Universidad de Huelva

Departamento de Química "Profesor José Carlos Vílchez Martín"

Metagenomic characterization, bioactive properties and biotechnological applications of the extremophilic microorganisms inhabiting Odiel saltern ponds

Memoria para optar al grado de doctora
presentada por:

Patricia del Rocío Gómez Villegas

Fecha de lectura: 20 de julio de 2021

Bajo la dirección de los doctores:

Rosa María León Bañares

Javier Vigara Fernández

Huelva, 2021

UNIVERSIDAD DE HUELVA

FACULTAD DE CIENCIAS EXPERIMENTALES

DEPARTAMENTO DE QUÍMICA
"PROFESOR JOSÉ CARLOS VÍLCHEZ MARTÍN"

TESIS DOCTORAL

"CARACTERIZACIÓN METAGENÓMICA, PROPIEDADES BIOACTIVAS Y APLICACIONES BIOTECNOLÓGICAS DE LOS MICROORGANISMOS EXTREMÓFILOS QUE HABITAN LAS BALSAS DE LAS SALINAS DEL ODIEL"

"METAGENOMIC CHARACTERIZATION, BIOACTIVE PROPERTIES AND BIOTECHNOLOGICAL APPLICATIONS OF THE EXTREMOPHILIC MICROORGANISMS INHABITING ODIEL SALTERN PONDS"

PROGRAMA DE DOCTORADO
CIENCIA Y TECNOLOGÍA INDUSTRIAL Y AMBIENTAL

MEMORIA PRESENTADA PARA OPTAR AL GRADO DE DOCTORA POR:

Patricia Del Rocío Gómez Villegas

TRABAJO PRESENTADO BAJO LA DIRECCIÓN DE:

Dra. Rosa María León Bañares
Dr. Javier Vigara Fernández

HUELVA, 2021

INDEX

Abstract

Abstract

Extremophilic microorganisms are those that live under the most severe conditions for life on Earth, including extreme values of temperature, pressure, pH, radiation, or salinity, among others. What is really surprising is that these microorganisms, not only tolerate, but require for their proliferation conditions which are considered lethal for most individuals.

In this doctoral thesis, we focus on a specific type of extremophilic microorganisms, the so-called halophiles, living in hypersaline environments where the concentration of salt reaches ten times the salinity of the sea. These microorganisms proliferate in environments such as salt lakes, salt mines, brine, and salt mines. This work focuses on the study of the microbial population of Odiel salterns, located in the marshlands of the Odiel river in the city of Huelva (Spain).

In many occasions, the microbial diversity in hypersaline environments has been underestimated due to the lack of suitable methods for its study, given that for their extremophilic nature many of these microorganisms do not proliferate well in the laboratory. However, halophiles are an excellent source of resources, as they possess specially adapted enzymes and have a large battery of metabolites to cope with the extreme conditions in which they live.

In this work, a complete characterization of the microbial communities that inhabit Odiel saltern ponds is carried out, and the applications of some of the compounds produced by the isolated halophilic microorganisms are studied. Different methods for the characterization of the microbial population at extreme salinity are addressed **(Chapter 1)**. The bioactive properties **(Chapter 2)** and the biotechnological applications **(Chapter 3)** of the metabolites from the isolated microorganisms were analyzed, to conclude with a further insight into the dynamics of the microbial diversity across the salinity gradient **(Chapter 4)**.

In **Chapter 1** the characterization of prokaryotic population in the highest salinity rafts of the Odiel salterns (33% NaCl) is presented. We combined two culture-independent strategies based on molecular techniques, clone library generation, and high throughput sequencing, both focused on the coding gene of 16S rRNA. The results showed that both methods are comparable in the determination of the majority genera, although metagenomics gives more information about the minority ones. Among the most abundant microorganisms, haloarchaea of the genera *Halorubrum* and *Haloquadratum*, in

addition to the bacterium *Salinibacter ruber* were found. On the other hand, the capacity of the biomass collected from the crystallizer pond to produce different extracellular hydrolases and halocins was assessed, and furthered in the following two chapters.

In **Chapter 2** the evaluation of the antioxidant, antimicrobial and bioactive properties of various extracts of two halophile archaea strains isolated from Odiel salterns is reported. These haloarchaea were phylogenetically classified as *Haloarcula* sp. HM1 and *Halobacterium* sp. HM2. The most outstanding results were found in the acetone extracts of both species, which had high antioxidant, antimicrobial, anti-inflammatory, and melanogenic capacity. In addition, aqueous extracts of both haloarchaea exhibited a considerable inhibition ability over the enzyme acetylcholinesterase, related to neurological disorders.

In **Chapter 3**, the amylase activity of an isolated halophilic archaeon is characterized using biochemical and proteomic approaches. Amylases are one of the most widely used enzymes in the industry, where the tolerance of halophilic proteins to very extreme conditions can be of high applied interest. After a screening within different strains of isolated haloarchaea, the one with the highest amylase activity was identified as *Haloarcula* sp. HS. This microorganism showed amylase activity in both the cell and extracellular extract, with maxima at 60°C and 25% NaCl. Up to three different amylases of the so-called α-amylase family were identified. In addition, the effectiveness of extracellular amylase activity was tested to treat bakery residues under high salinity.

Finally, in **Chapter 4** the study of microbial diversity in the Odiel salterns ponds along the salinity gradient (3.5, 7.5, 15, and 30% NaCl) is described. The microbial communities of eukaryotes and prokaryotes were characterized by the massive sequencing of the 16S and 18S rRNA coding genes, together with the analysis of the most abundant pigments. It was found that green microalgae (*Chlorophyta*) dominate phytoplankton in all salinities and that the phylum *Proteobacteria* is displaced by the phyla *Bacteroidetes* and *Euryarcheaota* as salinity increases. Finally, the evaluation of the role of microbial carotenoids in the trophic chain indicated that these pigments could pass to higher organisms such as flamingos through the small crustacean *Artemia*.

Resumen

Los microorganismos extremófilos son aquellos que viven bajo las condiciones más severas para la vida en la Tierra, incluyendo valores extremos de temperatura, presión, pH, radiación, o salinidad, entre otros. Lo realmente sorprendente es que estos microorganismos, no solo toleran, sino que requieren para su proliferación condiciones que se consideran letales para la mayoría de los individuos.

Dentro de los microorganismos extremófilos, esta tesis doctoral se ha centrado en el estudio de un tipo concreto de ellos, los denominados halófilos, que habitan en ambientes hipersalinos, donde la concentración de sal llega a superar en diez veces la salinidad del mar. Estos microorganismos proliferan en lugares como lagos salados, minas de sal, salmueras y salinas. Este trabajo está centrado en el estudio de la población microbiana de salinas del Odiel, ubicadas en las marismas del río Odiel en la ciudad de Huelva (España).

La diversidad microbiana en ambientes hipersalinos ha estado subestimada por la falta de métodos adecuados para su estudio, dado que por su carácter extremófilo muchos de estos microorganismos no proliferan bien en laboratorio. Sin embargo, los halófilos suponen una excelente fuente de recursos, ya que poseen enzimas especialmente adaptadas y una gran batería de metabolitos con potencial interés biotecnológico, que utilizan para hacer frente a las condiciones extremas en las que viven.

En este trabajo se realiza una caracterización completa de las comunidades microbianas que habitan en las balsas de las salinas del Odiel, y se estudian las aplicaciones de algunos de los compuestos producidos por los microorganismos halófilos aislados. Se abordan distintos métodos para la caracterización de la población microbiana a salinidad extrema **(Capítulo 1)**, seguido del análisis de las propiedades bioactivas **(Capítulo 2)** y aplicaciones biotecnológicas **(Capítulo 3)** de los metabolitos producidos por los microrganismos aislados, para concluir con el estudio de la evolución de la biodiversidad microbiana a lo largo del gradiente de salinidad **(Capítulo 4)**.

En el **Capítulo 1** se presenta la caracterización de la población de microorganismos procariotas en las balsas de mayor salinidad (33% NaCl). Se combinaron dos estrategias independientes de cultivo basadas en técnicas moleculares, la generación de genotecas y la secuenciación masiva, ambas centradas en el gen codificante del ARNr 16S. Los resultados mostraron que ambos métodos son comparables en cuanto a la determinación de los géneros

mayoritarios, aunque la metagenómica otorga más información sobre los minoritarios. Dentro de los microorganismos más abundantes, se encontraron haloarqueas de los géneros *Halorubrum* y *Haloquadratum*, además de la bacteria *Salinibacter ruber*. Por otro lado, se evaluó la capacidad de la biomasa recolectada de las balsas de cristalización para producir distintas hidrolasas extracelulares y halocinas, sobre lo que se profundiza en los dos siguientes capítulos.

En el **Capítulo 2** se relata la evaluación de las propiedades antioxidantes, antimicrobianas y bioactivas de diversos extractos de dos cepas de arqueas halófilas aisladas de las salinas del Odiel. Estas haloarqueas se clasificaron filogenéticamente como *Haloarcula* sp. HM1 y *Halobacterium* sp. HM2. Los resultados más destacables se encontraron en los extractos de acetona de ambas especies, los cuales presentaron alta capacidad antioxidante, antimicrobiana, anti-inflamatoria y melanogénica. Además, los extractos acuosos de ambas haloarqueas exhibieron inhibición sobre la enzima acetilcolinesterasa, relacionada con desórdenes neurológicos.

En el **Capítulo 3**, se detalla la caracterización bioquímica y proteómica de la actividad amilasa de una arquea halófila aislada. Las amilasas son unas de las enzimas más empleadas en la industria, donde las proteínas de halófilos pueden resultar útiles al tolerar condiciones muy extremas. Tras realizar un cribado con distintas cepas de haloarqueas aisladas, se identificó la que presentaba mayor actividad amilasa como *Haloarcula* sp. HS. Este microorganismo mostró actividad amilasa tanto en el extracto celular como extracelular, con máximos a 60°C y 25% NaCl. Se identificaron hasta tres amilasas distintas de la familia de las denominadas α-amilasas. Además, se probó la efectividad de la actividad amilasa extracelular para tratar residuos de panadería bajo elevada salinidad.

Finalmente, en el **Capítulo 4** se describe el estudio de la diversidad microbiana en las balsas de las salinas del Odiel a lo largo del gradiente de salinidad (3,5; 7,5; 15 y 30% NaCl). Las comunidades microbianas de eucariotas y procariotas se caracterizaron mediante la secuenciación masiva de los genes codificantes para el ARNr 16S y 18S, junto al análisis de los pigmentos más abundantes. Se comprobó que las microalgas verdes (*Chlorophyta*) dominan el fitoplancton en todas las salinidades y que el filo *Proteobacteria* es desplazado por los filos *Bacteroidetes* y *Euryarcheaota* conforme aumenta la salinidad. Por último, la evaluación del papel de los carotenoides microbianos en la cadena trófica indicó que estos pigmentos podrían pasar a organismos superiores como los flamencos a través del pequeño crustáceo *Artemia*.

Introduction

1. Extremophilic microorganisms

The term extremophile incudes all those organisms that achieve their optimal growth in extreme environmental conditions for life on Earth. This word was first introduced by MacElory in 1974, and comes from Latin *extremus* and Greek *philiā* (φιλία) meaning literally "extreme lover". This term must not be confused with extremotolerant or extremotroph, which refers to the organisms that proliferate optimally under normal conditions for life but also resist extreme environmental conditions. By contrast, extremophilic organisms, not only tolerate extreme conditions but usually require them for survival and growth. Extensive global research efforts have revealed the great diversity of extremophiles, which inhabit environments that were previously considered inhospitable for life. Extremophiles have been found at depths of 6.7 Km inside the Earth's crust, more than 10 Km deep inside the ocean, at pressures of up to 110 MPa; from extreme acid (pH 0) to extreme basic conditions (pH 13); and from hydrothermal vents at 122 °C to frozen seawater, at −20 °C [1,2].

An environment is considered as moderate when it presents pH near neutral, temperature between 20 and 40°C, air pressure 1 atm, and adequate levels of available water, nutrients, and salt. However, many other habitats with harsh conditions for a normal life are found in nature, such as hot springs, geysers, polar waters and soils, saline and soda lakes, deserts, and hydrothermal vents. Also, other man-made extreme conditions like coolhouses, steam-heated buildings, solar lakes, and acid mine waters have been introduced into the biosphere. Extreme environments include high temperature, pH, pressure, salt concentration, ionizing radiations, as well as, low temperature, pH, nutrient concentration, and water availability, and also high levels of radiation, harmful heavy metals, and toxic compounds as organic solvents [3].

Extremophiles include members of the three domains of life, Bacteria, Archaea, and Eukarya (Figure 1). Most extremophiles are found in the microbial world, being able to tolerate a range of environmental extremes much broader than other life forms. Among them, a high proportion are archaea, which are usually quite adapted to different extreme conditions and hold commonly extremophilic records, although they are often less versatile than bacteria and eukaryotes. Generally, extremophilic microorganisms may be divided into two distinct categories: specialists, adapted to a single extreme; and generalists adapted to multiple extremes.

Extremophilic microorganisms are classified according to the conditions in which they grow as thermophiles and hyperthermophiles, that grow at high or very high temperatures, respectively; psychrophiles, which proliferate best at low temperatures; acidophiles and alkaliphiles, which are adapted to acidic or basic pH values, respectively; barophiles or piezophiles, that flourish under high pressure; halophiles, which require high concentrations of NaCl for growth; xerophiles, that prosper with low water availability; metallophiles, that grow in high concentrations of metals or heavy metals; oligotrophic, that grow in nutritionally limited conditions; endolith, that inhabit inside rocks; radiophiles, that proliferate under high radiation levels; microaerophiles, that grow best in the presence of a small amount of free oxygen; and some other extremophiles that have evolved mainly due to anthropogenic activities, and proliferate under high concentration of nuclides and pollutants. Moreover, these organisms are normally polyextremophiles, being adapted to live in habitats where various physicochemical parameters reach extreme values. Therefore, they can be, for example, thermoacidophiles or haloalkaliphiles [4–6].

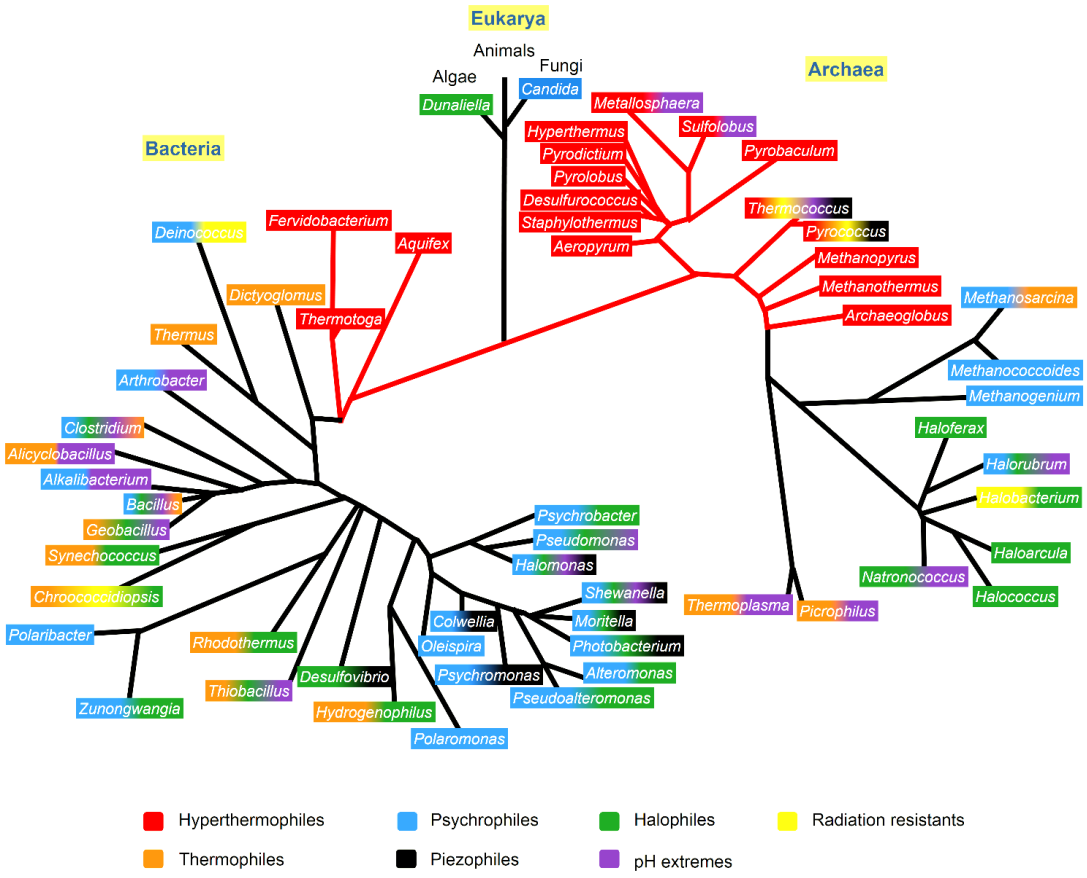

Figure 1. Phylogenetic tree of extremophiles, including at least one species of each genus. The different extremophilic characteristics are highlighted by the color code, as shown in Dalmaso *et al*. [7].

The research on extremophiles has gained increasing interest in view of the biotechnological potential of these microorganisms and their biomolecules. Due to the fact that extremophilic microorganisms have evolved to cope with the extreme environments where they live, they can be an excellent source of compounds for diverse industrial processes in which harsh conditions are required. Noteworthy are the enzymes of these microbes, so-called extremozymes, which can work under high salt, temperature, and/or pressure [8]; organic osmolites or extremolytes, that protect cells from damage by external stresses and minimize the denaturation of biopolymers [9]; and pigments, that protect the cells from multiple stressors [10]. All these compounds present multiple applications in diverse sectors, including medicine, pharmacy, food and textile industry, detergency, bioremediation, and biorefinery [11–13].

Furthermore, studies on extremophiles are essential for the emerging field of astrobiology, as they define the boundary conditions for life known so far. These microorganisms constitute the basis of study for the origin of life on Earth and the exploration of life on other planets [14]. The groundbreaking discoveries of a great variety of extremophilic microorganisms on Earth have considerably broadened the range of habitats where life could be found on other planets. Therefore, extraterrestrial environments previously thought to be uninhabitable have been shown to be theoretically habitable [4]. The ancient and versatile halophilic archaea are especially attractive models for astrobiology, being able to survive in a variety of planetary environments and with relevance for *in situ* life detection [15].

There is still a huge diversity of extremophilic microorganisms waiting to be explored. Hence, many novel and useful species with their respective metabolites are expected to be discovered and utilized for improving the quality of life. In this work, the extremophilic community of a practically unexplored extreme environment has been characterized, focusing especially on extreme halophilic archaea and their biomolecules for diverse biotechnological applications.

2. Halophilic microorganisms

Halophiles, from Greek *halos* and *philein*, are literally salt-loving organisms, which means that they need high salt concentrations for growth. Halophilic organisms are commonly classified according to the salt (NaCl) concentration needed for their optimum growth, as proposed by Kushner in

1978. Thus, halophiles can be divided into slightly halophilic, with optimum growth between 0.2 and 0.5 M salt; moderately halophilic, growing best with 0.5-2.5 M salt; and extremely halophilic, which require above 2.5 M salt for their optimum growth. In addition, two more categories have to be considered, non-halophiles, living best in media containing less than 0.2 M salt, and halotolerant organisms, that do not need salt for growth but tolerate high salt concentrations [16,17]. However, it must be taken into account that the minimum, optimum and maximum salt concentrations often depend on the medium composition and growth temperature [18]. In addition, the tolerance to salt can vary according to environmental and/or nutritional factors [19].

2.1. Habitats

Hypersaline environments are usually polyextreme ecosystems where high salinity is not the only limiting condition. In these media, alkaline pH, high or low temperature, low nutrient, water, and oxygen availability, high UV radiation, high concentrations of heavy metals, and/or other toxic compounds are usually present. Therefore, halophiles often display additional extremophilisms, such as the thermophilic alkaliphilic extremely halophilic members of the *Natranaerobius* genus [20,21].

Habitats for halophilic microorganisms include marshlands, salt lakes, man-made salterns, either coastal or inland, hypersaline deep-sea masses, subterranean brines, salted food, animal hides, salt mines, saline soils, and dessert salt crusts. Water bodies are considered hypersaline when they exceed the salinity of the sea (3.5% w/v), and they are classified into thalassohaline and athassohaline environments [22]. Thalassohaline environments are derived from the evaporation of seawater, and reflect the ionic composition of the sea, with NaCl as the main component of brines. Their pH is around neutrality and thus, they are preferred for most known halophilic microorganisms. Examples of thalassohaline environments are coastal solar salterns and the Great Salt Lake (Utah, USA), which despite not having a connection with the sea, presents a similar salt composition to that of seawater. On the other hand, water in athalassohaline environments has not a marine origin but is formed mainly from salt deposits by evaporation procedures in continental water bodies. Therefore, the salt composition of these lakes varies considerably from one to another. A remarkable example of this environment is the Dead Sea, which typical features are the high concentrations of the divalent cations magnesium and calcium rather

than sodium, and the slightly acid pH. Other athassohaline salt lakes are extremely alkaline, such as Mono Lake (California, USA) and soda lakes in East African Rift Valley, characterized by high concentrations of carbonate salts, especially sodium carbonate [23–25].

2.2. Biodiversity

The earliest modern-day report on halophilic microorganisms was done in 1914 by Pierce [26], although the proliferation of halophiles has been observed during the salt-making process along with human history. During the 20th century, studies on halophilic microorganisms were based on culture approaches, until new molecular and genome sequencing techniques appeared, allowing the development of culture-independent and genetic methods. These innovative techniques have revealed that the diversity of halophiles was underestimated with the culture-dependent methods, as well as their applications to industrial and environmental biotechnology [27,28]. Halophiles are found in all three domains of life: *Archaea*, *Bacteria*, and *Eukarya*, as shown in Figure 2, although, the tolerance to salt and the strategies adopted to cope with salt stress are quite different in each group [29].

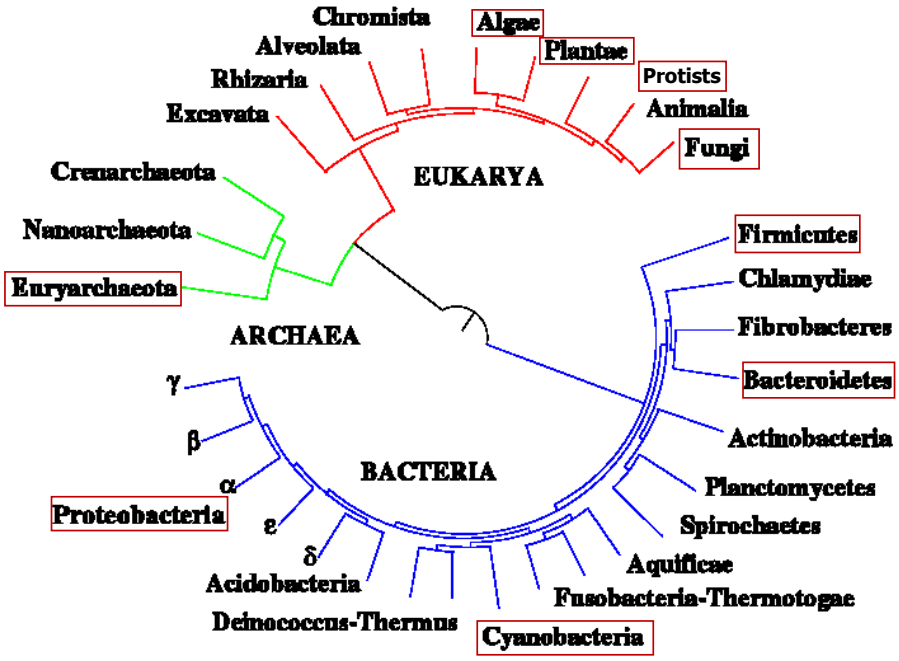

Figure 2. Distribution of halophiles within the three domains of life. The phylogenetic tree of life is adapted from Ciccarelli *et al.* [30] and generated using iTOL (Interactive Tree Of Life), an online phylogenetic tree viewer and Tree Of Life resource. Groups in red boxes contain at least one halophile, based on the information from Edbeib *et al.* [31].

Within the eukaryotic members, several species of green algae are moderate halophiles, such as the unicellular green algae of the genus *Dunaliella*, which proliferate at moderate salinities and are the main primary producers in many hypersaline environments. Ubiquitous extreme halophilic species are *Dunaliella salina*, *Dunaliella parva,* and *Dunaliella viridis*, which lack a robust cell wall and can grow until salt saturation. Other algae usually found in hypersaline environments, but rarely abundant, are diatoms, which are surrounded by silica cell walls. Diverse species have been found at approximately 2M NaCl, and some of them up to 3M NaCl. Yeasts and filamentous fungi tolerate hypersaline environments, growing better under aerobic conditions at moderate temperatures and acidic or neutral pH. Among the protozoa in hypersaline environments, the more widely studied is *Fabrea salina*, although other representatives are also present. Finally, several complex multicellular eukaryotes can survive in hypersaline environments, as the brine shrimp, *Artemia salina,* brine flies, rotifers, flatworms, copepods, and ostracods. Also, a variety of obligate and facultative halophytic plants, and the moderate halophytes as *Salicornia europaea* are found in hypersaline environments [19,32].

A great diversity of halophilic bacteria exists in nature, including gram-positive and gram-negative, phototrophic and heterotrophic, as well as, aerobic and anaerobic bacteria. Most moderately or extremely halophilic species are included in the following phyla: *Actinobacteria*, *Bacteroidetes*, *Cyanobacteria*, *Firmicutes*, *Proteobacteria*, *Spirochaetes*, *Tenericutes,* and *Thermotogae*. Among them, *Cyanobacteria*, also known as blue-green algae, dominate the planktonic biomass and play an ecological role as major contributors to photosynthesis in many hypersaline lakes. All the halophilic members of the phylum *Actinobacteria* belong to the order *Actinomycetales*, while halophilic bacterial species of the phylum *Bacteroidetes* are spread into the three classes of this group. Within *Bacteroidetes, Salinibacter ruber* must be highlighted as one of the few extremely halophilic members of the domain *Bacteria* [33]. Numerous halophilic species have been reported as members of the phyla *Firmicutes* and *Proteobacteria*, distributed into different families, while there are few moderately halophilic species belonging to the phyla *Spirochaetes* and *Tenericutes*. Finally, halophiles belonging to the phylum *Thermotogae* are common inhabitants of deep, hot oil reservoirs located in marine or continental ecosystems [21,34].

Halophilic archaea or haloarchaea are a phylogenetically coherent group of salt-requiring prokaryotes, that grow best at the highest salinities (3.4–5.1 M NaCl). They are included in the phylum *Euryarchaeota*, within the class

Halobacteria, which encompasses to the date around 70 genera and 260 species, classified in three orders and six families: *Halobacteriales* (families *Halobacteriaceae*, *Haloarculaceae*, *Halococcaceae*), *Haloferacales* (families *Haloferacaceae* and *Halorubraceae*), and *Natrialbales* (family *Natrialbaceae*) [18]. In addition, a novel group of *Halobacteria* identified by metagenomics was established as the new class *Nanohaloarchaea* [35] and its phylogenetic position has been highly debated. By phylogenetic inference, it has been shown that *Nanohaloarchaea* and *Halobacteria* represent two independent lines that are derived from two distinct but related methanogen Class II lineages. This fact implies that adaptation to high salinity emerged twice independently in *Archaea* and that the similarities between *Nanohaloarchaea* and *Halobacteria* likely result from convergent evolutionary processes [36]. Haloarchaeal cells are rod-, coccus- or disk-shaped, triangular, and even square-shaped. Many species are pleomorphic, especially when the ionic conditions of the media are altered, and most lyse below 1–1.5 M NaCl [19]. Most species of *Halobacteria* prefer near neutral pH values, but there are also many obligate alkaliphilic species. Haloarchaea mainly lead an aerobic chemoheterotrophic lifestyle, although there is considerable metabolic diversity within the group, and some of them can also grow anaerobically or even in strictly anaerobic conditions. Anaerobic photoheterotrophic growth, using light energy absorbed by the bacteriorhodopsin proton pump, has also been observed in some species [18].

Finally, halophilic viruses may be included as members of hypersaline habitats. The number of virus particles exceeds the numbers of cells from 10 to 100 times in most hypersaline environments. To date, around 100 haloviruses infecting extremely halophilic archaea have been reported, being currently the most described viruses of extremophiles [37].

Contrarily, few viruses infecting halophilic bacteria have been found and very little is known about eukaryotic haloviruses. The known haloviruses include tailed and tailless icosahedral, pleomorphic, and lemon-shaped forms and they are classified according to their host range, genome type, and replication mode [37]. The ecology of haloviruses was first studied by Wais and Daniels in 1985 [38] in the halophilic archaea *Halobacterium*. Later studies have revealed that the viral diversity increased up to salt concentrations of 15%, and then decreases as salinity increases. At the highest salinities (>25% NaCl), viral lysis appears to be more common than grazing by heterotrophic protists [24].

2.3. Strategies for salt adaptation

All halophilic microorganisms maintain their cytoplasm isosmotic with the surrounding hypersaline medium. However, there are two substantially different strategies used to cope with osmotic stress, known as "high-salt-in" and "low-salt-in". The first implies the accumulation of molar concentrations of potassium and chloride, while the second is based on the accumulation of organic osmoregulatory solutes.

The "high salt-in" strategy is energetically much less costly than the synthesis of organic compatible solutes but requires an extensive adaptation of the whole intracellular machinery to the presence of high ionic concentrations [39]. Probably for that reason, only a small number of specialized groups have adopted this strategy: the aerobic extremely halophilic archaea of the *Halobacteriales* order, the aerobic extremely halophilic bacteria *Salinibacter ruber* (*Bacteroidetes*), which is physiologically similar but phylogenetically unrelated with haloarchaea [33], and the fermentative obligatory anaerobic bacteria of the order *Halanaerobiales* (*Firmicutes*).

The ''high-salt-in'' strategy permits the colonization of the environments with the highest salinity, but these adaptations make the cells strictly dependent on the continuous presence of high salt concentrations to maintain their structural integrity and viability. The proteomes of the aerobic haloarchaea and *Salinibacter ruber* are quite acid and low hydrophobic [40]. Their proteins present a large excess of the acidic amino acids glutamate and aspartate and low content of the basic amino acids lysine and arginine.

Similarly, the proteins of these microorganisms show a low content of hydrophobic amino acids, generally offset by an increase in the hydroxylated amino acids serine and threonine. High salt inside the cells is needed to maintain the weak hydrophobic interactions and to shield the negative charges, allowing proteins to maintain their proper conformation. The peculiar ionic composition found in the cytoplasm of these microorganisms and the gradients over their cell membrane are the result of the cooperative action of different ion pumps, antiporters, and other transport proteins, which are shown in Figure 3 [19,31,32,41,42].

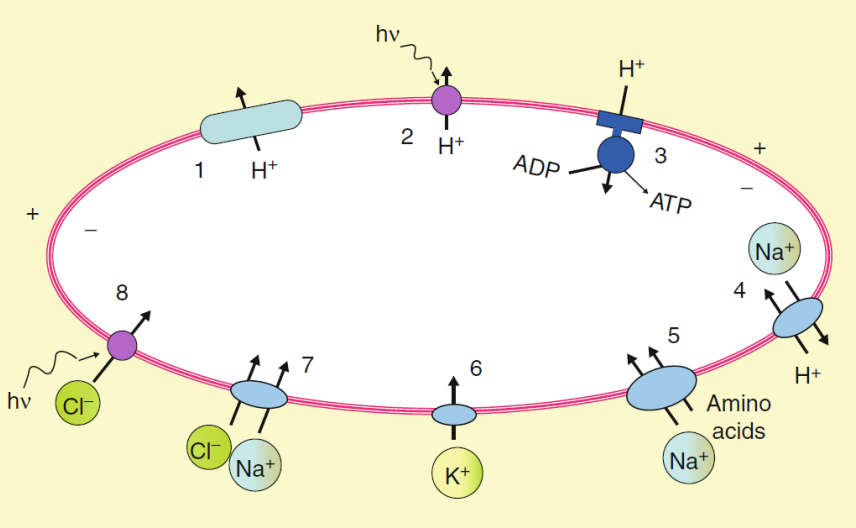

Figure 3. Ion movements in the aerobic halophilic archaea (adapted from Oren [41])**. [1]**, proton extrusion via respiratory electron transport; **[2]**, light-driven proton extrusion mediated by bacteriorhodopsin; **[3]**, ATP formation by ATP synthase, driven by the proton gradient. Alternatively, this system can generate a proton gradient at the expense of ATP during fermentative growth on arginine; **[4]**, electrogenic sodium/proton antiporter; **[5]**, sodium gradient-driven inward amino acids transport; **[6]**, potassium uniport, driven by the membrane potential; **[7]**, light-independent chloride transport system, probably coupled with inward transport of sodium; **[8]**, halorhodopsin, the primary, light-driven chloride pump.

Conversely, the strategy of "low-salt-in" or "salt-out" implies the maintenance of cytoplasm with a much lower salt concentration than the outside medium. This option is widespread in most halophilic and halotolerant bacteria, halophilic methanogenic archaea, and halophilic eukaryotic microorganisms. Osmotic equilibrium is provided by organic solutes that are either produced by the cells or uptaken from the medium and accumulated, while ions are actively pumped out of the cells. This strategy is energetically costly because of the production of massive amounts of solutes and the need to prevent salts from reaching the cytoplasm.

Compatible solutes display a general stabilizing effect over the proteins preventing their denaturation. They are uncharged or zwitterionic molecules with low-molecular weight, soluble in water, and not inhibitory to enzymatic activities even in molar concentrations. As the intracellular concentrations of the organic solutes can be regulated accordingly to the salinity of the medium, they provide fast flexibility and adaptability to a wide range of salinities. In addition, few adaptations of the proteome are needed because these molecules barely interfere with the enzymatic activity.

The number of organic compatible solutes is extensive, including amino acids and derivatives, sugars, heterosides, and polyols, as shown in Figure 4 [43]. Some of them are widely distributed among halophiles, while others are more exclusive for specific groups. For example, glycerol and other polyols are broadly used by halophilic algae and fungi, but rarely in prokaryotes. Many prokaryotes contain cocktails of diverse compatible solutes rather than relying on a single compound. Among *Bacteria* cyclic amino acid derivatives as ectoine and hydroxyectoine are very usual. Also, glycine betaine is commonly employed by many different microorganisms, like cyanobacteria, while proline is especially used in the *Firmicutes* but also present in some microalgae, such diatoms. Unusual compatible solutes, such as β- amino acids and derivatives are mainly found in halophilic methanogens. Similarly, sulfotrehalose is found in some alkaliphilic haloarchaea together with KCl [19,32,39,42]. Protozoa are known to regulate osmotic pressure with contractile vacuoles that expel water. Besides, halophilic protists exploit organic solutes as major osmolytes and potentially have higher intracellular salt content than marine protists [44].

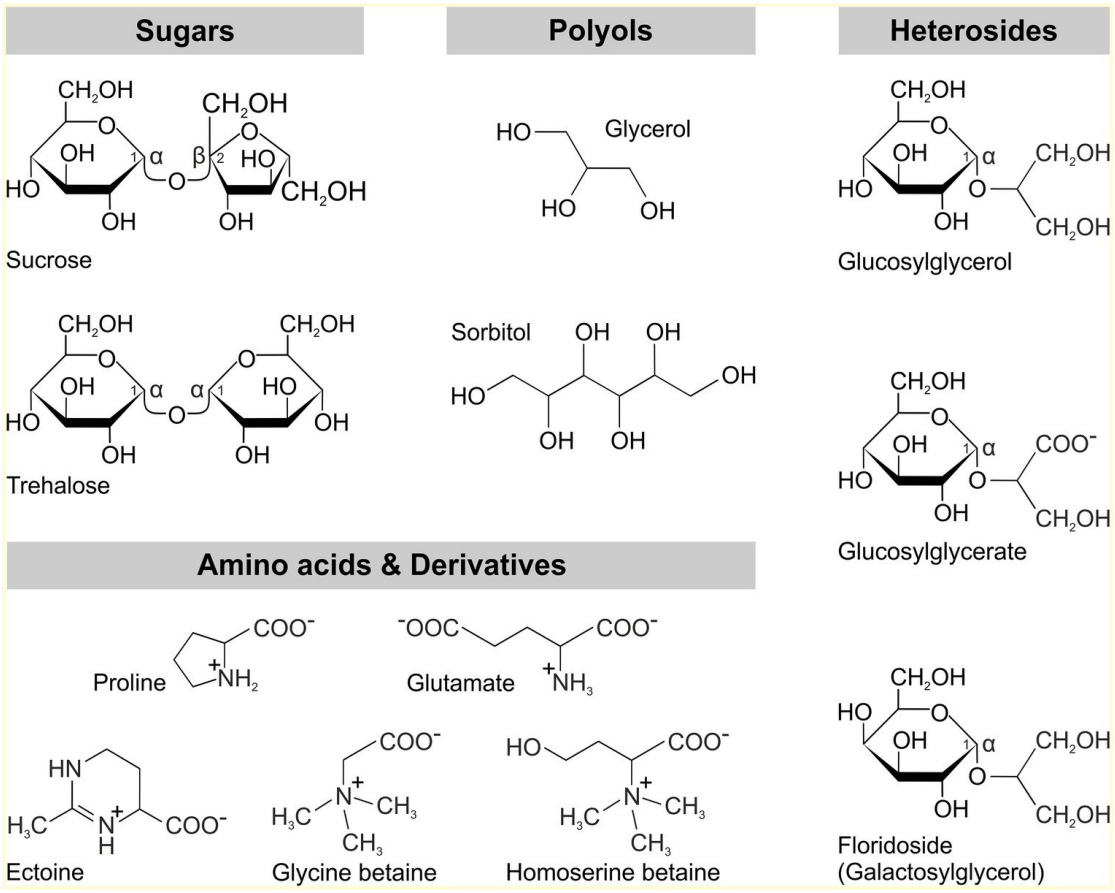

Figure 4. Different types of compatible solutes found in microorganisms (adapted from Kirsch *et al* [43]).

3. Metabolic interactions between the biota in salterns

Solar salterns have been build worldwide to obtain common salt from seawater. These salt flats consist of a series of shallow evaporation and crystallizer ponds connected by canals, in which brine is directed into smaller ponds as salinity increases through evaporation. During the process of evaporation, sequential precipitation of salts, calcium carbonate, calcium sulfate (gypsum), and NaCl (halite) occurs [19]. Saltern crystallizer ponds are ideal habitats to study the behavior of halophilic microorganisms in their natural medium at saturating salt concentrations since microbial communities in these environments are simple and usually archive very high population densities. In each pool, the salinity is almost constant, which allows the existence of a specific microbial community at the prevalent salt concentration [45].

The earliest set of evaporation ponds have salinities near the seawater (~4%), and therefore, their microbiota is similar to those of the sea. In the following evaporation ponds, in which the salinity is increased up to around 20%, is usual to find microbial mats of photosynthetic unicellular and filamentous cyanobacteria and purple and green sulfur bacteria at the bottom, as well as a variety of sulfur-oxidizing, sulfate-reducing, homoacetogenic, methanogenic and heterotrophic bacteria and archaea in the anoxic zones of the mats and in the sediment. When the salinity increases to around 15%, gypsum precipitates and accumulates on the bottom, showing sometimes beautifully colored layers of cyanobacteria and photosynthetic purple bacteria. The crystallizer ponds are located in the last step of the salt-making process. In these pools, when the salinity reaches 30% the NaCl precipitates as halite crystals, which are harvested whenever a sufficient layer is accumulated on the bottom. At this salinity, the most striking microbial communities are found in planktonic populations, which confer a reddish color to the brines. In these crystallizer ponds haloarchaea dominate the microbiota and nearly all other microbial activity ceases [18,19,27].

With respect to the metabolic processes performed to obtain energy and carbon for growth, halophilic microorganisms are as diverse as expected in view of the large phylogenetic diversity of the organisms. The metabolic processes found up to almost salt saturation include oxygenic and anoxygenic photosynthesis, aerobic and anaerobic respiration, fermentation, and chemoautotrophic sulfur oxidation. Contrarily, other metabolic processes have not been shown to occur at salt concentrations above 15%, for example, sulfate

reduction with acetate as electron donor, methanogenesis by reduction of carbon dioxide with hydrogen, or by splitting of acetate, and autotrophic nitrification. This fact could be due to the upper salt concentration limit, at which a dissimilatory process can occur, and the balance between the amount of energy generated in this metabolism and the energy cost of the osmotic adaptations [34].

The crystallizer ponds, where salinity reaches saturation, constitute the more extreme environment of solar salterns. The microbial population in these crystallizer pools is worldwide dominated by the flat, square-shaped, and red haloarchaea *Haloquadratum walsbyi*, the extremely halophilic rod-shaped red bacteria *Salinibacter ruber*, and the unicellular green alga *Dunaliella* as the primary producer. Forty years ago, Borowitzka provided a simple picture of the relationships within the biota in salt-saturated waters [46].

Although the trophic simplicity at such high salinity is still accepted, the microbial diversity of halophilic archaea has been revealed much more extensive than previously thought. *Dunaliella* photosynthetically produces glycerol, which is massively accumulated intracellularly as an osmotic solute. Glycerol has been often postulated to be the most important source of organic carbon for the heterotrophic prokaryotes in hypersaline ecosystems. Nonetheless, the heterotrophic activities are undoubtedly rather more complex than the simple aerobic oxidation of glycerol to carbon dioxide. Aerobic haloarchaea can use different substrates as carbon and energy sources, including simple sugars, sugar alcohols, and glycerol, which are frequently oxidized incompletely, and products such as acetic acid, lactic acid, and pyruvic acid are excreted. Studies on *Haloquadratum walsbyi* and *Salinibacter ruber* have revealed that both possess glycerol kinase genes involved in glycerol metabolization, although other experiments showed that *Salinibacter ruber* was unable to grow in glycerol and that glycerol was not used by *Haloquadratum walsbyi*. Thus, more research will be needed to determine whether glycerol is imported by both organisms into their natural environments [18,45].

Another possible key substrate in saltern ecosystems is dihydroxyacetone, which has been suggested to derive from the metabolism of *Dunaliella*, when excess glycerol has to be metabolized after osmotic downshock, or as a possible overflow compound of carbon metabolism produced by *Salinibacter ruber*. In addition, an efficient uptake system for dihydroxyacetone has been identified in the genome of *Haloquadratum*, the main component of the microbial consortium in most saltern crystallizer ponds around the globe. Hence, the glycerol

synthetized by *Dunaliella* would be first converted by *Salinibacter ruber* to dihydroxyacetone, which could be further employed by *Haloquadratum* and maybe other members of the *Halobacteria* group [18,45].

Furthermore, many aerobic halophilic archaea use pyruvate as one of their preferred growth substrates, and it is also excreted by some halophilic archaea in the presence of glucose. Besides, just like glycerol and dihydroxyacetone, pyruvate can be a substrate for the respiration metabolism of the microbial community in crystallizer ponds [47,48]. Acetate and D-lactate are also released to the medium by halophilic archaea in crystallizer ponds, and some haloarchaeal species are able to grow in acetate as the single substrate or in combination with other carbon sources [18].

4. The reddish color in brines: carotenoids and retinal proteins

Hypersaline systems, as salterns and salt lakes, are usually pink-red colored due to the presence of dense communities of different types of carotenoid-rich microorganisms. In brines of natural salt lakes and crystallization ponds, with total salt concentrations exceeding 30%, the predominant colored microorganisms are the halophilic archaea of the class *Halobacteria* that contain bacterioruberin carotenoids and sometimes retinal proteins as bacteriorhodopsin and halorhodopsin. In addition, β-carotene-rich species of the unicellular green alga *Dunaliella*, and the bacteria *Salinibacter* that contain the carotenoid salinixanthin and the retinal protein xanthorhodopsin, may contribute to this reddish color [18,40].

Carotenoids are lipophilic isoprenoid compounds that include a wide range of carotenes and xanthophylls. The halophilic microalgae *Dunaliella salina* and some other related species produce massive amounts of the C_{40} carotenoid β-carotene, and *Salinibacter ruber* synthetizes the C_{40}-carotenoid acyl glycoside salinixanthin. Instead, members of the *Halobacteria* produce C_{50}-carotenoids, mainly the open-chain carotenoid α-bacterioruberin but also some minor amounts of different derivatives, being monoanhydrobacterioruberin and bisanhydrobacterioruberin the most frequent. All these carotenoid pigments, β-carotene, salinixanthin, as well as α-bacterioruberin and derivatives, seem to protect the cells against photo-oxidative damage. Besides, salinixanthin acts as a light-harvesting antenna for xanthorhodopsin, which is the proton-pumping retinal pigment of *Salinibacter* [49,50].

As aforementioned, many halophilic prokaryotes possess membrane-bound retinal proteins, named rhodopsins, which encompass photoactive proteins containing a retinal chromophore. Rhodopsins are found in all domains of life and are divided into two groups. While lower organisms utilize the family of microbial rhodopsins for light energy conversion and intracellular signaling, animal rhodopsins are a specialized subset of G protein-coupled receptors used for photosensory functions. Animal and microbial rhodopsins have almost no sequence homology and differ largely in their functions, but they share the common structure of seven transmembrane α-helices with the N- and C-terminus facing outwards from and inside of the cell, respectively. The first microbial rhodopsin found was the light-driven proton pump bacteriorhodopsin in the halophilic archaea *Halobacterium salinarum* in the early 1970s [51,52], and from then many others retinal proteins with novel functions have been described, as the light-driven inward chloride pump halorhodopsin and sensory rhodopsins, employed as light sensors to direct phototactic movement in motile species. In *Salinibacter*, retinal proteins have also been found, including the light-driven retinal containing proton pump xanthorhodopsin, a putative light-driven chloride pump, and retinal-based light sensors [18,53].

In crystallizer ponds and salt lakes, β-carotene-rich *Dunaliella salina* is typically present in numbers between 10^3 and 10^4 cells per mL, while prokaryotic microorganisms usually reach 10^7-10^8 cells per mL. In the past, the red color of brines was attributed to the microalgae of the genus *Dunaliella*, as the quantity of β-carotene present in these cells often greatly exceeds that of the haloarchaeal bacterioruberin pigments. However, nowadays, the main contributors to this typical red color appear to be halophilic archaea, and the reason suggested is, not only their higher number, but also the different distribution of the carotenoids in cells. In microalgae, β-carotene has a very small *in vivo* optical cross-section, because of the dense packing of the pigment in granules attached to the thylakoid membranes in the chloroplast, while in the haloarchaea, bacterioruberin are distributed more or less evenly over the entire cell membrane.

In addition, salinixanthin pigments have never been shown to contribute greatly to the overall optical properties of the waters, since its presence has been found to be minor in comparison with the amount of bacterioruberin pigments from the halophilic archaea that inhabit the same brines [54]. Furthermore, retinal pigments from the biomass collected from natural brines have never showed a prominent absorption peak that can be attributed to them. Thus, the main factor

causing the characteristic red color of hypersaline brines worldwide must be bacterioruberin, the characteristic carotenoid of haloarchaea [18,55].

The three main types of carotenoids found in hypersaline systems can be easily differentiated by their characteristic absorption spectra, as shown in Figure 5. β-Carotene has its absorption maximum at 450 nm, with a minor peak at ~480 nm, while bacterioruberin spectrum is dominated by a peak near 496 nm, a minor peak at ~530 nm, and a shoulder at ~470 nm and the absorption spectrum of salinixanthin shows a peak at ~482 nm and a broad shoulder around 506–510 nm. In addition, retinal proteins of the halophilic prokaryotes are purple-colored and can be distinguished from carotenoids, with an absorbance maximum at 570–580 nm [18,55]. Therefore, the optical properties of the brines can be exploited for remote monitoring of the salinity and population distributions of microbial communities.

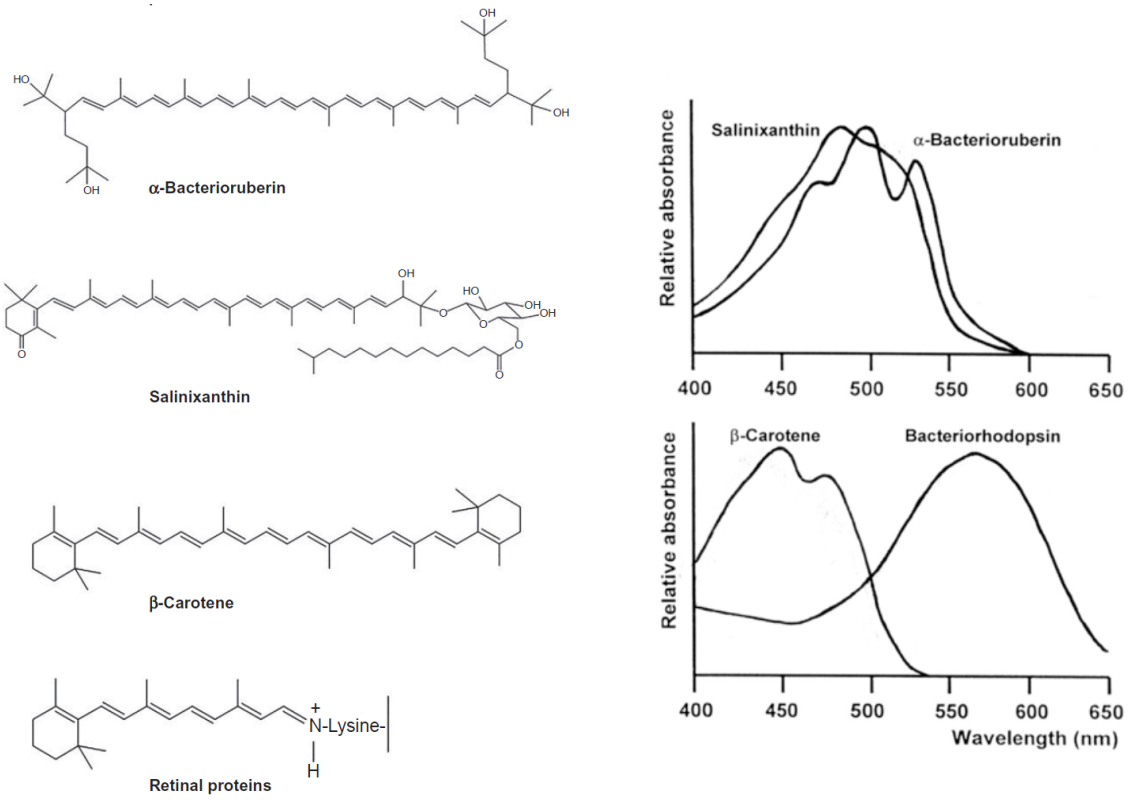

Figure 5. The principal orange, red and purple pigments encountered in the biomass of saltern crystallizer ponds, and their absorption spectra (adapted from Oren [18,55]): α-bacterioruberin, the main carotenoid of the halophilic archaea of the class *Halobacteria*; salinixanthin, the primary carotenoid of the halophilic bacteria *Salinibacter ruber*; all-trans β-carotene, the principal carotenoid accumulated by *Dunaliella* species; and the retinal group bound by a Schiff base to a lysine residue in bacteriorhodopsin, halorhodopsin and other retinal proteins.

The appearance of red colors in the crystallizer brines of salterns for the production of common salt from seawater is usually considered as a positive factor for the process. Pigmented microorganisms absorb solar radiation, and thereby they increase the water temperature and the evaporation rate. There is evidence that the microorganisms may directly interact with the brine and influence the formation of the halite (NaCl) crystals during the evaporation process. In recent studies, better quality salt was obtained in the presence of a halophilic consortium [56].

There is a great interest for the biotechnological exploitation of the pigments produced by halophilic microorganisms. Carotenoids are quite appreciated for their benefits on health, due to their ability to quench oxygen radicals [57], while retinal pigments as bacteriorhodopsin are currently finding many applications in the emerging field of bioelectronics [58,59]. Among the carotenoids, β-carotene is nowadays one of the most valuable, being extensively used as a colorant, food additive, and cosmetic. The halophilic microalgae *Dunaliella salina* is considered the richest natural source of β-carotene, and some hyperaccumulative species are of interest for its industrial production [60,61].

5. Features of halophilic archaea

Halophilic archaea or haloarchaea belong to the *Archaea* domain, which constitutes one of the three domains in which all living beings are classified, together with *Bacteria* and *Eukarya*, as proposed by Carl Woese in 1990 [62]. Until then, archaea were located in the domain *Prokaryote*, which included all microorganisms without a defined nucleus. However, new studies carried out at the molecular level showed that, within prokaryotes, archaea showed as many differences with respect to the bacteria group as this one with eukaryotes. Archaea have an architecture similar to that of bacteria, but in many other respects, they differ from them, presenting even greater phylogenetic proximity to eukaryotes [63]. Therefore, due to their independent evolutionary history and their biochemical differences from other life forms, they settled in a separate domain.

5.1. Cellular composition

Haloarchaea exhibit specific characteristics of the domain archaea, including eukaryotic-like deoxyribonucleic acid (DNA) replication, transcription and translation machinery, branched-chain, ether-linked archaeal lipids, and a

cell wall S-layer composed of a glycoprotein, lacking the lipopolysaccharide (LPS) cell walls typical of many bacteria [19]. In addition, most exhibit distinctive features such as gas vesicles, purple membrane, and red-orange carotenoids.

Halophilic archaea are Gram-negative and their size varies between 1 and 15 μm. Regarding their shape, cells show great variability, and even some do not have it well-defined or permanent. They adopt different structures (Figure 6), including rods (*Halobacterium*), cocci (*Halococcus*), discs (*Halarchaeum acidiphilum*), squares (*Haloquadratum walsbyi*), triangles (*Haloarcula japonica*), and even pleomorphic (*Haloferax*), particularly when the growing conditions are unfavorable [64,65]. In addition, many haloarchaea are motile thanks to their flagella, called archaella, which allows them to swim slowly, presumably as a response to nutrient-limited conditions. They also possess genetic components for chemotaxis analogous to those found in bacterial species [66].

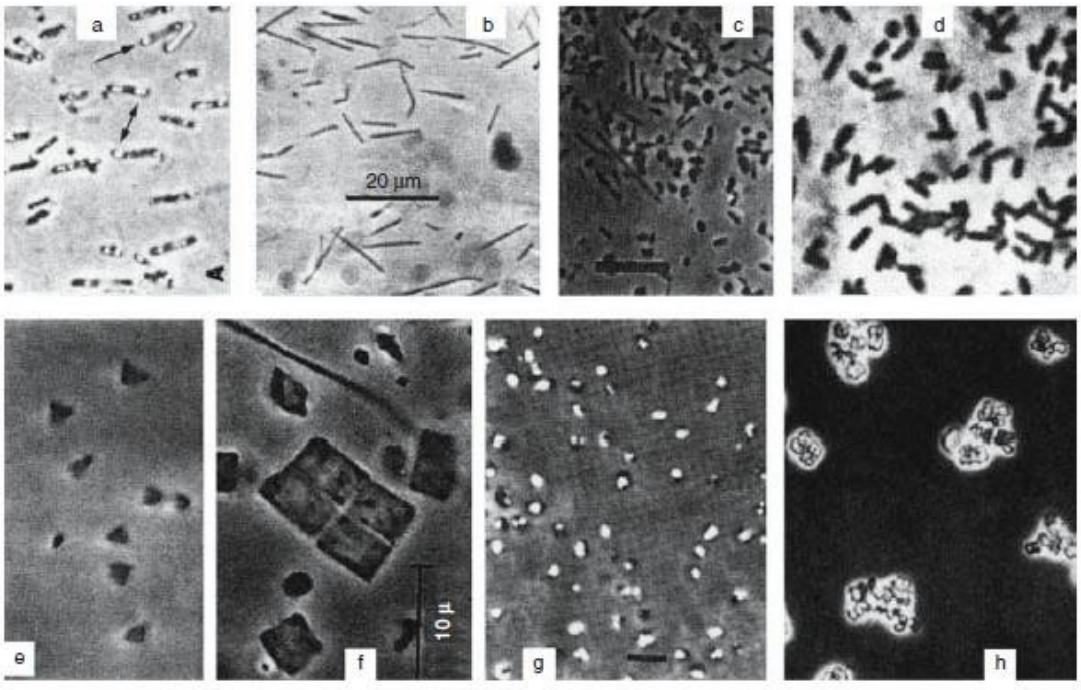

Figure 6. Microscope view of different species of halophilic archaea (adapted from Oren [67]): **a:** *Halobacterium salinarum,* **b:** *Natronobacterium gregoryi*, **c:** *Halorubrum lacusprofundi*, **d:** *Natronomonas pharaonis*, **e:** *Haloarcula japonica*, **f:** *Haloquadratum walsbyi*, **g:** *Halogeometricum borinquense*, **h:** *Natrononococcus occultus*.

Moreover, some haloarchaeal species, as *Haloquadratum Walsby*, produce internal gas vesicles, which are filled by diffusion with gases dissolved in the environment. These gas vesicles are composed of two structural proteins: the hydrophobic GvpA that forms the core of the cylinders and the hydrophilic

GvpC that cross-links the GvpA subunits at the outside and provides strength to the vesicles. Their function is to allow cells to float on the surface of the brines, in response to a need for oxygen or light. Also, some of them produce extracellular polysaccharides (EPS), which are composed of a heteropolysaccharide mainly made of mannose and some sugars, amino acids, uronic acids, and sulfate [64,68].

The cell wall of haloarchaea is devoid of peptidoglycan but, instead, presents a variety of chemical compounds, such as polysaccharides, proteins, and glycoproteins. The absence of peptidoglycan gives them resistance to the antibiotics that inhibit the synthesis of the bacterial cell walls, such as β-lactams [67,69]. In most halophilic archaea, the cell wall is constituted by hexagonal glycoprotein subunits, organized in a single layer called the S-layer, which protects cells against osmotic stress and pH disturbances. However, it is very sensitive to detergents such as sodium dodecyl sulfate (SDS), and urea. Glycoproteins contain high levels of negatively charged acidic amino acids that easily interact with sodium and potassium ions and allow the uptake of water molecules, promoting cell wall hydration and increasing nutrient solubility. This type of wall requires high concentrations of salt to maintain its stability, although some members present several polymers in their cell walls that confer them stability under lower salinities [70,71].

The most distinctive feature of the membranes of halophilic *Archaea* is the nature of their lipids. These lipids are made up of a bilayer of isoprenyl-L-glycerol ethers which form a matrix in which various proteins are embedded. They have branched fatty acid chains linked to glycerol by ether bonds (Figure 7), which are more stable to temperature and oxidation compared to ester bonds present in bacteria [72]. Concretely, membrane lipids are mainly composed of polar lipids which include phospholipids, sulfolipids, and glycolipids, while the other minority lipids are neutral lipids, including C_{20} and C_{30} isoprenoids, glycerol ethers, quinones, and carotenoids. Phosphatidylglycerol phosphate methyl ester (PGP-Me) represents 50 to 80% of the membrane polar lipids, and it plays an important role in the stability of the membrane at high salinities, thanks to its very acidic nature.

The type and composition of polar lipids, in particular that of glycolipids, have been used in the chemotaxonomic differentiation of the genera of *Halobacteria* [67,71,73]. In addition, their cytoplasmic membranes often have retinal proteins (bacteriorhodopsin, halorhodopsin, and sensory rhodopsins) and, with the exception of a few species, all members of the class *Halobacteria*

produce membrane pigments of the C_{50} carotenoid type bacterioruberin, which serve as protection against photo-oxidative damage and as structural reinforcements for the plasma membranes. The production of these pigments depends on the nutritional status of the cell and the salinity of the medium [64,67,74].

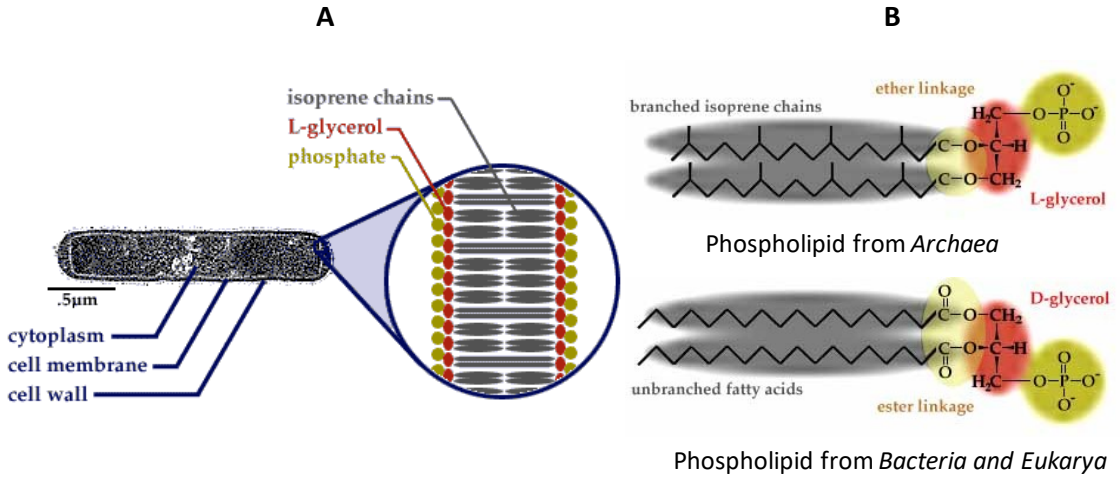

Figure 7. Basic cell structure and phospholipids of *Archaea* are shown (adapted from on-line resources of the University of California, Berkeley, USA). **A:** The three primary regions of archaeal cells are the cytoplasm, cell membrane, and cell wall. Above, these three regions are labelled, with an enlargement at right of the cell membrane structure. **B:** Comparison of cell membrane lipid between *Archaea*, *Bacteria* and *Eukarya*. Archaeal cell membranes are chemically different from all other living things, including L-glycerol molecules and isoprene derivatives in place of fatty acids.

Furthermore, a specific feature within the haloarchaeal group is undoubtedly their acidic proteome. The majority of their proteins have an isoelectric point around 4 and also a low content of hydrophobic amino acids. As has been previously mentioned, these proteins are adapted to work under the presence of high concentrations (3-4 M) of KCl in the cytoplasm, which is used to balance the osmotic pressure with respect to the surrounding hypersaline medium. Thus, high salt is needed to maintain the structure and function of their proteins [22,39]. An additional distinctive characteristic is found in the protein secretory pathway used by the halophilic archaea. In eukaryotes, bacteria, and non-halophilic archaea, the general secretory (Sec) pathway is used by most secreted proteins to pass across the cytoplasmic membrane in an unfolded state. By contrast, *in silico* predictions and some *in vivo* experiments have revealed that the vast majority of haloarchaeal-secreted proteins were substrates of the twin-arginine translocation (Tat) pathway for the secretion of folded proteins. This

mechanism would provide an adaptation to extremely high-salt conditions, allowing the proteins to be folded correctly in the controlled cytoplasmic environment where chaperones are present [75].

5.2. Genetic traits

Since the first complete genome sequence of the model organism *Halobacterium* sp. NRC-1 was published in 2000 [76], many other genome sequences of different strains of haloarchaea have become available. Similar to bacteria, the genome of extremely halophilic archaea is usually constituted by a single circular chromosome of 2 to 4 Mbp, with the difference that it is associated with proteins homologous to eukaryotic histones. Many species contain, in addition to this main chromosome, extra genes in large plasmids (megaplasmids), which have been named mini-chromosomes due to the fact that some of them comprise up to 30% of total DNA and contain essential genes for life. The genome of haloarchaea is highly GC-rich, presenting around 70% of CG content in the main chromosome, and close to 60% in the mini-chromosomes.

Another remarkable aspect is that the genomes of haloarchaea encode multiple isoforms of genes that are present as a single copy in other organisms. This might be due to a requirement for regulatory and metabolic flexibility in haloarchaea, but it is also possible that these redundant homologs have accumulated as a result of lateral gene transfer [64,77,78]. It is also noticeable the fact that several haloarchaeal species are polyploid and that polyploidy might even be a general trait of haloarchaea. The possible evolutionary advantages of polyploidy for haloarchaea might be a low mutation rate and high resistance to radiation and desiccation [79].

Haloarchaea possess, like other archaea, a range of eukaryote-like features that make them distinct from bacteria at the molecular level, including eukaryotic homologous polymerases and transcription factors [64]. As in eukaryotes, multiple origins of replication have been observed in haloarchaea, although their number varies depending on the genera [80]. The transcription in *Archaea* appears to possess an intriguing mosaic of eukaryal-like basal transcription machinery and bacterial-like regulatory mechanisms. Archaea, like bacteria, utilize only one type of RNA polymerase (RNAP) to transcribe all genes but its subunit composition and architecture is strikingly similar to eukaryotic RNAP-II. Also, the organization of functionally related genes in multicistronic transcription units (operons) is similar to bacteria [81]. Primary transcripts are

comparable to those of bacteria, with triphosphorylation, without introns or poly (A) tails, and often polycistronic, encoding several polypeptide chains. RNA polymerases are similar to those of eukaryotes, formed of at least 10 subunits, which makes them more complex machinery than that of bacteria, which is formed of 5 subunits [82].

In addition, archaeal transfer RNAs (tRNAs) contain at least 47 different modifications, some of them, including archaeosine or agmatidine, specific to the archaeal domain [83]. However, as in eukaryotes, the initiator tRNA carries methionine instead of N-formylmethionine typical of bacteria [84]. Ribosomes of archaea are similar in size and composition to those of bacteria. They contain three molecules of ribonucleic acid (RNA): 16S, 23S, and 5S rRNA and from 50 to 70 proteins depending on the species. However, the primary structures of rRNA and ribosomal proteins are closer to those of eukaryotes. Ribosomes, as well as aminoacyl-tRNA synthetases, are adapted to function at high salinities and in some species require high KCl concentrations (3-4 M) [85].

In contrast to other extremophilic microorganisms, which require specialized culturing equipment, haloarchaea can be grown in any microbiology laboratory using standard media supplemented with salt. As a result, many methods for genetic have been developed and standardized for some species of *Haloferax* and *Halobacterium*, including a facile transformation system, selectable markers, cloning and expression vectors, reporter genes, and systems for gene replacement and knockouts. In addition, an increasing number of genome sequences are available for different genera of haloarchaea, which are highly tractable model systems for genetic studies [77,86].

Furthermore, *Archaea* comprise a reservoir of new molecular tools as the CRISPR-Cas (CRISPR: Clustered Regularly Interspaced Short Palindromic Repeats and Cas: CRISPR associated), which are unique defense mechanisms, since they are able to adapt to new invaders and are heritable. These systems facilitate the sequence-specific elimination of invading genetic elements in prokaryotes and they are found in 45% of bacteria and 85% of archaea [87]. This function of CRISPR as an immune system was first discovered in haloarchaea by Mojica [88], and since then it has become one of the most powerful tools for genome editing [89].

5.3.Metabolism

The metabolism of the *Archaea* resembles in its complexity those of *Bacteria* and lower *Eukarya*, although they present unique variants of classical pathways such as the Embden-Meyerhof-Parnas (EMP), or the Entner-Doudoroff (ED) pathways. The metabolism of halophilic archaea differs considerably between the distinct members, being aerobic and anaerobic representatives. There are carbohydrate-utilizing species, such as *Haloarcula marismortui*, *Halococcus saccharolyticus*, and *Haloferax mediterranei*, which catabolize hexoses (glucose, fructose), pentoses (arabinose, xylulose), sucrose, lactose, and some other non-carbohydrate-utilizing species that thrive mainly on amino acids.

The members of the family *Halobacteriaceae* use the tricarboxylic acid cycle (TCA) in the process of aerobic degradation of carbon and, if necessary, a combination of the glyoxylate cycle and the respiratory electron transport. Glucose oxidation can be performed by a modified ED pathway, and the resulting pyruvate is further oxidized by pyruvate oxidoreductase and the tricarboxylic acid cycle, while some species can degrade fructose and sucrose by a modified version of the EMP pathway. The central intermediary metabolism in halophilic archaea, inferred from experimental and bioinformatics studies, is represented in Figure 9.

Moreover, many haloarchaea can grow on single carbon sources such as sugars, glycerol, and acetate, while using ammonia as a nitrogen source, and some species can metabolize aliphatic and aromatic hydrocarbons and long-chain fatty acids, as *Haloferax*, *Halobacterium*, and *Halococcus* which can grow on crude oil vapor. In addition, many species of haloarchaea also produce exo-enzymes such as proteases, lipases, DNAses, and amylases to degrade organic polymeric substances extracellularly, making small organic molecules available as carbon and energy source.

Several halophilic archaea are facultative anaerobes that grow by fermentation of different sugars or arginine. Variants of anaerobic growth documented within the *Halobacteriaceae* include the use of alternative electron acceptors such as nitrate, dimethylsulfoxide, trimethylamine N-oxide, or fumarate. A completely different mode of anaerobic growth displayed by some haloarchaea is photoheterotrophy, which consists of the use of light energy absorbed by retinal-based pigments. The light-driven proton pump bacteriorhodopsin can drive anaerobic growth of *Halobacterium salinarum*, in

combination with the use of organic substrates as carbon sources, since photoautotrophy has not been demonstrated in the archaeal domain yet [101–103].

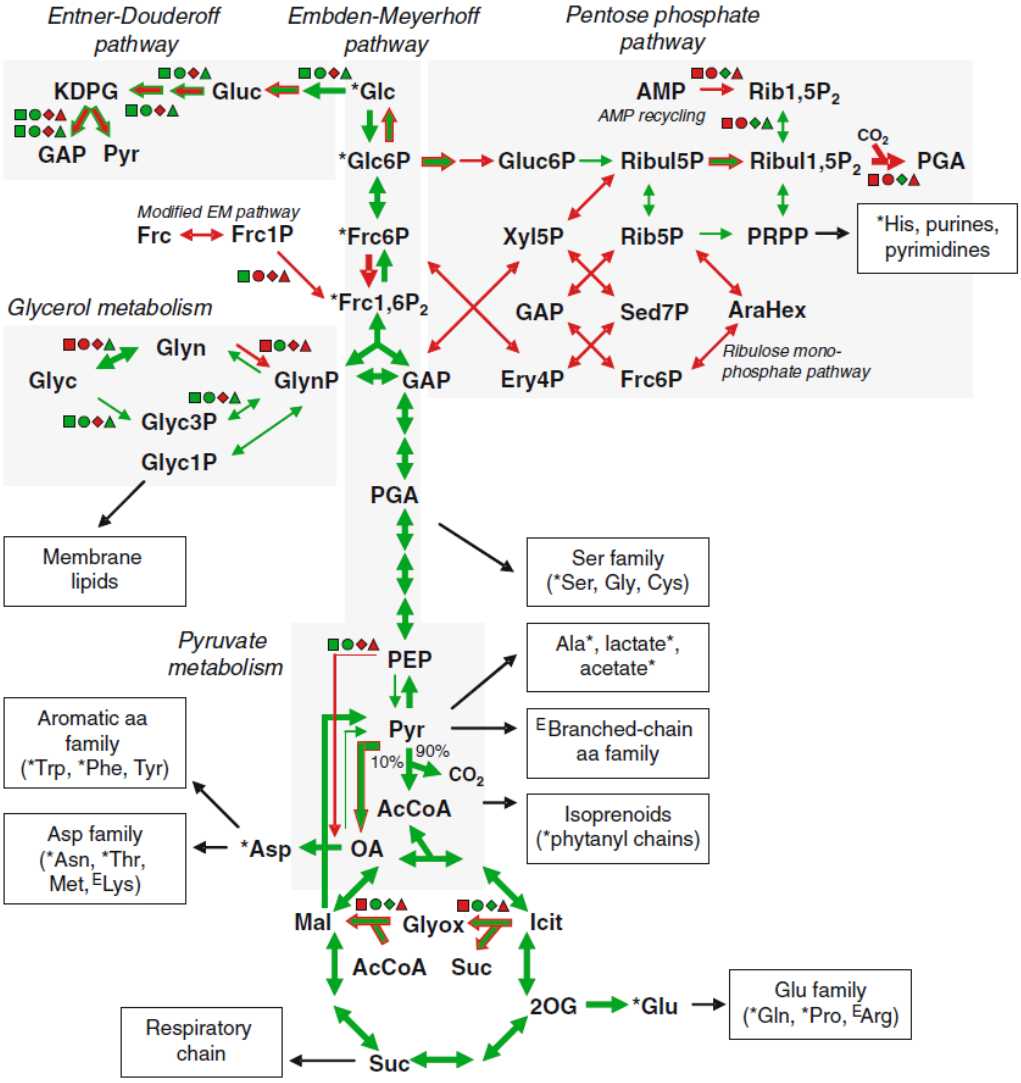

Figure 9. The central intermediary metabolism in halophilic archaea (adapted from Falb *et al*, [101]). The reaction arrows depict the reconstructed metabolism of the reference species *H. salinarum* (green reaction exists, red reaction absent). The four geometric symbols illustrate differences in enzyme gene sets between the four sequenced haloarchaea (square: *H. marismortui*, circle: *H. walsbyi*, diamond: *N. pharaonis*, triangle: *H. salinarum*, green gene exists, red gene absent). Reactions investigated experimentally in *H. salinarum* are highlighted by bold arrows (green reaction exists, red reaction absent). Experimentally verified reactions, without current genetic evidences in the *H. salinarum* genome are denoted with green arrows with a red border, while reactions experimentally excluded but probable enzyme genes in the *H. salinarum* genome are indicated with red arrows with a green border. Compounds that have been identified through labeling studies are marked by asterisks. Proposed essential amino acids for *H. salinarum* are indicated (E).

Compounds: AraHex—D-arabino-3-hexulose-6P, Ery4P—erythrose-4P, Frc—fructose, GAP—glyceraldehyde-3P, Glc—glucose, Gluc—gluconate, Glyn—glycerone, Glyc—glycerol, Glyox—glyoxylate, Icit—isocitrate, KDPG—2-dehydro-3-deoxy-6-phosphogluconate, Mal—malate, OA—oxalacetate, 2-OG—2-oxoglutarate, PEP—phosphoenolpyruvate, PGA—3-phosphoglycerate, Pyr—pyruvate, Rib5P—ribose-5P, Ribul5P—ribulose- 5P, Suc—succinate, Xyl5P—xylulose-5P, Sed7P—sedoheptulose 7-phosphate, AcCoA—acetyl-CoA.

The special metabolic requirements of the diverse halophilic archaea must be taken into account for their isolation and culture in the laboratory. For example, organic-nutrient-rich growth media typically gives rise to the growth of colonies belonging to the genera *Halorubrum*, *Haloferax*, and *Haloarcula*. Besides, high concentrations of yeast extract or other rich sources of nutrients are required for the growth *Halobacterium salinarum*, whereas carbohydrates, amino acids, fats, and proteins do not support the growth of *Halosimplex carlsbadense*, an organism that only grows in a defined medium with acetate and glycerol, acetate and pyruvate, or pyruvate alone [102]. Similarly, pyruvate is the preferred substrate in the cultivation of the flat square *Haloquadratum walsbyi*, which cultivation was not possible until more than 20 years after its discovery [104,105].

Furthermore, many haloarchaea when grown in carbon-excess conditions accumulate polyhydroxyalkanoates (PHAs), produced as carbon and energy storage. Chemically, these compounds consist mostly of poly-β-hydroxybutyrate (PHB) and poly-β-hydroxyvalerate (PHV) or copolymers (poly-β-hydroxybutyrate-co-3-hydroxyvalerate; PHBV). Besides, the production of PHAs has been broadly described in the strain *Haloferax mediterranei*, others haloarchaea, with more or less pronounced PHA production capacity, have been isolated from different saline environments, including diverse genera such as *Haloarcula*, *Halococcus*, *Haloterrigena*, *Haloqudratum*, *Halogeometricum,* and *Natrinema*, among others [106–108].

5.4.Biosynthesis of pigments

Haloarchaea produce large quantities of red-orange carotenoids, as well as diverse rhodopsins. The most abundant pigments are bacterioruberins, and several retinal proteins, including bacteriorhodopsin, halorhodopsin, and sensory rhodopsins. It has been proposed that retinal, the polyene chromophore of bacteriorhodopsin, and bacterioruberin are synthesized from the common precursor, lycopene, and some studies suggest that the accumulation of

bacterioopsin, the bacterioruberin apoprotein, promotes retinal production by inhibiting bacterioruberin biosynthesis [90,91].

The biochemical pathway for the formation of the different carotenoid pigments encountered in halophilic archaea has been recently elucidated by Yang and coworkers [92], who have described the biosynthetic pathway of bacterioruberin from lycopene in *Haloarcula japonica* (Figure 8). Subsequent metagenomic studies on 100 haloarchaeal species have revealed that all the genomes analyzed contain the genes involved in the conversion of lycopene into bacterioruberin previously identified in *Haloarcula japonica* [93].

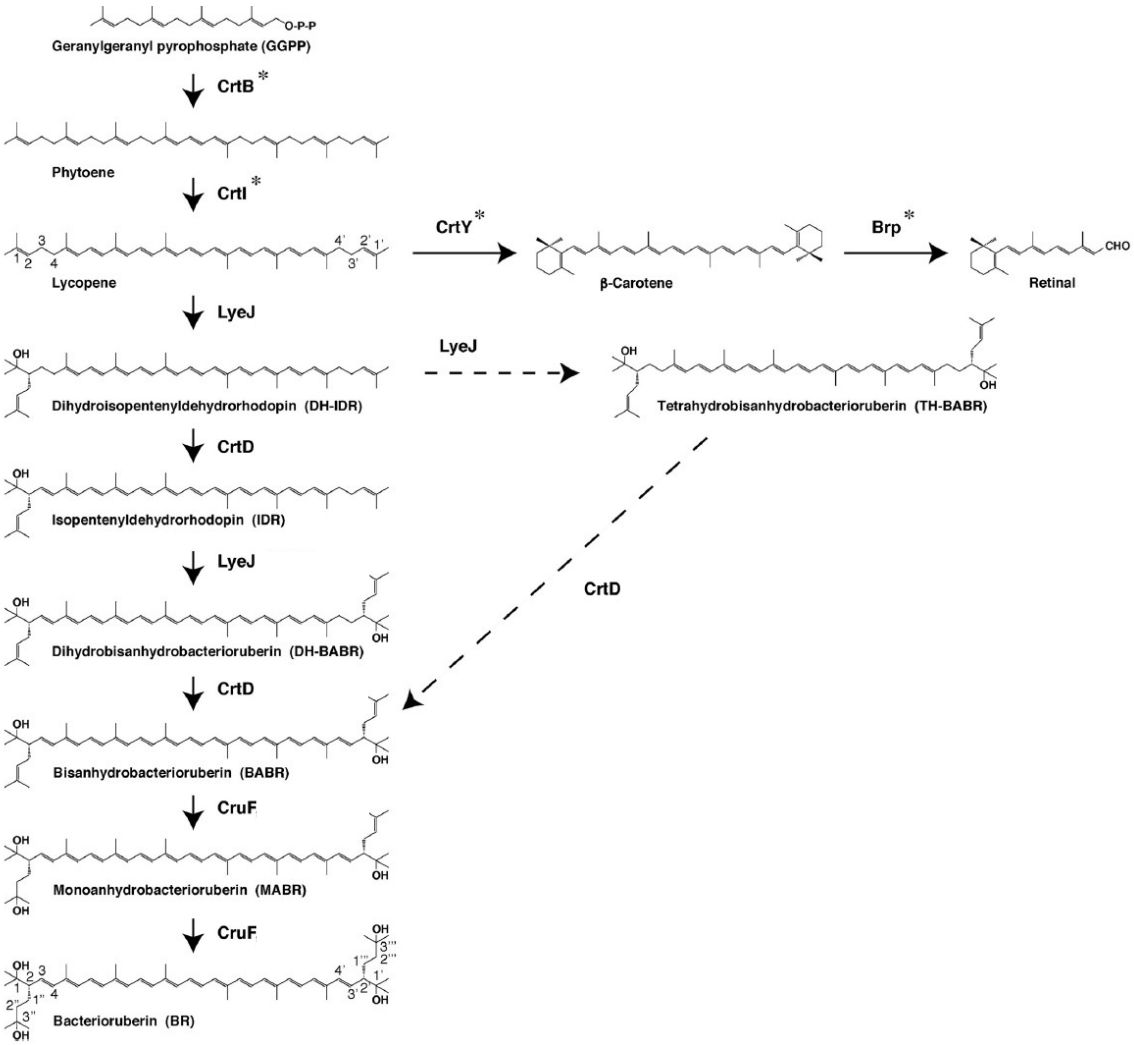

Figure 8. Proposed main steps in the carotenoid and retinal biosynthetic pathways of *Haloarcula japonica* (adapted from Yang, *et al* [92]). Solid arrows signify the main carotenoid biosynthetic steps. The dashed arrows indicate other possible carotenoid biosynthetic steps. Asterisks indicate the unidentified carotenoid biosynthetic enzymes.

Bacterioruberin (BR) is the most abundant carotenoid found in the *Halobacteriaceae* family, but also considerable quantities of its precursors trisanhydrobacterioruberin (TABR), bisanhydroruberin (BABR), and monoanhydrobacterioruberin (MABR), are present in many species [50,94–96]. More than 30 carotenoids, including 7 geometric isomers for bacterioruberin, BABR, and MABR, have been identified in some species [97]. In addition, smaller amounts of biosynthetic intermediates such as β-carotene and lycopene have been also found and even occasionally, ketocarotenoids, as canthaxanthin, have been identified in halophilic archaea [74].

Bacterioruberin has 50 carbon atoms with 13 conjugated carbon double bonds and 4 hydroxyl groups, which gives it an effective antioxidant power. The ability of carotenoids to block free radicals is related to the number of conjugated double bonds and hydroxyl groups that they present. Therefore, chemically bacteriorruberin possess a higher antioxidant potential than the well-known β-carotene, which has only 11 double conjugate bonds, a fact that has been verified experimentally [98]. Bacterioruberin protects archaea against fatal injuries caused by high light intensities, UV radiation, and exposure to oxidant species. Furthermore, given its dipolar nature, bacterioruberin preserves the plasma membrane, modulating its fluidity and permeability to oxygen and other molecules, which favors the survival in hypersaline media [99], or even it could be associated with retinal proteins [100].

Haloarchaea synthesize terpenoid backbones through the mevalonate pathway, which provides the isopentenyl pyrophosphate (IPP), which is subsequently converted to geranylgeranyl pyrophosphate (GGPP) [74]. The colorless carotenoid phytoene is produced by the condensation of two molecules of GGPP by the enzyme phytoene synthase (CrtB). Later, lycopene is generated from phytoene via a series of desaturation reactions that are catalyzed by phytoene desaturase (CrtI). Thereafter, the way is divided into the retinal biosynthetic pathway and the bacterioruberin biosynthetic pathway. In retinal synthesis, the cyclization of lycopene to β-carotene is catalyzed by lycopene β-cyclase (CrtY), and β-carotene is then cleaved to form a retinal (C_{20}) by β-carotene dioxygenase (Brp). Meanwhile, in the bacterioruberin biosynthetic pathway, lycopene is used as a precursor and converted to bacterioruberin by the addition of two C_5 isoprene units and the introduction of two double bonds, and four hydroxyl groups into the lycopene (Figure 8).

The three main bacterioruberin biosynthetic enzymes characterized to generate bacterioruberin from lycopene, are a bifunctional lycopene elongase and 1,2-hydratase (LyeJ), a carotenoid 3,4-desaturase (CrtD), and a C_{50} carotenoid 2″,3″-hydratase (CruF). However, other enzymes involved and the complete pathway for bacterioruberin biosynthesis from lycopene are still unknown [92] (Figure 8).

6.Biotechnological applications of haloarchaea

Halophilic archaea are microorganisms particularly interesting for biotechnology since they have the cellular machinery fully adapted to these harsh conditions and also, produce several compounds in response to their extreme surroundings. Therefore, many biocompounds, such as their enzymes (haloenzymes), lipids, carotenoids, rhodopsins or polyhydroxyalkanoates (PHAs), have been on the focus of many researchers around the world during the last decades. Also, new biotechnological trends utilizing novel and unique molecules found in halophiles are now being studied, including their halocins, exopolysaccharides (EPS) or gas vesicles.

Currently, the majority of the microbial cell factories utilized for the production of high-value compounds on an industrial scale are bacterial, fungal or algae based and, the only commercially available products of archaeal cell factories are those produced by halophiles, including bacterioruberin, bacteriorhodopsin and ether-lipids [109]. A representation of the valuable compounds produced by haloarchaeal cell factories is shown in Figure 10.

The unique trait of haloenzymes to work under hypersaline conditions has extended the range of already available biocatalysts and industrial processes in which high salt concentration inhibits the activity of most enzymes. Besides, enzymes from haloarchaea are usually poly-extremotolerant and can also withstand several harsh conditions such as extreme pH and temperature, low-water availability, as well as, high concentration of organic solvents and/or surfactants [8,25,110].

Special attention has been received the glycoside hydrolases, which are a large group of enzymes related to carbohydrate metabolism that include amylases, pullulanases, dextranases, hyaluronidases, xylosidases, and cellulases. These enzymes and other hydrolases, including proteases, liapases, and esterases are often excreted by haloarchaea into the medium [111].

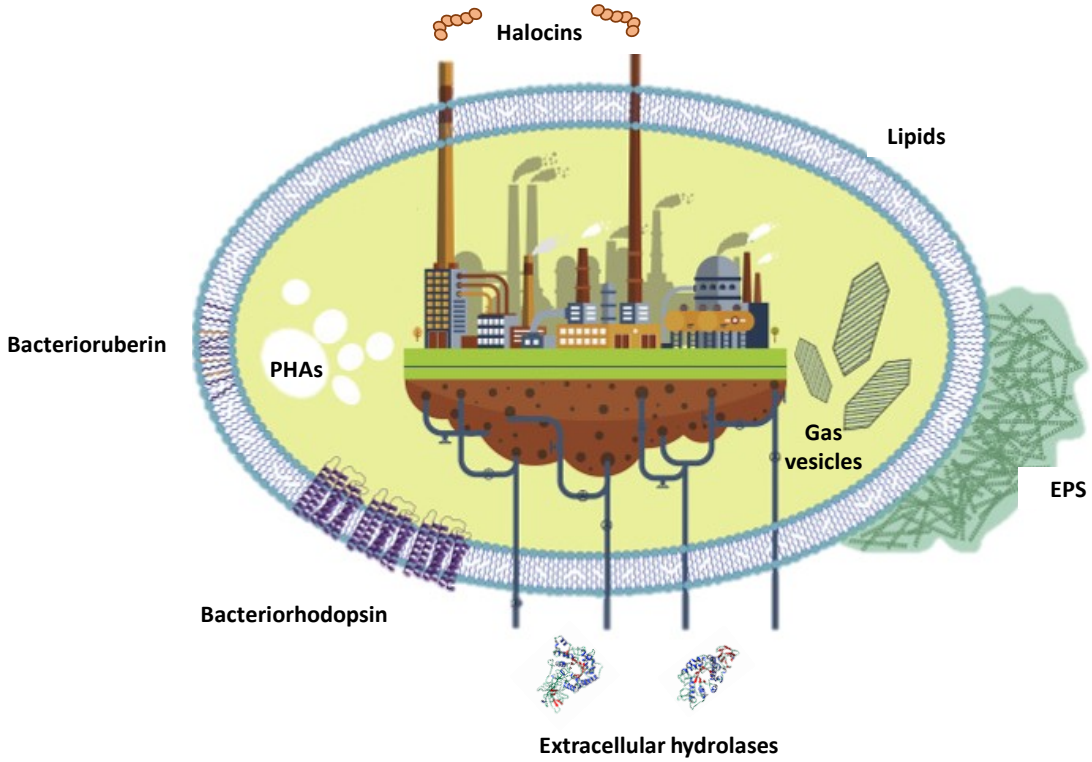

Figure 10. Depiction of haloarchaeal cell factory producing diverse value-added products (modified from Pfeifer *et al* [109]).

Among hydrolases, the α-amylases are currently the most important in industry, with several applications in paper, textile, chemical, pharmaceutical, detergent, and beverage industries [112–114]. Also, halophilic cellulolytic enzymes have been used for the transformation of biopolymers into useful products such as biofuels. Other significant hydrolases are proteases, with wide applications in detergent, beer, food, leather tanning, and pharmaceutical industries [115,116]. Besides, lipases from haloarchaea are useful in the production of fatty acids, in baking, in detergents, as biocatalysts in processing diesel, and for the conversion of vegetable oil into fuel [117,118]. Cloning and expressing haloenzymes in non-halophilic hosts such as *E. coli* is often very difficult due to the fact that many proteins may misfold in absence of a high salt concentration. Thus, it is essential to develop efficient systems to produce halophilic proteins in halophiles [25].

Carotenoids are commonly used as colorants and vitamins in food products. These carotenoids are normally produced by chemical synthesis, however, increasing awareness against synthetic additives has led to the search

for natural sources of carotenoids, which also present a series of additional benefits for health due to their anticancer, antimutagenic, and antioxidant properties [57,99]. Halophilic archaea are an interesting source of carotenoid production that has not yet been deeply exploited due to the difficulties of their isolation, in addition to the lack of information about the composition of their carotenoids and the conditions for carotenoid accumulation [119]. There are several reports supporting the high antioxidant power, of bacterioruberin, and its use in biomedicine and as promoters of human health are ongoing [93,120].

The retinal pump bacteriorhodopsin has a wide range of potential applications that include protein films, artificial retinal implants, light modulators, three-dimensional optical memories, color photochromic sensors, photochromic and electrochromic papers and ink, biological camouflage, and photodetectors for biodefense and non-defense purposes [121]. Several patents and inventions have exploited the capability of bacteriorhodopsin to convert light energy to chemical energy or electricity, or for the development of image sensing systems such as robotic vehicle navigation, surveillance work, and biosensing [122]. In addition, due to the fact that bacteriorhodopsin is identical to the rhodopsin found in the retina, it possesses immense applications in the medical field, as it has been proved for the treatment of blind people suffering from photoreceptor disorders [123].

The unique composition of archaeal lipids makes them more resistant to stress than phospholipids from other organisms, being highly interesting for liposome-based applications in drug delivery, adjuvant additives and antigen presenting scaffolds for vaccines. In this sense, archaeosomes from halophiles are particularly engaging due to their great biocompatibility [109]. Moreover, gas vesicle buoyancy organelles, which are stable, non-toxic, and genetically engineerable, have been used for the display of antigenic proteins for vaccines and delivery of therapeutic proteins [19]. Also, their exopolysaccharides can be used in the food industry as gelling agents, stabilizers and thickeners, as well as in the pharmaceutical and cosmetic industries [124].

Furthermore, halophiles produce a wide range of secondary metabolites to survive in extreme environments. In this respect, haloarchaea comprise a powerful repository of many bioactive compounds with antimicrobial and anticancer agents. Concretely, in the constant search for new antibiotics, is worth highlighting the properties of halocins. These molecules are peptides that inhibit

the growth of closely related haloarchaea by affecting the bioenergetic steady-state across the membrane, thus their use as antibiotics is promising [125–127].

Haloarchaea have also been explored for their potential to produce bioplastics such as polyhydroxyalkanoates (PHAs), which provide an eco-friendly alternative to conventional plastics. Due to their excellent biocompatibility and biodegradability, PHAs can be applied in the packaging industry for the production of bottles and containers, in biomedicine, as osteosynthetic materials, and in pharmacy for the controlled release of medicines [128]. The production of PHAs in haloarchaea presents some key factors for reducing costs, as for example the fact that the high salt concentration in the culturing media diminishes the need for sterilization. Also, since cells lysis at lower salt concentrations and plastics are released to the medium, the downstream processing is cost-effective. As a last resort, PHAs can be produced from inexpensive industrial wastes and carbon sources reducing, even more, the costs [129,130].

Halophiles are becoming increasingly valuable for bioremediation since many industrial processes release contaminated brine effluent into the environment. Selected species are being targeted for their use in the biodegradation of contaminants, including polychlorinated biphenyls (PCBs), herbicides, hydrocarbons, aromatic compounds, and phenols [131,132]. Additionally, some are being used to trait high-salt wastewaters polluted with nitrates and nitrites [133,134].

Halophilic archaea are a leading group of microorganisms in the newly developing field of astrobiology and may be key to the search for life elsewhere in the universe. Recent discoveries have suggested the presence of freezing and thawing brine on Mars, therefore, any liquid water that is present or may have been present on the planet is expected to be hypersaline [64].

Among halophiles, halophilic archaea of the family *Halobacteriaceae* are the best adapted to life at extremes of salinity on Earth. In addition, many species resist freezing temperatures, low-water availability, and high UV or ionizing radiation. They have shown to be highly tolerant to perchlorate, which is present in Martian soils, and even some species are able to use this compound as an electron acceptor to support anaerobic growth [135]. Also, many species can use light as an energy source through bacteriorhodopsin. Finally, the presence of bacterioruberin, their typical carotenoids, makes haloarchaea easy to identify by

Raman spectroscopy, which part of the instrumentation to explore life in Mars during ExoMars missions [135,136].

7. Solar salterns in the river Odiel marshlands

Odiel salterns, like other coastal solar salt flats, are employed primarily for the production of edible and industrial sodium chloride. In these saltworks a series of pans are distributed with the aim of concentrating seawater to facilitate the sequential precipitation of calcite ($CaCO_3$), gypsum ($CaSO_4$) followed by halite (NaCl), leaving behind salts of magnesium and potassium [137]. These ecosystems make an excellent model for studying the diversity patterns due to the maintenance of constant salinity in each pond with minimal disturbances.

Several studies have described microbial populations, mainly centered on prokaryotic communities, that inhabit saltern ponds worldwide, from the Mediterranean coasts of Spain [138] and Tunisia [139] to places as distant as Mexico [140] and India [141]. In this context, the microbial population of the brines from Odiel salterns has been scarcely studied until now. Thus, this environment supposes newer ecological niches for the exploration of the diversity of halophilic microorganisms and the discovery of unique bioactive compounds.

Odiel saltworks are located in an area of extraordinary natural value, on the shores of the Atlantic Ocean (Figure 11A), in the heart of the Odiel Marshlands Natural Park (Figure 11B), in the city of Huelva (SW, Spain). Salt flats are spread over an area of 1,300 hectares, with a total of 12 crystallizing basins where the seawater rests until it reaches the optimum level of salt concentration (Figure 11A).

The entry of seawater is carried out in a natural way, using the tides with the highest coefficient, while crystallization of salt occurs thanks to the natural evaporation process of seawater by the action of the sun and the wind. The salt harvest is carried out for two months, in which up to 6000 tons of salt are removed per day. Later, the salt is washed and accumulated in a spectacular mountain of salt that is a typical element of these marshlands (Figure 11C). All this process occurs in perfect coexistence with the species that inhabit here and, proof it is the declaration of this space as a Biosphere Reserve by UNESCO.

Figure 11. **Distinct views of solar salterns in river Odiel marshlands. A**: Satellite view of salterns ponds. Note the red and white colors of the crystallization pools due to the precipitation of salt (white) and the proliferation of halophilic microorganisms (red). **B**: Picture of Odiel marshlands Natural Park. **C**: The monumental mountain of salt view from the city of Huelva.

Odiel marshlands and salterns harbor a wide diversity of animals (Figure 12), including migratory birds as the spectacularly colorful flamingos. This bird is born white and obtains its typical red hues from the pigments acquired in its diet, through carotenoid-rich microbial sources present in these habitats. Besides, they are also able of metabolizing those pigments into others [142]. Concretely, the major carotenoid present in the blood and feathers of seaside birds as flamingos is canthaxanthin, but also astaxanthin and a rare β-carotene derivative (4-keto-α-carotene) have been found in distinct species [143].

The ingested microorganisms by flamingos may include the microalga *Dunaliella*, which accumulates β-carotene, the small shrimps *Artemia*, that can produce canthaxanthin from β-carotene [144], or even haloarchaea (*Halobacteriaceae*), which synthetizes bacterioruberin and have been recently proposed as contributors to the characteristic pink-red color of flamingos' feathers [145]. In addition, the presence of bacterioruberin has been detected in *Artemia* when fed with haloarchaeal species [146], indicating that it could pass to the food chain.

Figure 12. **Biodiversity in Odiel marshes and salt flats. A**: Small shrimps *Artemia*. **B**: Marine fiddler crab (family Ocypodidae) **C**: European flamingos (*Phoenicopterus roseus*). **D:** Other typical species of birds found in this environment, including herons (family *Ardeidae*) and sandpipers (genus *Calidris*).

References

1. Horikoshi, K.; Bull, A.T. Prologue: Definition, Categories, Distribution, Origin and Evolution, Pioneering Studies, and Emerging Fields of Extremophiles BT - Extremophiles Handbook. In; Horikoshi, K., Ed.; Springer Japan: Tokyo, 2011; pp. 3–15 ISBN 978-4-431-53898-1.
2. Rampelotto, P.H. Extremophiles and extreme environments. *Life* **2013**, *3*, 482–485, doi:10.3390/life3030482.
3. Satyanarayana, T.; Raghukumar, C.; Shivaji, S. Extremophilic microbes: Diversity and perspectives. *Curr. Sci.* **2005**, *89*, 78–90.
4. Rothschild, L.J.; Mancinelli, R.L. Life in extreme environments. *Nature* **2001**, *409*, 1092–1101.
5. Gupta, G.N.; Srivastava, S.; Khare, S.K.; Prakash, V. Extremophiles: An Overview of Microorganism from Extreme Environment. *Int. J. Agric. Environ. Biotechnol.* **2014**, *7*, 371, doi:10.5958/2230-732x.2014.00258.7.
6. Arora, N.K.; Panosyan, H. Extremophiles: applications and roles in environmental sustainability. *Environ. Sustain.* **2019**, *2*, 217–218, doi:10.1007/s42398-019-00082-0.

7. Dalmaso, G.Z.L.; Ferreira, D.; Vermelho, A.B. Marine extremophiles a source of hydrolases for biotechnological applications. *Mar. Drugs* **2015**, *13*, 1925–1965, doi:10.3390/md13041925.

8. Dumorné, K.; Córdova, D.C.; Astorga-Eló, M.; Renganathan, P. Extremozymes: A potential source for industrial applications. *J. Microbiol. Biotechnol.* **2017**, *27*, 649–659, doi:10.4014/jmb.1611.11006.

9. Lentzen, G.; Schwarz, T. Extremolytes: Natural compounds from extremophiles for versatile applications. *Appl. Microbiol. Biotechnol.* **2006**, *72*, 623–634, doi:10.1007/s00253-006-0553-9.

10. García-lópez, E.; Alcázar, A. Color-producing extremophiles. **2015**.

11. Babu, P.; Chandel, A.K.; Singh, O. V. *Extremophiles and Their Applications in Medical Processes*; 2015; ISBN 978-3-319-12807-8.

12. Raddadi, N.; Cherif, A.; Daffonchio, D.; Neifar, M.; Fava, F. Biotechnological applications of extremophiles, extremozymes and extremolytes. *Appl. Microbiol. Biotechnol.* **2015**, *99*, 7907–7913, doi:10.1007/s00253-015-6874-9.

13. Zhu, D.; Adebisi, W.A.; Ahmad, F.; Sethupathy, S.; Danso, B.; Sun, J. Recent Development of Extremophilic Bacteria and Their Application in Biorefinery. *Front. Bioeng. Biotechnol.* **2020**, *8*, 1–18, doi:10.3389/fbioe.2020.00483.

14. Zaremba-Niedzwiedzka, K.; Caceres, E.F.; Saw, J.H.; Backstrom, D.; Juzokaite, L.; Vancaester, E.; Seitz, K.W.; Anantharaman, K.; Starnawski, P.; Kjeldsen, K.U.; et al. Asgard archaea illuminate the origin of eukaryotic cellular complexity. *Nature* **2017**, *541*, 353–358, doi:10.1038/nature21031.

15. DasSarma, S.; DasSarma, P.; Laye, V.J.; Schwieterman, E.W. Extremophilic models for astrobiology: haloarchaeal survival strategies and pigments for remote sensing. *Extremophiles* **2020**, *24*, 31–41, doi:10.1007/s00792-019-01126-3.

16. Kushner, D.J. Life in high salt and solute concentrations: halophilic bacteria. *Microb. life Extrem. Environ.* **1978**.

17. Kushner, D.; Kamekura, M. Physiology of halophilic eubacteria. In *Halophilic Bacteria*; Rodriguez-Valera, F., Ed.; CRC Press: Boca Ratón, 1988; pp. 109–138.

18. Oren, A. *The microbiology of red brines*; 1st ed.; Elsevier Inc., 2020; Vol. 113; ISBN 9780128207093.

19. DasSarma, S.; DasSarma, P. Halophiles. In *eLS*; John Wiley & Sons, Ltd: Chichester, UK, 2017; pp. 1–13 ISBN 9780470015902.

20. Bowers, K.J.; Mesbah, N.M.; Wiegel, J. Biodiversity of poly-extremophilic Bacteria: Does combining the extremes of high salt, alkaline pH and elevated temperature approach a physico-chemical boundary for life? *Saline Systems* **2009**, *5*, 1–8, doi:10.1186/1746-1448-5-9.

21. de la Haba, R.R.; Sánchez-Porro, C.; Marquez, M.C.; Ventosa, A. Taxonomy of Halophiles. In *Extremophiles Handbook*; Horikoshi, K., Ed.; Springer Japan: Tokyo, 2011; pp. 255–308 ISBN 978-4-431-53898-1.

22. Ventosa, A.; Joaquiˊ, J.; Nieto, J.J.; Oren, A. *Biology of Moderately Halophilic Aerobic*

Bacteria; 1998; Vol. 62;.

23. Oren, A. The dying Dead Sea: The microbiology of an increasingly extreme environment. *Lakes Reserv. Res. Manag.* **2010**, *15*, 215–222, doi:10.1111/j.1440-1770.2010.00435.x.

24. Oren, A. Ecology of Halophiles BT - Extremophiles Handbook. In; Horikoshi, K., Ed.; Springer Japan: Tokyo, 2011; pp. 343–361 ISBN 978-4-431-53898-1.

25. Ghosh, S.; Kumar, S.; Khare, S.K. Microbial Diversity of Saline Habitats: An Overview of Biotechnological Applications. **2019**, 65–92, doi:10.1007/978-3-030-18975-4_4.

26. Pierce GJ The behavior of certain microorganisms in brine. *Carnegie Inst Washingt. Pub* **1914**, 49 – 69.

27. Ventosa, A.; de la Haba, R.R.; Sanchez-Porro, C.; Papke, R.T. Microbial diversity of hypersaline environments: a metagenomic approach. *Curr. Opin. Microbiol.* **2015**, *25*, 80–87, doi:10.1016/j.mib.2015.05.002.

28. Vera-Gargallo, B.; Ventosa, A. Metagenomic insights into the phylogenetic and metabolic diversity of the prokaryotic community dwelling in hypersaline soils from the odiel saltmarshes (SW Spain). *Genes (Basel).* **2018**, *9*, doi:10.3390/genes9030152.

29. Ma, Y.; Galinski, E.A.; Grant, W.D.; Oren, A.; Ventosa, A. Halophiles 2010: Life in saline environments. *Appl. Environ. Microbiol.* 2010, *76*, 6971–6981.

30. Ciccarelli, F.D.; Doerks, T.; von Mering, C.; Creevey, C.J.; Snel, B.; Bork, P. Toward Automatic Reconstruction of a Highly Resolved Tree of Life. *Science (80-.).* **2006**, *311*, 1283–1287, doi:10.1126/science.1123061.

31. Edbeib, M.F.; Wahab, R.A.; Huyop, F. Halophiles: biology, adaptation, and their role in decontamination of hypersaline environments. *World J. Microbiol. Biotechnol.* **2016**, *32*, 1–23, doi:10.1007/s11274-016-2081-9.

32. Oren, A. Microbial life at high salt concentrations: Phylogenetic and metabolic diversity. *Saline Systems* **2008**, *4*, 1–13, doi:10.1186/1746-1448-4-2.

33. Antón, J.; Oren, A.; Benlloch, S.; Rodríguez-Valera, F.; Amann, R.; Rosselló-Mora, R. Salinibacter ruber gen. nov., sp. nov., a novel, extremely halophilic member of the Bacteria from saltern crystallizer ponds. *Int. J. Syst. Evol. Microbiol.* **2002**, *52*, 485–491, doi:10.1099/00207713-52-2-485.

34. Oren, A. Diversity of Halophiles BT - Extremophiles Handbook. In; Horikoshi, K., Ed.; Springer Japan: Tokyo, 2011; pp. 309–325 ISBN 978-4-431-53898-1.

35. Narasingarao, P.; Podell, S.; Ugalde, J.A.; Brochier-Armanet, C.; Emerson, J.B.; Brocks, J.J.; Heidelberg, K.B.; Banfield, J.F.; Allen, E.E. De novo metagenomic assembly reveals abundant novel major lineage of Archaea in hypersaline microbial communities. *ISME J.* **2012**, *6*, 81–93, doi:10.1038/ismej.2011.78.

36. Aouad, M.; Taib, N.; Oudart, A.; Lecocq, M.; Gouy, M.; Brochier-Armanet, C. Extreme halophilic archaea derive from two distinct methanogen Class II lineages. *Mol. Phylogenet. Evol.* **2018**, *127*, 46–54, doi:10.1016/j.ympev.2018.04.011.

37. Atanasova, N.S.; Oksanen, H.M.; Bamford, D.H. Haloviruses of archaea, bacteria, and eukaryotes. *Curr. Opin. Microbiol.* **2015**, *25*, 40–48, doi:10.1016/j.mib.2015.04.001.

38. Wais, A.C.; Daniels, L.L. Populations of bacteriophage infecting Halobacterium in a transient brine pool. *FEMS Microbiol. Ecol.* **1985**, *1*, 323–326.

39. Oren, A. Life at high salt concentrations, intracellular KCl concentrations, and acidic proteomes. *Front. Microbiol.* **2013**, *4*, doi:10.3389/fmicb.2013.00315.

40. Oren, A. Salinibacter: An extremely halophilic bacterium with archaeal properties. *FEMS Microbiol. Lett.* **2013**, *342*, 1–9, doi:10.1111/1574-6968.12094.

41. Oren, A. Life at High Salt Concentrations BT - The Prokaryotes: Prokaryotic Communities and Ecophysiology. In; Rosenberg, E., DeLong, E.F., Lory, S., Stackebrandt, E., Thompson, F., Eds.; Springer Berlin Heidelberg: Berlin, Heidelberg, 2013; pp. 421–440 ISBN 978-3-642-30123-0.

42. Gunde-Cimerman, N.; Plemenitaš, A.; Oren, A. Strategies of adaptation of microorganisms of the three domains of life to high salt concentrations. *FEMS Microbiol. Rev.* **2018**, *42*, 353–375, doi:10.1093/femsre/fuy009.

43. Kirsch, F.; Klähn, S.; Hagemann, M. Salt-Regulated Accumulation of the Compatible Solutes Sucrose and Glucosylglycerol in Cyanobacteria and Its Biotechnological Potential. *Front. Microbiol.* **2019**, *10*, doi:10.3389/fmicb.2019.02139.

44. Harding, T.; Brown, M.W.; Simpson, A.G.B.; Roger, A.J. Osmoadaptative strategy and its molecular signature in obligately halophilic heterotrophic protists. *Genome Biol. Evol.* **2016**, *8*, 2241–2258, doi:10.1093/gbe/evw152.

45. Elevi Bardavid, R.; Khristo, P.; Oren, A. Interrelationships between Dunaliella and halophilic prokaryotes in saltern crystallizer ponds. *Extremophiles* 2008, *12*, 5–14.

46. Borowitzka, L.J. The microflora. In *Salt lakes*; Springer, 1981; pp. 33–46.

47. Oren, A. Pyruvate: A key Nutrient in Hypersaline Environments? *Microorganisms* **2015**, *3*, 407–416, doi:10.3390/microorganisms3030407.

48. Oren, A. Probing saltern brines with an oxygen electrode: What can we learn about the community metabolism in hypersaline systems? *Life* **2016**, *6*, 1–11, doi:10.3390/life6020023.

49. Boichenko, V.A.; Wang, J.M.; Antón, J.; Lanyi, J.K.; Balashov, S.P. Functions of carotenoids in xanthorhodopsin and archaerhodopsin, from action spectra of photoinhibition of cell respiration. *Biochim. Biophys. Acta - Bioenerg.* **2006**, *1757*, 1649–1656, doi:10.1016/j.bbabio.2006.08.012.

50. Jehlička, J.; Edwards, H.G.M.; Oren, A. Bacterioruberin and salinixanthin carotenoids of extremely halophilic Archaea and Bacteria: A Raman spectroscopic study. *Spectrochim. Acta - Part A Mol. Biomol. Spectrosc.* **2013**, *106*, 99–103, doi:10.1016/j.saa.2012.12.081.

51. Oesterhelt, D.; Stoeckenius, W. Rhodopsin-like protein from the purple

membrane of Halobacterium halobium. *Nat. new Biol.* **1971**, *233*, 149–152.

52. Oesterhelt, D.; Stoeckenius, W. Functions of a new photoreceptor membrane. *Proc. Natl. Acad. Sci.* **1973**, *70*, 2853–2857.

53. Kandori, H. Retinal proteins: Photochemistry and optogenetics. *Bull. Chem. Soc. Jpn.* **2020**, *93*, 76–85, doi:10.1246/bcsj.20190292.

54. Oren, A.; Rodríguez-Valera, F. The contribution of halophilic Bacteria to the red coloration of saltern crystallizer ponds11Non-standard abbreviations: The names of genera of the family Halobacteriaceae were abbreviated using three-letter abbreviations as recommended in Int. J. Syst. E. *FEMS Microbiol. Ecol.* **2001**, *36*, 123–130, doi:https://doi.org/10.1016/S0168-6496(01)00124-6.

55. Oren, A. Microbial diversity and microbial abundance in salt-saturated brines: why are the waters of hypersaline lakes red? *Nat. Resour. Environ. Issues* **2009**, *15*, 49.

56. Chasanah, E.; Pratitis, A.; Ambarwati, D.; Fithriani, D.; Susilowati, R. Application of halophilic bacteria in traditional solar salt pond: a preliminary study. In Proceedings of the IOP Conference Series: Earth and Environmental Science; IOP Publishing, 2020; Vol. 404, p. 12035.

57. Rao, A. V.; Rao, L.G. Carotenoids and human health. *Pharmacol. Res.* 2007, *55*, 207–216.

58. Wagner, N.L.; Greco, J.A.; Ranaghan, M.J.; Birge, R.R. Directed evolution of bacteriorhodopsin for applications in bioelectronics. *J. R. Soc. Interface* **2013**, *10*, 20130197.

59. Li, Y.T.; Tian, Y.; Tian, H.; Tu, T.; Gou, G.Y.; Wang, Q.; Qiao, Y.C.; Yang, Y.; Ren, T.L. A review on bacteriorhodopsin-based bioelectronic devices. *Sensors (Switzerland)* **2018**, *18*, 1–21, doi:10.3390/s18051368.

60. Ben-Amotz, A.; Shaish, A.; Avron, M. The biotechnology of cultivating Dunaliella for production of β-carotene rich algae. *Bioresour. Technol.* **1991**, *38*, 233–235, doi:https://doi.org/10.1016/0960-8524(91)90160-L.

61. Borowitzka, M.A.; Siva, C.J. The taxonomy of the genus Dunaliella (Chlorophyta, Dunaliellales) with emphasis on the marine and halophilic species. *J. Appl. Phycol.* **2007**, *19*, 567–590, doi:10.1007/s10811-007-9171-x.

62. Woese, C.R.; Kandler, O.; Wheelis, M.L. Towards a natural system of organisms: proposal for the domains Archaea, Bacteria, and Eucarya. *Proc. Natl. Acad. Sci.* **1990**, *87*, 4576–4579.

63. Robertson, C.E.; Harris, J.K.; Spear, J.R.; Pace, N.R. Phylogenetic diversity and ecology of environmental Archaea. *Curr. Opin. Microbiol.* **2005**, *8*, 638–642.

64. Fendrihan, S.; Legat, A.; Pfaffenhuemer, M.; Gruber, C.; Weidler, G.; Gerbl, F.; Stan-Lotter, H. Extremely halophilic archaea and the issue of long-term microbial survival. In *Life in Extreme Environments*; Springer Netherlands: Dordrecht, 2007; Vol. 9781402062, pp. 125–140 ISBN 9781402062858.

65. Amoozegar, M.A.; Siroosi, M.; Atashgahi, S.; Smidt, H.; Ventosa, A. Systematics

of haloarchaea and biotechnological potential of their hydrolytic enzymes. *Microbiol. (United Kingdom)* **2017**, *163*, 623–645, doi:10.1099/mic.0.000463.

66. Thornton, K.L.; Butler, J.K.; Davis, S.J.; Baxter, B.K.; Wilson, L.G. Haloarchaea swim slowly for optimal chemotactic efficiency in low nutrient environments. *Nat. Commun.* **2020**, *11*, doi:10.1038/s41467-020-18253-7.

67. Oren, A. Adaptation of Halophilic Archaea to Life at High Salt Concentrations. In *Salinity: Environment - Plants - Molecules*; 2006.

68. Oren, A. Industrial and environmental applications of halophilic microorganisms. *Environ. Technol.* **2010**, *31*, 825–834, doi:10.1080/09593330903370026.

69. Kandler, O.; König, H. Cell wall polymers in Archaea (Archaebacteria). *Cell. Mol. Life Sci. C.* **1998**, *54*, 305–308.

70. Klingl, A. S-layer and cytoplasmic membrane–exceptions from the typical archaeal cell wall with a focus on double membranes. *Front. Microbiol.* **2014**, *5*, 624.

71. Oren, A. Taxonomy of halophilic Archaea: current status and future challenges. *Extremophiles* **2014**, *18*, 825–834, doi:10.1007/s00792-014-0654-9.

72. Kate, M. Membrane lipids of archaea. In *New comprehensive biochemistry*; Elsevier, 1993; Vol. 26, pp. 261–295 ISBN 0167-7306.

73. Tenchov, B.; Vescio, E.M.; Sprott, G.D.; Zeidel, M.L.; Mathai, J.C. Salt tolerance of archaeal extremely halophilic lipid membranes. *J. Biol. Chem.* **2006**, *281*, 10016–10023.

74. Calegari-Santos, R.; Diogo, R.A.; Fontana, J.D.; Bonfim, T.M.B. Carotenoid Production by Halophilic Archaea Under Different Culture Conditions. *Curr. Microbiol.* **2016**, *72*, 641–651, doi:10.1007/s00284-015-0974-8.

75. Feng, J.; Wang, J.; Zhang, Y.; Du, X.; Xu, Z.; Wu, Y.; Tang, W.; Li, M.; Tang, B.; Tang, X.F. Proteomic analysis of the secretome of haloarchaeon Natrinema sp. J7-2. *J. Proteome Res.* **2014**, *13*, 1248–1258, doi:10.1021/pr400728x.

76. Ng, W.V.; Kennedy, S.P.; Mahairas, G.G.; Berquist, B.; Pan, M.; Shukla, H.D.; Lasky, S.R.; Baliga, N.S.; Thorsson, V.; Sbrogna, J. Genome sequence of Halobacterium species NRC-1. *Proc. Natl. Acad. Sci.* **2000**, *97*, 12176–12181.

77. Berquist, B.R.; Müller, J.A.; DasSarma, S. 27 Genetic Systems for Halophilic Archaea. *Methods Microbiol.* **2006**, *35*, 649–680, doi:10.1016/S0580-9517(08)70030-8.

78. Leigh, J.A.; Albers, S.V.; Atomi, H.; Allers, T. Model organisms for genetics in the domain Archaea: Methanogens, halophiles, Thermococcales and Sulfolobales. *FEMS Microbiol. Rev.* **2011**, *35*, 577–608, doi:10.1111/j.1574-6976.2011.00265.x.

79. Zerulla, K.; Soppa, J. Polyploidy in haloarchaea: Advantages for growth and survival. *Front. Microbiol.* **2014**, *5*, 1–8, doi:10.3389/fmicb.2014.00274.

80. Lestini, R.; Delpech, F.; Myllykallio, H. DNA replication restart and cellular dynamics of Hef helicase/nuclease protein in Haloferax volcanii. *Biochimie* **2015**,

118, 254–263, doi:10.1016/j.biochi.2015.07.022.

81. Werner, F. Structure and function of archaeal RNA polymerases. *Mol. Microbiol.* **2007**, *65*, 1395–1404, doi:10.1111/j.1365-2958.2007.05876.x.

82. Bell, S.D.; Jackson, S.P. Mechanism and regulation of transcription in archaea. *Curr. Opin. Microbiol.* **2001**, *4*, 208–213, doi:10.1016/S1369-5274(00)00190-9.

83. Phillips, G.; de Crécy-Lagard, V. Biosynthesis and function of tRNA modifications in Archaea. *Curr. Opin. Microbiol.* **2011**, *14*, 335–341.

84. Yatime, L.; Schmitt, E.; Blanquet, S.; Mechulam, Y. Functional Molecular Mapping of Archaeal Translation Initiation Factor 2. *J. Biol. Chem.* **2004**, *279*, 15984–15993, doi:10.1074/jbc.M311561200.

85. Londei, P. Archaeal Ribosomes. *Encycl. Life Sci.* **2010**, 1–5, doi:10.1002/9780470015902.a0000293.pub2.

86. Atomi, H.; Imanaka, T.; Fukui, T. Overview of the genetic tools in the Archaea. *Front. Microbiol.* **2012**, *3*, 1–13, doi:10.3389/fmicb.2012.00337.

87. Maier, L.-K.; Alkhnbashi, O.S.; Backofen, R.; Marchfelder, A. CRISPR and Salty: CRISPR-Cas systems in Haloarchaea. In *RNA Metabolism and Gene Expression in Archaea*; Springer, 2017; pp. 243–269.

88. Mojica, F.J.M.; Díez-Villaseñor, C.; García-Martínez, J.; Soria, E. Intervening sequences of regularly spaced prokaryotic repeats derive from foreign genetic elements. *J. Mol. Evol.* **2005**, *60*, 174–182, doi:10.1007/s00239-004-0046-3.

89. Ishino, Y.; Krupovic, M.; Forterre, P. History of CRISPR-Cas from Encounter with a Mysterious. *J. Bacteriol.* **2018**, *200*, e00580-17.

90. Dummer, A.M.; Bonsall, J.C.; Cihla, J.B.; Lawry, S.M.; Johnson, G.C.; Peck, R.F. Bacterioopsin-Mediated regulation of bacterioruberin biosynthesis in Halobacterium salinarum. *J. Bacteriol.* **2011**, *193*, 5658–5667, doi:10.1128/JB.05376-11.

91. Peck, R.F.; Pleşa, A.M.; Graham, S.M.; Angelini, D.R.; Shaw, E.L. Opsin-mediated inhibition of bacterioruberin synthesis in halophilic archaea. *J. Bacteriol.* **2017**, *199*, 1–13, doi:10.1128/JB.00303-17.

92. Yang, Y.; Yatsunami, R.; Ando, A.; Miyoko, N.; Fukui, T.; Takaichi, S.; Nakamura, S. Complete biosynthetic pathway of the C50 carotenoid bacterioruberin from lycopene in the extremely halophilic archaeon Haloarcula japonica. *J. Bacteriol.* **2015**, *197*, 1614–1623, doi:10.1128/JB.02523-14.

93. Giani, M.; Garbayo, I.; Vílchez, C.; Martínez-Espinosa, R.M. Haloarchaeal carotenoids: Healthy novel compounds from extreme environments. *Mar. Drugs* **2019**, *17*, 1–13, doi:10.3390/md17090524.

94. Mandelli, F.; Miranda, V.S.; Rodrigues, E.; Mercadante, A.Z. Identification of carotenoids with high antioxidant capacity produced by extremophile microorganisms. *World J. Microbiol. Biotechnol.* **2012**, *28*, 1781–1790, doi:10.1007/s11274-011-0993-y.

95. de la Vega, M.; Sayago, A.; Ariza, J.; Barneto, A.G.; León, R. Characterization of a

bacterioruberin-producing Haloarchaea isolated from the marshlands of the Odiel river in the southwest of Spain. *Biotechnol. Prog.* **2016**, *32*, 592–600, doi:10.1002/btpr.2248.

96. Sahli, K.; Gomri, M.A.; Esclapez, J.; Gómez-Villegas, P.; Ghennai, O.; Bonete, M.; León, R.; Kharroub, K. Journal of Basic Microbiology. *J. Basic Microbiol.* **2020**, doi:10.1002/jobm.202000083.

97. Squillaci, G.; Parrella, R.; Carbone, V.; Minasi, P.; La Cara, F.; Morana, A. Carotenoids from the extreme halophilic archaeon Haloterrigena turkmenica: identification and antioxidant activity. *Extremophiles* **2017**, *21*, 933–945, doi:10.1007/s00792-017-0954-y.

98. Yatsunami, R.; Ando, A.; Yang, Y.; Takaichi, S.; Kohno, M.; Matsumura, Y.; Ikeda, H.; Fukui, T.; Nakasone, K.; Fujita, N.; et al. Identification of carotenoids from the extremely halophilic archaeon Haloarcula japonica. *Front. Microbiol.* **2014**, *5*, doi:10.3389/fmicb.2014.00100.

99. Abbes, M.; Baati, H.; Guermazi, S.; Messina, C.; Santulli, A.; Gharsallah, N.; Ammar, E. *Biological properties of carotenoids extracted from Halobacterium halobium isolated from a Tunisian solar saltern*; 2013;

100. Yoshimura, K.; Kouyama, T. Structural Role of Bacterioruberin in the Trimeric Structure of Archaerhodopsin-2. *J. Mol. Biol.* **2008**, *375*, 1267–1281, doi:10.1016/j.jmb.2007.11.039.

101. Falb, M.; Müller, K.; Königsmaier, L.; Oberwinkler, T.; Horn, P.; Von Gronau, S.; Gonzalez, O.; Pfeiffer, F.; Bornberg-Bauer, E.; Oesterhelt, D. Metabolism of halophilic archaea. *Extremophiles* **2008**, *12*, 177–196, doi:10.1007/s00792-008-0138-x.

102. Andrei, A.Ş.; Banciu, H.L.; Oren, A. Living with salt: Metabolic and phylogenetic diversity of archaea inhabiting saline ecosystems. *FEMS Microbiol. Lett.* **2012**, *330*, 1–9, doi:10.1111/j.1574-6968.2012.02526.x.

103. Bräsen, C.; Esser, D.; Rauch, B.; Siebers, B. Carbohydrate metabolism in archaea: Current insights into unusual enzymes and pathways and their regulation. *JAMA Ophthalmol.* **2014**, *132*, 326–331, doi:10.1128/MMBR.00041-13.

104. Henk, B.; te, P.E.M.; Francisco, R. Isolation and cultivation of Walsby's square archaeon. *Environ. Microbiol.* **2004**, *6*, 1287–1291, doi:10.1111/j.1462-2920.2004.00692.x.

105. Burns, D.G.; Camakaris, H.M.; Janssen, P.H.; Dyall-Smith, M.L. Combined use of cultivation-dependent and cultivation-independent methods indicates that members of most haloarchaeal groups in an Australian crystallizer pond are cultivable. *Appl. Environ. Microbiol.* **2004**, *70*, 5258–5265, doi:10.1128/AEM.70.9.5258-5265.2004.

106. Rodriguez-Valera, F.; Lillo, J.A.G. Halobacteria as producers of polyhydroxyalkanoates. *FEMS Microbiol. Lett.* **1992**, *103*, 181–186, doi:10.1016/0378-1097(92)90308-B.

107. Legat, A.; Gruber, C.; Zangger, K.; Wanner, G.; Stan-Lotter, H. Identification of

polyhydroxyalkanoates in Halococcus and other haloarchaeal species. *Appl. Microbiol. Biotechnol.* **2010**, *87*, 1119–1127, doi:10.1007/s00253-010-2611-6.

108. Koller, M. Polyhydroxyalkanoate biosynthesis at the edge of water activitiy-haloarchaea as biopolyester factories. *Bioengineering* **2019**, *6*, 1–33, doi:10.3390/bioengineering6020034.

109. Pfeifer, K.; Ergal, İ.; Koller, M.; Basen, M.; Schuster, B.; Rittmann, S.K.M.R. Archaea Biotechnology. *Biotechnol. Adv.* **2021**, *47*, doi:10.1016/j.biotechadv.2020.107668.

110. Litchfield, C.D. Potential for industrial products from the halophilic Archaea. *J. Ind. Microbiol. Biotechnol.* **2011**, *38*, 1635–1647, doi:10.1007/s10295-011-1021-9.

111. Karray, F.; Ben Abdallah, M.; Kallel, N.; Hamza, M.; Fakhfakh, M.; Sayadi, S. Extracellular hydrolytic enzymes produced by halophilic bacteria and archaea isolated from hypersaline lake. *Mol. Biol. Rep.* **2018**, *45*, 1297–1309, doi:10.1007/s11033-018-4286-5.

112. Gupta, R.; Gigras, P.; Mohapatra, H.; Goswami, V.K.; Chauhan, B. Microbial α-amylases: a biotechnological perspective. *Process Biochem.* **2003**, *38*, 1599–1616, doi:10.1016/S0032-9592(03)00053-0.

113. Monteiro De Souza, P. Application of microbial-amylase in industry-a review. *Brazilian J. Microbiol.* **2010**, *41*, 850–861.

114. Kumar, S.; Grewal, J.; Sadaf, A.; Hemamalini, R.; K. Khare, S. Halophiles as a source of polyextremophilic α-amylase for industrial applications. *AIMS Microbiol.* **2016**, *2*, 1–26, doi:10.3934/microbiol.2016.1.1.

115. Li, Q.; Yi, L.; Marek, P.; Iverson, B.L. Commercial proteases: Present and future. *FEBS Lett.* **2013**, *587*, 1155–1163, doi:10.1016/j.febslet.2012.12.019.

116. Razzaq, A.; Shamsi, S.; Ali, A.; Ali, Q.; Sajjad, M.; Malik, A.; Ashraf, M. Microbial proteases applications. *Front. Bioeng. Biotechnol.* **2019**, *7*, 1–20, doi:10.3389/fbioe.2019.00110.

117. Guerrand, D. Lipases industrial applications: Focus on food and agroindustries. *OCL - Oilseeds fats, Crop. Lipids* **2017**, *24*, doi:10.1051/ocl/2017031.

118. Chandra, P.; Enespa; Singh, R.; Arora, P.K. *Microbial lipases and their industrial applications: A comprehensive review*; BioMed Central, 2020; Vol. 19; ISBN 1293402001.

119. Rodrigo-Baños, M.; Garbayo, I.; Vílchez, C.; Bonete, M.J.; Martínez-Espinosa, R.M. Carotenoids from Haloarchaea and their potential in biotechnology. *Mar. Drugs* 2015, *13*, 5508–5532.

120. Corral, P.; Amoozegar, M.A.; Ventosa, A. Halophiles and Their Biomolecules: Recent Advances and Future Applications in Biomedicine. *Mar. Drugs* **2019**, *18*, 33, doi:10.3390/md18010033.

121. Saeedi, P.; Moosaabadi, J.M.; Sebtahmadi, S.S.; Mehrabadi, J.F.; Behmanesh, M.; Mekhilef, S. Potential applications of bacteriorhodopsin mutants. *Bioengineered* **2012**, *3*, 326–328, doi:10.4161/bioe.21445.

122. Trivedi, S.; Choudhary, O.P.; Gharu, J. Different Proposed Applications of Bacteriorhodopsin. *Recent Patents DNA Gene Seq.* **2011**, *5*, 35–40, doi:10.2174/187221511794839273.

123. Busskamp, V.; Duebel, J.; Balya, D.; Fradot, M.; Viney, T.J.; Siegert, S.; Groner, A.C.; Cabuy, E.; Forster, V.; Seeliger, M.; et al. Genetic reactivation of cone photoreceptors restores visual responses in retinitis pigmentosa. *Science (80-.).* **2010**, *329*, 413–417, doi:10.1126/science.1190897.

124. Poli, A.; Di Donato, P.; Abbamondi, G.R.; Nicolaus, B. Synthesis, production, and biotechnological applications of exopolysaccharides and polyhydroxyalkanoates by Archaea. *Archaea* **2011**, *2011*, doi:10.1155/2011/693253.

125. Torreblanca, M.; Ventosal, A. Is a Rods. *Lett. Appl. Microbiol.* **1994**, 201–205.

126. O'Connor, E.; Shand, R. Halocins and sulfolobicins: The emerging story of archaeal protein and peptide antibiotics. *J. Ind. Microbiol. Biotechnol.* **2002**, *28*, 23–31, doi:10.1038/sj/jim/7000190.

127. Karthikeyan, P.; Bhat, S.G.; Chandrasekaran, M. Halocin SH10 production by an extreme haloarchaeon Natrinema sp. BTSH10 isolated from salt pans of South India. *Saudi J. Biol. Sci.* **2013**, *20*, 205–212, doi:10.1016/j.sjbs.2013.02.002.

128. Quillaguamán, J.; Guzmán, H.; Van-Thuoc, D.; Hatti-Kaul, R. Synthesis and production of polyhydroxyalkanoates by halophiles: Current potential and future prospects. *Appl. Microbiol. Biotechnol.* **2010**, *85*, 1687–1696, doi:10.1007/s00253-009-2397-6.

129. Abdallah, M. Ben; Karray, F.; Sayadi, S. Production of polyhydroxyalkanoates by two halophilic archaeal isolates from Chott El Jerid using inexpensive carbon sources. *Biomolecules* **2020**, *10*, doi:10.3390/biom10010109.

130. Mitra, R.; Xu, T.; Xiang, H.; Han, J. Current developments on polyhydroxyalkanoates synthesis by using halophiles as a promising cell factory. *Microb. Cell Fact.* **2020**, *19*, 1–30, doi:10.1186/s12934-020-01342-z.

131. Le Borgne, S.; Paniagua, D.; Vazquez-Duhalt, R. Biodegradation of organic pollutants by halophilic bacteria and archaea. *J. Mol. Microbiol. Biotechnol.* **2008**, *15*, 74–92, doi:10.1159/000121323.

132. Rezaei Somee, M.; Dastgheib, S.M.M.; Shavandi, M.; Zolfaghar, M.; Zamani, N.; Ventosa, A.; Amoozegar, M.A. Halophiles in bioremediation of petroleum contaminants: challenges and prospects. In *Bioremediation for Environmental Sustainability*; Elsevier, 2021; pp. 251–291.

133. Nájera-Fernández, C.; Zafrilla, B.; Bonete, M.J.; Martínez-Espinosa, R.M. Role of the denitrifying Haloarchaea in the treatment of nitrite-brines. *Int. Microbiol.* **2012**, *15*, 111–119, doi:10.2436/20.1501.01.164.

134. Singh, A.; Singh, A.K. Haloarchaea: worth exploring for their biotechnological potential. *Biotechnol. Lett.* **2017**, *39*, 1793–1800, doi:10.1007/s10529-017-2434-y.

135. Oren, A. Halophilic archaea on Earth and in space: Growth and survival under extreme conditions. *Philos. Trans. R. Soc. A Math. Phys. Eng. Sci.* **2014**, *372*,

doi:10.1098/rsta.2014.0194.

136. Veneranda, M.; Lopez-Reyes, G.; Antonio Manrique-Martinez, J.; Sanz-Arranz, A.; Medina, J.; Pérez, C.; Quintana, C.; Moral, A.; Rodríguez, J.A.; Zafra, J.; et al. Raman spectroscopy and planetary exploration: testing the ExoMars/RLS system at the Tabernas Desert (Spain). *Microchem. J.* **2021**, *165*, 106149, doi:10.1016/j.microc.2021.106149.

137. Javor, B. Industrial microbiology of solar salt production. In Proceedings of the Journal of Industrial Microbiology and Biotechnology; 2002; Vol. 28, pp. 42–47.

138. Ventosa, A.; Fernández, A.B.; León, M.J.; Sánchez-Porro, C.; Rodriguez-Valera, F. The Santa Pola saltern as a model for studying the microbiota of hypersaline environments. *Extremophiles* **2014**, *18*, 811–824, doi:10.1007/s00792-014-0681-6.

139. Baati, H.; Guermazi, S.; Amdouni, R.; Gharsallah, N.; Sghir, A.; Ammar, E. Prokaryotic diversity of a Tunisian multipond solar saltern. *Extremophiles* **2008**, *12*, 505–518, doi:10.1007/s00792-008-0154-x.

140. Dillon, J.G.; Carlin, M.; Gutierrez, A.; Nguyen, V.; McLain, N. Patterns of microbial diversity along a salinity gradient in the Guerrero Negro solar saltern, Baja CA Sur, Mexico. *Front. Microbiol.* **2013**, *4*, doi:10.3389/fmicb.2013.00399.

141. Mani, K.; Taib, N.; Hugoni, M.; Bronner, G.; Bragança, J.M.; Debroas, D. Transient dynamics of archaea and bacteria in sediments and brine across a salinity gradient in a solar saltern of Goa, India. *Front. Microbiol.* **2020**, *11*, doi:10.3389/fmicb.2020.01891.

142. Amat, J.A.; Rendon, M.A. Flamingo coloration and its significance. *Flamingos Behav. Biol. Relatsh. with Humans* **2016**, 77–96.

143. Fox, D.L.; Hopkins, T.S. Comparative metabolic fractionation of carotenoids in three flamingo species. *Comp. Biochem. Physiol.* **1966**, *17*, doi:10.1016/0010-406x(66)90125-3.

144. Davies, B.H. The mechanism of the conversion of B-carotene into canthaxanthin by the brine shrimp, artemia salina. **1970**, *33*, 601–615.

145. Martínez-Espinosa, R.M.; Torregrosa-Crespo, J. Haloarchaea May Contribute to the Colour of Avian Plumage in Marine Ecosystems. **2021**.

146. Xie, W.; Ma, Y.; Ren, B.; Gao, M.; Sui, L. Artemia nauplii enriched with archaea Halorubrum increased survival and challenge tolerance of Litopenaeus vannamei postlarvae. *Aquaculture* **2021**, *533*, 736087, doi:10.1016/j.aquaculture.2020.736087.

Objectives

Halophilic microorganisms are an extraordinary source of useful compounds for several industrial applications. However, the microbial population inhabiting extreme saline environments has been underestimated due to the difficulties found in the isolation and cultivation of these microorganisms. In this sense, the main objectives of this Thesis are:

1. Validate two different culture-independent approaches, the clone library generation and high throughput sequencing, for the analysis of the microbial population living in the extreme environment of Odiel salterns **(Chapter 1)**.

2. Characterize the prokaryotic microbial population living in the brine from the crystallization ponds of Odiel salterns at saturating salinity, and evaluate the ability of this microbiota to excrete haloenzymes **(Chapter 1)**.

3. Assess diverse bioactive properties of the extracts obtained from two haloarchaea strains isolated from Odiel solar salterns **(Chapter 2)**.

4. Perform the biochemical and proteomic characterization of the amylase activity from the haloarchaea *Haloarcula* sp. HS isolated from Odiel salterns, and evaluate its potential use for the treatment of bakery waste **(Chapter 3)**.

5. Study the dynamics of the microbial communities across the salinity gradient in the brine of Odiel salterns **(Chapter 4)**.

6. Trace the transformations of the microbial pigments through the trophic chain in Odiel salt flats **(Chapter 4)**.

Results and Discussion

Chapter 1

Characterization of the Microbial Population Inhabiting a Solar Saltern Pond of the Odiel Marshlands (SW Spain)

This chapter has been published as: **Gómez-Villegas, P**.; Vigara, J.; León, R. Characterization of the Microbial Population Inhabiting a Solar Saltern Pond of the Odiel Marshlands (SW Spain). *Mar. Drugs* 2018, *16*, 332. https://doi.org/10.3390/md16090332

marine drugs

MDPI

Article

Characterization of the Microbial Population Inhabiting a Solar Saltern Pond of the Odiel Marshlands (SW Spain)

Patricia Gómez-Villegas, Javier Vigara and Rosa León *

Laboratory of Biochemistry and Molecular Biology, Faculty of Experimental Sciences, Marine International Campus of Excellence (CEIMAR), University of Huelva, 21071 Huelva, Spain; patgomvil@gmail.com (P.G.-V.); vigara@uhu.es (J.V.)

* Correspondence: rleon@uhu.es; Tel.: +34-959-219-951

Received: 28 June 2018; Accepted: 8 September 2018; Published: 12 September 2018

Abstract: The solar salterns located in the Odiel marshlands, in southwest Spain, are an excellent example of a hypersaline environment inhabited by microbial populations specialized in thriving under conditions of high salinity, which remains poorly explored. Traditional culture-dependent taxonomic studies have usually under-estimated the biodiversity in saline environments due to the difficulties that many of these species have to grow at laboratory conditions. Here we compare two molecular methods to profile the microbial population present in the Odiel saltern hypersaline water ponds (33% salinity). On the one hand, the construction and characterization of two clone PCR amplified-16S rRNA libraries, and on the other, a high throughput 16S rRNA sequencing approach based on the Illumina MiSeq platform. The results reveal that both methods are comparable for the estimation of major genera, although massive sequencing provides more information about the less abundant ones. The obtained data indicate that *Salinibacter ruber* is the most abundant genus, followed by the archaea genera, *Halorubrum* and *Haloquadratum*. However, more than 100 additional species can be detected by Next Generation Sequencing (NGS). In addition, a preliminary study to test the biotechnological applications of this microbial population, based on its ability to produce and excrete haloenzymes, is shown.

Keywords: halo-extremophyles; archaea; 16S rRNA metagenomics; haloenzymes; Odiel marshlands

1. Introduction

The study of the microbial population inhabiting extreme saline environments has gained increasing interest in the last years due to its usually uncompleted characterization, which is essential to understand the ecology of these ecosystems [1] and also because archaea have revealed themselves as the key to understand the origin of eukaryotic cells [2]. Furthermore, these halo-extremophyles microorganisms can be an excellent source of useful compounds and proteins with special properties and potential industrial applications [3,4] such as antioxidant pigments [5,6], haloestable enzymes [7], antimicrobial compounds [8] or antitumor agents [9]. Haloenzymes have unique characteristics that allow them to be stable and functional at saline concentrations as high as 5 M and tolerate high temperatures without losing their activity [10]. This fact makes halotolerant archaea a potential source of enzymes for food, textile, pharmaceutical or chemical industries [11].

The extreme conditions that prevail in salt brines, which include high light intensity, UV radiation, elevated temperatures and salt concentrations near saturation, support a considerable diversity of halophilic microorganisms belonging mainly to the haloarchaea group [12]. Traditional ecological studies, based on serial dilutions or streaking on agar plates for single-cell isolation, have usually

underestimated this biodiversity due to the difficulties of some species to grow at lab conditions. Examples of this are the unsuccessful attempts to culture some generally abundant archaea genera, such as the square-shaped *Haloquadratum* [13]; or the discrepancy commonly found between the characterization of microbial communities by culture-independent and culture-dependent methods.

The application of molecular techniques, based on the comparison of highly conserved DNA reference sequences, such as the genes encoding for ribosomal RNA (16S rRNA, 5S rRNA), has allowed to overcome this limitation, making possible the comparison of different microbial communities and the discovery of a good number of uncultured new species. Examples of these culture-independent methods include: random fragment length polymorphisms (RFLP) [14], fluorescence *in situ* hybridization with rRNA-targeted probes [15], denaturing gradient gel electrophoresis (DGGE) [16] and more recently metagenomic approaches [17,18], which have facilitated the profiling of complex microbial communities. Culture-independent characterization of the microbial assemblages in different halophilic habitats has shown that diversity within the domain archaea is broader than that previously inferred from culture-dependent surveys [19].

The solar salterns located in the Odiel Marshlands (Huelva), at the southwest of Spain, are an excellent example of a hypersaline environment inhabited by microbial populations specialized in thriving under conditions of high salinity, which remains poorly explored [20]. In this work, we have used two independent methods to study the prokaryotic diversity present in these salterns. We have constructed and characterized two libraries of PCR amplified 16S rRNA genes obtained using genomic DNA extracted from a water sample of the brines as template; and we have used a high throughput 16S rRNA massive sequencing approach based on the Illumina MiSeq platform to profile the same genomic sample. This double approach has allowed us, not only to explore the microbial diversity of this water environment but also to validate the results of the PCR gene library by comparison with the NGS approach. Furthermore, the ability of this microbial population to produce and excrete haloenzymes with applied interest has been studied.

2. Results

2.1. Construction of a 16S rRNA Library and Identification of the Obtained Sequences

Two 16S rRNA libraries clone libraries, one for archaea and another one for bacteria, were constructed from an environmental water sample collected at the end of the summer, in the crystallizer ponds located in the Marshlands of the Odiel river in the southwest coast of Spain. The procedure for the libraries construction is detailed in Section 4.4 and the specific primers used listed in Table S1 (Supplementary Material). The main chemical characteristics of the water at the collection time are summarized in Table 1. The salt composition was similar to that reported for other thalassohaline marine solar salterns at this degree of salinity, which was 33.2% at the time of sample collection.

Table 1. Chemical composition of the water sample collected from the evaporation ponds located in the Natural Reserve of Odiel Marshlands in the southwest Spain.

Density ($g \cdot mL^{-1}$)	Brine Composition ($g \cdot L^{-1}$)						Total Salinity
	$CaSO_4$	$MgSO_4$	$MgCl_2$	NaCl	KCl	NaBr	
1.212	1.40	23.06	34.08	265.38	7.51	0.84	332.30

A selection of 50 clones from both clone libraries, 25 clones per each library, were analysed. The preliminary comparison of the obtained sequences with the National Center for Biotechnology Information database (NCBI) revealed that many of the clones in the 16S rRNA libraries were redundant. In the archaeal library, the 25 clones studied corresponded to 11 different species, belonging to six genera (Figure 1). Most clones corresponded to the archaea genus *Halorubrum*, followed by the peculiar square-shaped haloarchaea *Haloquadratum* [13,21]. These two genera represented respectively 32% and 28% of the total archaeal clones obtained, followed by *Halonotius* (12%) and *Halobellus* (8%).

The least abundant genera identified were *Haloarcula* and *Halorientalis*, each one represented 4% of the total clones (Figure 1). Three clones could not be directly affiliated to any currently described genera, since they did not reach the 95% of sequence identity with any of the sequences of the database. The Shannon biodiversity index was calculated as previously reported [22], obtaining a value of 2.07. Despite the small number of clones analysed this score indicates a wide range of diversity.

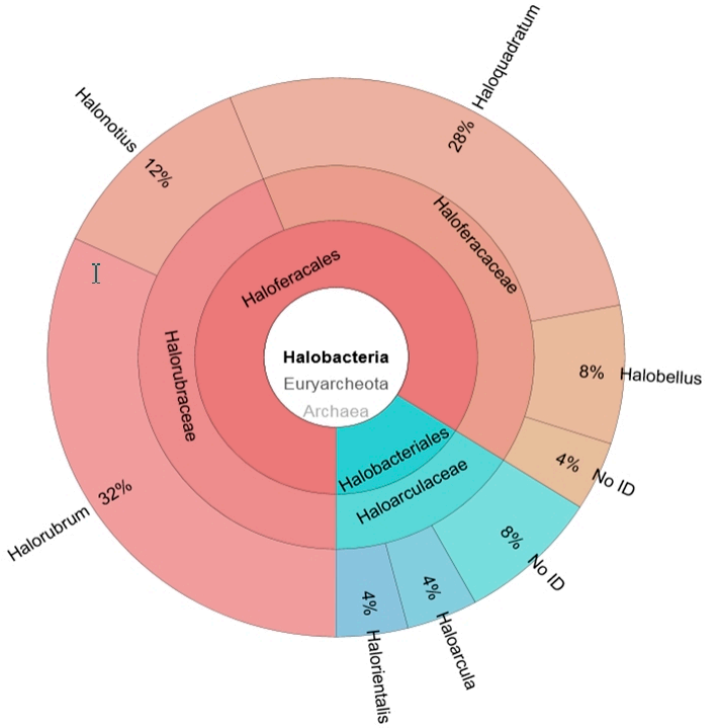

Figure 1. Distribution of the clones from the archaeal 16S rRNA clone library among different genera. 16S rRNA fragments obtained by amplification with archaeal specific primers were cloned into pGEMT vector for the construction of a clone library. The inserted sequence of 25 of the obtained clones were analysed and compared with the NCBI to identify the original genera. Data are expressed as percentages of the total archaeal population. Only sequences that shared over 95% 16S rRNA sequence identity with a known one was assigned to a specific genus.

To obtain additional information, a molecular phylogenetic analysis has been done including all the 16S rRNA encoding sequences obtained from the analysis of the archaeal library and several reference sequences obtained from the NCBI data base. The evolutionary history was inferred by using the Maximum Likelihood method based on the General Time Reversible model [23] (Figure 2).

Some of the amplified 16S rRNA sequences obtained in the archaea library showed 100% of identity or were closely related, showing $\leq$3% sequence divergence, with species already classified and could be assigned at species level. As it is shown in Figure 2, the sequences Col.10/11/12 and Col. 1/4/14/15/18/19/20 can be assigned to the species *Halonotius pteroides* and *Haloquadratum walsbyi*, respectively. The *Haloquadratum* sequences found (Col.1/14/15/18/19/20) displayed sequence divergences lower than 1% with *H. walsbyi*. By contrast, sequences related to *Halorubrum* genus (Col.21/25, Col.13/22, Col.23/24, Col.3, Col.16), *Halobellus* genus (Col.6/9) and *Haloarcula* genus (Col.17) showed high percentage of identity with several reference species. In addition, sequences clustering within *Halorientalis* genus (Col.7) presented more than 3% divergence with the reference sequences; being impossible their assignation to a particular species in these cases. Finally, two of the sequences which could not be directly assigned to a genus (Col.5, Col.8) clustered within the *Haloarcula* clade, while Col.2 is strongly related to the genus *Hallobelus*.

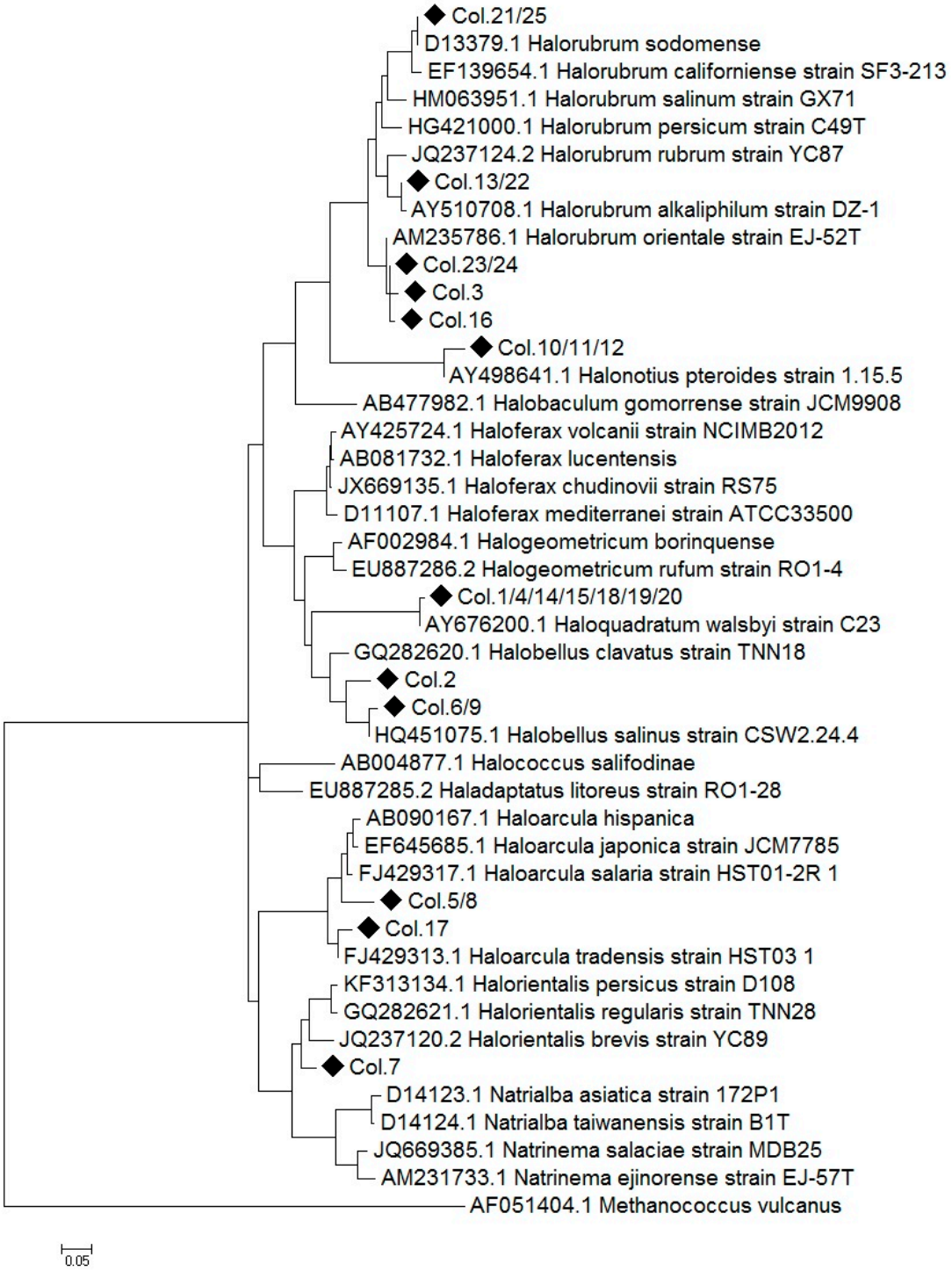

Figure 2. Molecular Phylogenetic Analysis by Maximum Likelihood method. The tree represents the relationship among the 16S rRNA sequences from strains isolated from the saltern ponds of the Odiel Marshlands and reference archaeal sequences. Multiple alignments were generated by MUSCLE and the tree was constructed with MEGA 7, using 1000 bootstrap replicates. The name and the NCBI access number are indicated for all the reference sequences. Black diamonds represent 16S rDNA Sequences from the isolates and "Col. N" denotes the colony number. When an identical sequence was obtained from different colonies it was denoted as "Col. N1/N2." The tree is drawn to scale, branch lengths represent the number of substitutions per site. Scale bar indicate 5% sequence divergence. The sequence of *Methanococcus vulcanus* was used as the outgroup.

By contrast, all the clones isolated from the bacterial gene library contained 16S rRNA sequences with 99–100% sequence identity to a unique bacterial species, *Salinibacter ruber*, which is usually present in hypersaline ponds [24]. The chosen primers have been shown to be very specific for each prokaryotic group studied, since archaea sequences have not been obtained in the bacterial library, nor have bacterial sequences been detected in the archaeal library. This specificity makes impossible the use of these primers to create a common bacterial/archaeal library.

2.2. Metagenomic Microbial Profiling by High-throughput 16S rRNA Sequencing

As a second approach, the identification of the microbial population present in the hypersaline water from the Odiel saltern ponds was performed by next-generation sequencing of the 16S rRNA gene, using the Illumina MiSeq platform as detailed in Materials and Methods. The analysis was set up in quadruplicate by two independent sequencing services, Stabvida (SBV) and Life Sequencing (LFS). Bioinformatic processing with the software pipelines described in Materials and Methods allowed us to cluster the obtained reads into a limited number of operational taxonomic units, between 117 and 356, depending on the sequencing reaction and the bioinformatic treatment of the obtained sequences (Table 2). The mean quality of the processed sequences was denoted by the Q scores and the Shannon biodiversity index (*H'*), calculated including the whole prokaryotic population and following previously described procedures [22,25].

Table 2. Sequence data statistics.

Reaction	Raw Sequence Reads	Mean Read Length (bp)	Sequences after Denoising	Mean Quality (Q Score)	OTUs	Shannon Index
SBV-1	349 726	250	49 100	>28	177	2.75
SBV-2	204 766	250	19 537	>28	117	2.65
LFS-1	57 148	299.8	25 479	37.16	228	2.77
LFS-2	156 520	299.6	71 623	37.25	356	3.03

The number of sequences and Operational Taxonomic Units (OTUs) obtained from Stabvida (SBV) and Life Sequencing (LFS) are shown. The mean quality, expressed as Q scores and the Shannon biodiversity index for each sequencing run have also been included.

Both 16S rRNA NGS analysis indicate that the most abundant reads correspond to the halophilic bacteria *Salinibacter* and the archaeal genera *Halorubrum*, *Haloquadratum* and *Halonotius*, although there are significant discrepancies between their relative abundance. *Salinibacter* represents between 38% and 42% of the total reads. *Halorubrum* (13–19%), *Haloquadratum* (9–18%) and *Halonotius* (8–9%) are the main archaeal genera, followed by *Halobellus* (3–4%), *Natronomonas* (2.5–3%). *Haloplanus* and *Halohasta* each represent around 3% of the total sequences after the analysis of Life Sequencing and only trace amounts (0.1%) in the data from Stabvida. *Halomicroarcula*, *Salinivenus*, *Halovenus*, *Halomicrobium*, *Halorientalis*, *Haloarcula* and *Halosimplex*, with relative abundances between 0.7% and 1.5%, are also present in both analyses. Genera with relative abundances lower than 0.2% have not been shown in Figure 3, but the complete list of sequenced genera is shown in Supplementary Material (Table S2).

It is interesting to note that the NGS analysis revealed the presence of trace amounts of genus such as *Spiribacter* (0.1%), a moderate halophilic bacteria usually found in medium salinity habitats [26] and other minor bacteria, not revealed in the clone library approach (Table S2).

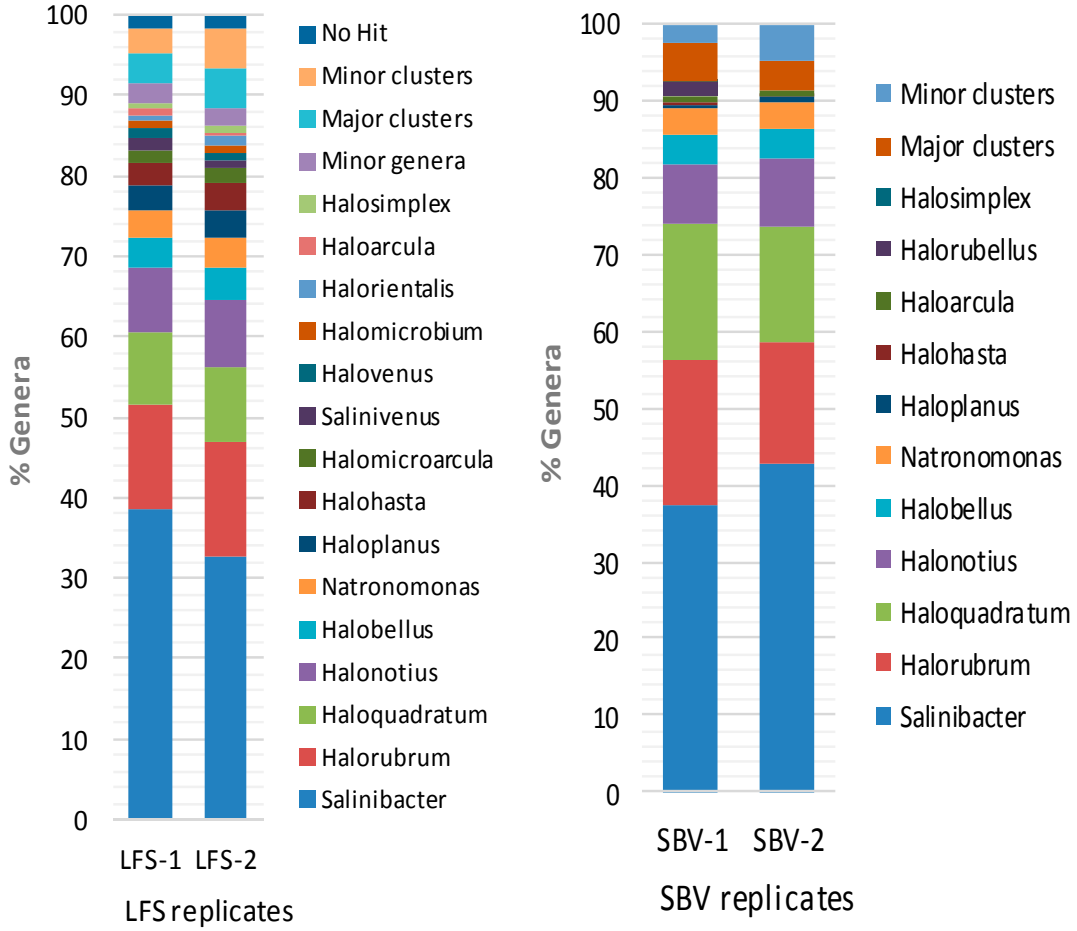

Figure 3. Relative abundance of the genera found by the metagenomic approaches. Operational Taxonomic Units (OTUs) distribution in Odiel saline ponds (33% salinity) obtained from Illumina MiSeq sequencing of the 16S rRNA V3, V4 hypervariable regions. Four data sets were obtained from two different sequencing services. The graphic shows the percentage of the genera with more than 0.2% abundance. Minor genera include all the genera below 0.2%. The sequences that clustered together but could not been affiliated to a genus are named as "clusters" and have been divided in "Major clusters" (>0.2%) and "Minor clusters" (<0.2%). "No hit" represents the sequences which did not cluster with any other obtained sequence.

2.3. Comparison of Clone Library and 16S rRNA Metagenomic Approaches to Identify the Archaeal Microbiota of the Odiel Saltern Ponds Water

The relative abundances of the main genera obtained from the two NGS platforms are compared with those obtained by affiliation of the 25 sequences gathered from the archaeal clone library (Figure 4). Despite the low number of sequences retrieved from the clone library, there was a considerable degree of agreement between the main genera obtained by this method and by the NGS approaches, as it is supported by a correlation coefficient of 0.97 when comparing clone library results versus the mean of NGS results. Similarly, a correlation coefficient of 0.96 was obtained when we compared both NGS methods (Mean LSF vs. Mean SVB).

The estimated percentage of *Halorubrum* and *Haloquadratum* obtained by the clone library approach are almost identical to those obtained by the Stabvida analysis, being the standard deviation (SD) for these values 2 and 0.34 respectively, while the percentages of *Halonotius* and *Halobellus* are of the same order than those obtained by Life Sequencing (SD 2.48 and 0.35, respectively) or Stabvida (SD 1.78 and 1.41, respectively). *Halorientalis* and *Haloarcula* which represented about 4% of the library clones are also present in the massive 16S rRNA analysis but at lower percentage than that estimated by the clone library approach. Standard deviations in these cases were respectively 1.42 and 1.77, comparing

the results of the clone library with the Life Sequencing results; and 2.82 and 2.12 respectively, when comparing with Stabvida results. Massive sequencing provides more information about the less abundant species, although the analysis of higher number of archaeal clones could have allowed the identification of more minor genera by the clone library approach.

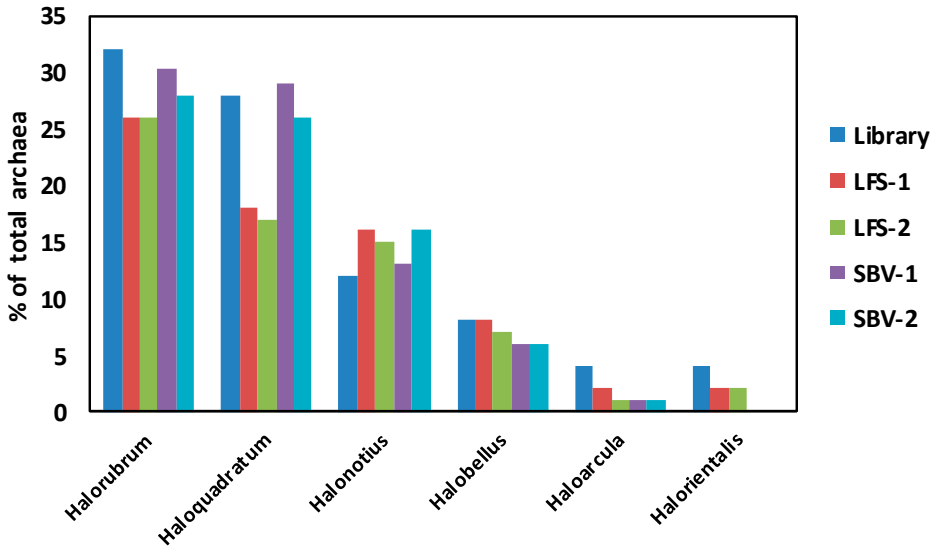

Figure 4. Comparison of the main archaeal genera present in the Odiel saline ponds. Percentage of the different archaea genera over the total archaea population found in the Odiel saline ponds obtained by the two different culture-independent approaches previously described: construction of a clone library (Library) and massive 16S rRNA sequencing, including the two replicates from each Metagenomic Service (LFS and SBV). Only the most abundant genera are shown.

2.4. Evaluation of Halocin Activity

Massive 16S rRNA sequencing has revealed an extremely low representation of the genus *Haloferax* (0.021%) in the Odiel Saltern ponds (Table S2). However, *Haloferax* is a metabolically versatile genus, able to grow on complex substrates and degrade polymeric substances with a wide salt tolerance in laboratory cultures [27]. To investigate the possible reasons for the low presence of *Haloferax* in the Odiel saltern water, we studied the potential ability of the biomass isolated from the Odiel saterns to specifically inhibit the growth of the control *Haloferax* species, *Haloferax lucetense.* The results show the inhibition of *H. lucetense* growth in the presence of the concentrated biomass isolated from the Odiel saltern ponds, indicating the presence of halocin activity (Figure 5A), which could be an important factor to explain the practically absence of species of the *Haloferax* genus in the hypersaline water from the Odiel saltern ponds.

2.5. Haloenzymes Production by the Archaeal Enriched Biomass Isolated from the Odiel Saltern Ponds

Simple and sensitive plate assays were optimized for the detection of archaeal extracellular enzymes produced by the biomass isolated from the hypersaline water (33%) of the Odiel salterns. The biomass was enriched, concentrated and dropped on agar plates supplemented with different carbon sources to detect the excretion of α-amylase, protease, lipase, cellulase and laccase as described in Materials and Methods.

The amylase (Figure 5B), protease (Figure 5C) and lipase (Figure 5D) activities, assayed as described in Material and Methods following the degradation of starch, skimmed milk and Tween 80, respectively, were positive. Cellulase and exo-lacasse activities, assayed in the presence of carboxymethyl cellulose (Figure 5E) and bromophenol blue (Figure 5F), were also detected.

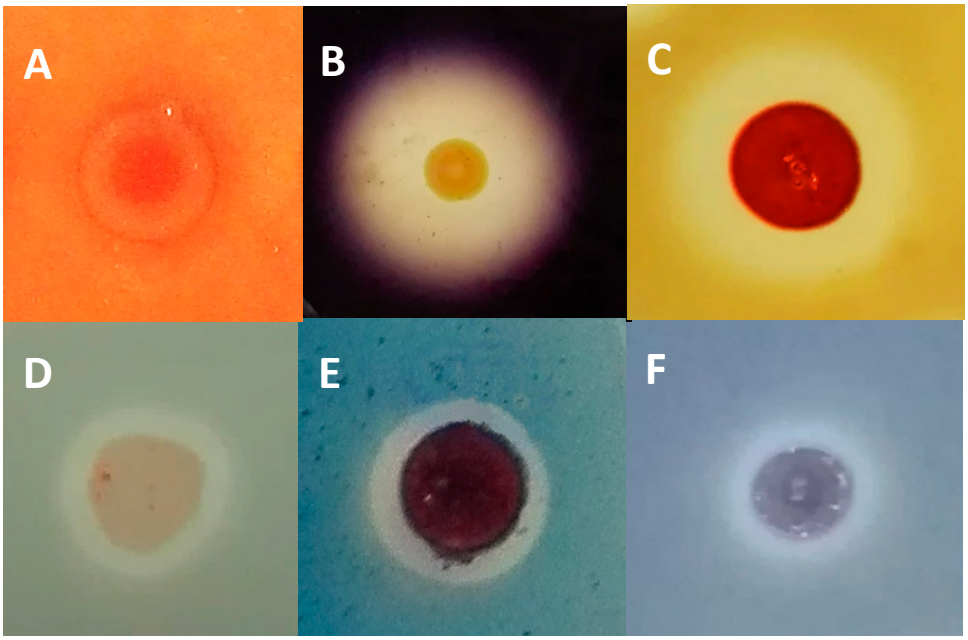

Figure 5. Detection of extracellular halocin and enzymatic activities in the enriched archaeal biomass by plate assay. The biomass obtained from the Odiel salterns water was enriched and concentrated as detailed in Material and Methods and used to test extracellular: halocin (**A**), amylase (**B**), protease (**C**), lipase (**D**), cellulase (**E**) and laccase (**F**) activities by the plate assays described in Materials and Methods.

3. Discussion

3.1. Microbiological Diversity in Hypersaline Solar Saltern Ponds

Despite the existence of many studies about the microbiota inhabiting thalassosaline water ponds all around the word, it is difficult to establish comparisons among them, due to the variety of experimental procedures used to determine microbial composition and the dramatic influence of the water salinity, which can range between the 3.5% of the sea water to the 37% of NaCl saturation.

Numerous studies have described the prokaryotic communities that inhabit saltern crystallizer ponds as distant as the Mediterranean coast of Spain [15,18], Australia [28] or Mexico [29], among others. However, the microbial profile of the Odiel salterns, differently from that of other Spanish salterns, such as Santa Pola in Alicante [24,30] or Isla Cristina in Huelva [18], has been poorly studied. To our knowledge, the only survey about the microbiota of the Odiel Marshlands is a recent study by Vera-Gargallo and Ventosa [20], which focused on studying the assemblage and the metabolic strategies of the microbiota thriving in these hypersaline soils but no information about the aquatic microbial composition of this location has been previously reported.

Most hypersaline ponds, regardless their location, are dominated by the archaeal genera species *Haloquadratum* and *Halorubrum* [31], which coexists and compete for the same hypersaline environments. *Haloquadratum* was the predominant genus followed by *Halorubrum*, in three crystallizer ponds as geographically distant as Australia at 34% salinity [28], Santa Pola (Spain) at 32% salinity [18] and in Bingöl (Turkey) at 25% salinity [32]. Conversely, our results at 33% salinity suggest that in Odiel Salters this relation is inverse, being the most abundant archaeal genus *Halorubrum* followed by *Haloquadratum*, which often dominates the microbial communities in hypersaline waters and was not cultured in a laboratory until 2004 [13,21]. This difference could be attributed to changes in environmental conditions, due to the diverse geographical situations [18]. There are also some interesting exceptions, such as the Maras salterns in the Peruvian Andes, in which around 31% of the detected sequences were related to the usually low abundant *Halobacterium* and no *Halorubrum* was detected [33]; the Adriatic solar saltern crystallizers studied by Pašić et al. [34], where the

presence of the usually abundant *Haloquadratum* was rare; or the Pomorie Salterns (Bulgaria) where the predominant archaea genus was *Halanaeroarchaeum*, which reached 28% of the total archaeal community [35]. The aforementioned study carried out by Vera-Gargallo and Ventosa about saline soils from Odiel saltmarshes reveals that *Haloquadratum* was not found in these soils; in contrast to our results from hypersaline water in the same location, which suggest that this is one of the dominant archaeal genus. However, other genera identified in our work, such as *Halorubrum*, *Haloarcula* and *Halobellus*, are also present in the soil samples studied [20]. The predominant microbial genera and their estimated composition in other hypersaline ponds with salinity similar to our study are summarized in Table 3. The most complete studies have been done in Santa Pola, in the Mediterranean coast of Spain and showed that *Haloquadratum* was the most abundant microorganism and that its relative abundance increased with salinity. In hypersaline ponds in Australia (34%) [28] the three most abundant haloarchaeal genera were the same that we observed in the Odiel ponds. However, it is important to notice that in this study and in the study carried out by Kambourova et al. in Bulgaria [35], the bacterial contribution to the prokaryotic community was not considered because the study was based on clone libraries with archaeal specific primers. This comparison confirms that although there are some common genera, which are found in almost all hypersaline ponds, such as *Halorubrum* or *Haloquadratum*, the relative abundance of hypersaline genera is specific of each geographic location. In addition, identifications at species level returned unique lineages which appeared to be specific of the investigated environments.

Salinibacter ruber, was first identified in Santa Pola, Spain (Alicante, Spain) and, despite not being an archaea, it is usually one of the most abundant microorganisms present in hypersaline waters [24]. In Santa Pola ponds with salinities of 19%, 33% and 37% the abundance of *Salinibacter* was reported to be 6.4%, 4.7% and 9.1%, respectively [18]. Our results suggest that the bacteria *Salinibacter ruber* is the dominant microorganism in the Odiel saltern water with a salinity of 33%, reaching around 40% of the total prokaryotic community (Figure 3), which is the highest *Salinibacter* abundance reported in solar salterns to our knowledge. The libraries for the metagenomics studies were built with the universal primers, which have been designed to target V3 and V4 hypervariable regions from both bacterial and archaeal 16S rRNA [36]; however, additional research is needed to determine if the high percentage of reads corresponding to *Salinibacter* obtained in our metagenomic study corresponds to such a percentage of the bacterium abundance or can be influenced by a potential bias in the library construction.

It is interesting to note the low abundance that we have found for the genus *Haloferax* in the Odiel evaporation pond. Although it grows optimally at 2.5 M NaCl (15% salinity) [37], *Haloferax* has been described to grow at salinities of 33.7% with growth rates higher than any other comparable extreme halophile [27]. Despite these characteristics, *Haloferax* is usually found at low percentage, around 1%, in solar saltern ponds with medium and high salinity (10–37%), as described for example in Santa Pola, Spain [30]. Curiously, the relative abundance that we have found in the Odiel evaporation pond for *Haloferax* is even lower, reaching about 0.021% of the total prokaryotic community. There are several studies that have shown the excretion of halocins or archeocins by archaeal species [38,39], demonstrating the importance of such halocins for interspecies competition in hypersaline environments. The results of our growth inhibitory studies support the possible production of halocins against *Haloferax* by the dominant species and give a possible explanation to the limited presence in the Odiel salterns of *Haloferax*, which should be apparently more qualified to dominate hypersaline ecosystems than the usual dominant species [27].

Table 3. Comparison of prokaryotic diversity at genus level in the Odiel hypersaline pond (33%) and other hypersaline ponds with similar salinity.

Sample	Santa Pola (Spain)	Santa Pola (Spain)	Odiel Salterns (Spain) *	Pomorie (Bulgaria) **	Bajool (Australia) **
Salinity	**33%**	**37%**	**33%**	**34%**	**34%**
Ref.	[18,30]	[30]	**This study**	[35]	[28]
%	*Haloquadratum* 29.5 *Haloruburm* 23.1 *Natronomonas* 5.7 *Salinibacter* 4.7 *Haloplanus* 3.4	*Haloquadratum* 58 *Salinibacter* 9.1 *Nanosalina* 4.0 *Haloruburm* 3.2 *Nanosalinarum* 1.7 *Halomicrobium* 1	*Salinibacter* 37.8 *Halorubrum* 15.5 *Haloquadratum* 12.8 *Halonotius* 8.3 *Halobellus* 3.8 *Natromonas* 3.4 *Haloplanus* 2 *Halohasta* 1.7 *Halorientalis* 0.96 *Haloarcula* 0.67	*Halanaeroarchaeum* 27.8 *Halorubrum 24* *Halonotius 15.7* *Halobellus 6.5* *Halovenus 6.5* *Natronomonas 2.8*	*Haloquadratum 47* *Halorubrum 17.6* *Halonotius 11.7* *Haloplanus-like 11.7* *Natronomonas 2.9*

* Mean of four 16S rRNA NGS data sets. ** In these studies, only archaea were considered.

3.2. PCR Library versus 16S rRNA Massive Sequencing

Cloning-based methods have been successfully used for years [40], however the availability of new benchtop NGS technologies has made more popular the use of 16S rRNA high-throughput for sequencing and profiling of microbial communities including that of hypersaline habitats [41].

Here we demonstrate that, although NGS 16S rRNA sequencing offers a more complete view of the microbial community inhabiting the saline ponds of the Odiel Marshlands, providing more information about the less abundant genera, both NGS and 16S rRNA clone library approaches are comparable regarding the estimation of the major genera found in the sample. This is in agreement with the results obtained by other authors, such as González-Pimentel [42], who compared both approaches to study the microbial diversity in lava tubes from Canary Islands.

We have observed that there is a good general agreement in the relative abundance of the main genera distribution obtained in both NGS analysis (SBV and LFS), however there are discrepancies for some genera. Since both massive sequence services have used the same platform (My Seq Illumina), primers and starting genomic DNA, the small discrepancies and the higher sensitivity of LFS analysis can be greatly attributed to differences in the bioinformatic analysis and other factors such as details of PCR libraries preparation. Furthermore, we observed that the use of different tools for the denoising and clustering step (i.e., using DADA2 instead of DEBLUR plugging) caused the removal of potentially valid sequences and yield different results from the same raw data (data not shown).

Shannon index value, which indicates the uniformity of species and its abundance in the obtained OTUs, increases as both the richness and the evenness of the community increase [43]. The Shannon index values calculated for our NGS studies were on average 2.9 for LFS replicates and 2.7 for SVB replicates (Table 2), while the Shannon index calculated for the clone library data was 2.07. This value is in accordance with previous studies carried out by clone library approaches, which reported values between 1.64 and 2.10 in Australia (34% salinity) [28], 1.8 (37% salinity) and 1.6 (38% salinity) in Mexico [29], while Shannon indexes from NGS are substantially higher. This difference is probably due to the small number of sequences analysed by the clone library technique when compared to NGS. It is necessary to remember that both, clone library and 16S rRNA massive sequencing, methods are based on the PCR amplification of a fraction of the highly conserved reference sequence 16S rRNA. Consequently, both methods share the possible bias inherent to PCR amplification of a single gene and the limitations of 16S rRNA for the resolution of closely related species [44]. Some authors have pointed the higher sensitivity and accuracy of whole genome metagenomic sequencing approach [44]. However, the lower cost of the massive sequencing of 16S rRNA and the existence of wide information and databases for the 16S rRNA sequences have converted this approach in the most commonly used method for exploring bacterial communities. It is important to note that to obtain accurate values in the characterization of microbial communities by single gene amplification methods primers must be validated [45], as were the IlluAdp16S primers (Table S1 in Supplementary Material) used in this

study [36]; and robust bioinformatic pipelines should be chosen to process the sequencing data, since different bioinformatic treatments usually yield different relative genera abundances.

3.3. Archaeal Halo-Exoenzymes

Haloarchaeal hydrolases are halophilic and usually thermostable exoenzymes able to catalyse clean and ecologically-friendly processes with high specificity. They have interesting features which make them very attractive for many industrial applications, such as paper, textile, food, detergent and pharmaceutical industries [46]. In addition, lipases and esterases could be used in biofuel production [47], while cellulases and laccases could be of interest for the conversion of plant biomass into fuel and renewable products [48] and the detoxification of the treated lignocelluloses substrates [49,50], respectively. Despite all these interesting studies no application of archaeal haloenzymes at industrial scale has been described so far [10,51].

Halophilic termoestable α-amylases have been found in different genera, including *Haloferax* [52], *Haloterrigena* [53] and *Halomonas* [54]. Some haloarchaeal isolates, such as *Haloarcula marismortui*, produce salt-dependent thermoactive lipases and esterases [55]. Extracellular organic-solvent tolerant proteases have been found in *Halobacterium* sp. [56] and *Natrialba magadii* [57]. However, only few cellulases [58–60] and laccases [61,62] producing halophiles have been reported.

In this work, we have demonstrated that the enriched biomass analysed presents different hydrolases activities, including α-amylase, protease, lipase/esterase, cellulose and laccase. Further studies will focus on the isolation and identification of the strains which show the higher activity for each enzyme, followed by the characterization of the parameters that enable the best activity.

4. Materials and Methods

4.1. Sample Collection and Chemical Composition of the Brine

Samples were obtained at the end of the summer from the salt evaporation ponds located in the natural reserve of Odiel Marshlands, at the estuary of the Odiel and Tinto rivers in the Southwest Spain (Latitude: 37.2395, longitude: −6.95287). The salt concentration in the crystallizer pond was 33.2% at the collection time. Climatological features of the location are characteristic of the Mediterranean maritime climate with hot dry summers and rainy autumns and winters. The mean insolation rate exceeds 3000 h per year, the average annual rainfall and air temperature are 506 mm and 18.3 °C, respectively [20]. The ionic composition and the main physicochemical parameters of the seawater brine at the time of sample collection were determined according to following standard methods: ISO 2480-1973 "Determination of sulphate contents-barium sulphate gravimetric method"; ISO 2481-1973 "Determination of halogens expressed as chlorine-mercuric method", ISO 2482-1973 "Determination of calcium and magnesium contents-EDTA complexometric method"; ECSS/SC 2482-1979 "Determination of potassium content by flame atomic absorption spectrophotometric method".

4.2. Genomic DNA Extraction

For genomic DNA extraction, fresh biomass was harvested by centrifugation of a 500 mL water sample at 11,000 rpm. The resulting pellet was washed with ammonium formate 4 M, freeze-dried and used for genomic DNA extraction with the GeneJET Genomic Purification kit (Thermo Fisher Scientific, Waltham, MA, USA), following the instructions of the manufacturer. Quantification of the genomic DNA obtained and assessment of its purity was done on a Nanodrop Spectrophotometer ND-1000 (Thermo Fisher Scientific).

4.3. Amplification of 16S rRNA Encoding Gene and Construction of Clone Libraries

16S rRNA fragments were amplified with the primer sets: Arc340F/Arc1000R [6,63] for archaea and 341F/907R [64,65] for bacteria (Table S1) using 1 µL of genomic DNA, isolated as previously described, as template. Polymerase chain reactions (PCR) were performed in a total volume of 25 µL

containing 1 µL of genomic DNA, 10 pM of each primer, 0.2 mM dNTPs, 0.5 U Taq DNA polymerase from Bioline, 2.5 µL of specific 10X buffer and 1.5 µL of 2.5 mM $MgCl_2$ buffer using an Eppendorff thermo-cycler. The PCR program was 0.5 min at 96 °C, 0.5 min at 50 °C and 1 min at 72 °C for 30 cycles, followed by 10 min of final primer extension.

4.4. Construction and Analysis of Clone Libraries

The PCR products, obtained with both bacterial and archaeal primer sets, were subjected to agarose electrophoretic separation. The bands obtained for each PCR reaction (with around 660 bp for archaea and 560 bp for bacteria) were purified with the GeneJET Gel Extraction Kit (Thermo Fisher Scientific), ligated to pGEM-T vector (Promega, Madison, WI, USA) according to the manufacturer's instructions and cloned into *Escherichia coli* DH5α competent cells to establish two clone libraries, one for archaea and another one for bacteria. A selection of 50 clones, 25 per each library, were analysed by extraction of the plasmidic DNA, Sanger-sequencing of the 16S rRNA DNA encoding fragments (Stabvida, Lisbon, Portugal) and comparison of the obtained sequences with the National Center for Biotechnology Information 16S rRNA database (NCBI, http://www.ncbi.nih.gov) by using the advanced BLASTN search tool. Sequences with more than 98% length coverage and more than 95% of sequence identity were assigned to a described genus. Sequences with high identity (>97%) were assigned to specific species. Sequences which showed percentage of identity lower than 95% can be potential novel species or genera but further evidence is needed to confirm it.

4.5. High-Throughput 16S rRNA Sequencing

For High-throughput 16S rRNA based microbial profiling, the same genomic DNA was analysed on the Illumina MiSeq platform. Analysis was set up in quadruplicate by two independent Sequencing services: Life Sequencing (Valencia, Spain) and Stabvida (Lisbon, Portugal). In both cases the PCR libraries were prepared by targeting the V3-V4 hypervariable regions of the 16S rRNA [36] with the previously validated [66] IlluAdp16S primers (Table S1) and sequenced using the Illumina MiSeq Reagent kits, V2× 250bp or V3× 300 bp, following Illumina recommendations for Library preparation and metagenomic sequencing. R1 and R2 reads were overlapped using PEAR program version 0.9.1 [67]. Raw data were processed for denoising, filtering (minimum quality threshold of Q20) and clustering using different approaches.

Samples sequenced by STABVIDA (SBV) were processed with QIIME2 v2018.02 [68] and Deblur plugin [69]. The resulting sequences were clustered in operational taxonomic Units (OTUs) and taxonomic assignments were done by scikit-learn naïve Bayes machine learning, which was trained using the SILVA database (version 128) with a clustering threshold of 97% similarity. Samples sequenced by Life Sequencing (LFS) were processed with CUTADAPT 1.8.1 [70] and UCHIME [71] programs. The resulting sequences were clustered in operational taxonomic Units (OTUs) with a threshold of 97%. Those clean FASTA files were BLAST [66] against NCBI 16s rRNA database using BLASTN version 2.2.29+. The resulting XML files were processed using a Python script developed by Life sequencing S.L.-ADM (Paterna, Valencia, Spain) in order to annotate each sequence at different phylogenetic levels.

The Q scores, which represent the probability that a base call is erroneous in a logarithmic base and the Shannon biodiversity index (H'), which indicates the uniformity of species and its abundance in the obtained OTUs were calculated following previously described procedures [22,25] and included as sequence quality indicators.

4.6. Extracellular Hydrolases Test

Biomass from the saltern water samples was harvested by centrifugation at 11,000 rpm and resuspended in the archaea enrichment medium (ATCC 1176 medium). Typically, 5 L of environmental water were centrifuged to obtain 50 mL of culture, which was incubated at 37 °C and 100 rpm for 7 days. The biomass growth was quantified by measuring the O.D. at 580 nm in a UV–Vis spectrophotometer

Ultrospec 3100 pro. Culture media contained (per litre): 10 g Glucose, 156 g NaCl, 13 g $MgCl_2 \cdot 6H_2O$, 20 g $MgSO_4 \cdot 7H_2O$, 1 g $CaCl_2 \cdot 6H_2O$, 4 g KCl, 0.2 g $NaHCO_3$, 0.5 g NaBr, 5 g yeast extract. The pH of medium was adjusted to 7 before autoclaving. After 7 days of growth, the culture was collected by centrifugation at 11,000 rpm and the pellet was resuspended (1/100) using the aforementioned medium. This enriched-concentrated archaea mixture was used to detect different hydrolase activities by platting 20 µL drops of the concentrated biomass on 1% agar plates with the indicated medium supplemented with starch, skim milk, carboxymethylcellulose, bromophenol blue and Tween 80 as substrates to test for α-amylase, protease, cellulase, laccase and lipase activities, respectively.

To test for amylase activity, starch (1% w/v) was added to the glucose-less agar ATCC 1176 medium. After incubation, the plates were flooded with Lugol reagent solution. The presence of a clear zone around the cells indicated starch hydrolysis. The biomass was screened for proteolytic activity by using ATCC 1176 agar medium supplemented with skimmed milk (1% w/v). Protease activity detection was based on the presence of a clear zone around the cells growth due to casein hydrolysis. Screening of cellulase production was done on ATCC 1176 agar medium containing carboxymetylcellulose (0.5% w/v) instead of glucose as carbon source. Plates were flooded with 0.1% Congo red dye for 20 min followed by treatment with 1 M NaCl for 15 min and finally with 1 M HCl for 5 min in order to increase the halo contrast as described by Sazci et al. [72]. The presence of clearance zones around the cells, as a result of carboxymetylcellulose hydrolysis, indicated production of cellulase. Laccase activity assay was carried out on agar Petri dishes containing the ATCC 1176 medium supplemented with the dye bromophenol blue (0.02% w/v), according to Tekere et al. [73]. The formation of discoloration halos around the cells caused by dye degradation showed laccase activity. Lipase activity was screened on nutrient agar plates containing per litre: 10 g peptone, 150 g NaCl, 1 g $CaCl_2 \cdot 2H_2O$ Tween 80 (0.1% v/v). Opaque halos around the cells resulting from the precipitation of calcium oleate revealed lipase activity [74].

All the plates were incubated at 37 °C and the results were checked periodically from the 3th to 10th day of assay, by measuring the diameters of clearance zones or halos around each archaeal drop. All the tests were done in triplicate.

4.7. Growth Inhibition Test

Halocin activity was determined by observing growth inhibition of a presumably susceptible archaea strain. The enriched biomass, obtained as described for hydrolase activities, was tested against *Haloferax lucetense* (CECT 5871), which was purchased from CECT (Spanish Collection of Culture Type). *H. lucetense* was grown on the medium specified by the CECT (MHE 25 Medium; CECT 188) and 1 mL of the culture was completely spread across the surface of a Petri dish. When the plate was totally dried, a 20 µL drop of the enriched biomass was spotlessly placed in the centre of the Petri dish. The inhibition of *H. lucetense* growth was measured by the formation of a clearance zone around the enriched biomass drop added.

Supplementary Materials: The following are available online at http://www.mdpi.com/1660-3397/16/9/332/s1, Table S1: Sequences of the primers used, Table S2: Complete list of sequenced genera.

Author Contributions: For research articles with several authors, a short paragraph specifying their individual contributions must be provided. The following statements should be used "Conceptualization, R.L. and J.V.; Methodology, P.G.-V.; R.L. and J.V.; Software, P.G.-V.; Validation, P.G.-V.; R.L. and J.V.; Investigation, P.G.-V.; Writing-Original Draft Preparation, R.L.; Writing-Review & Editing, P.G.-V.; R.L. and J.V.; Visualization, P.G.-V.; Supervision, R.L. and J.V.; Funding Acquisition, R.L.", please turn to the CRediT taxonomy for the term explanation. Authorship must be limited to those who have contributed substantially to the work reported.

Funding: This research was funded by INTERREG VA España–Portugal (POCTEP) 2014–2020 Cooperation Program, grant number 0055_ALGARED_PLUS_5_E and SUBV. COOP.ALENTEJO-ALGARVE-ANDALUCIA 2017.

Acknowledgments: The authors would like to thank the company Salinas del Odiel S.L. and J. Ariza from the University of Huelva for kindly providing the water samples.

Conflicts of Interest: "The authors declare no conflict of interest." "The funders had no role in the design of the study; in the collection, analyses, or interpretation of data; in the writing of the manuscript and in the decision to publish the results."

References

1. Oren, A. Halophilic microbial communities and their environments. *Curr. Opin. Biotechnol.* **2015**, *33*, 119–124. [CrossRef] [PubMed]
2. Zaremba-Niedzwiedzka, K.; Caceres, E.F.; Saw, J.H.; Backstrom, D.; Juzokaite, L.; Vancaester, E.; Seitz, K.W.; Anantharaman, K.; Starnawski, P.; Kjeldsen, K.U.; et al. Asgard archaea illuminate the origin of eukaryotic cellular complexity. *Nature* **2017**, *541*, 353–358. [CrossRef] [PubMed]
3. Litchfield, C.D. Potential for industrial products from the halophilic Archaea. *J. Ind. Microbiol. Biotechnol.* **2011**, *38*, 1635–1647. [CrossRef] [PubMed]
4. Coker, J.A. Extremophiles and biotechnology: Current uses and prospects. *F1000Research* **2016**, *5*, 396. [CrossRef] [PubMed]
5. Mandelli, F.; Miranda, V.S.; Rodrigues, E.; Mercadante, A.Z. Identification of carotenoids with high antioxidant capacity produced by extremophile microorganisms. *World J. Microbiol. Biotechnol.* **2012**, *28*, 1781–1790. [CrossRef] [PubMed]
6. de la Vega, M.; Sayago, A.; Ariza, J.; Barneto, A.G.; Leon, R. Characterization of a bacterioruberin-producing Haloarchaea isolated from the marshlands of the Odiel river in the southwest of Spain. *Biotechnol. Prog.* **2016**, *32*, 592–600. [CrossRef] [PubMed]
7. Kumar, S.; Karan, R.; Kapoor, S.; Singh, S.P.; Khare, S.K. Screening and isolation of halophilic bacteria producing industrially important enzymes. *Brazilian J. Microbiol.* **2012**, *43*, 1595–1603. [CrossRef]
8. Price, L.B.; Shand, R.F. Halocin S8: A 36-amino-acid microhalocin from the haloarchaeal strain S8a. *J. Bacteriol.* **2000**, *182*, 4951–4958. [CrossRef] [PubMed]
9. Chen, L.; Wang, G.; Bu, T.; Zhang, Y.; Wang, Y.; Liu, M.; Lin, X. Phylogenetic analysis and screening of antimicrobial and cytotoxic activities of moderately halophilic bacteria isolated from the Weihai Solar Saltern (China). *World J. Microbiol. Biotechnol.* **2010**, *26*, 879–888. [CrossRef]
10. Kumar, S.; Grewal, J.; Sadaf, A.; Hemamalini, R.; Khare, S.K. Halophiles as a source of polyextremophilic α-amylase for industrial applications. *AIMS Microbiol.* **2016**, *2*, 1–26. [CrossRef]
11. Oren, A. Industrial and environmental applications of halophilic microorganisms. *Environ. Technol.* **2010**, *31*, 825–834. [CrossRef] [PubMed]
12. Thombre, R.S.; Shinde, V.D.; Oke, R.S.; Dhar, S.K.; Shouche, Y.S. Biology and survival of extremely halophilic archaeon Haloarcula marismortui RR12 isolated from Mumbai salterns, India in response to salinity stress. *Sci. Rep.* **2016**, *6*, 25642. [CrossRef] [PubMed]
13. Bolhuis, H.; Te Poele, E.M.; Rodriguez-Valera, F. Isolation and cultivation of Walsby's square archaeon. *Environ. Microbiol.* **2004**, *6*, 1287–1291. [CrossRef] [PubMed]
14. Martínez-Murcia, A.J.; Acinas, S.G.; Rodriguez-Valera, F. Evaluation of prokaryotic diversity by restrictase digestion of 16S rDNA directly amplified from hypersaline environments. *FEMS Microbiol. Ecol.* **1995**, *17*, 247–255. [CrossRef]
15. Anton, J.; Llobet-Brossa, E.; Rodriguez-Valera, F.; Amann, R. Fluorescence in situ hybridization analysis of the prokaryotic community inhabiting crystallizer ponds. *Environ. Microbiol.* **1999**, *1*, 517–523. [CrossRef] [PubMed]
16. Benlloch, S.; López-López, A.; Casamayor, E.O.; Øvreås, L.; Goddard, V.; Daae, F.L.; Smerdon, G.; Massana, R.; Joint, I.; Thingstad, F.; et al. Prokaryotic genetic diversity throughout the salinity gradient of a coastal solar saltern. *Environ. Microbiol.* **2002**, *4*, 349–360. [CrossRef] [PubMed]
17. Narasingarao, P.; Podell, S.; Ugalde, J.A.; Brochier-Armanet, C.; Emerson, J.B.; Brocks, J.J.; Heidelberg, K.B.; Banfield, J.F.; Allen, E.E. De novo metagenomic assembly reveals abundant novel major lineage of Archaea in hypersaline microbial communities. *Isme J.* **2011**, *6*, 81. [CrossRef] [PubMed]
18. Fernández, A.B.; Vera-Gargallo, B.; Sánchez-Porro, C.; Ghai, R.; Papke, R.T.; Rodriguez-Valera, F.; Ventosa, A. Comparison of prokaryotic community structure from Mediterranean and Atlantic saltern concentrator ponds by a metagenomic approach. *Front. Microbiol.* **2014**, *5*, 196. [CrossRef] [PubMed]

19. DeLong, E.F.; Pace, N.R. Environmental Diversity of Bacteria and Archaea. *Syst. Biol.* **2001**, *50*, 470–478. [CrossRef] [PubMed]
20. Vera-Gargallo, B.; Ventosa, A. Metagenomic Insights into the Phylogenetic and Metabolic Diversity of the Prokaryotic Community Dwelling in Hypersaline Soils from the Odiel Saltmarshes (SW Spain). *Genes* **2018**, *9*, 152. [CrossRef] [PubMed]
21. Burns, D.G.; Camakaris, H.M.; Janssen, P.H.; Dyall-Smith, M.L. Combined use of cultivation-dependent and cultivation-independent methods indicates that members of most haloarchaeal groups in an Australian crystallizer pond are cultivable. *Appl. Environ. Microbiol.* **2004**, *70*, 5258–5265. [CrossRef] [PubMed]
22. Shannon, C.E. A mathematical theory of communication. *Bell Syst. Tech. J.* **1948**, *27*, 379–423. [CrossRef]
23. Thomas, R.H. Molecular Evolution and Phylogenetics. *Heredity* **2001**, *86*, 385. [CrossRef]
24. Antón, J.; Rosselló-mora, R.; Amann, R.; Anto, J. Extremely Halophilic Bacteria in Crystallizer Ponds from Solar Salterns Extremely Halophilic Bacteria in Crystallizer Ponds from Solar Salterns. *Appl. Environ. Microbiol.* **2000**, *66*, 3052–3057. [CrossRef] [PubMed]
25. Keshri, J.; Mishra, A.; Jha, B. Microbial population index and community structure in saline-alkaline soil using gene targeted metagenomics. *Microbiol. Res.* **2013**, *168*, 165–173. [CrossRef] [PubMed]
26. León, M.J.; Aldeguer-Riquelme, B.; Antón, J.; Sánchez-Porro, C.; Ventosa, A. *Spiribacter aquaticus* sp. nov., a novel member of the genus Spiribacter isolated from a saltern. *Int. J. Syst. Evol. Microbiol.* **2017**, *67*, 2947–2952. [CrossRef] [PubMed]
27. Oren, A.; Hallsworth, J.E. Microbial weeds in hypersaline habitats: The enigma of the weed-like *Haloferax mediterranei*. *FEMS Microbiol. Lett.* **2014**, *359*, 134–142. [CrossRef] [PubMed]
28. Oh, D.; Porter, K.; Russ, B.; Burns, D.; Dyall-Smith, M. Diversity of *Haloquadratum* and other haloarchaea in three, geographically distant, Australian saltern crystallizer ponds. *Extremophiles* **2010**, *14*, 161–169. [CrossRef] [PubMed]
29. Dillon, J.G.; Carlin, M.; Gutierrez, A.; Nguyen, V.; McLain, N. Patterns of microbial diversity along a salinity gradient in the Guerrero Negro solar saltern, Baja CA Sur, Mexico. *Front. Microbiol.* **2013**, *4*, 399. [CrossRef] [PubMed]
30. Ventosa, A.; Fernández, A.B.; León, M.J.; Sánchez-Porro, C.; Rodriguez-Valera, F. The Santa Pola saltern as a model for studying the microbiota of hypersaline environments. *Extremophiles* **2014**, *18*, 811–824. [CrossRef] [PubMed]
31. Cray, J.A.; Bell, A.N.W.; Bhaganna, P.; Mswaka, A.Y.; Timson, D.J.; Hallsworth, J.E. The biology of habitat dominance; can microbes behave as weeds? *Microb. Biotechnol.* **2013**, *6*, 453–492. [CrossRef] [PubMed]
32. Çınar, S.; Mutlu, M.B. Comparative analysis of prokaryotic diversity in solar salterns in eastern Anatolia (Turkey). *Extremophiles* **2016**, *20*, 589–601. [CrossRef] [PubMed]
33. Maturrano, L.; Santos, F.; Rosselló-Mora, R.; Antón, J. Microbial diversity in Maras salterns, a hypersaline environment in the Peruvian Andes. *Appl. Environ. Microbiol.* **2006**, *72*, 3887–3895. [CrossRef] [PubMed]
34. Pašić, L.; Bartual, S.G.; Ulrih, N.P.; Grabnar, M.; Velikonja, B.H. Diversity of halophilic archaea in the crystallizers of an Adriatic solar saltern. *FEMS Microbiol. Ecol.* **2005**, *54*, 491–498. [CrossRef] [PubMed]
35. Kambourova, M.; Tomova, I.; Boyadzhieva, I.; Radchenkova, N.; Vasileva-Tonkova, E. Unusually High Archaeal Diversity in a Crystallizer Pond, Pomorie Salterns, Bulgaria, Revealed by Phylogenetic Analysis. *Archaea* **2016**, *2016*. [CrossRef] [PubMed]
36. Klindworth, A.; Pruesse, E.; Schweer, T.; Peplies, J.; Quast, C.; Horn, M.; Glöckner, F.O. Evaluation of general 16S ribosomal RNA gene PCR primers for classical and next-generation sequencing-based diversity studies. *Nucleic Acids Res.* **2013**, *41*, 1–11. [CrossRef] [PubMed]
37. Payá, G.; Bautista, V.; Camacho, M.; Castejón-Fernández, N.; Alcaraz, L.A.; Bonete, M.J.; Esclapez, J. Small RNAs of Haloferax mediterranei: Identification and potential involvement in nitrogen metabolism. *Genes* **2018**, *9*. [CrossRef] [PubMed]
38. Atanasova, N.S.; Pietilä, M.K.; Oksanen, H.M. Diverse antimicrobial interactions of halophilic archaea and bacteria extend over geographical distances and cross the domain barrier. *Microbiologyopen* **2013**, *2*, 811–825. [CrossRef] [PubMed]
39. Charlesworth, J.C.; Burns, B.P. Untapped resources: Biotechnological potential of peptides and secondary metabolites in archaea. *Archaea* **2015**, *2015*. [CrossRef] [PubMed]
40. Baker, G.C.; Smith, J.J.; Cowan, D.A. Review and re-analysis of domain-specific 16S primers. *J. Microbiol. Methods* **2003**, *55*, 541–555. [CrossRef] [PubMed]

41. Gibtan, A.; Park, K.; Woo, M.; Shin, J.K.; Lee, D.W.; Sohn, J.H.; Song, M.; Roh, S.W.; Lee, S.J.; Lee, H.S. Diversity of extremely halophilic archaeal and bacterial communities from commercial salts. *Front. Microbiol.* **2017**, *8*, 1–11. [CrossRef] [PubMed]
42. Gonzalez-Pimentel, J.L.; Miller, A.Z.; Jurado, V.; Laiz, L.; Pereira, M.F.C.; Saiz-Jimenez, C. Yellow coloured mats from lava tubes of La Palma (Canary Islands, Spain) are dominated by metabolically active Actinobacteria. *Sci. Rep.* **2018**, *8*, 1944. [CrossRef] [PubMed]
43. Magurran, A.E. *Measuring Biological Diversity*; John Wiley & Sons, 2013; ISBN 1118687922.
44. Poretsky, R.; Rodriguez-R, L.M.; Luo, C.; Tsementzi, D.; Konstantinidis, K.T. Strengths and limitations of 16S rRNA gene amplicon sequencing in revealing temporal microbial community dynamics. *PLoS ONE* **2014**, *9*. [CrossRef] [PubMed]
45. Fouhy, F.; Clooney, A.G.; Stanton, C.; Claesson, M.J.; Cotter, P.D. 16S rRNA gene sequencing of mock microbial populations-impact of DNA extraction method, primer choice and sequencing platform. *BMC Microbiol.* **2016**, *16*, 1–13. [CrossRef] [PubMed]
46. Amoozegar, M.A.; Siroosi, M.; Atashgahi, S.; Smidt, H.; Ventosa, A. Systematics of haloarchaea and biotechnological potential of their hydrolytic enzymes. *Microbiol.* **2017**, *163*, 623–645. [CrossRef] [PubMed]
47. Schreck, S.D.; Grunden, A.M. Biotechnological applications of halophilic lipases and thioesterases. *Appl. Microbiol. Biotechnol.* **2014**, *98*, 1011–1021. [CrossRef] [PubMed]
48. Gunny, A.A.N.; Arbain, D.; Edwin Gumba, R.; Jong, B.C.; Jamal, P. Potential halophilic cellulases for in situ enzymatic saccharification of ionic liquids pretreated lignocelluloses. *Bioresour. Technol.* **2014**, *155*, 177–181. [CrossRef] [PubMed]
49. Rezaei, S.; Tahmasbi, H.; Mogharabi, M.; Firuzyar, S.; Ameri, A.; Khoshayand, M.R.; Faramarzi, M.A. Efficient decolorization and detoxification of reactive orange 7 using laccase isolated from paraconiothyrium variabile, kinetics and energetics. *J. Taiwan Inst. Chem. Eng.* **2015**, *56*, 113–121. [CrossRef]
50. Vithanage, L.N.G.; Barbosa, A.M.; Borsato, D.; Dekker, R.F.H. Value adding of poplar hemicellulosic prehydrolyzates: Laccase production by *Botryosphaeria rhodina* MAMB-05 and its application in the detoxification of prehydrolyzates. *BioEnergy Res.* **2015**, *8*, 657–674. [CrossRef]
51. Waditee-Sirisattha, R.; Kageyama, H.; Takabe, T. Halophilic microorganism resources and their applications in industrial and environmental biotechnology. *AIMS Microbiol.* **2016**, *2*, 42–54. [CrossRef]
52. Bajpai, B.; Chaudhary, M.; Saxena, J. Production and Characterization of alpha-Amylase from an Extremely Halophilic Archaeon, *Haloferax* sp. HA10. *Food Technol. Biotechnol.* **2015**, *53*, 11–17. [CrossRef] [PubMed]
53. Santorelli, M.; Maurelli, L.; Pocsfalvi, G.; Fiume, I.; Squillaci, G.; La Cara, F.; Del Monaco, G.; Morana, A. Isolation and characterisation of a novel alpha-amylase from the extreme haloarchaeon *Haloterrigena turkmenica*. *Int. J. Biol. Macromol.* **2016**, *92*, 174–184. [CrossRef] [PubMed]
54. Uzyol, K.S.; Akbulut, B.S.; Denizci, A.A.; Kazan, D. Thermostable a-amylase from moderately halophilic *Halomonas* sp. AAD21. *Turk. J. Biol.* **2012**, *36*, 327–338. [CrossRef]
55. Camacho, R.M.; Mateos, J.C.; Gonzalez-Reynoso, O.; Prado, L.A.; Cordova, J. Production and characterization of esterase and lipase from *Haloarcula marismortui*. *J. Ind. Microbiol. Biotechnol.* **2009**, *36*, 901–909. [CrossRef] [PubMed]
56. Akolkar, A.V.; Deshpande, G.M.; Raval, K.N.; Durai, D.; Nerurkar, A.S.; Desai, A.J. Organic solvent tolerance of *Halobacterium* sp. SP1 (1) and its extracellular protease. *J. Basic Microbiol.* **2008**, *48*, 421–425. [CrossRef] [PubMed]
57. Ruiz, D.M.; De Castro, R.E. Effect of organic solvents on the activity and stability of an extracellular protease secreted by the haloalkaliphilic archaeon *Natrialba magadii*. *J. Ind. Microbiol. Biotechnol.* **2007**, *34*, 111–115. [CrossRef] [PubMed]
58. Wang, C.-Y.; Hsieh, Y.-R.; Ng, C.-C.; Chan, H.; Lin, H.-T.; Tzeng, W.-S.; Shyu, Y.-T. Purification and characterization of a novel halostable cellulase from *Salinivibrio* sp. strain NTU-05. *Enzyme Microb. Technol.* **2009**, *44*, 373–379. [CrossRef]
59. Simankova, M.V.; Chernych, N.A.; Osipov, G.A.; Zavarzin, G.A. *Halocella cellulolytica* gen. nov., sp. nov., a new obligately anaerobic, halophilic, cellulolytic bacterium. *Syst. Appl. Microbiol.* **1993**, *16*, 385–389. [CrossRef]
60. Yu, H.-Y.; Li, X. Alkali-stable cellulase from a halophilic isolate, *Gracilibacillus* sp. SK1 and its application in lignocellulosic saccharification for ethanol production. *Biomass Bioenergy* **2015**, *81*, 19–25. [CrossRef]

61. Uthandi, S.; Saad, B.; Humbard, M.A.; Maupin-Furlow, J.A. LccA, an archaeal laccase secreted as a highly stable glycoprotein into the extracellular medium by *Haloferax volcanii*. *Appl. Environ. Microbiol.* **2010**, *76*, 733–743. [CrossRef] [PubMed]
62. Rezaie, R.; Rezaei, S.; Jafari, N.; Forootanfar, H.; Khoshayand, M.R.; Faramarzi, M.A. Delignification and detoxification of peanut shell bio-waste using an extremely halophilic laccase from an *Aquisalibacillus elongatus* isolate. *Extremophiles* **2017**, *21*, 993–1004. [CrossRef] [PubMed]
63. Gantner, S.; Andersson, A.F.; Alonso-Sáez, L.; Bertilsson, S. Novel primers for 16S rRNA-based archaeal community analyses in environmental samples. *J. Microbiol. Methods* **2011**, *84*, 12–18. [CrossRef] [PubMed]
64. Muyzer, G.; de Waal, E.C.; Uitterlinden, A.G. Profiling of complex microbial populations by denaturing gradient gel electrophoresis analysis of polymerase chain reaction-amplified genes coding for 16S rRNA. *Appl. Environ. Microbiol.* **1993**, *59*, 695–700. [PubMed]
65. Teske, A.; Wawer, C.; Muyzer, G.; Ramsing, N.B. Distribution of sulfate-reducing bacteria in a stratified fjord (Mariager Fjord, Denmark) as evaluated by most-probable-number counts and denaturing gradient gel electrophoresis of PCR-amplified ribosomal DNA fragments. *Appl. Environ. Microbiol.* **1996**, *62*, 1405–1415. [PubMed]
66. Altschul, S.F.; Gish, W.; Miller, W.; Myers, E.W.; Lipman, D.J. Basic local alignment search tool. *J. Mol. Biol.* **1990**, *215*, 403–410. [CrossRef]
67. Zhang, J.; Kobert, K.; Flouri, T.; Stamatakis, A. PEAR: A fast and accurate Illumina Paired-End reAd mergeR. *Bioinformatics* **2014**, *30*, 614–620. [CrossRef] [PubMed]
68. Caporaso, J.G.; Kuczynski, J.; Stombaugh, J.; Bittinger, K.; Bushman, F.D.; Costello, E.K.; Fierer, N.; Pena, A.G.; Goodrich, J.K.; Gordon, J.I.; et al. QIIME allows analysis of high-throughput community sequencing data. *Nat. Methods* **2010**, *7*, 335–336. [CrossRef] [PubMed]
69. Amir, A.; McDonald, D.; Navas-Molina, J.A.; Kopylova, E.; Morton, J.T.; Zech Xu, Z.; Kightley, E.P.; Thompson, L.R.; Hyde, E.R.; Gonzalez, A.; et al. Deblur Rapidly Resolves Single-Nucleotide Community Sequence Patterns. *mSystems* **2017**, *2*. [CrossRef] [PubMed]
70. Martin, M. Cutadapt removes adapter sequences from high-throughput sequencing reads. *EMBnet.journal* **2011**, *17*, 10. [CrossRef]
71. Edgar, R.C.; Haas, B.J.; Clemente, J.C.; Quince, C.; Knight, R. UCHIME improves sensitivity and speed of chimera detection. *Bioinformatics* **2011**, *27*, 2194–2200. [CrossRef] [PubMed]
72. Sazci, A.; Erenler, K.; Radford, A. Detection of cellulolytic fungi by using Congo red as an indicator: A comparative study with the dinitrosalicyclic acid reagent method. *J. Appl. Bacteriol.* **1986**, *61*, 559–562. [CrossRef]
73. Tekere, M.; Mswaka, A.Y.; Zvauya, R.; Read, J.S. Growth, dye degradation and ligninolytic activity studies on Zimbabwean white rot fungi. *Enzym. Microb. Technol.* **2001**, *28*, 420–426. [CrossRef]
74. Lanka, S.; Latha, J.N.L. A short review on various screening methods to isolate potential lipase producers: Lipases-the present and future enzymes of biotech industry. *Int. J. Biol. Chem.* **2015**, *9*, 207–219. [CrossRef]

Supplementary material

Table S1. Sequences of the primers used.

Target	Name	Sequence	Reference
Bacterial 16S rRNA	341F	CCTACGGGAGGCAGCAG	Muyzer et al., 1993
	907R	CCGTCAATTCMTTTGAGTTT	Teske et al., 1996
Archaeal 16S rRNA	Arc340F	CCCTAYGGGGYGCASCAG	Grantner 2011
	Arc1000R	GGCCATGCACYWCYTCTC	De la Vega et al., 2016
V3-V4 16SrRNA	IlluAdp16SF	CCTACGGGNGGCWGCAG	Klindworth et al., 2013
hypervariable regions	IlluAdp16SR	GACTACHVGGGTATCTAATCC	

Table S2. Percentage of the microbial genera found in the two replicates for each sequencing service

LFS-1

Genera	Percentage %
Salinibacter	38.523
Halorubrum	13.077
Haloquadratum	9.023
Halonotius	7.895
Halobellus	3.73
Natronomonas	3.447
Haloplanus	3.045
Halohasta	2.957
No Hit	1.766
Halomicroarcula	1.541
Salinivenus	1.436
Cluster 1274	1.339
Cluster 468	1.305
Halovenus	1.276
Cluster 450	1.043
Halomicrobium	0.857
Halorientalis	0.794
Haloarcula	0.752
Halosimplex	0.664
Cluster 69	0.545
Cluster 356	0.283
Cluster 20	0.283
Halanaeroarchaeur	0.275
Cluster 452	0.258
Salarchaeum	0.253
Halovarius	0.182
Cluster 470	0.161
Cluster 469	0.148
Cluster 317	0.135
Cluster 482	0.131
Cluster 451	0.127
Arhodomonas	0.122
Halobaculum	0.113
Spiribacter	0.093
Cluster 1280	0.089
Cluster 37	0.076
Cluster 454	0.068
Cluster 401	0.068
Halorhabdus	0.068
Bacteroides	0.062
Cluster 1278	0.063
Blautia	0.06
Cluster 368	0.059
Cluster 360	0.059
Halorubellus	0.055
Halalkalicoccus	0.05

Cluster 512	0.051
Cluster 64	0.051
Cluster 475	0.051
Cluster 1285	0.051
Halapricum	0.046
Cluster 461	0.046
Cluster 462	0.046
Nevskia	0.042
Limimonas	0.042
Cluster 474	0.042
Aliifodinibius	0.042
Eubacterium	0.038
Roseivivax	0.038
Salinigranum	0.034
Cluster 457	0.034
Butyrivibrio	0.034
Halococcus	0.034
Cluster 473	0.03
Cluster 75	0.03
Faecalibacterium	0.03
Cluster 1286	0.03
Cluster 561	0.03
Rhodovibrio	0.03
Cluster 1293	0.03
Halolamina	0.029
Cluster 319	0.03
Alcanivorax	0.03
Halogeometricum	0.025
Salinirubrum	0.025
Haloferax	0.021
Halanaerobium	0.021
Lactobacillus	0.021
Psychroflexus	0.017
Butyricicoccus	0.017
Flintibacter	0.017
Fimbriiglobus	0.017
Prevotella	0.013
ascolarctobacteriu	0.013
Coprococcus	0.012
Bradyrhizobium	0.013
Oscillibacter	0.013
Halobacterium	0.013
Dactylococcopsis	0.013
Halobiforma	0.012
Roseburia	0.013
Parabacteroides	0.012
Akkermansia	0.013
Azoarcus	0.008
Acinetobacter	0.008
Halomonas	0.008

Salisaeta	0.008
Faecalibaculum	0.008
Reyranella	0.008
Halarchaeum	0.008
Coraliomargarita	0.008
Clostridium	0.008
Halogranum	0.008
Halopelagius	0.008
Lachnoclostridium	0.008
Alistipes	0.008
Longibacter	0.008
Collinsella	0.008
Anaerotaenia	0.008
Novosphingobium	0.008
Halodesulfurarchaeu	0.008
Bryobacter	0.008
Sphingomonas	0.004
Murimonas	0.004
Ruminococcus	0.004
Flexistipes	0.004
Haloarchaeobius	0.004
Halopeptonella	0.004
Anaerotignum	0.004
Ruminiclostridium	0.004
Guyparkeria	0.004
Heliimonas	0.004
Halosiccatus	0.004
Corynebacterium	0.004
Fusicatenibacter	0.004
Halanaerobaculum	0.004
Delftia	0.004
Weissella	0.004
Caulobacter	0.004
Natrinema	0.004
Chryseolinea	0.004
Desulfosporosinus	0.004
Planctopirus	0.004
Clostridia;[3]Clostri	0.004
Barnesiella	0.004
Microbacterium	0.004
Herbiconiux	0.004
Alkalispirillum	0.004
Singulisphaera	0.004
Bacillus	0.004
Pseudomonas	0.004
Longimonas	0.004
Halanaerobacter	0.004
Moraxella	0.004
Streptococcus	0.004

LFS-2

Genera	Percentage %
Salinibacter	32.645
Halorubrum	14.139
Haloquadratum	9.462
Halonotius	8.344
Halobellus	4.057
Haloplanus	3.608
Halohasta	3.574
Natronomonas	3.319
Cluster 355	1.865
Halomicroarcula	1.846
Cluster 307	1.723
No Hit	1.503
Cluster 303	1.502
Halorientalis	1.129
Halomicrobium	1.065
Salinivenus	0.939
Halosimplex	0.887
Halovenus	0.823
Haloarcula	0.514
Salinirubrum	0.37
Cluster 420	0.361
Cluster 21	0.309
Cluster 321	0.279
Cluster 306	0.273
alanaeroarchaeur	0.252
Cluster 465	0.247
Halovarius	0.238
Salarchaeum	0.236
Cluster 316	0.187
Cluster 480	0.173
Cluster 2204	0.162
Halobaculum	0.138
Cluster 463	0.127
Cluster 478	0.122
Cluster 256	0.122
Arhodomonas	0.116
Cluster 427	0.1
Halalkalicoccus	0.101
Cluster 304	0.1
Halapricum	0.096
Halorhabdus	0.09
Salinigranum	0.086
Cluster 88	0.083
Cluster 49	0.082
Halorubellus	0.076
Cluster 123	0.062
Cluster 421	0.06
Cluster 323	0.059

Cluster 354	0.057
Haladaptatus	0.056
Cluster 486	0.056
Spiribacter	0.053
Cluster 437	0.052
Cluster 150	0.051
Cluster 521	0.045
Cluster 428	0.045
Cluster 57	0.043
Alcanivorax	0.043
Fimbriiglobus	0.042
Cluster 513	0.034
Halococcus	0.032
Limimonas	0.032
Cluster 258	0.032
Cluster 485	0.031
Aliifodinibius	0.031
Cluster 967	0.029
Cluster 452	0.029
Halolamina	0.03
Cluster 2221	0.028
Cluster 474	0.026
Cluster 1074	0.026
Faecalibacterium	0.026
Cluster 446	0.026
Cluster 102	0.026
Haloferax	0.028
Cluster 476	0.025
Cluster 113	0.025
Cluster 2207	0.025
Cluster 2231	0.025
Cluster 831	0.023
Cluster 431	0.023
Bacteroides	0.025
Cluster 1009	0.023
Cluster 479	0.022
Halogeometricum	0.022
Cluster 555	0.022
Cluster 158	0.022
Cluster 509	0.02
Cluster 472	0.02
Halobacterium	0.021
Cluster 582	0.02
Cluster 508	0.02
Cluster 116	0.019
Cluster 432	0.019
Cluster 637	0.019
Cluster 783	0.019
Prevotella	0.019
Cluster 109	0.017

Cluster 617	0.017
Cluster 576	0.017
Lactobacillus	0.018
Cluster 557	0.017
Cluster 502	0.015
Halogranum	0.015
Cluster 488	0.015
Cluster 2719	0.015
Cluster 348	0.015
Halopelagius	0.016
Reyranella	0.016
Cluster 985	0.015
Cluster 1682	0.015
Cluster 1253	0.015
Cluster 497	0.015
Cluster 2278	0.015
Halanaerobium	0.015
Cluster 2266	0.015
Cluster 2214	0.014
Cluster 811	0.014
Cluster 475	0.014
Cluster 501	0.014
lodesulfurarchaeu	0.014
Halorussus	0.012
Rhodovibrio	0.012
Cluster 495	0.012
Halobiforma	0.012
Dactylococcopsis	0.012
Nevskia	0.012
Cluster 433	0.012
Cluster 422	0.011
Cluster 579	0.011
Cluster 571	0.011
Paludibaculum	0.011
Ruminococcus	0.012
Cluster 112	0.011
Cluster 2240	0.011
Cluster 155	0.011
Blautia	0.012
Halomarina	0.011
Acinetobacter	0.008
Lacibacterium	0.008
ostridia;[3]Clostri	0.008
Paracoccus	0.008
Oscillibacter	0.008
Halarchaeum	0.008
Psychroflexus	0.007
Alistipes	0.007
Halomonas	0.007
Lachnoclostridium	0.007

Longibacter	0.006
Microbacterium	0.006
Streptococcus	0.007
Novosphingobium	0.006
Roseivivax	0.007
Planctopirus	0.006
Dorea	0.006
Aquabacterium	0.005
Haemophilus	0.005
Sphingomonas	0.005
Halopenitus	0.005
Donghicola	0.005
Bradyrhizobium	0.005
Halanaerobacter	0.005
Roseovarius	0.005
Azoarcus	0.005
Ralstonia	0.005
Singulisphaera	0.005
Stenotrophomona	0.005
Pseudomonas	0.005
Massilia	0.003
Scopulibacillus	0.003
Caulobacter	0.003
Agrobacterium	0.003
Celeribacter	0.003
Anaerotaenia	0.003
Slackia	0.003
Chryseolinea	0.003
Roseburia	0.003
Collinsella	0.003
Haloarchaeobius	0.003
Veillonella	0.003
Anaerobacillus	0.003
Halobium	0.003
Steroidobacter	0.003
Ochrobactrum	0.003
Zavarzinella	0.002
Halostella	0.002
Marinobacter	0.002
Acetitomaculum	0.002
Fusicatenibacter	0.002
Enterorhabdus	0.002
Acidipila	0.002
Actinomyces	0.002
Gemmiger	0.002
Alkalilimnicola	0.002
Alloprevotella	0.002
Agathobacter	0.002
Clostridium	0.002
Thioalkalivibrio	0.002

Moraxella	0.002
Delftia	0.002
Heliimonas	0.002
Halocella	0.002
Longimonas	0.002
Herbinix	0.002
Marinilabilia	0.002
Comamonas	0.002
Bifidobacterium	0.002
Rheinheimera	0.002
Eubacterium	0.002
Eisenbergiella	0.002
Tabrizicola	0.002
Pseudohongiella	0.002
Cetobacterium	0.002
Muricomes	0.002
Butyricimonas	0.002
Flexistipes	0.002
Ruminiclostridium	0.002
Barnesiella	0.002
Salisaeta	0.002
Roseospirillum	0.002
Dialister	0.002
Longibaculum	0.002
Geotoga	0.002
Taibaiella	0.002
Wenzhouxiangella	0.002
Natronococcus	0.002
Halosiccatus	0.002
seudoflavonifracto	0.002
Marseilla	0.002
Brevundimonas	0.002
Romboutsia	0.002
Desulfovermiculus	0.002
Halorhodospira	0.002
Halanaerobaculum	0.002
Hydrogenovibrio	0.002
Rhizobium	0.002
Gracilimonas	0.002
Negativibacillus	0.002
Puniceicoccus	0.002
Thioprofundum	0.002
Bryobacter	0.002
Alkalispirillum	0.002
Desulfonatronum	0.002

SBV-1

Genera	Percentage %
Salinibacter	37.289
Halorubrum	18.792
Haloquadratum	18.012
Halonotius	7.809
Halobellus	3.692
Natronomonas	3.33
Halobacteriaceae NC	3.153
Halapricum	2.187
Halococcus	1.45
Nanohaloarchaeon NC	1.181
Haloarcula	0.713
Haloplanus	0.713
Halobacteria NC	0.448
Others	0.445
Halovenus	0.31
Sphingobacteriales NC	0.193
Halohasta	0.12
Halobaculum	0.088
Halosimplex	0.055
Halorubellus	0.02

SBV-2

Genera	Percentage %
Salinibacter	42.601
Halorubrum	16.123
Haloquadratum	14.798
Halonotius	9.147
Halobellus	3.527
Natronomonas	3.481
NA Halobacteriaceae	3.255
Halapricum	1.976
Halococcus	1.362
Haloplanus	0.819
Haloarcula	0.706
Haloarchaea NC	0.676
Halobacteriaceae	0.43
Halovenus	0.287
NA Bacteria	0.225
Halohasta	0.097
Gemmata	0.077
Others	0.413

Chapter 2

Antioxidant, Antimicrobial, and Bioactive Potential of Two New Haloarchaeal Strains Isolated from Odiel Salterns (Southwest Spain)

This chapter has been published as: **Gómez-Villegas, P.**; Vigara, J.; Vila, M.; Varela, J.; Barreira, L.; Léon, R. Antioxidant, Antimicrobial, and Bioactive Potential of Two New Haloarchaeal Strains Isolated from Odiel Salterns (Southwest Spain). *Biology* 2020, *9*, 298. https://doi.org/10.3390/biology9090298

biology

MDPI

Article

Antioxidant, Antimicrobial, and Bioactive Potential of Two New Haloarchaeal Strains Isolated from Odiel Salterns (Southwest Spain)

Patricia Gómez-Villegas [1], Javier Vigara [1], Marta Vila [1], João Varela [2], Luísa Barreira [2] and Rosa Léon [1,*]

1 Laboratory of Biochemistry, Department of Chemistry, University of Huelva, Avda. de las Fuerzas Armadas s/n, 21071 Huelva, Spain; patgomvil@gmail.com (P.G.-V.); vigara@uhu.es (J.V.); marta.vila@dpcm.uhu.es (M.V.)

2 Centre of Marine Sciences, University of Algarve, Campus of Gambelas, 8005-139 Faro, Portugal; jvarela@ualg.pt (J.V.); lbarreir@ualg.pt (L.B.)

* Correspondence: rleon@uhu.es; Tel.: +34-95-921-9951

Received: 15 August 2020; Accepted: 17 September 2020; Published: 18 September 2020

Simple Summary: Halophilic archaea are microorganisms that inhabit in extreme environments for life, under salt saturation, high temperature and elevated UV radiation. The interest in these microorganisms lies on the properties of their molecules, that present high salt and temperature tolerance, as well as, antioxidant power, being an excellent source of compounds for several biotechnological applications. However, the bioactive properties from haloarcahaea remain scarcely studied compared to other groups as plants or algae, usually reported as good health promoters. In this work we describe the isolation and the molecular identification of two new haloarchaeal strains from Odiel salterns (SW Spain), and the antioxidant, antimicrobial and bioactive potential of their extracts. The results revealed that the extracts obtained with acetone presented the highest activities in the antioxidant, antimicrobial and anti-inflammatory assays, becoming a promising source of metabolites with applied interest in pharmacy, cosmetics and food industry.

Abstract: The need to survive in extreme environments has furnished haloarchaea with a series of components specially adapted to work in such conditions. The possible application of these molecules in the pharmaceutical and industrial fields has received increasing attention; however, many potential bioactivities of haloarchaea are still poorly explored. In this paper, we describe the isolation and identification of two new haloarchaeal strains from the saltern ponds located in the marshlands of the Odiel River, in the southwest of Spain, as well as the in vitro assessment of their antioxidant, antimicrobial, and bioactive properties. The acetone extract obtained from the new isolated *Haloarcula* strain exhibited the highest antioxidant activity, while the acetone extracts from both isolated strains demonstrated a strong antimicrobial activity, especially against other halophilic microorganisms. Moreover, these extracts showed a remarkable ability to inhibit the enzyme cyclooxygenase-2 and to activate the melanogenic enzyme tyrosinase, indicating their potential against chronic inflammation and skin pigmentation disorders. Finally, the aqueous protein-rich extracts obtained from both haloarchaea exhibited an important inhibitory effect on the activity of the acetylcholinesterase enzyme, involved in the hydrolysis of cholinergic neurotransmitters and related to several neurological diseases.

Keywords: antioxidant; anti-inflammatory; antimicrobial; bioactive substances; haloarchaea

1. Introduction

Halophilic archaea or haloarchaea are a group of extremophilic microorganisms inhabiting hypersaline environments, such as salt lakes and salterns. They thrive in harsh conditions for life, including low water availability, high salt concentration, and elevated solar irradiance, which implies high temperature and ultra-violet (UV) radiation [1,2]. The biotechnological interest in the haloarchaeal group has increased due to their ability to produce a wide variety of compounds such as exopolysaccharides, carotenoids, and proteins adapted to work in such extreme conditions. The tolerance of these enzymes to elevated saline concentrations and temperatures, the high antioxidant power and therapeutic potential of haloarchaeal carotenoids or the good jellifying properties and thermal stability of the exopolysacharides secreted by many archaea make these metabolites highly appreciated for numerous biotechnological applications, including biomedical, pharmaceutical, cosmetic, environmental or industrial purposes [3,4]. Furthermore, considering that only a small part of the existing archaeal species has been discovered and studied, it is expected that many other metabolites with unexplored bioactivities can be obtained from this extraordinary group of microorganisms, as pointed in recent reviews [5].

Haloarchaea have shown to be particularly suitable for the production of extremozymes, which can tolerate high temperatures and saturating salt concentrations, conditions required in food, detergent and textile sectors [6,7]. In addition, a common feature within the haloarchaeal group is their ability to secrete halocins, which are peptides or proteins able to inhibit the growth of susceptible microorganisms living in the same habitat [8,9]. These molecules are also resistant to extreme conditions and could be a source of new antimicrobial compounds. Moreover, most haloarchaea can produce and accumulate carotenoids, which are responsible for their red color. Carotenoids are antioxidant compounds with an important role as human health enhancers, and it is widely known that their regular consumption helps to prevent many degenerative diseases, such as neurodegeneration, cancer, cardiovascular diseases, macular degeneration and cataracts [10,11].

Carotenoids from haloarchaea have shown anticancer and antihemolytic activities [12], and the ability to increase sperm cells viability after cryopreservation [13]. Furthermore, many natural carotenoids are used as food preservatives and pharmaceutical and cosmetic compounds due to their antioxidant and pro-vitamin properties [14]. Bacterioruberin (BR) and its derivatives, monoanhydrobacterioruberin (MABR) and bisanhydrobacterioruberin (BABR), are the main carotenoids synthesized by halophilic archaea [15–17]. These carotenoids have 50 carbon atoms (C_{50}) and possess a longer system of conjugated double bonds than the C_{40} carotenoids usually found in other organisms such as plants, microalgae, fungi and bacteria [14]. Some C_{40} carotenoids, such as phytoene, lycopene and β-carotene have also been found in haloarchaea, but at such low quantities that they have been proposed as metabolic intermediates for the biosynthesis of C_{50} carotenoids [18,19]. Even though carotenoids play a unique important role in cell protection against oxidative damage, bacterioruberin appears also to be a stabilizer of the cell membrane under osmotic stress [20]. Because of the structure of bacterioruberin, it can be inferred that its antioxidant potential might be even higher than that of β-carotene, due to the fact that it has 13 conjugated double bonds and four hydroxyl groups, compared to the 9 conjugated double bonds and none hydroxyl group of β-carotene [16]. For those reasons, the antioxidant power of haloarchaeal extracts and their potential as alternative to current food preservatives and as drug leads should be more deeply studied.

Pigments from different kinds of marine microorganisms have shown effective antibacterial properties. Examples of this are the red pigment prodigiosin, isolated from the sponge-associated bacterium *Serratia marcescens* [21]; or the chlorophyll a derivatives obtained from the microalga *Isochrysis galbana* [22]. Recently, the antimicrobial activity of pigments from some halophilic bacteria has been tested against bacteria and fungi [23]; however, so far, the studies about the antimicrobial activity of haloarchaeal pigments or extracts thereof are scarce [19,24].

The main aim of this work is to explore the bioactive properties of different extracts obtained from two new strains of haloarchaea isolated from the Odiel solar saltern (SW Spain), focusing on their

antioxidant and antimicrobial activities; and their capability to modulate the activity of disease-related enzymes involved in melanin biosynthesis, neurological degeneration, carbohydrate metabolism, and inflammatory response, through in vitro assays.

2. Materials and Methods

2.1. Sample Collection

Water samples were collected from a crystallizer pond located in the natural reserve of the Odiel Marshlands, in the southwest of Spain (Latitude: 37.2395, longitude: −6.95287). The ionic composition and the physicochemical parameters of the water brine were determined by the standard methods, as previously reported [20].

2.2. Archaea Isolation

The biomass from 2 L of the collected water samples was harvested by centrifugation at 19,800× *g*, resuspended in 20 mL of archaeal medium (ATCC 1176 medium) and used for the isolation of archaeal colonies on agar plates. Typically, 1 mL of serial dilution corresponding to 1:10, 1:100 and 1:1000 were spread on agar medium containing 20% of salt. After incubation at 37 °C for 15 days, red and pink colonies were visible. Selected colonies were purified by at least three streaking rounds on fresh agar plates. The isolates were preserved in 20% glycerol (w/v) at −80 °C for further use.

2.3. Preliminary Selection of Archaeal Strains with Antimicrobial Activity

Halocin activity was determined by observing growth inhibition of the archaea *Haloferax lucetense* (CECT 5871), which was purchased from CECT (Spanish Collection of Culture Type, Valencia, Spain) and whose susceptibility to the halocin activity of the species inhabiting Odiel salterns was previously probed [25]. *H. lucetense* was grown on the medium specified by the CECT (MHE 25 Medium; CECT 188), and 1 mL of the culture was completely spread across the surface of a Petri dish. When the plate was totally dried, a 20 µL drop of the culture of each previously isolated colony was spotlessly placed onto the Petri dish. The inhibition of *H. lucetense* growth was measured by the formation of a clearance zone around each drop added.

2.4. Identification of the Selected Microorganisms

Genomic DNA of each strain was extracted using the GeneJET Genomic Purification kit (Thermo Fisher Scientific, Waltham, MA, USA), following the manufacturer's instructions. Quantification of the genomic DNA obtained, and the assessment of its purity was done on a Nanodrop Spectrophotometer ND-1000 (Thermo Fisher Scientific). The full length of the 16S rRNA encoding gene was amplified with the archaeal specific primers 21F (5'-TTCCGGTTGATCCTGCCGGA-3') and 1492R (5'-GGTTACCTTGTTACGACTT-3'). Polymerase chain reactions (PCR) were performed in a total volume of 25 µL containing: 1 µL of genomic DNA, 10 pM of each primer, 0.2 mM dNTPs, 0.2 U REDTaq®DNA polymerase from Sigma Aldrich (St. Louis, Missouri, USA) 2.5 µL of specific 10X buffer and 1.5 µL of 2.5 mM $MgCl_2$ buffer using an Eppendorf thermo-cycler. The thermal profile corresponded to 0.5 min at 96 °C, 0.5 min at 55 °C and 1 min at 72 °C for 30 cycles, followed by 10 min of final primer extension. The PCR products were analyzed by electrophoresis on a 1 % agarose gel to check their quality and sent to Stabvida (Lisbon, Portugal) for Sanger sequencing. The 1.4 kb 16S rRNA gene sequences obtained were compared to those available at the GenBank and the European Molecular Biology Laboratory (EMBL) databases using advanced Basic Local Alignment Search Tool (BLAST), Megablast and BLASTn, searches at the National Center for Biotechnology Information (NCBI) [26].

2.5. Archaeal Culture Conditions

The medium used for haloarchaeal growth contained (per liter): 10 g glucose, 156 g NaCl, 13 g $MgCl_2 \cdot 6H_2O$, 20 g $MgSO_4 \cdot 7H_2O$, 1 g $CaCl_2 \cdot 6H_2O$, 4 g KCl, 0.2 g $NaHCO_3$, 0.5 g NaBr and 5 g yeast extract. The pH was adjusted to 7 before autoclaving. The cultures were incubated in Erlenmeyer flasks at 37 °C at 100 rpm for one week.

2.6. Preparation of Archaeal Extracts

When cultures reached the stationary phase of growth, 1 L of each culture was collected by centrifugation at 19,800× *g* for 30 min at 4 °C. The obtained cellular pellets were subjected to five freezing-unfreezing cycles, by successive 1 min immersions in liquid nitrogen/hot water (60 °C). The obtained cell lysates were treated overnight with 100 mL of cold acetone (−20 °C) in the dark. Then, acetone extracts were centrifuged at 4 °C and 19,800× *g* for 30 min. The resulting pellet, containing the proteins precipitated with cold acetone and the acetone supernatant, containing carotenoids and other lipophilic compounds, were dried in a rotary vacuum evaporator and freeze-dried for further study. The total content of carotenoids in acetone extracts was determined by measuring the absorbance of the sample at 494 nm in a cuvette with a 1 cm path length and using the specific absorption coefficient $E_1{}^{1\%} = 2500$ (100 mL g^{-1} cm^{-1}) according to Hiyana et al. [27]. Similarly, the concentration of proteins in the acetone precipitated extracts, hereinafter called aqueous extract, was determined by Bradford's method [28].

Potential bioactive compounds excreted into the culture medium by the selected archaea were recovered from 500 mL of each culture medium by successive liquid/liquid extractions with 50 mL of four organic solvents in this order: hexane, dichloromethane, ethyl acetate, and chloroform. The extraction with each solvent was repeated three times. All the fractions were evaporated to dryness in a rotary evaporator under reduced pressure at 50 °C, freeze-dried, and stored until further use.

2.7. Antioxidant Activity Assays

Different assays were conducted to test the antioxidant activity of archaea cell extracts and all the extracellular extracts obtained from the culture medium, as previously described. Each freeze-dried extract was homogenized and dissolved in DMSO (at 10 mg mL^{-1}) except for the acetone precipitate, which was resuspended in phosphate-buffered saline (PBS) buffer. All samples were tested at a concentration of 1 mg mL^{-1}. Butylated hydroxytoluene (BHT, 1 mg mL^{-1}) was used as positive control in the 1,1-Diphenyl-2-picrylhydrazyl (DPPH), 2,2′-azino-bis(3-ethylbenzothiazoline-6-sulfonic acid (ABTS) and nitric oxide (NO) radical scavenging assays, and in the ferrocyanide reduction potential (FRP), while the metal chelator EDTA (1 mg mL^{-1}) was employed as positive control in the copper (CCA) and iron (ICA) chelating assays. The solvent employed to dissolve the extracts (DMSO or PBS) was used as negative control. All the measurements were carried out at least six times on 96-well plates. The radical scavenging activity was expressed as percent of inhibition relative to the negative control, following the formula:

$$\%\ Scavenging\ activity = 100 - \frac{Abs\ sample \times 100}{Abs\ negative\ control}$$

When the activity of a sample was higher than 65%, the concentration of the extract providing 50% reduction of the radical scavenging activity (IC_{50} or EC_{50}) was calculated by sigmoidal fitting of the data, using the GraphPad Prism 6 program. These values were calculated from a graph built by plotting the log of the radical scavenging activity (%) against the normalized sample concentration, according to the concentration of proteins or carotenoids in the extracts.

2.7.1. DPPH Assay

1,1-Diphenyl-2-picrylhydrazyl radical scavenging assay was performed by the method of Sachindra et al. [29] with some modifications. A solution of DPPH 0.12 mM was prepared in methanol; 200 µL of this DPPH solution were mixed with 22 µL of each extract solution. The absorbance decrease at 517 nm was recorded in a microplate reader, after incubation at 25 °C for 30 min in the dark. A color control prepared with 200 µL of methanol and 22 µL of each extract sample was included in all the assays.

2.7.2. ABTS Assay

Free radical scavenging activity of the extracts was determined by the $ABTS^+$ (2,2′-azino-bis (3-ethylbenzothiazoline-6-sulfonic acid)) radical cation decolorization assay [30]. $ABTS^+$ cation radical was generated by the reaction between ABTS (7 mM in water) and potassium persulfate (2.5 mM), in the dark at room temperature for 12–16 h. The $ABTS^+$ solution was then diluted with methanol to obtain an absorbance of 0.700 at 734 nm. After the addition of 10 µL of each extract to 190 µL of the diluted $ABTS^+$ solution, the samples were incubated for 6 min in the dark and the absorbance at 734 nm was measured after the incubation.

2.7.3. Nitric Oxide (NO) Assay

The capacity to scavenge the free radical NO was evaluated according to Baliga et al. [31]. Briefly, 50 µL of extracts were mixed with 50 µL of sodium nitroprusside (10 mM in PBS) and incubated for 90 min at room temperature before adding 50 µL of Griess reagent. After that, the absorbance was measured at 546 nm.

2.7.4. Ferrocyanide Reducing Power (FRP) Assay

The reducing power assay was performed according to Tundis et al. [32]. The assay solution was prepared by mixing 50 µL of sample solution, 50 µL of distilled water and 50 µL of potassium ferrocyanide (1%). After 20 min of incubation, 50 µL of TCA (10%) and 10 µL of $FeCl_3$ (0.1%) were added and the mix was incubated 10 min before measuring the absorbance at 700 nm.

2.7.5. Metal Chelating Activity on Iron and Copper Ions

Both assays were conducted according to Megías et al. [33]. Iron chelating activity (ICA) was determined by measuring the formation of the Fe^{2+}-ferrozine, by measuring the absorbance at 562 nm. Copper chelating activity (CCA) was determined using pyrocatechol violet (PV), detecting the color change at 632 nm.

2.8. Inhibition of Carbohydrate-Hydrolyzing Enzymes

The ability of the obtained extracts to inhibit the carbohydrate-hydrolyzing enzymes α-amylase and α-glucosidase was tested by incubating dilutions of the haloarchaeal extracts (1 mg mL^{-1}), prepared in sodium phosphate buffer 0.1 M pH 7, with the corresponding enzymes. Acarbose (1 mg mL^{-1}) was used as positive control and the buffer was employed as negative control. A blank, made with the buffer without the corresponding assayed enzyme, was also included. All the assays were conducted in 96 well plates and repeated at least six times. The inhibitory activity was calculated according to the formula:

$$\%\ Inhibitory\ activity = 100 \times \frac{Abs\ sample - Abs\ blank}{Abs\ negative\ control}$$

2.8.1. α-Amylase Inhibition Test

The α-amylase inhibition assay was performed as previously described by Iauk et al. [34]. Briefly, 40 µL of sample were mixed with 40 µL of amylase solution (100 U mL^{-1} in buffer) and 40 µL of starch

solution (0.1% in buffer sodium phosphate buffer 0.1M pH 7) and incubated 10 min at 37 °C. After that, 20 µL of HCl (1 M) and 100 µL of iodide solution (5 mM I_2 + 5 mM KI, in dH_2O) were added and the absorbance at 580 nm was read.

2.8.2. α-Glucosidase Inhibition Test

The α-glucosidase inhibition assay was performed according to Iauk et al. [34]. Concisely, 50 µL of sample were added to 100 µL of enzyme solution (1.0 U mL^{-1}) and incubated 10 min at room temperature. Then, 50 µL of 5mM p-nitrophenyl-a-D glucopyranoside was added and, after another incubation of 5 min at 25 °C, the absorbance was read at 405 nm.

2.9. Acetylcholinesterase (AChE) Activity

The AChE activity was measured by the Ellman method as described by Orhan et al. [35]. Typically, 20 µL of each sample (10 mg mL^{-1} in DMSO) were mixed with 140 µL of 0.1 mM sodium phosphate buffer (pH 8.0) and 20 µL of an AChE (EC.3.1.1.7) solution (0.28 U mL^{-1}) from electric eel, and incubated at room temperature for 15 min. The reaction was started by adding 10 µL of ATChI (acetylthiocholine iodide, 4 mg mL^{-1}) together with 20 µL of DTNB (5,5-dithiobis-2-nitrobenzoic acid, 1.2 mg mL^{-1}). The hydrolysis of ATChI was monitored at 412 nm, by the formation of the yellow 5-thio-2-nitrobenzoate anion as a result of the reaction between DTNB and the thiocholine produced from the reaction catalyzed by the enzyme. Results were expressed as percentages of activity relative to the negative control, as indicated above. Galantamine (1 mg mL^{-1}) was used as positive inhibitory control, while the sample solvent was set as the negative control. All the reactions were carried out in 96-well microplates and repeated at least six times.

2.10. Tyrosinase (TYRO) Activity

The effect of the different extracts on the tyrosinase activity was determined, by the method reported by Nerya et al. [36] with some modifications. Essentially, 70 µL of samples (10 mg mL^{-1}) dissolved in phosphate buffer 25 mM pH 6.5 were mixed with 30 µL of TYRO (333 U mL^{-1} in phosphate buffer, pH 6.5) and incubated for 5 min. After that, 110 µL of substrate (L-tyrosine, 2 mM in water) were added and further incubated for 30 min at room temperature, before reading the optical densities at 492 nm. The assays were done with six replicates for each sample in 96 well plates and arbutin (1 mg mL^{-1}) was used as positive control. Results were expressed as percentage of activity relative to a negative control as previously detailed, containing the buffer in place of the sample.

2.11. Cyclooxygenase 2 (COX-2) Activity

The anti-inflammatory activity of the extracts was studied by testing the inhibition of the enzyme cyclooxygenase 2 (COX-2), using the fluorometric COX-2 Inhibitor Screening Kit, Biovision K547-100 (Life Science, Milpitas, CA, USA). This assay is based on the fluorometric detection of Prostaglandin G2, the intermediate product generated by the COX enzyme from arachidonic acid. All the extracts were tested at a concentration of 1 mg mL^{-1} and solved in PBS, except the acetone ones, which were prepared in acetone to obtain a better solubility. All the assays were conducted in triplicate, following the manufacturer's indications. The reactions were started by adding 10 µL of the provided arachidonic acid, using 10 µL of the samples in a final volume of 100 µL of reaction mixture. Celecoxib (2 mM) was employed as positive control and the corresponding solvents, PBS and acetone, were used as negative control of COX-2 inhibition. The fluorometric detection (Ex/Em = 535/587 nm) was recorded in a fluorimeter FLUOstar Omega, BMG LABTECH, and the percentage of inhibition was calculated from the slope for all samples, including Enzyme Control (EC) as follows:

$$\%\ Relative\ Inhibition = \frac{Slope\ of\ EC - Slope\ of\ Sample}{Slope\ of\ EC} \times 100$$

2.12. Antimicrobial Activity

2.12.1. Strains and Media

The antimicrobial activity of the extracts obtained from the two selected haloarchaea strains was tested against different kinds of microorganisms including bacteria, microalgae, yeast, and archaea. The bacteria included in the assays were fish pathogens, kindly provided by the Andalusian Institute of Agriculture research: *Streptococcus parauberis* DSM 6631T, *Lactococcus garvieae* CECT 4531T, *Tenacibaculum maritimum* CECT 4276, *Tenacibaculum soleae* CECT 7292T, *Pseudomonas anguilliseptica* CECT 899T, *Pseudomonas moraviensis* DSM 16007T, *Pseudomonas plecoglossicida* DSM 15088T, *Edwardsiella tarda* CECT 849T, *Edwardsiella tarda* CECT 849T, *Vibrio anguillarum* CECT 522T, *Vibrio harveyi* CECT 525T, *Vibrio tapetis* CECT 4600T, *Aeromonas salmonicida salmonicida* CECT 894T, *Pseudomonas baetica* a390T, *Mycobacterium marinum* CECT 7091T, *Yersinia ruckeri* CECT 4319T, *Photobacterium damsela damselae* CECT 626T; common human pathogenic bacteria: *Micrococcus luteus* CECT 245, *Bacillus cereus* CECT 40 and *Staphylococcus aureus*, provided by the Microbiology and Parasitology Department of the University of Seville and the Gram negative *Escherichia coli* DH5α, related to human pathogenic strains. Among the microalgae, two freshwater species, *Chlorella sorokiniana* and *Chlamydomonas reinhardtii* 21gr, and two hypersaline species, *Dunaliella salina* and *Dunaliella bardawil* were tested. Antifungal activity was assayed against three different yeasts; *Saccharomyces cerevisiae* F13A, *Rhodotorula* sp., and *Rhodospirillum toruloides* 1854, supplied by the University of Algarve. Finally, the inhibitory activity of the obtained extracts against different haloarchaeal genera was studied in: *Haloferax* CECT 5871, *Halogeometricum*, *Halogiper*, *Halorubrum*, *Haloterrigena*, and *Natrinema*, generously given by the University of Mentouri's Bothers in Constantine, Algeria. All the tested species are listed in Table 1, in the Results section.

Table 1. Antimicrobial activity of acetone extracts.

	Target Microorganisms	Acetone Extract	
		***H. hispanica* HM1**	***H. salinarum* HM2**
Human pathogenic bacteria	*Bacillus cereus*	+	+
	Escherichia coli	+	−
	Micrococcus luteus	+	++
	Staphylococcus aureus	+	+
Marine fish pathogenic bacteria	*Aeromonas salmonicida* CECT 894T	−	−
	Edwardsiella tarda CECT 849T	−	−
	Lactococcus garvieae CECT 4531T	−	−
	Nocardia seriolae DSM 44129T	−	−
	Photobacterium damsela damselae CECT 626T	+	++
	Pseudomonas anguilliseptica CECT 899T	++	++
	Pseudomonas baetica A390T	−	−
	Pseudomonas moraviensis DSM 16007T	−	−
	Pseudomonas plecoglossicida DSM 15088T	−	−
	Streptococcus iniae CECT 7363T	−	−
	Streptococcus parauberis DSM 6631T	−	+
	Tenacibaculum soleae CECT 7292T	+	−
	Vibrio aestuarianus CECT 625T	−	−
	Vibrio anguillarum CECT 522T	+	+
	Vibrio harveyi CECT 525T	++	++
	Vibrio tapetis CECT 4600T	+	++
	Yersinia ruckeri CECT 4319T	+	+

Table 1. *Cont.*

	Target Microorganisms	Acetone Extract	
		H. hispanica **HM1**	***H. salinarum*** **HM2**
Halophilic archaea and bacteria	*Haloferax lucentense*	+	++
	Haloferax mediterranei	+++	+++
	Halogeometricum	+++	+++
	Halogiper	++	++
	Halorubrum	++	+++
	Haloterrigena	++	++
	Natrinema	+	+
	Salinibacter ruber	+++	+++
Microalgae	*Chlamydomonas reinhardtii* 21GR	+	++
	Chlorella sorokiniana	+	++
	Dunaliella bardawil	+++	++++
	Dunaliella salina	+++	++++
Yeasts	*Rhodospirillum toruloides* 1854	−	−
	Rhodotorula sp.	−	−
	Saccharomyces cerevisiae F13A	−	−

Microbial susceptibility was tested by agar diffusion assays and expressed as a function of the diameter of the growth inhibition zone: halo from 0.5 to 1 cm (+), halo from 1 to 2 cm (++), halo from 2 to 4 cm (+++) and halo from 4 to 6 cm (++++); absence of susceptibility (−). For a visual aspect of the halos, please refer to Figure 4.

Human pathogenic bacteria were cultured in LB (Luria–Bertani) medium, while fish pathogens were cultured in TSB (Tryptic Soy Broth) medium. Fresh water microalgae were cultured in TAP (Tris-Acetate-Phosphate) medium, whereas halophilic microalgae were cultured in modified Johnson's medium [37,38]. Finally, YPD (Yeast extract-Peptone-Dextrose) and MHE 25 (CECT 188) media were used for yeast and archaea growth, respectively.

2.12.2. Agar Diffusion Method

The indicator strains were grown in liquid media until they reached the late exponential phase of growth. Then, 1 mL inoculums of approximately 10^7 UFC mL^{-1} were spread across agar plates with their appropriate growth media. Once cell suspensions were completely dried, a 10 µL drop of each extract (10 mg DW mL^{-1}) was added to the plate. The extracts obtained from the culture media were resuspended in water or DMSO/water (1:4), while the precipitate and the supernatant obtained by extraction with acetone were diluted in PBS and acetone/water (1:4), respectively. The absence of toxicity of all the solvents was confirmed before the assays. The inhibition of growth was checked after the corresponding incubation period; 24 h at 37 °C for human pathogenic bacteria; 24 h at 25 °C for fish pathogenic bacteria; 48 h at 25 °C and light (100 µE m^{-2} s^{-1} of intensity) for fresh water microalgae; 7 days at 25 °C and light (100 µE m^{-2} s^{-1} of intensity) for hypersaline water microalgae; 24 h at 30 °C for yeasts; and 7 days at 37 °C for haloarchaea. The antimicrobial activity was determined measuring the size of the inhibition zone around the spotted drops. All the experiments were carried out in triplicate.

2.12.3. MIC Determination

Several dilutions of the active extracts were assayed to determine their Minimal Inhibitory Concentration (MIC) for the most susceptible microorganisms of each tested group using the agar diffusion method, as previously described, to detect the lowest extract concentration able to inhibit the growth of the selected microorganisms.

2.13. Statistical Analysis

The results were expressed as the mean ± SD of at least triplicate experiments. The data were submitted to one-way variance analysis (ANOVA) and the differences between means were evaluated by a Duncan's Multiple Range Test. The data were analyzed using the statistical and data analysis solution for Microsoft Excel (XLSTAT 2020, New York, NY, USA). Differences were considered significant at $p < 0.05$.

3. Results and Discussion

3.1. Isolation, Selection, and Identification of Haloarchaeal Strains

Two new haloarchaeal strains were isolated from environmental water samples, collected at the end of the summer from a salt evaporation pond located in the natural reserve of Odiel Marshlands, where rivers Tinto and Odiel flow into the Atlantic Ocean in the city of Huelva (SW Spain). The total salinity of the water collected was 33.23 g L^{-1}, being the composition of the brine of 1.40 g $CaSO_4$, 23.06 g $MgSO_4$, 34.08 g $MgCl_2$, 265.38 g NaCl, 7.51 g KCl and 0.84 g NaBr per liter.

These strains were chosen among a series of haloarchaeal colonies initially isolated from the water samples by serial dilution and successive streaking rounds on agar plates. Those which showed the most vigorous growth and exhibited the highest halocin activity, preliminary tested against *Haloferax lucentense*, were selected to further investigate their antimicrobial potential against a wide number of pathogenic bacteria and other bioactivities, such antioxidant and anti-inflammatory activities as well as their neuroprotective, melanogenic, or antidiabetic potential properties.

Amplification of the complete 16S rRNA sequence encoding gene from the new haloarchaeal strains was performed using the primers 21F y 1492R and procedures described in the materials and method section. Comparison of the obtained sequences (Supplementary Materials) with the NCBI database using the BLASTn tool revealed that the two new strains isolated belong to the genus *Haloarcula* and *Halobacterium*, respectively. The first isolate shared a 98.68% of sequence identity with *Haloarcula hispanica,* consequently it was designated as *Haloarcula hispanica* HM1. The 16S rRNA gene of the second haloarchaea isolated, on the other hand, showed high percentage of identity with the corresponding sequence of *Halobacterium salinarum* (97.53%). In addition, a Molecular Phylogenetic Analysis was conducted using the Molecular Evolutionary Genetics Analysis (MEGA) program version 7, including the sequences obtained and the complete sequences of a series of 16S rRNA coding genes available in the NCBI database for several members of the corresponding genus (Figure 1). In both cases, *Haloferax volcanii* was used as outgroup and the bootstrap was set at 1000 replicates. The 16S rRNA encoding sequence of the first isolate forms a cluster with the corresponding genes of *H. hispanica* and is closely related with the sequence of other *Haloarcula* species (Figure 1A). Otherwise, the 16S rRNA sequence of the second haloarchaea isolated clusters together with *H. salinarum* sequences and is highly related with the sequence of several species of the genus *Halobacterium* (Figure 1B).

Haloarcula [39,40] and *Halobacterium* [41,42] genera belong to the *Halobacteriaceae* family within the *Halobacteriales* order. Currently, ten recognized species are included in the *Haloarcula* genus: *H. amylolytica* [43], *H. argentinensis* [44], *H. vallismortis* [45], *H. marismortui* [46], *H. hispanica* [47], *H. japonica* [48], *H. quadrata* [49], *H. sinaiiensis* [50], *H. Salaria* and *H. Tradensis* [51]; while to date, five species comprise the *Halobacterium* genus: *H. Jilantaiense* [52], *H. litoreum* [53], *H. noricense* [54], *H. rubrum* [55] and *H. salinarum* [56]. Several strains of these species have been described due to the divergence of their 16S RNA coding gene sequences, as is the case of the two strains proposed here, which have been designated as *Haloarcula hispanica* HM1 and *Halobacterium salinarum* HM2.

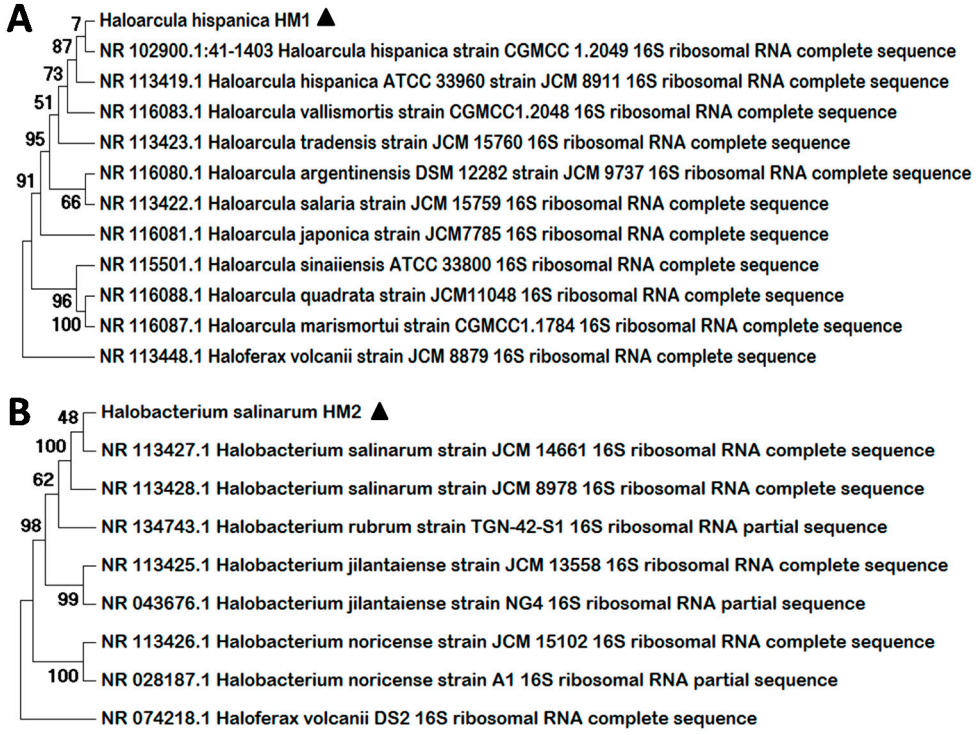

Figure 1. Molecular Phylogenetic Analysis by Maximum Likelihood Method. The trees represent a comparison among the 16S rRNA sequences from the new strains isolated, *H. hispanica* HM1 (**A**) and *H. salinarum* HM2 (**B**), and a series of reference archaeal sequences. Multiple alignments were generated by MUSCLE (MUltiple Sequence Comparison by Log-Expectation) and the trees were constructed with MEGA 7. The numbers at nodes indicate the bootstrap values calculated for 1000 replicates. The name and the NCBI access number are indicated for all the reference sequences. Black triangles indicate the new strains identified.

3.2. Bioactive Properties of the Extracts from H. Hispanica HM1 and H. Salinarum HM2

A total of 12 extracts, six from each of the new isolated haloarchaeal strains, were obtained from cultures of *H. hispanica* HM1 and *H. salinarum* HM2 harvested at the end of the stationary phase of growth. Hexane, dichloromethane, ethyl acetate, and chloroform extracellular extracts were recovered from the culture media, while acetone and aqueous extracts were obtained from the archaea biomass. The potential bioactive properties of all these extracts was tested as detailed below.

3.2.1. Antioxidant Capacity

The antioxidant potential of all the extracts was tested in radical scavenging assays, based on DPPH, ABTS, or NO, by the ferrocyanide reduction potential (FRP), and ICA and CCA metal chelation assays. The half maximal inhibitory concentration (IC_{50}) or the half maximal effective concentration (EC_{50}) was calculated using the prism program version 6 for the extracts that exhibited antioxidant activities higher than 65% (Figure 2).

None of the extracellular extracts obtained from the culture media was found to have antioxidant activity, while cellular extracts showed a considerable antioxidant activity, being able to scavenge DPPH, and ABTS radicals, reduce ferrocyanide and chelate copper, but not scavenge NO radicals or chelate iron. The aqueous extracts obtained from *H. hispanica* HM1 and *H. salinarum* HM2 biomass showed a moderate antioxidant capacity on DPPH, ABTS, and CCA assays, with inhibition values between 20 and 30%, and an important ability to reduce ferrocyanide, with values around 70 and 80%.

A

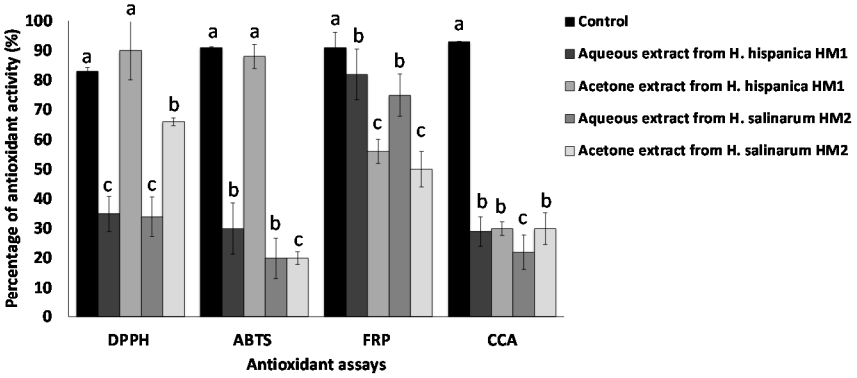

B

		IC_{50} value (μg mL^{-1})		EC_{50} value (μg mL^{-1})
		DPPH	*ABTS*	*FRP*
***H. hispanica* HM1**	*Aqueous extracts*	-	-	3.12
	Acetone extracts	2.06	3.89	-
***H. salinarum* HM2**	*Aqueous extracts*	-	-	3.59
	Acetone extracts	8.99	-	-

Figure 2. Antioxidant activity of aqueous and acetone extracts (1 mg mL^{-1}) obtained from the haloarchaeal strains *H. hispanica* HM1 and *H. salinarum* HM2, determined by DPPH (1,1-Diphenyl-2-picrylhydrazyl) and ABTS (2,2′-azino-bis(3-ethylbenzothiazoline-6-sulfonic acid)) radical scavenging assays, or FRP (Ferrous ion reduction potential) and CCA (Copper chelating activity). For each assay, the data were submitted to one-way variance analysis (ANOVA). Bars are followed by different superscript letters (a, b or c), which denote groups with significant differences according to the Duncan's Multiple Range Test ($p < 0.05$) (**A**). The half maximal inhibitory or effective concentration (IC_{50} or EC_{50}) were calculated when the activity was higher than 65% (**B**). These values were normalized to the content of proteins and carotenoids in the extracts, being the protein concentration of the aqueous extract 47 and 30 μg per mg DW and the carotenoid content of 10 and 12 μg per mg DW, respectively, for *H. hispanica* HM1 and *H. salinarum* HM2.

The acetone extracts obtained from *H. hispanica* HM1 presented high antioxidant activity when assayed on ABTS (88%; IC_{50} = 3.89 μg mL^{-1}) or DPPH (90%; IC_{50} = 2.06 μg mL^{-1}), which was even higher than that of the BHT positive control, however showed medium (56%) or low (30%) antioxidant activity when assayed on FRP or CCA, respectively. Acetone extracts from *H. salinarum* HM2, on the other hand, exhibited a high antioxidant activity when assayed with DPPH (66%; IC_{50} = 8.90 μg mL^{-1}) and only low (20–30%) or medium (50%) activity when tested on the other antioxidant assays, showing that differences can be observed between the same type of fractions obtained from both tested haloarchaea.

In addition, the aqueous extracts, obtained from the acetone precipitate of *H. hispanica* HM1, exhibited higher antioxidant activity in FRP assay (82%; EC_{50} = 3.12 μg mL^{-1}) than the same extract from *H. salinarum* HM2 (75%; EC_{50} = 3.59 μg/mL). These results suggest that *H. hispanica* HM1 extracts possess a higher antioxidant potential than the *H. salinarum* HM2 ones.

The results obtained entail a complete study about the antioxidant capacity of haloarchaea, as a wide range of antioxidant assays have been employed. In agreement with the results obtained for the new two strains isolated, *H. hispanica* HM1 and *H. salinarum* HM2, extracts from several haloarchaeal species have been reported to show antioxidant activity in the DPPH assay, which is the test most commonly used for this purpose. Examples of this are *Halogeometricum rufum*, *Halogeometricum limi*, *Haladaptatus litoreus*, *Haloplanus vescus*, *Halopelagius inordinatus*, *Halogranum rubrum*, and *Haloferax volcanii*, whose IC_{50} values varied from 2.5 to 10 μg mL^{-1} [12] and *Haloterrigena turkmenica* with an IC_{50} of 4.49 μg mL^{-1} [57]. Regarding the aqueous protein-rich extracts, there are no available reports for comparison in the case of haloarchaea. The fact that different extracts from the studied archaea showed

antioxidant activity makes us think that haloarchaea could have antioxidant compounds of different nature and polarity, present in different fractions. Polyphenolic compounds are usually related to the antioxidant activity of plants and algal extracts, [58–60]; however there is no evidence to the date of their production in haloarchaea, which antioxidant potential is mainly attributed to the presence of carotenoid pigments. Finally, moderate levels of copper ions chelating activity was found in extracts from both strains. This activity has been previously reported in saline microalgae [61], but has not been studied in haloarchaeal members as yet. Taken together, those results indicate that haloarchaeal extracts could be a promising source of antioxidant compounds with widespread applications as natural food preservatives, colorants and supplements [62], as well as sources of leads for pharmaceutical and cosmetic formulations to prevent oxidative damage [63].

3.2.2. In Vitro Neuroprotective, Antidiabetic, Melanogenic, and Anti-Inflammatory Properties of the Haloarchaeal Extracts

All the extracts were tested to determine their potential activity over the enzymes tyrosinase (TYRO), α-glucosidase, α-amylase, cyclooxygenase 2 (COX-2) and acetylcholinesterase (AChE), which are classical targets in the search for new drug leads for the treatment of diverse dermatological, metabolic, inflammatory, and neurological diseases.

Among all the tested enzymes, the highest percentage of activity inhibition was observed for COX-2, specifically in the acetone fraction of both haloarchaea, being the *H. hispanica* HM1 extracts more active, with a 65% of enzyme inhibition, than the same extracts of *H. salinarum* HM2, with 47% of COX-2 inhibition. Also, a slight inhibition of COX-2, around 15%, was found in the aqueous fractions of *H. salinarum* HM2 (Figure 3). COX is the central enzyme in the biosynthetic pathway of prostanoids, which are important biological mediators as prostaglandins, prostacyclin, and thromboxane. There are two known isoenzymes: COX-1 and COX-2. COX-1 is constitutively expressed in many tissues and is the predominant form in gastric mucosa and in kidney, while COX-2 is not expressed under normal conditions in most cells, but elevated levels are found during inflammation. Coxibs include a variety of powerful drugs, whose primary mechanism is the potent inhibition of the COX-2 enzyme. These drugs are used worldwide to treat diverse medical conditions as muscular skeletal pain and inflammation. Unfortunately, their use is limited due to negative effects on renal clearance and increased risk of cardiovascular pathology [64]. Therefore, there is a clear need to develop new COX-2 inhibitors free of the aforementioned problems, which can provide pain and inflammatory relief.

Regarding the antidiabetic potential, the aqueous and acetone extracts obtained from *H. hispanica* HM1 biomass exhibited inhibitory activities of 33 and 36%, respectively, on α-amylase activity. In the same way, glucosidase inhibition of 36% was achieved with the aqueous protein-rich extract of *H. salinarum* HM2. Both carbohydrate-hydrolyzing enzymes, α-glucosidase and α-amylase, have been proposed as targets to control the hyperglycemia associated with diabetes mellitus type 2 [65]. The inhibitory potential of these extracts was lower than that of the reference antidiabetic acarbose, which was about 65% for α-amylase and 80% for α-glucosidase (Figure 3).

With respect to the neuroprotective assay, acetone extracts obtained from the biomass of both archaea and all the extracts recovered from culture media showed the capacity of inhibiting acetylcholinesterase activity in a range from 20 to 37%, which was lower than the AChE inhibitory potential of the positive control, galantamine (78%). Conversely, aqueous extracts from both strains exhibited the antagonist activity; they were able to induce the activity of the enzyme by 45%–49% (Figure 3). Acetylcholinesterase catalyzes the hydrolysis of cholinergic neurotransmitters such as acetylcholine and others choline esters to terminate the synaptic transmission rapidly. The reversible inhibition of this enzyme is being explored as treatment for Alzheimer's disease [66], while acetylcholinesterase activation is required in cholinergic crisis related to acetylcholine accumulations [67].

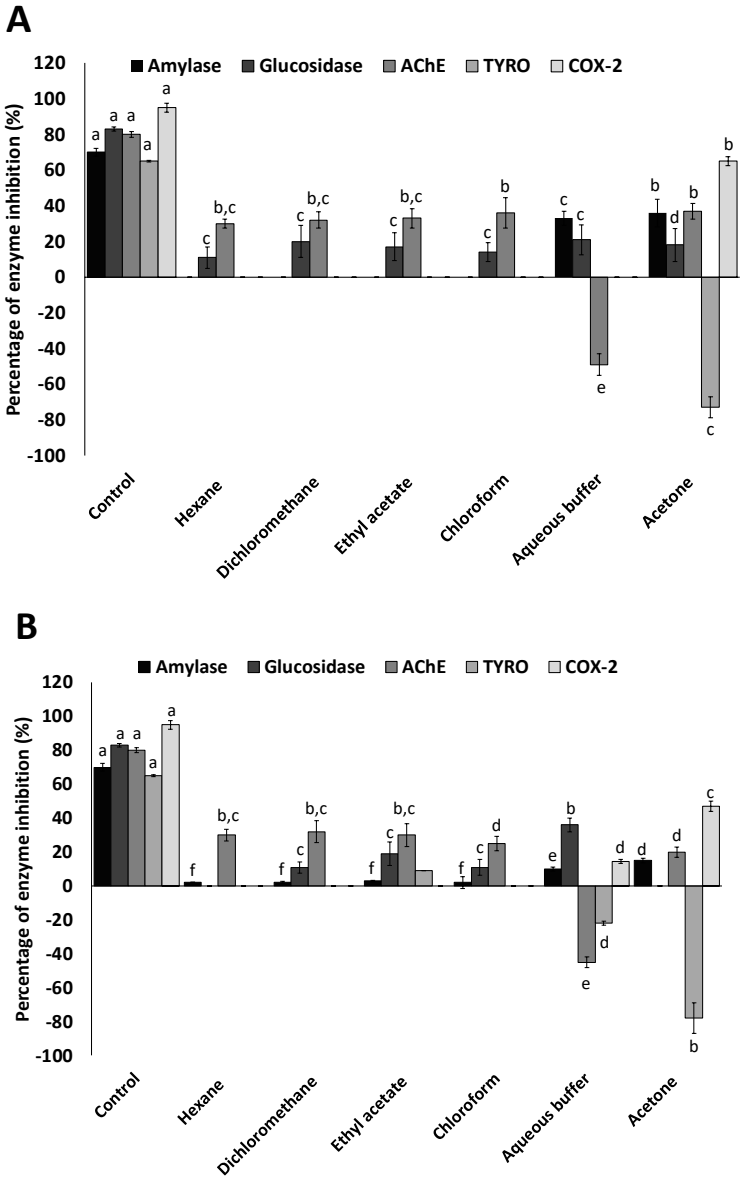

Figure 3. In vitro activity of haloarchaeal extracts on enzymes related to diabetic, neurodegenerative skin pigmentation, and inflammatory diseases. Percentages of inhibition of the enzymes: α-amylase, α-glucosidase, acetylcholinesterase (AChE), tyrosinase (TYRO) and cyclooxygenase 2 (COX-2) by the all extracts obtained in different solvents (hexane, dichloromethane, ethyl acetate, chloroform, aqueous buffer and acetone) from *H. hispanica* HM1 (**A**) and *H. salinarum* HM2 (**B**) strains are represented. A known inhibitor for each enzyme was included as control. For each assay, the data were submitted to one-way variance analysis (ANOVA). Bars are followed by different superscript letters (a–f), which denote groups with significant differences according to the Duncan's Multiple Range Test ($p < 0.05$).

Regarding tyrosinase activity, none of the extracts studied showed a significant ability to inactivate this oxidase involved in the synthesis of melanin. However, it is remarkable that the acetone extracts from both strains exhibited, in our experimental conditions, a high percentage of tyrosinase activation (73–78%). Although inhibitors of tyrosinase are used to alleviate skin hyperpigmentation and prevent age spots [68], inducers of this enzyme can stimulate melanogenesis and contribute to treat skin depigmentation disorders, such as vitiligo [69,70]. Many melanogenesis stimulators have been isolated from natural sources, but to our knowledge, this is the first report about the influence of archaeal extracts on tyrosinase activity. High repigmentation ratios of vitiligo patients treated with Dead Sea

Climatotherapy, which includes sea baths, have been reported [71]. The mineral composition of these saline waters seems to have positive effects in this and other skin conditions; however, the possible therapeutic role of the haloarchaea, which are usual inhabitants of hypersaline water, has not been investigated yet [72]. Furthermore, Vitiligo has also been found to be related to oxidative stress and to the activation/deactivation of acetylcholinesterase [73], and we have demonstrated that haloarchaeal extracts show antioxidant activity and the ability to induce acetylcholinesterase in vitro.

In this study, we have demonstrated that haloarchaeal extracts have interesting bioactive properties. Their ability to inhibit the COX-2 enzyme is especially remarkable, and although in vitro antidiabetic properties of the studied extracts were low, their ability to induce acetylcholinesterase and tyrosinase are noteworthy. To our knowledge, these results represent the first report on the potential applicability of haloarchaeal extracts as a potential source of compounds for the treatment of the aforementioned diseases. To date, the applicability of haloarchaea has been mainly focused on their carotenoids, which have been described as antiproliferative [20] and erythroprotective agents [12], and enhancers of sperm cells viability [13].

3.3. Antimicrobial Activity and MIC Determination

The antimicrobial activity of the different extracts obtained from the two new haloarchaeal strains was assayed against a collection of typical fish and human pathogenic bacteria, against representative microalgae and yeast species and over other haloarchaea typically found in hypersaline environments, by using the agar diffusion method.

This screening revealed that only the acetone extracts showed considerable antimicrobial activity. Acetone extracts from the two tested haloarchaeal strains, *H. hispanica* HM1 and *H. salinarum* HM2, showed to be active against bacteria, microalgae, and archaea, but not on yeasts. Zones of inhibition, with diameters which varied according to the susceptibility of the target microorganism from 0.5 to 6 cm, were used as indicators of antimicrobial activity (Figure 4). Both acetone extracts inhibited the growth of all the human pathogenic bacteria assayed and of most fish pathogenic bacteria studied, with inhibition halos ranging from 0.5 to 2 cm. In addition, both extracts exhibited important antimicrobial activity against microalgae, which was especially pronounced over halophilic microalgae from the *Dunaliella* genus, with inhibition halos sized from 2 to 6 cm. Moreover, high activity was found against all the tested extreme halophilic archaea and bacteria, with inhibition zones from 0.5 to 4 cm (Table 1).

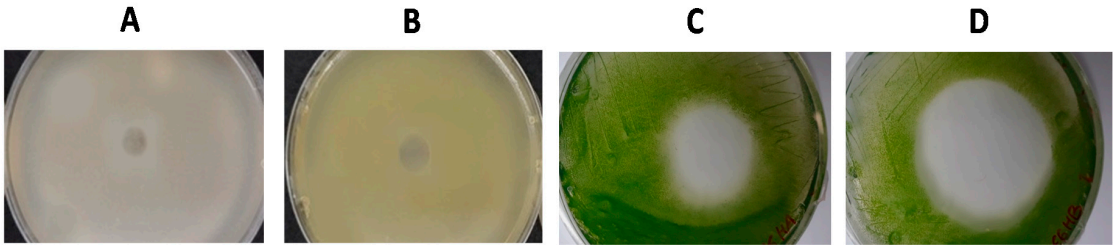

Figure 4. Antimicrobial activity of acetone extracts. Antimicrobial activity was indicated by zones of inhibition of growth or halos. Taking into account the diameter of the halo, the susceptibility of the different microorganisms to the extracts was classified in four reference groups: (**A**) 0.5–1 cm (+) in *Bacillus cereus*; (**B**) 1–2 cm (++) in *Staphylococcus aureus*; (**C**) 2–4 cm (+++) in *Dunaliella bardawil* and (**D**) 4–6 cm (++++) in *Dunaliella salina*.

Several dilutions of acetone extracts containing pigment concentrations of 100, 80, 40, 20, 10, 5 and 1 μg mL^{-1} were prepared to detect their MIC on different target microorganisms. For this purpose, one of the most susceptible microorganisms of each group was selected; *Micrococcus luteus* for human pathogenic bacteria, *Vibrio harveyi* for fish pathogenic bacteria, *Halogeometricum* for archaea, and *Dunaliella salina* for microalgae. The obtained results revealed that the extracts were more active against halophilic microorganisms, with MIC values of 10 μg mL^{-1} for *D. salina* and 5 μg mL^{-1}

for *Halogeometricum* (Figure 5); while for the bacteria species *M. luteus* and *V. harveyi*, MIC values were 100 μg mL^{-1}.

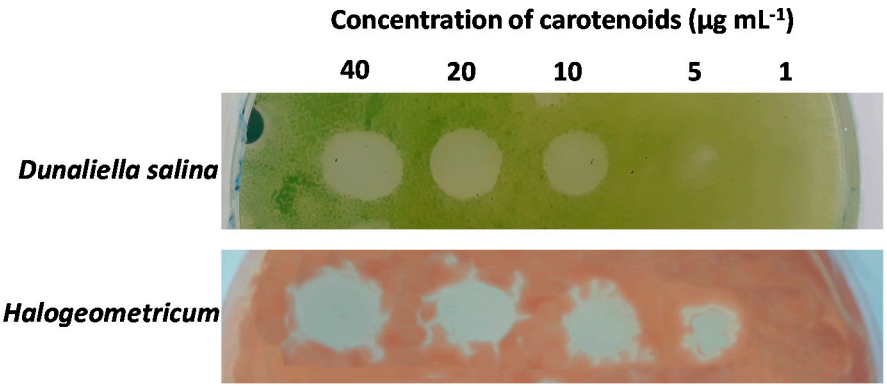

Figure 5. Minimal Inhibitory Concentration plate assay. Dilutions of the active extracts were assayed against one of the most susceptible microorganisms of each group. Halophilic microorganisms, represented by *Dunaliella salina* and *Halogeometricum*, showed to be more sensitive to the extracts.

Lipophilic extracts and pigments of diverse origin have shown antimicrobial activity against pathogenic human bacteria and fungi. In this sense, several studies have been carried out with positive results with pigments derived from plants and vegetables [59,74]; from algae [75,76] and from saline and halophilic bacteria [21,23,77], but to date the reports about the applicability of such extracts as antimicrobial agents are scarce. Recent studies report a moderate inhibitory effect of the extracts from the haloarchaea *Halorubrum* sp. on pathogenic bacteria, with inhibition halos up to 15 mm [24], which is quite lower than the results obtained is this work. Most studies about antimicrobial interactions between halophilic bacteria and archaea are focused on halocins [78–80]. Therefore, the present research entails a pioneer report on the effectiveness of haloarchaeal acetonic extracts against a wide range of different microorganisms belonging to the three domains of life. Likewise, this study represents the first outcome from the use of *Haloarcula* and *Halobacterium* as source of antimicrobial compounds.

4. Conclusions

This research explores the antioxidant, antimicrobial and other bioactive properties of the extracts obtained from two new isolated haloarchaea strains and confirms that they can be an exceptional source of new bioactive extracts, able to modulate the activity of several medically relevant enzymes, and with potential applicability in pharmacy and cosmetics. The acetone fractions, showed to be the most active extracts in most of the assays, being their antioxidant, antimicrobial, and anti-inflammatory potential especially remarkable. Moreover, acetone extracts from the two haloarchaea have shown for the first time to have the ability to activate the melanogenic enzyme tyrosinase and to inhibit the enzyme cyclooxygenase-2 (COX-2), implicated in the inflammatory response; while the aqueous extracts from both strains have demonstrated to enhance in vitro the acetylcholinesterase activity; this enzyme catalyzes the hydrolysis of cholinergic neurotransmitters and has been reported to be involved in neurological disorders and to have a role in apoptosis. In this study, we have untapped novel unexplored bioactivities of haloarchaea, which can be the source of potential new therapeutic compounds. However, many archaea species are still undiscovered, many potential bioactivities remain to be studied, and the isolation and identification of the compounds responsible for these activities is still a pending issue. Further work will be carried out to fully characterize the composition of the active extracts and their efficacy in in vivo assays.

Supplementary Materials: The following are available online at http://www.mdpi.com/2079-7737/9/9/298/s1, Figure S1: Sequences of the 16S rRNA genes amplified from the new haloarchaea.

Author Contributions: Conceptualization, P.G.-V. and R.L.; Data curation, P.G.-V.; Funding acquisition, M.V., J.V. (Javier Vigara) and R.L.; Investigation, P.G.-V. and M.V.; Methodology, P.G.-V., J.V. (João Varela) and L.B.; Supervision, J.V. (Javier Vigara), J.V. (João Varela), L.B. and R.L.; Validation, P.G.-V.; Writing—original draft, P.G.-V. and R.L.; Writing—review & editing, P.G.-V, J.V. (Javier Vigara), J.V. (João Varela), L.B. and R.L. All authors have read and agreed to the published version of the manuscript.

Funding: This research was funded by the European commission (INTERREG VA POCTEP-055 ALGARED _PLUS_5E), the Operative FEDER Program-Andalucía 2014-2020, the University of Huelva, and the SUBV. COOP.ALENTEJO-ALGARVE-ANDALUCIA 2019. P.G.-V. acknowledges financial support from the University of Huelva (EPIT 2016-17).

Acknowledgments: We thank Pajuelo from the University of Seville, Raposo from the University of Algarve, and Sally from the University of Mentouri brothers, Constantine (Algeria) for kindly providing the human pathogenic strains, the yeasts and the Algerian archaea tested in this research. Colaboration of López-Sanmartín, López-Fernández and Navas from the Andalusian Institute of Agriculture research, who provided the fish pathogenic strains is also acknowledged. The authors also thank to "Salinas del Odiel S.L." company for providing the water samples used in this study.

Conflicts of Interest: The authors declare no conflict of interest. The funders had no role in the design of the study; in the collection, analyses, or interpretation of data; in the writing of the manuscript, or in the decision to publish the results.

References

1. Oren, A. Halophilic microbial communities and their environments. *Curr. Opin. Biotechnol.* **2015**, *33*, 119–124. [CrossRef] [PubMed]
2. Ventosa, A.; Fernández, A.B.; León, M.J.; Sánchez-Porro, C.; Rodriguez-Valera, F. The Santa Pola saltern as a model for studying the microbiota of hypersaline environments. *Extremophiles* **2014**, *18*, 811–824. [CrossRef] [PubMed]
3. Singh, A.; Singh, A.K. Haloarchaea: Worth exploring for their biotechnological potential. *Biotechnol. Lett.* **2017**, *39*, 1793–1800. [CrossRef] [PubMed]
4. Oren, A. Industrial and environmental applications of halophilic microorganisms. *Environ. Technol.* **2010**, *31*, 825–834. [CrossRef] [PubMed]
5. Corral, P.; Amoozegar, M.A.; Ventosa, A. Halophiles and their biomolecules: Recent advances and future applications in biomedicine. *Mar. Drugs* **2020**, *18*, 33. [CrossRef]
6. Amoozegar, M.A.; Siroosi, M.; Atashgahi, S.; Smidt, H.; Ventosa, A. Systematics of haloarchaea and biotechnological potential of their hydrolytic enzymes. *Microbiol. (UK)* **2017**, *163*, 623–645. [CrossRef]
7. Desai, C.; Patel, P.; Markande, A.R.; Kamala, K.; Sivaperumal, P. Exploration of haloarchaea for their potential applications in food industry. *Int. J. Environ. Sci. Technol.* **2020**. [CrossRef]
8. Besse, A.; Peduzzi, J.; Rebuffat, S.; Carré-Mlouka, A. Antimicrobial peptides and proteins in the face of extremes: Lessons from archaeocins. *Biochimie* **2015**, *118*, 344–355. [CrossRef]
9. Litchfield, C.D. Potential for industrial products from the halophilic Archaea. *J. Ind. Microbiol. Biotechnol.* **2011**, *38*, 1635–1647. [CrossRef]
10. van den Berg, H.; Faulks, R.; Granado, H.F.; Hirschberg, J.; Olmedilla, B.; Sandmann, G.; Southon, S.; Stahl, W. The potential for the improvement of carotenoid levels in foods and the likely systemic effects. *J. Sci. Food Agric.* **2000**, *80*, 880–912. [CrossRef]
11. Bakker, M.F.; Peeters, P.H.M.; Klaasen, V.M.; Bueno-De-Mesquita, H.B.; Jansen, E.H.J.M.; Ros, M.M.; Travier, N.; Olsen, A.; Tjønneland, A.; Overvad, K.; et al. Plasma carotenoids, Vitamin C, tocopherols, and retinol and the risk of breast cancer in the European Prospective Investigation into Cancer and Nutrition cohort. *Am. J. Clin. Nutr.* **2016**, *103*, 454–464. [CrossRef] [PubMed]
12. Hou, J.; Cui, H.L. In Vitro Antioxidant, Antihemolytic, and Anticancer Activity of the Carotenoids from Halophilic Archaea. *Curr. Microbiol.* **2018**, *75*, 266–271. [CrossRef] [PubMed]
13. Zalazar, L.; Pagola, P.; Miró, M.V.; Churio, M.S.; Cerletti, M.; Martínez, C.; Iniesta-Cuerda, M.; Soler, A.J.; Cesari, A.; De Castro, R. Bacterioruberin extracts from a genetically modified hyperpigmented Haloferax volcanii strain: Antioxidant activity and bioactive properties on sperm cells. *J. Appl. Microbiol.* **2019**, *126*, 796–810. [CrossRef] [PubMed]
14. Kirti, K.; Amita, S.; Priti, S.; Mukesh Kumar, A.; Jyoti, S. Colorful World of Microbes: Carotenoids and Their Applications. *Adv. Biol.* **2014**, *2014*, 1–13. [CrossRef]

15. Fang, C.J.; Ku, K.L.; Lee, M.H.; Su, N.W. Influence of nutritive factors on C 50 carotenoids production by Haloferax mediterranei atcc 33500 with two-stage cultivation. *Bioresour. Technol.* **2010**, *101*, 6487–6493. [CrossRef] [PubMed]
16. Yatsunami, R.; Ando, A.; Yang, Y.; Takaichi, S.; Kohno, M.; Matsumura, Y.; Ikeda, H.; Fukui, T.; Nakasone, K.; Fujita, N.; et al. Identification of carotenoids from the extremely halophilic archaeon Haloarcula japonica. *Front. Microbiol.* **2014**, *5*. [CrossRef]
17. de la Vega, M.; Sayago, A.; Ariza, J.; Barneto, A.G.; León, R. Characterization of a bacterioruberin-producing Haloarchaea isolated from the marshlands of the Odiel river in the southwest of Spain. *Biotechnol. Prog.* **2016**, *32*, 592–600. [CrossRef] [PubMed]
18. Yang, Y.; Yatsunami, R.; Ando, A.; Miyoko, N.; Fukui, T.; Takaichi, S.; Nakamura, S. Complete biosynthetic pathway of the C50 carotenoid bacterioruberin from lycopene in the extremely halophilic archaeon Haloarcula japonica. *J. Bacteriol.* **2015**, *197*, 1614–1623. [CrossRef]
19. Giani, M.; Garbayo, I.; Vílchez, C.; Martínez-Espinosa, R.M. Haloarchaeal carotenoids: Healthy novel compounds from extreme environments. *Mar. Drugs* **2019**, *17*, 524. [CrossRef]
20. Abbes, M.; Baati, H.; Guermazi, S.; Messina, C.; Santulli, A.; Gharsallah, N.; Ammar, E. Biological properties of carotenoids extracted from Halobacterium halobium isolated from a Tunisian solar saltern. *BMC Complement. Altern. Med.* **2013**, *13*. [CrossRef]
21. Ibrahim, D.; Nazari, T.F.; Kassim, J.; Lim, S.H. Prodigiosin—an antibacterial red pigment produced by Serratia marcescens IBRL USM 84 associated with a marine sponge Xestospongia testudinaria. *J. Appl. Pharm. Sci.* **2014**, *4*, 1–6. [CrossRef]
22. Falaise, C.; François, C.; Travers, M.A.; Morga, B.; Haure, J.; Tremblay, R.; Turcotte, F.; Pasetto, P.; Gastineau, R.; Hardivillier, Y.; et al. Antimicrobial compounds from eukaryotic microalgae against human pathogens and diseases in aquaculture. *Mar. Drugs* **2016**, *14*, 159. [CrossRef] [PubMed]
23. Fariq, A.; Yasmin, A.; Jamil, M. Production, characterization and antimicrobial activities of bio-pigments by Aquisalibacillus elongatus MB592, Salinicoccus sesuvii MB597, and Halomonas aquamarina MB598 isolated from Khewra Salt Range, Pakistan. *Extremophiles* **2019**, *23*, 435–449. [CrossRef] [PubMed]
24. Sahli, K.; Gomri, M.A.; Esclapez, J.; Gómez-Villegas, P.; Ghennai, O.; Bonete, M.J.; León, R.; Kharroub, K. Bioprospecting and characterization of pigmented halophilic archaeal strains from Algerian hypersaline environments with analysis of carotenoids produced by *Halorubrum* sp. BS2. *J. Basic Microbiol.* **2020**. [CrossRef] [PubMed]
25. Gómez-Villegas, P.; Vigara, J.; León, R. Characterization of the Microbial Population Inhabiting a Solar Saltern Pond of the Odiel Marshlands (SW Spain). *Mar. Drugs* **2018**, *16*, 332. [CrossRef]
26. Altschul, S.F.; Gish, W.; Miller, W.; Myers, E.W.; Lipman, D.J. Basic local alignment search tool. *J. Mol. Biol.* **1990**, *215*, 403–410. [CrossRef]
27. Hiyama, T.; Nishimura, M.; Chance, B. Determination of carotenes by thin-layer chromatography. *Anal. Biochem.* **1969**, *29*, 339–342. [CrossRef]
28. Bradford, M.M. A rapid and sensitive method for the quantitation of microgram quantities of protein utilizing the principle of protein-dye binding. *Anal. Biochem.* **1976**, *72*, 248–254. [CrossRef]
29. Sachindra, N.M.; Sato, E.; Maeda, H.; Hosokawa, M.; Niwano, Y.; Kohno, M.; Miyashita, K. Radical scavenging and singlet oxygen quenching activity of marine carotenoid fucoxanthin and its metabolites. *J. Agric. Food Chem.* **2007**, *55*, 8516–8522. [CrossRef]
30. Re, R.; Pellegrini, N.; Proteggente, A.; Pannala, A.; Yang, M.; Rice-Evans, C. Antioxidant activity applying an improved ABTS radical cation decolorization assay. *Free Radic. Biol. Med.* **1999**, *26*, 1231–1237. [CrossRef]
31. Baliga, M.S.; Jagetia, G.C.; Rao, S.K.; Babu, S.K. Evaluation of nitric oxide scavenging activity of certain spices in vitro: A preliminary study. *Nahr. Food* **2003**, *47*, 261–264. [CrossRef] [PubMed]
32. Tundis, R.; Bonesi, M.; Sicari, V.; Pellicanò, T.M.; Tenuta, M.C.; Leporini, M.; Menichini, F.; Loizzo, M.R. Poncirus trifoliata (L.) Raf.: Chemical composition, antioxidant properties and hypoglycaemic activity via the inhibition of α-amylase and α-glucosidase enzymes. *J. Funct. Foods* **2016**, *25*, 477–485. [CrossRef]
33. Megías, C.; Pastor-Cavada, E.; Torres-Fuentes, C.; Girón-Calle, J.; Alaiz, M.; Juan, R.; Pastor, J.; Vioque, J. Chelating, antioxidant and antiproliferative activity of Vicia sativa polyphenol extracts. *Eur. Food Res. Technol.* **2009**, *230*, 353–359. [CrossRef]

34. Iauk, L.; Acquaviva, R.; Mastrojeni, S.; Amodeo, A.; Pugliese, M.; Ragusa, M.; Loizzo, M.R.; Menichini, F.; Tundis, R. Antibacterial, antioxidant and hypoglycaemic effects of *Thymus capitatus* (L.) Hoffmanns. et Link leaves' fractions. *J. Enzym. Inhib. Med. Chem.* **2015**, *30*, 360–365. [CrossRef]
35. Orhan, I.; Kartal, M.; Naz, Q.; Ejaz, A.; Yilmaz, G.; Kan, Y.; Konuklugil, B.; Şener, B.; Iqbal Choudhary, M. Antioxidant and anticholinesterase evaluation of selected Turkish Salvia species. *Food Chem.* **2007**, *103*, 1247–1254. [CrossRef]
36. Nerya, O.; Vaya, J.; Musa, R.; Izrael, S.; Ben-Arie, R.; Tamir, S. Glabrene and isoliquiritigenin as tyrosinase inhibitors from licorice roots. *J. Agric. Food Chem.* **2003**, *51*, 1201–1207. [CrossRef] [PubMed]
37. Johnson, M.K.; Johnson, E.J.; MacElroy, R.D.; Speer, H.L.; Bruff, B.S. Effects of Salts on the Halophilic Alga Dunaliella viridis1. *J. Bacteriol.* **1968**, *95*, 1461–1468. [CrossRef]
38. Shariati, M.; Hadi, M.R. Microalgal Biotechnology and Bioenergy in Dunaliella. In *Progress in Molecular and Environmental Bioengineering—From Analysis and Modeling to Technology Applications*; Capri, A., Ed.; In Tech: Cambridge, UK, 2011; Volume 1, pp. 483–506. [CrossRef]
39. Torreblanca, M.; Rodriguez-Valera, F.; Juez, G.; Ventosa, A.; Kamekura, M.; Kates, M. Classification of Non-alkaliphilic Halobacteria Based on Numerical Taxonomy and Polar Lipid Composition, and Description of Haloarcula gen. nov. and Haloferax gen. nov. *Syst. Appl. Microbiol.* **1986**, *8*, 89–99. [CrossRef]
40. Oren, A.; Arahal, D.R.; Ventosa, A. Emended descriptions of genera of the family Halobacteriaceae. *Int. J. Syst. Evol. Microbiol.* **2009**, *59*, 637–642. [CrossRef]
41. Elazari-Volcani, B. Genus XII. Halobacterium. In *Bergey's Manual of Determinative Bacteriology*, 7th ed.; Breed, R.S., Murray EGD, S.N., Eds.; The Williams & Wilkins Co.: Baltimore, MD, USA, 1957.
42. Sneath, P.H.A.; Mcgowan, V.; Skerman, V.B.D. Approved Lists of Bacterial Names. *Int. J. Syst. Evol. Microbiol.* **1980**, *30*, 225–420. [CrossRef]
43. Yang, Y.; Cui, H.-L.; Zhou, P.-J.; Liu, S.-J. Haloarcula amylolytica sp. nov., an extremely halophilic archaeon isolated from Aibi salt lake in Xin-Jiang, China. *Int. J. Syst. Evol. Microbiol.* **2007**, *57*, 103–106. [CrossRef] [PubMed]
44. Ihara, K.; Watanabe, S.; Tamura, T. *Haloarcula argentinensis* sp. nov. and *Haloarcula mukohataei* sp. nov., two new extremely halophilic archaea collected in Argentina. *Int. J. Syst. Bacteriol.* **1997**, *47*, 73–77. [CrossRef] [PubMed]
45. Gonzalez, C.; Gutierrez, C.; Ramirez, C. Halobacterium vallismortis sp. nov. An amylolytic and carbohydrate-metabolizing, extremely halophilic bacterium. *Can. J. Microbiol.* **1978**, *24*, 710–715. [CrossRef] [PubMed]
46. Oren, A.; Ginzburg, M.; Ginzburg, B.Z.; Hochstein, L.I.; Volcani, B.E. Haloarcula marismortui (Volcani) sp. nov., nom. rev., an extremely halophilic bacterium from the Dead Sea. *Int. J. Syst. Bacteriol.* **1990**, *40*, 209–210. [CrossRef]
47. Juez, G.; Rodriguez-Valera, F.; Ventosa, A.; Kushner, D.J. *Haloarcula hispanica* spec. nov. and *Haloferax gibbonsii* spec, nov., two new species of extremely halophilic archaebacteria. *Syst. Appl. Microbiol.* **1986**, *8*, 75–79. [CrossRef]
48. Takashina, T.; Hamamoto, T.; Otozai, K.; Grant, W.D.; Horikoshi, K. *Haloarcula japonica* sp. nov., a New Triangular Halophilic Archaebacterium. *Syst. Appl. Microbiol.* **1990**, *13*, 177–181. [CrossRef]
49. Oren, A.; Ventosa, A.; Gutiérrez, M.C.; Kamekura, M. *Haloarcula quadrata* sp. nov., a square, motile archaeon isolated from a brine pool in Sinai (Egypt). *Int. J. Syst. Evol. Microbiol.* **1999**, *49*, 1149–1155. [CrossRef]
50. Javor, B.; Requadt, C.; Stoeckenius, W. Box-shaped halophilic bacteria. *J. Bacteriol.* **1982**, *151*, 1532–1542. [CrossRef]
51. Namwong, S.; Tanasupawat, S.; Kudo, T.; Itoh, T. *Haloarcula salaria* sp. nov. and *Haloarcula tradensis* sp. nov. from salt in Thai fish sauce. *Int. J. Syst. Evol. Microbiol.* **2010**, *61*, 231–236. [CrossRef]
52. Yang, Y.; Cui, H.-L.; Zhou, P.-J.; Liu, S.-J. *Halobacterium jilantaiense* sp. nov., a halophilic archaeon isolated from a saline lake in Inner Mongolia, China. *Int. J. Syst. Evol. Microbiol.* **2006**, *56*, 2353–2355. [CrossRef]
53. Lü, Z.-Z.; Li, Y.; Zhou, Y.; Cui, H.-L.; Li, Z.-R. *Halobacterium litoreum* sp. nov., isolated from a marine solar saltern. *Int. J. Syst. Evol. Microbiol.* **2017**, *67*, 4095–4099. [CrossRef] [PubMed]
54. Gruber, C.; Legat, A.; Pfaffenhuemer, M.; Radax, C.; Weidler, G.; Busse, H.-J.; Stan-Lotter, H. *Halobacterium noricense* sp. nov., an archaeal isolate from a bore core of an alpine Permian salt deposit, classification of *Halobacterium* sp. NRC-1 as a strain of *H. salinarum* and emended description of *H. salinarum*. *Extremophiles* **2004**, *8*, 431–439. [CrossRef] [PubMed]

55. Han, D.; Cui, H.-L. *Halobacterium rubrum* sp. nov., isolated from a marine solar saltern. *Arch. Microbiol.* **2014**, *196*, 847–851. [CrossRef]
56. Ventosa, A.; Oren, A. *Halobacterium salinarum* nom. corrig., a name to replace *Halobacterium salinarium* (Elazari-Volcani) and to include *Halobacterium halobium* and *Halobacterium cutirubrum*. *Int. J. Syst. Evol. Microbiol.* **1996**, *46*, 347. [CrossRef]
57. Squillaci, G.; Parrella, R.; Carbone, V.; Minasi, P.; La Cara, F.; Morana, A. Carotenoids from the extreme halophilic archaeon Haloterrigena turkmenica: Identification and antioxidant activity. *Extremophiles* **2017**, *21*, 933–945. [CrossRef]
58. Huynh Thi Le, D.; Lu, W.-C.; Li, P.-H. Sustainable Processes and Chemical Characterization of Natural Food Additives: Palmyra Palm (Borassus Flabellifer Linn.) Granulated Sugar. *Sustainability* **2020**, *12*, 2650. [CrossRef]
59. Szabo, K.; Diaconeasa, Z.; Cătoi, A.F.; Vodnar, D.C. Screening of ten tomato varieties processing waste for bioactive components and their related antioxidant and antimicrobial activities. *Antioxidants* **2019**, *8*, 292. [CrossRef]
60. Maadane, A.; Merghoub, N.; Ainane, T.; El Arroussi, H.; Benhima, R.; Amzazi, S.; Bakri, Y.; Wahby, I. Antioxidant activity of some Moroccan marine microalgae: Pufa profiles, carotenoids and phenolic content. *J. Biotechnol.* **2015**, *215*, 13–19. [CrossRef]
61. Custódio, L.; Silvestre, L.; Rocha, M.I.; Rodrigues, M.J.; Vizetto-Duarte, C.; Pereira, H.; Barreira, L.; Varela, J. Methanol extracts from *Cystoseira tamariscifolia* and *Cystoseira nodicaulis* are able to inhibit cholinesterases and protect a human dopaminergic cell line from hydrogen peroxide-induced cytotoxicity. *Pharm. Biol.* **2016**, *54*, 1687–1696. [CrossRef]
62. Chaari, M.; Theochari, I.; Papadimitriou, V.; Xenakis, A.; Ammar, E. Encapsulation of carotenoids extracted from halophilic Archaea in oil-in-water (O/W) micro- and nano-emulsions. *Colloids Surf. B Biointerfaces* **2018**, *161*, 219–227. [CrossRef]
63. Jaswir, I.; Noviendri, D.; Hasrini, R.F.; Octavianti, F. Carotenoids: Sources, medicinal properties and their application in food and nutraceutical industry. *J. Med. Plant. Res.* **2011**, *5*, 7119–7131. [CrossRef]
64. D Tortorella, M.; Zhang, Y.; Talley, J. Desirable Properties for 3rd Generation Cyclooxygenase-2 Inhibitors. *Mini Rev. Med. Chem.* **2016**, *16*, 1284–1289. [CrossRef] [PubMed]
65. Saeedi, M.; Hadjiakhondi, A.; Nabavi, S.M.; Manayi, A. Heterocyclic Compounds: Effective alpha-Amylase and alpha-Glucosidase Inhibitors. *Curr. Top. Med. Chem.* **2017**, *17*, 428–440. [CrossRef]
66. Saxena, M.; Dubey, R. Target Enzyme in Alzheimer's Disease: Acetylcholinesterase Inhibitors. *Curr. Top. Med. Chem.* **2019**, *19*, 264–275. [CrossRef]
67. Rovenský, J.; Payer, J. Cholinergic crisis. In *Dictionary of Rheumatology*; Springer: Vienna, Austria, 2009; p. 41.
68. Pillaiyar, T.; Manickam, M.; Namasivayam, V. Skin whitening agents: Medicinal chemistry perspective of tyrosinase inhibitors. *J. Enzym. Inhib. Med. Chem.* **2017**, *32*, 403–425. [CrossRef] [PubMed]
69. Bae-Harboe, Y.-S.C.; Park, H.-Y. Tyrosinase: A Central Regulatory Protein for Cutaneous Pigmentation. *J. Investig. Dermatol.* **2012**, *132*, 2678–2680. [CrossRef]
70. Niu, C.; Aisa, H.A. Upregulation of Melanogenesis and Tyrosinase Activity: Potential Agents for Vitiligo. *Molecules* **2017**, *22*, 1303. [CrossRef]
71. Czarnowicki, T.; Harari, M.; Ruzicka, T.; Ingber, A. Dead Sea climatotherapy for vitiligo: A retrospective study of 436 patients. *J. Eur. Acad. Dermatol. Venereol.* **2011**, *25*, 959–963. [CrossRef]
72. Carbajo, J.M.; Maraver, F. Salt water and skin interactions: New lines of evidence. *Int. J. Biometeorol.* **2018**, *62*, 1345–1360. [CrossRef]
73. Schallreuter, K.U.; Elwary, S.M.A.; Gibbons, N.C.J.; Rokos, H.; Wood, J.M. Activation/deactivation of acetylcholinesterase by H_2O_2: More evidence for oxidative stress in vitiligo. *Biochem. Biophys. Res. Commun.* **2004**, *315*, 502–508. [CrossRef]
74. Boo, H.O.; Hwang, S.J.; Bae, C.S.; Park, S.H.; Heo, B.G.; Gorinstein, S. Extraction and characterization of some natural plant pigments. *Ind. Crops Prod.* **2012**, *40*, 129–135. [CrossRef]
75. Manilal, A.; Sujith, S.; Selvin, J.; Kiran, G.S.; Shakir, C.; Lipton, A.P. Potencial de los antimicrobianos de los organismos marinos de la costa sureste de la India frente a patógenos multirresistentes del camarón y humanos. *Sci. Mar.* **2010**, *74*, 287–296. [CrossRef]
76. Karpiński, T.M.; Adamczak, A. Fucoxanthin—An antibacterial carotenoid. *Antioxidants* **2019**, *8*, 239. [CrossRef] [PubMed]

77. Chen, L.; Wang, G.; Bu, T.; Zhang, Y.; Wang, Y.; Liu, M.; Lin, X. Phylogenetic analysis and screening of antimicrobial and cytotoxic activities of moderately halophilic bacteria isolated from the Weihai Solar Saltern (China). *World J. Microbiol. Biotechnol.* **2010**, *26*, 879–888. [CrossRef]
78. Atanasova, N.S.; Pietilä, M.K.; Oksanen, H.M. Diverse antimicrobial interactions of halophilic archaea and bacteria extend over geographical distances and cross the domain barrier. *Microbiologyopen* **2013**, *2*, 811–825. [CrossRef]
79. Mazguene, S.; Rossi, M.; Gogliettino, M.; Palmieri, G.; Cocca, E.; Mirino, S.; Imadalou-Idres, N.; Benallaoua, S. Isolation and characterization from solar salterns of North Algeria of a haloarchaeon producing a new halocin. *Extremophiles* **2018**, *22*, 259–270. [CrossRef]
80. Quadri, I.; Hassani, I.I.; l'Haridon, S.; Chalopin, M.; Hacène, H.; Jebbar, M. Characterization and antimicrobial potential of extremely halophilic archaea isolated from hypersaline environments of the Algerian Sahara. *Microbiol. Res.* **2016**, *186*, 119–131. [CrossRef]

Supplementary material

***Haloarcula hispanica* HM1, 16S RNA coding gene sequence**

GGAATCGATTAGCCCTGCTAGTCGCACGGGTCTTAGACTCCGTAGGCATATAGCTCAGTAACACGTGGC
CAAACTACCCTACAGACCGCGATAACCTCGGGAAACTGAGGCCAATAGCGGATATAACTCTCAGGCTG
GAGTGCCGAGAGTTAGAAACGTTCCGGCGCTGTAGGATGTGGCTGCGGCCGATTAGGTAGATGGTGG
GGTAACGGCCCACCATGCCGATAATCGGTACGGGTTGTTGGAGAGCAAGAACCCGGAGACGGTATTT
GAGACAAGATACCGGGCCCTACGGGGCGCAGCAGGCGGGAAACCTTTACACTGCACGACAGTGCGAT
AGGGGGACTCCGAGTGTGAGGGCATATAGCCCTCGCTTTTCTGTACCGTAAGGTGGTACAGGAACAAG
GACTGGGCAAGACCGGTGCCAGCCGCCGCGGTAATACCGGCAGTCCAAGTGATGGCCGATATTATTGG
GCCTAAAGCGTCCGTAGCCGGCCGGACAAGTCCGTTGGGAAATCGACGAGCTCAACGCGTCGGCGTCC
AGCGGAAACTGTCCGGCTTGGGGCCGGAAGACTTGGGGGGTACGTCCGGGGTAGGAGTGAAATCCTG
TAATCCTGGACGGACCACCAATGGGGAAACCACCTCAGGAAGCCGGACCCGACGGTGAGGGACGAAA
GCCAGGGTCTCGAACCGGATTAGATACCCGGGTAGTCCTAGCTGTAAACGATGCTCGCTAGGTGTGCC
GTAGGCCACGAGCATGCGATGCGCCGTAGGGAAGCCGAGAAGCGAGCCGCCTGGGAAGTACGTCTGC
AAGGATGAAACTTAAAGGAATTGGCGGGGGAGCACCACAACCGGAGGAGCCTGCGGTTTAATTGGAC
TCAACGCCGGAAATCTCACCGGTCCCGACAGTAGTAATGACGGTCAGGTTGACGACTTTACCCGACGCT
ACTGAGAGGAGGTGCATGGCCGCCGTCAGCTCGTACCGTGAGGCGTCCTGTTAAGTCAGGCAACGAG
CGAGACCCGCACTTCTAGTTGCCAGCAATACCCTTGAGGTAGTTGGGTACACTAGGAGGACTGCCGCT
GCTAAAGCGGAGGAAGGAACGGGCAACGGTAGGTCAGTATGCCCCGAATGGACCGGGCAACACGCG
GGCTACAATGGCTCTGACAGTGGGATGCAACGCCGAGAGGCGACGCTAATCTCCAAACGGAGTCGTA
GTTCGGATTGCGGGCTGAAACCCGCCCGCATGAAGCTGGATTCGGTAGTAATCGCGTGTCAGAAGCGC
GCGGTGAATACGTCCCTGCTCCTTGCACACACCGCCCGTCAAAGCACCCGAGTGGGGTCCGGATGAGG
CCGTCATGCGACGGTCGAATCCT

***Halobacterium salinarum* HM2, 16S RNA coding gene sequence**

GGATCGATTAGCCATGCTAGTTGTGCGGGTTTAGACCCGCAGCGGAAGCTCAGTAACACGTGGCCAAG
CTACCCTGTGGACGGGAATACTCTCGGGAAACTGAGGCTAATCCCCGATAACGCTTTGCTCCTGGAAG
GGGCAAAGCCGGAAACGCTCCGGCGCCACAGGATGCGGCTGCGGTCGATTAGGTAGACGGTGGGGT
AACGGCCCACCGTGCCCATAATCGGTACGGGTTGTGAGAGCAAGAGCCCGGAGACGGAATCTGAGAC
AAGATTCCGGGCCCTACGGGGCGCAGCAGGCGCGAAACCTTTACACTGTACGAAAGTGCGATAAGGG
GACTCCGAGTGTGAAGGCATAGAGCCTTCACTTTTGTACACCGTAAGGTGGTGCACGAATAAGGACTG
GGCAAGACCGGTGCCAGCCGCCGCGGTAATACCGGCAGTCCGAGTGATGGCCGATCTTATTGGGCCTA
AAGCGTCCGTAGCTGGCTGAACAAGTCCGTTGGGAAATCTGTCCGCTTAACGGGCAGGCGTCCAGCGG
AAACTGTTCAGCTTGGGACCGGAAGACCTGAGGGGTACGTCTGGGGTAGGAGTGAAATCCTGTAATCC
TGGACGGACCGCCGGTGGCGAAAGCGCCTCAGGAGAACGGATCCGACAGTGAGGGACGAAAGCTAG
GGTCTCGAACCGGATTAGATACCCGGGTAGTCCTAGCTGTAAACGATGTCCGCTAGGTGTGGCGCAGG
CTACGAGCCTGCGCTGTGCCGTAGGGAAGCCGAGAAGCGGACCGCCTGGGAAGTACGTCTGCAAGGA
TGAAACTTAAAGGAATTGGCGGGGGAGCACTACAACCGGAGGAGCCTGCGGTTTAATTGGACTCAAC
GCCGGACATCTCACCAGCCCCGACAGTAGTAATGACGGTCAGGTTGATGACCTTACCCGAGGCTACTG
AGAGGAGGTGCATGGCCGCCGTCAGCTCGTACCGTGAGGCGTCCTGTTAAGTCAGGCAACGAGCGAG
ACCCGCACTCCTAATTGCCAGCAGTACCCTTTGGGTAGCTGGGTACATTAGGTGGACTGCCGCTGCCAA
AGCGGAGGAAGGAACGGGCAAGCCCCGAATGGGCTGGGCAACACGCGGGCTACAATGGTCGAGACA
ATGGGAAGCCACTCCGAGAGGAGGCGCTAATCTCCTAAACTCGATCGTAGTTCGGATTGAGGGCTGAA
ACTCGCCCTCATGAAGCTGGATCGGTAGGTCAGTATTCGGTAGTAATCGCGTGTCAGCAGCGCGCGGT
GAATACGTCCCTGCTCCTTGCACACACCGCCCGTCAAATCACCCGAGTGGGGTTCGGATGAGGCCGGC
ATGCGCTGGTCAAATCGGC

Chapter 3

Biochemical Characterization of the Amylase Activity from the New Haloarchaeal Strain Haloarcula sp. HS Isolated in the Odiel Marshlands

This chapter has been published as: **Gómez-Villegas, P.**; Vigara, J.; Romero, L.; Gotor, C.; Raposo, S.; Gonçalves, B.; Léon, R. Biochemical Characterization of the Amylase Activity from the New Haloarchaeal Strain Haloarcula sp. HS Isolated in the Odiel Marshlands. Biology 2021, 10,337. https://doi.org/10.3390/biology10040337

biology

MDPI

Article

Biochemical Characterization of the Amylase Activity from the New Haloarchaeal Strain *Haloarcula* sp. HS Isolated in the Odiel Marshlands

Patricia Gómez-Villegas [1], Javier Vigara [1], Luis Romero [2], Cecilia Gotor [2], Sara Raposo [3], Brígida Gonçalves [3] and Rosa Léon [1,*]

1 Laboratory of Biochemistry, Department of Chemistry, Marine International Campus of Excellence (CEIMAR), University of Huelva, Avda. de las Fuerzas Armadas s/n, 21071 Huelva, Spain; patgomvil@gmail.com (P.G.-V.); vigara@uhu.es (J.V.)
2 Instituto de Bioquímica Vegetal y Fotosíntesis, Consejo Superior de Investigaciones Científicas and Universidad de Sevilla, Avenida Américo Vespucio 49, 41092 Seville, Spain; lromero@ibvf.csic.es (L.R.); gotor@ibvf.csic.es (C.G.)
3 CIMA—Centre for Marine and Environmental Research, FCT, Campus de Gambelas, Universidade do Algarve, 8005-139 Faro, Portugal; sraposo@ualg.pt (S.R.); bgrodrigues@ualg.pt (B.G.)
* Correspondence: rleon@uhu.es; Tel.: +34-959-219-951

Simple Summary: Amylases are a group of enzymes that degrade starch into simple sugars. These proteins are produced by a wide variety of organisms and are supposed to be one of the most valuable industrial enzymes. However, the extreme conditions required for many industrial operations limit the applicability of most amylases found in nature. In this context, halophilic archaea entail an excellent source of novel proteins that tolerate harsh conditions, as they live in environments with high salt concentration and temperature. In this work, a screening of haloarchaea, isolated from Odiel salterns in the southwest of Spain, was carried out to select a new strain with a high amylase activity. This microorganism was identified as *Haloarcula* sp. HS and showed amylase activities in both, the cellular and the extracellular extracts. Both amylase activities were poly-extremotolerant, as their optimal yields were achieved at 60 °C and 25% NaCl. Additionally, the study of the protein sequences from *Haloarcula* sp. HS allowed the identification of three different amylases, which conserved the typical structure of the alpha-amylase family. Finally, the applicability of the extracellular amylase to treat bakery wastes under high salinity conditions was demonstrated.

Abstract: Alpha-amylases are a large family of α,1-4-endo-glycosyl hydrolases distributed in all kingdoms of life. The need for poly-extremotolerant amylases encouraged their search in extreme environments, where archaea become ideal candidates to provide new enzymes that are able to work in the harsh conditions demanded in many industrial applications. In this study, a collection of haloarchaea isolated from Odiel saltern ponds in the southwest of Spain was screened for their amylase activity. The strain that exhibited the highest activity was selected and identified as *Haloarcula* sp. HS. We demonstrated the existence in both, cellular and extracellular extracts of the new strain, of functional α-amylase activities, which showed to be moderately thermotolerant (optimum around 60 °C), extremely halotolerant (optimum over 25% NaCl), and calcium-dependent. The tryptic digestion followed by HPLC-MS/MS analysis of the partially purified cellular and extracellular extracts allowed to identify the sequence of three alpha-amylases, which despite sharing a low sequence identity, exhibited high three-dimensional structure homology, conserving the typical domains and most of the key consensus residues of α-amylases. Moreover, we proved the potential of the extracellular α-amylase from *Haloarcula* sp. HS to treat bakery wastes under high salinity conditions.

Keywords: amylase; extremozymes; haloarchaea; enzymatic characterization; proteomics

check for updates

Citation: Gómez-Villegas, P.; Vigara, J.; Romero, L.; Gotor, C.; Raposo, S.; Gonçalves, B.; Léon, R. Biochemical Characterization of the Amylase Activity from the New Haloarchaeal Strain *Haloarcula* sp. HS Isolated in the Odiel Marshlands. *Biology* **2021**, *10*, 337. https://doi.org/10.3390/biology10040337

Academic Editor: Xuehong Zhang

Received: 22 February 2021
Accepted: 15 April 2021
Published: 16 April 2021

1. Introduction

Haloarchaea are the main representatives of extreme halophiles, which can thrive in media with salt concentrations ranging from 20 to 30% [1,2]. These singular microorganisms are characterized by the accumulation of large amounts of KCl in the cytoplasm, to maintain the osmotic balance with the medium, in contrast to moderate or facultative halophiles, which usually store compatible solutes for the same purpose [3]. Therefore, intra- and extracellular proteins from haloarchaea are specially adapted to work properly at high salt concentrations. These proteins possess exceptional features that make them distinguishable from non-halophilic proteins; they have a unique amino acid composition with acidic surfaces and low overall hydrophobicity, to prevent aggregation and, at the same time, retain flexibility in such high salinity [4]. Most haloarchaeal enzymes are considered poly-extremotolerant, as they work appropriately under more than one extreme condition, usually elevated temperatures, in addition to high salinity. For this reason, enzymes from these halophilic microorganisms can be of interest in many harsh industrial and biotechnological processes [5,6].

Amylases are a diverse group of hydrolase or transferase enzymes that degrade large alpha-linked polysaccharides, such as starch and related oligosaccharides, and are one of the most required enzymes in industrial operations. They stand for about 30% of the world enzyme market, and this value is expected to grow in the following years, due to the global increase in the demand for bakery and sugar-derived products, biofuels, detergents, breweries, animal feeds, pharmaceuticals, paper, and textiles [7,8]. At present, the best market for amylases is in the production of maltose and glucose syrups from corn, which are used as sweeteners for soft drinks [9,10]. They are also required for the enhancement of dough for baking, for clarification of fruit juices and beers, and in the pretreatment of animal feed to improve the digestibility of fiber [11]. In addition, amylases are widely used in textile and paper industries to remove the starch employed for the desizing process and the coating treatment, respectively. Moreover, several hydrolytic enzymes, including amylases, are usually added to detergents because they permit the use of milder conditions in laundry and automatic dishwashing, making them eco-friendlier. Other interesting fields of application of amylases are biomedicine and pharmacy, to treat digestive disorders or as reporter genes in molecular biology [12]. Furthermore, amylases are widely used for the conversion of starch-rich agronomic and food wastes into fermentable sugars, which are required as feedstocks for the production of fuels and chemicals with high demand and market value [13].

Amylases are ubiquitous ancient enzymes found in plants, animals, and microorganisms. Among them, bacteria of the genus *Bacillus* or fungi belonging to the *Aspergillus* genus are the most preferred source of amylases for large-scale production [14]. Hydrolytic amylases can be classified into two broad categories—endoamylases, which hydrolyze the interior of the starch molecule; and exo-amylases, which successively degrade starch from the non-reducing ends [9]. Most endoamylases belong to the α-amylase family (EC 3.2.1.1) and cleave internal α,1-4 glycosidic bonds between glucose units, producing oligosaccharides with varying lengths and α-limit dextrins. Additionally, α-amylases are typically divided into two groups, according to the hydrolysis products and the degree of starch hydrolysis; saccharifying α-amylases that produce free sugars, and liquefying α-amylases that break down the starch polymer without producing free sugars [5]. The mechanism of action and the catalytic properties of these amylases are well-known and can be correlated with their structural characteristics, as was detailed in several reviews [7,15,16].

The ability of haloarchaea to produce and excrete hydrolytic enzymes, including amylases to degrade extracellular polysaccharides, as many other microorganisms do, was previously described [6]. However, the application of archaeal amylases, which could be beneficial to many industrial operations that require extreme conditions, remains scarcely studied when compared to those from other microorganisms. Intracellular or cell-associated amylases from haloarchaea are particularly understudied, although they are an important haloarchaeal trait and can represent an interesting source of halotolerant enzymes.

The saltern ponds of the Odiel Marshlands are an interesting saline ecosystem, which harbors a rich diversity of prokaryotic and eukaryotic microorganisms. Our previous studies showed that at very high salinity (33%), the most abundant archaea species belong to the genera *Halorubrum* and *Haloquadratum* [17]. Metagenomic microbial profiling by high-throughput 16S rRNA sequencing revealed the existence of various strains that belonged to the *Haloarcula* genus. Although the abundance of these representatives was quite low, with less than 0.2% of the total sequenced reads, our data suggest that some of the haloarchaea of this group are able to produce bioactive compounds [18] and excrete hydrolytic haloenzymes, including proteases, amylases, or lipases [17].

In this study, a collection of haloarchaea isolated from the saltern ponds of the Odiel Marshlands was screened for their amylolytic activity, and the one that exhibited the highest activity was selected and identified on the basis of its 16S rRNA coding gene. The extracellular and cellular starch-degrading activities of the selected archaea were characterized, revealing different optimal parameters and modes of action. To get a further insight into the identity of these starch-degrading enzymes, the proteome composition of the partially purified cell-free supernatant and the cellular extracts was analyzed by tryptic digestion, followed by nano-liquid chromatography coupled to an electrospray ionization tandem mass spectrometry system. This study allowed the identification of three amylase sequences (two were exclusively cell-associated and one was also found in the extracellular medium) with high homology to amylases of other haloarchaeal species, and the typical alpha-amylase conserved regions. Furthermore, the potential applicability of the amylase enzymes of this new haloarchaea on the treatment of bakery waste was assessed and compared with a commercial amylase.

2. Materials and Methods

2.1. Screening and Selection of Amylase Producing Haloarchaea

The screening of amylase-producing haloarchaea was performed by detection of the extracellular amylase activity of the isolates on starch agar plates, with 20% NaCl. The plates were flooded with commercial Lugol's iodine solution, 0.5% I_2 and 1% KI (*w/v*) (Chem Lab, Zedelgem, Belgium), every three days, to check the formation of degradation halos around the colonies. The isolate that presented the highest ratio of halo zone with respect to colony diameter was chosen for further studies. Screenings were done in triplicates.

2.2. Identification of the Selected Microorganism

Genomic DNA of the isolated amylase-producing strain was purified using the GeneJET Genomic Purification kit (Thermo Fisher Scientific, Waltham, MA, USA), following the manufacturer's instructions. The quantification and the purity assessment of the genomic DNA obtained was done on a Nanodrop Spectrophotometer ND-1000 (Thermo Fisher Scientific). The full length of the 16S rRNA encoding gene was amplified with the archaeal specific primers 21F (5′-TTCCGGTTGATCCTGCCGGA-3′) and 1492R (5′-GGTTACCTTGTTACGACTT-3′). Polymerase chain reactions (PCR) were performed in a total volume of 25 µL, using an Eppendorf thermo-cycler. The reaction mixture contained—1 µL of genomic DNA, 0.2 U REDTaq®DNA polymerase from Sigma Aldrich (St. Louis, MO, USA), and 2.5 µL of its specific 10× buffer that contained 10 pM of each primer, 0.2 mM dNTPs, and 2.5 mM $MgCl_2$. The thermal profile was set to 0.5 min at 96 °C, 0.5 min at 55 °C, and 1 min at 72 °C for 30 cycles, followed by 10 min of final extension. The PCR products were analyzed by electrophoresis, on a 1% agarose gel to check their quality, and sent to Stabvida (Lisbon, Portugal) for Sanger sequencing. The 1.4 kb 16S rRNA gene sequences obtained were compared to those available at the GenBank and the European Molecular Biology Laboratory (EMBL) databases, using the Basic Local Alignment Search Tool (BLAST) at the National Center for Biotechnology Information (NCBI) [19].

2.3. Culture Conditions for Enzyme Production

All cultures were incubated at 37 °C with a shaking rate of 100 rpm, with either standard rich medium or minimal medium. The standard rich medium for archaea growth contained per liter—156 g NaCl, 13 g $MgCl_2 \cdot 6H_2O$, 20 g $MgSO_4 \cdot 7H_2O$, 1 g $CaCl_2 \cdot 6H_2O$, 4 g KCl, 0.2 g $NaHCO_3$, 0.5 g NaBr, and 5 g yeast extract, with a pH value of 7, measured before autoclaving. For the minimal medium, yeast extract was substituted for 1% (*w/v*) of ammonium acetate. The amylase activity was induced by the addition of starch (3 g L^{-1}) to either the rich or the minimal medium.

2.4. Partial Purification of Cell-Associated and Extracellular Amylases

Haloarcula sp. HS cells were first cultured in the rich medium, containing yeast extract and starch. When the culture reached the end of the exponential phase ($OD_{580} \approx 3$), cells were harvested through centrifugation, washed, and transferred to the minimal medium, where the biomass was cultivated until the extracellular starch was completely exhausted, about 3 days after the transference. Starch content was periodically measured every 24 h, by mixing 1 mL of culture medium with 5 µL of commercial Lugol's iodine solution and by reading the absorbance at 580 nm. Then, the biomass was harvested by centrifugation for 20 min at 12,000 rpm and 4 °C. The supernatant was 100-fold concentrated by an ultrafiltration process in an Amicon® system with a 10 kDa cut-off membrane and used as the source of the extracellular amylase. The specific amylase activity in the medium supernatant was 8 U mg^{-1} and it was increased to 350 U mg^{-1} in the concentrated supernatant, with a purification factor of 43.75. On its part, the cell pellet was disrupted by sonication in phosphate buffer (50 mM, 20% NaCl, pH 7) and centrifuged again to remove the cell debris and unbroken cells. The obtained cell extract was loaded onto a DEAE Sephacel™ column equilibrated with the same phosphate buffer. The absorbed proteins were eluted using a linear gradient of NaCl from 0 to 500 mM and a final washing with NaCl 1 M, with a flow rate of 15 mL h^{-1}. All fractions that presented amylase activity were collected and used as the cellular amylase source. In this case, the specific activity was increased from 20 U mg^{-1} in the crude cell extract to 120 U mg^{-1} in the partially purified preparation, with a purification factor of 6. Determination of the protein content in all the obtained extracts was performed according to the Bradford method [20], using bovine serum albumin (BSA) as standard.

2.5. Amylase Activity Assay

Unless otherwise indicated, the amylase activity was measured following the degradation of soluble starch by the standard iodine assay, based on the decrease of the absorbance at 580 nm of the iodine–starch complex produced by starch hydrolysis. The standard reaction mixture contained 50 µL of enzyme solution, 100 µL of 1% (*w/v*) potato starch solution in 20% NaCl, and 100 µL of phosphate buffer (50 mM, pH 7, 20% NaCl). The reaction mixture was incubated at 50 °C for 30 min, previously set as the best time to conserve the linearity of the activity. The reaction was stopped by cooling on ice and 100 µL were employed to reveal the remaining starch, by mixing 5 µL of four times diluted commercial Lugol's iodine solution with the sample. Thereafter, 1 mL of distilled water was added to the sample before reading the absorbance at 580 nm. A standard curve was prepared with soluble starch. One unit of amylase activity was defined as the amount of enzyme degrading one microgram of starch per minute from soluble starch, under the assay conditions. To study the substrate specificity, potato starch was substituted by the indicated compounds (carboxymethyl cellulose, sucrose, and lactose) at a concentration of 1% (*w/v*), and incubated in the same conditions.

To analyze the starch hydrolysis products, aliquots were withdrawn from the incubation mixture at the initial reaction time and after 2 h of incubation at 50 °C. The reaction mixture contained 300 µL of the corresponding amylase extract and 600 µL of 1% (*w/v*) potato starch solution in 20% NaCl (*w/v*). The hydrolysis products were examined by a high-performance liquid chromatographic (HPLC) system (Merck-Hitachi LaChrom

Elite), equipped with a refractive index detector (Merck-Hitachi L-2490) and an Aminex® HPX-87H Column (Bio-Rad, Hercules, CA, USA), using an isocratic elution method with 5 mM H_2SO_4 at 50 °C, and a flow rate of 0.6 mL min^{-1}. Glucose, maltose, and dextrin standards were obtained from Merck, Sigma-Aldrich (St. Louis, MO, USA).

2.6. Native Electrophoresis and Zymogram

The presence of amylase activity in the concentrated supernatant and the cell extract was revealed by in situ staining of a native PAGE containing 0.2% of soluble starch in the separating gel. A volume of 15 µL of the sample was mixed with 5 µL of loading dye and electrophoretically separated into two parallel gels of acrylamide, 10% supplemented with starch 0.2% (*w/v*) and run at 130 V. After electrophoresis, one of the gels was incubated in phosphate buffer (50 mM, pH 7, 20% NaCl) at 50 °C and 50 rpm for 1 h. Subsequently, the gel was stained with commercial Lugol´s reagent and the appearance of clear bands revealed the amylase activity. Meanwhile, the other gel was stained with 0.1% (*w/v*) Coomasie Brillant Blue R-250 in 45% (*v/v*) ethanol-10% (*v/v*) acetic acid, and faded with 25% (*v/v*) ethanol-10% (*v/v*) acetic acid. Molecular markers (NativeMark™ Unstained Protein Ladder, Thermo Fisher Scientific, Waltham, MA, USA) were used as a reference for the molecular weight of proteins. Molecular mass estimation of the proteins was calculated by plotting the log (MW) as a function of Rf (migration distance of the protein/migration distance of the dye front).

2.7. Effect of NaCl, Temperature, pH, Metals, and Detergents on the Amylase Activities of the New Isolated Strain Haloarcula sp. HS

The effect of salt concentration was evaluated until a maximum of 32% NaCl with intervals of 4% salinity increase. The desired NaCl concentration was obtained by adding the required NaCl to the phosphate buffer (50 mM, pH 7) and to the 1% (*w/v*) starch solution. The influence of temperature on cell-associated and extracellular amylase activities was studied in phosphate buffer (50 mM, pH 7, 20% NaCl), over the range of 30–80 °C, with temperature increments of 10 °C. For pH studies, amylase activity was measured at 50 °C and 20% of salt, in the following buffers—50 mM acetate for pH 2 and 3; 50 mM MES for pH from 4 to 6; and 50 mM Tris-HCl for pH from 7 to 11. All the assays were done at least in triplicates, and the results were presented as a percentage of relative activity.

To test the influence of different metals on cell-associated and extracellular amylase activities $MgSO_4$, $CaCl_2$, $CuCl_2$, $FeCl_2$, $FeCl_3$, or EDTA (ethylenediaminetetraacetic acid), were added to the reaction mixture, in a final concentration of 10 mM. Similarly, the effect of various surfactants were studied, including Tween20 (Polyoxyethylene (20) sorbitan monolaurate), Tween80 (Polyoxyethylene (80) sorbitan monooleate), Triton-X100 (2-[4-(2, 4, 4-trimethylpentan-2-yl) phenoxy] ethanol), CHAPS (3-[(3-Cholamidopropyl) dimethylammonio]-1-propanesulfonate), SB-12 (N-Dodecyl-N,N-dimethylammonio-3-propane sulfonate), and SDS (sodium dodecyl sulfate), in a final concentration of 0.5% (*w/v*). Amylase residual activity was measured as previously detailed for the standard assay and expressed as a percentage, with respect to a control sample incubated in the absence of additives. All the determinations were conducted in triplicates.

2.8. Proteomic Analysis

For the proteomic analysis, the concentrated supernatant and the partially purified cell extract fractions with starch degrading activity were dialyzed for 48 h, against a solution of 1% $NaHCO_3$ and 0.01% EDTA in milli-Q water, to eliminate excess salt. The proteins were first precipitated with TCA/acetone and resuspended in ammonium bicarbonate-trifluoroethanol (50%). After that, the proteins were treated with dithiothreitol, 10 mM, and methyl ethanethiosulfonate, 10 mM. Prior to trypsin digestion, the samples were diluted with ammonium bicarbonate 25 mM, until the concentration of trifluoroethanol was under 5%. The digestion with trypsin was done overnight at 37 °C. Subsequently, the samples were analyzed by LC-MS/MS in a triple quadrupole-TOF system (5600 plus, ABSciex, Vaughan, ON, Canada), equipped with a nano-electrospray ion source, coupled to

a nano-HPLC (Eksigent, Vaughan, ON, Canada). The Analyst TF 1.7 software was used for equipment controlling and data acquisition. Peptide mass tolerance was set to 25 ppm and 0.05 Da, for fragment masses, and only 1 or 2 missed cleavages were allowed. The peptide and protein identifications were performed using the Protein Pilot software (version 5.0.1, SCIEX, Vaughan, ON, Canada), with the Paragon algorithm. The search was conducted against the Uniprotproteome_Haloarcula_hispanica database 11_24_2020. The false discovery rate (FDR) was set to 0.01 for both peptides and proteins. Protein comparison was performed with the Basic Local Alignment Search Tool for proteins (BLASTp) of the NCBI (National Center for Biotechnology Information). The obtained sequences were analyzed using the CLC Workbench software (version 8, Qiagen, Hilden, Germany).

2.9. Identification of Amylase Coding Genes Based on Protein Sequences

With the aim of completing the full protein sequences of the amylases identified, the sequences of their encoding genes were amplified by PCR, using sets of primers specifically designed on the basis of the sequences of peptides obtained in the proteomic analysis. Concretely, six pairs of primers were employed to cover almost the full length of the DNA sequences of the three amylases found, obtaining two overlapping sequences for each amylase gene (Table 1).

Table 1. Sequences of the primers employed for the amylase encoding genes amplification.

Primers	Forward (5′-3′)	Reverse (5′-3′)
AMY_HS1	ACCGGCAGTAAGCAGGCGTCTC GGCTCGTCGGGCTGAAGGACC	GGCGGCGTCCCAGCGAATACC CCCTCTCGCTCGTAGACGTACAGGTC
AMY_HS2	CGTCGGCGAATCGGTCGAACT GGAACGCGACAGTGGAACCGGA	GTCGCGTTTCCGGTTCCACTGTC CGAAGTGCAGAACGACCACGAGCG
AMY_HS3	GGAGACGGCCCGGTCGAACA GCCGGCGATAGCGACGAAT	CGCGTCGAAGGGCGATTC TCGTACGGGATTCGGAGGAGG

Primer sets used for PCR amplification of the three amylase coding genes found in *Haloarcula* sp. HS. For each gene (*AMY_HS1*, *AMY_HS2*, and *AMY_HS3*), two pairs of primers were designed on the basis of the sequences of the peptides obtained by proteomics.

Polymerase chain reactions were performed in a total volume of 25 µL, using an Eppendorf thermo-cycler. The reaction mixtures contained—1 µL of genomic DNA, 0.2 U REDTaq®DNA polymerase from Sigma Aldrich (St. Louis, MO, USA), and 2.5 µL of its specific 10× buffer that contained 10 pM of each primer, 0.2 mM dNTPs, and 2.5 mM $MgCl_2$. The thermal profile was set to 0.5 min at 96 °C, 0.5 min at 62 °C, and 1 min at 72 °C for 30 cycles, followed by 10 min of final extension. The PCR products were analyzed by electrophoresis on a 1% agarose gel and sent to Stabvida (Lisbon, Portugal) for Sanger sequencing. The sequences obtained were translated to protein and both, DNA and protein sequences, were compared to those available at National Center for Biotechnology Information (NCBI) databases, using the Basic Local Alignment Search Tool (BLAST). Finally, different alignments were conducted in the CLC Workbench software (version 8, Qiagen), the predicted structural models were built using the Phyre2 [21] and NetSurfP [22] online web servers, and three-dimensional (3D) molecular graphics were analyzed in the UCSF Chimera version 1.15 [23] (University of California, Oakland, CA, USA). Physicochemical characteristics of the proteins were obtained using the ProtParam tool (ExPASy) [24].

2.10. Starch Hydrolysis from Bakery Waste

Bread from bakery waste was chosen for the present experiment. Bread crumbs were dried on a stove at 70 °C and milled in a porcelain mortar to obtain a fine powder. Starch was recovered by mashing dried crumbs in distilled water, in saltwater at 20% NaCl (*w/v*), and in saturated saline solution (33% NaCl). The ability of the extracellular amylase of *Haloarcula* sp. HS to degrade the starch from bread was comparatively tested against a commercial α-amylase (Megazyme cat. no. E-BSTAA). Starch and enzyme solutions were

mixed in a proportion of 1:1 (*v*/*v*) in a final volume of 1 mL. The hydrolysis of the starch was performed for 15 min at 60 °C in 50 mM acetate buffer pH 5. The amount of remaining starch was measured by the iodine-starch method. A control, containing starch recovered from bread without the enzyme solution, was incubated in the same conditions. All assays were conducted in triplicates.

3. Results

3.1. Selection of Amylase-Producing Haloarchaea Isolated from Odiel Salterns Ponds

An in vitro screening was carried out to select the best amylase-producing strain, among a collection of archaea previously isolated from the saltern ponds of the Odiel Marshlands (SW, Spain) with a salinity of 33%. Amylase activity of each isolate was screened for 9 days on starch-agar plates, as detailed in Material and Methods (Figure 1A). Eight colonies showed a considerable amylase activity, and that with the largest halo was selected and identified, by amplification and sequencing of its 16S rRNA full-length coding gene (Supplementary Material, Figure S1), followed by the comparison of the obtained sequence with the NCBI database using the BLASTn tool. The results showed that the selected strain was closely related to the *Haloarcula* genus, showing 98% homology with different species of this taxonomic group. Therefore, the new strain isolated was named *Haloarcula* sp. HS.

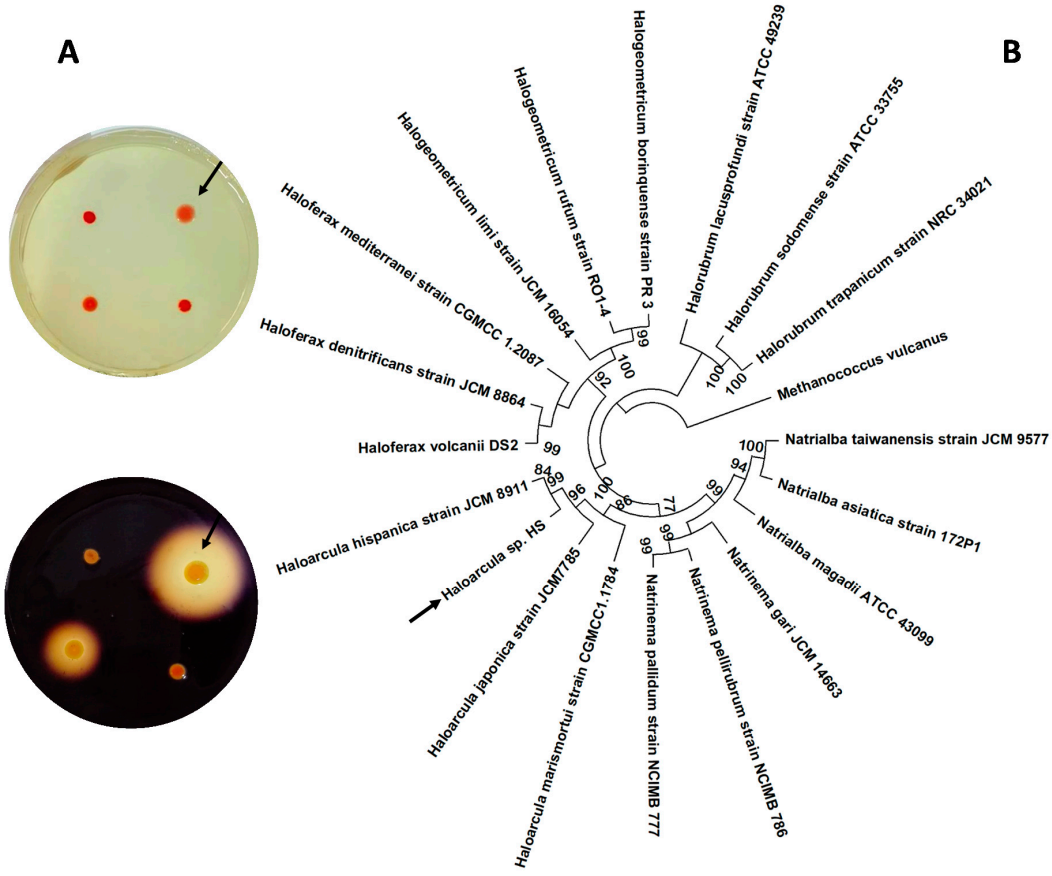

Figure 1. (**A**) In vitro selective screening for amylase-releasing haloarchaea. Semi-quantitative estimation of amylase activity from four haloarchaeal strains isolated from the Odiel Marshlands, grown on starch agar plates (**top**) and revealed with Lugol´s iodine solution (**down**), as detailed in the Material and Methods section. (**B**) Molecular phylogenetic analysis by the maximum likelihood method. The tree represents a comparison among the complete 16S rRNA coding gene sequences, including a series of reference haloarchaeal species and the new isolated strain, *Haloarcula* sp. HS. Multiple alignments were generated by MUSCLE (MUltiple Sequence Comparison by Log-Expectation) and the tree was constructed with MEGA X. The numbers at the nodes indicate the bootstrap values calculated for 1000 replicates. Arrows point to the new strain *Haloarcula* sp. HS.

Molecular phylogenetic analysis was performed using the Molecular Evolutionary Genetics Analysis (MEGA X) [25], on a series of reference haloarchaeal species and on the new isolated strain, *Haloarcula* sp. HS (Figure 1B). The hyperthermophilic archaea *Methanococcus vulcanus* was used as an outgroup and the bootstrap was set at 1000 replicates. The 16S rRNA encoding sequence of the isolate clustered with the corresponding genes of the representatives of the *Haloarcula* genus, especially close to the species *Haloarcula hispanica*.

3.2. Optimization of a Two-Stage Culture Strategy to Induce the Production of Amylase

In the studied archaea, significant levels of amylase activity were only found when the biomass was grown under inductive conditions in the presence of starch. The culture conditions that induced the production of amylases are widely studied for bacteria and hyperthermophilic archaea, as reviewed by Mehta and Satyanarayana [5], but more limited information exists on the production of amylase in haloarchaea [26,27]. Most authors agree that amylase production is growth-associated and is strongly induced by starch.

To establish the best culture conditions for the production and excretion of amylase by *Haloarcula* sp. HS, the haloarchaea was cultured in a (i) rich medium, which contained yeast extract and a (ii) minimal medium, in which the yeast extract was substituted by ammonium acetate. In both cases, starch (3 g L^{-1}) was added to the culture medium, as detailed in Materials and Methods. The optical density of the cultures, protein secretion into the media, and hydrolysis of extracellular starch were followed in both, rich and minimal medium cultures. As shown in Figure 2, cell growth and protein secretion were higher when the microorganism was grown in the rich media, which contained yeast extract. In this medium, the studied archaea reached the stationary phase of growth in about 4 days and excreted 3 mg L^{-1} of proteins into the culture medium. The archaea cultured in the minimal medium exhibited very slow growth and excreted much fewer proteins to the culture medium, about 1 mg L^{-1}, after 30 h of culture. However, starch degradation activity was much higher for the archaea cultured in the minimal medium, which despite a much lower biomass, showed an initial starch degradation rate 5.5 times higher than that of the rich medium. Although starch was completely hydrolyzed in both media, there was a 24 h lag phase before starch degradation started in the medium with yeast extract, probably due to the presence of more easily assimilable carbon sources in this medium.

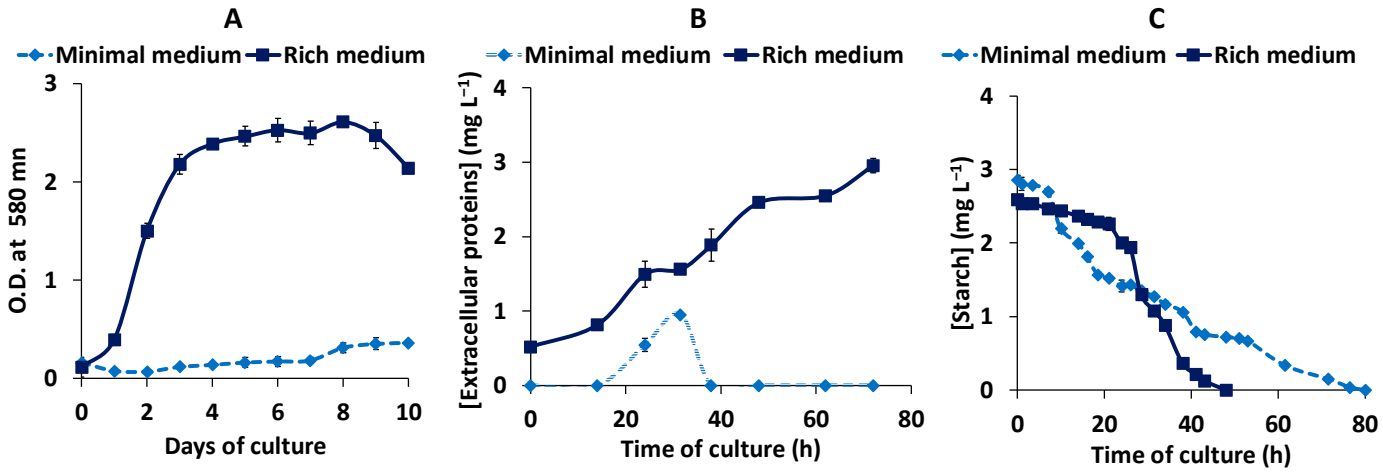

Figure 2. Time course evolution of *Haloarcula* sp. HS cultures in rich and minimal media. Optical density (**A**), secretion of proteins (**B**), and starch hydrolysis (**C**) were measured during the time of culture in rich (■) and minimal (♦) broths. All data are expressed as the mean ± SD of at least triplicate experiments.

For this reason, a two-step culture was set up to get both, a high biomass and amylase productivity. Cells were first grown in a rich medium in order to obtain a large amount of biomass, and when the culture reached the end of the exponential phase of growth, at

the third day of culture, the cells were transferred to the fresh minimal medium to induce the production of amylase, and was cultured for another 4 days. Through this two-step approach, high starch consumption activity and a high protein excretion were achieved, reaching an extracellular protein concentration of 10 mg L^{-1} and undetected levels of extracellular starch, on the 7th day of culture (Figure 3).

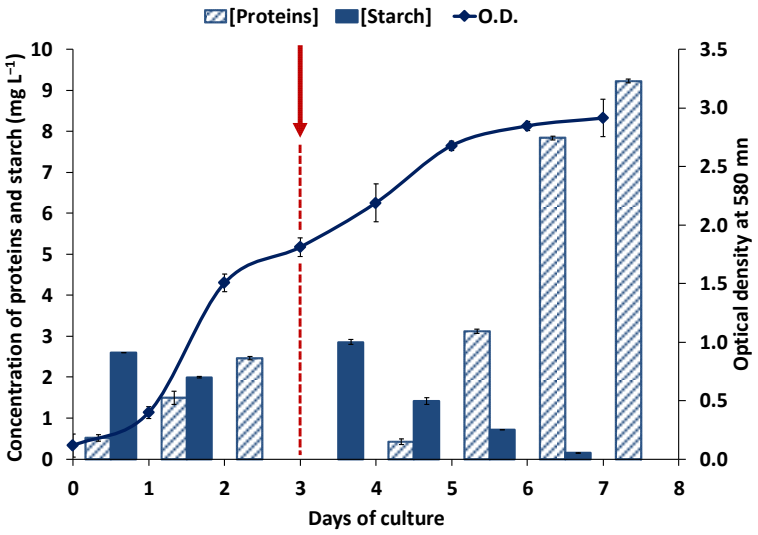

Figure 3. Time course evolution of *Haloarcula* sp. HS in the two-step culture. Optical density, secreted proteins, and starch concentration were measured along the full cultivation time. The red arrow indicates the moment of transference of the cells from the rich to the fresh minimum medium. All data are expressed as the mean ± SD of at least triplicate experiments.

3.3. Extracellular and Cell-Associated Amylase Activities in Haloarcula sp. HS

To identify the enzyme responsible for the amylase activity and characterize its properties, the haloarchaeal strain *Haloarcula* sp. HS was grown in a two-stage culture with starch (3 g L^{-1}), as previously described (Figure 3). Cell-associated proteins and the concentrated extracellular proteins excreted into the cultured medium were electrophoretically separated in a polyacrylamide gel containing starch. After electrophoresis, the gel was split lengthwise with a razor blade. One half was stained with Coomassie blue and the other with Lugol's iodine solution to detect both proteins and amylase activity, respectively. The zymogram analysis proved the presence of amylase activity in both samples, the culture medium, and the crude extract. A unique band with amylase activity was observed in the culture medium, after a 100-fold concentration step through ultrafiltration with a 10 kDa cut-off membrane, as indicated in Material and Methods. However, in the crude extract, two bands with starch hydrolyzing activity were observed, indicating the presence of several cell-associated enzymes with amylase activity (Figures 4 and S2). The crude extract was partially purified through ion-exchange chromatography in DEAE Sephacel^{TM}, as indicated in the Materials and Methods section. All fractions with amylase activity were pooled and used as the source of cellular amylase. The electrophoretic analysis of the purified extracts showed a unique band with amylase activity (Figure 4A). The size of the observed bands was between 20 and 27 kDa, however, the protein mobility was strongly affected by the starch added to the polyacrylamide gel and these apparent sizes observed were not representative.

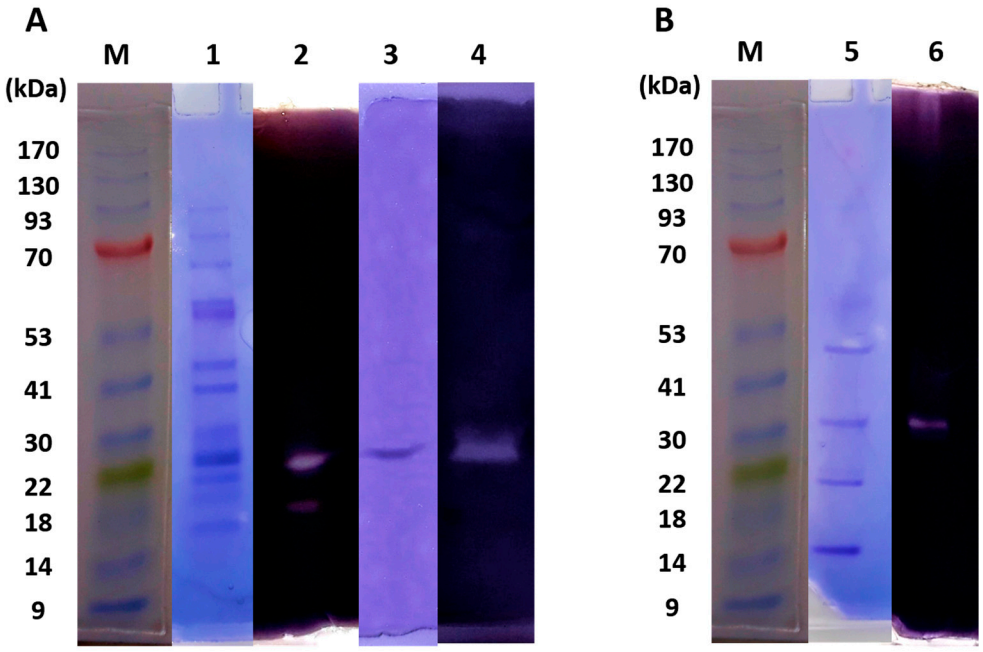

Figure 4. Native-PAGE and zymogram of cell-associated (**A**) and extracellular (**B**) proteins obtained from *Haloarcula* sp. HS. Lanes 1, 3, and 5—samples on native-PAGE followed by Coomassie Blue staining. Lanes 2, 4, and 6—samples on native PAGE followed by Lugol´s solution staining. Lane M—molecular mass marker in kDa, lanes 1 and 2—crude extract, lanes 3 and 4—partially purified crude extract, and lanes 5 and 6—concentrated supernatant. The whole gels for each staining are available in Supplementary Material, Figure S2.

3.4. Characterization of Extracellular and Cell-Associated Amylase Activities

A series of in vitro experiments were carried out with the extracellular and cellular amylase-enriched extracts to characterize the hydrolysis products, the substrate specificity, and the optimal kinetic parameters of the amylase activity of these extracts. Both, extracellular and cellular, enzymatic preparations were incubated with 1 mg of starch in the standard conditions, described in Material and Methods, excepting that the incubation time was fixed at 2 h. The products of starch hydrolysis were identified by HPLC and an IR detector, as detailed in Materials and Methods. A parallel reaction with a commercial α-amylase purchased from Megazyme (cat. no. E-BSTAA) was done in the same conditions for comparison. The results (Table 2) revealed that starch degradation was almost complete in all cases, being especially efficient in the case of the extracellular amylase extract, with a remaining starch of only 1.7%. The main product obtained with the three enzymatic sources was maltose, which represents between 73.8% and 86.1% of the total carbohydrate content in the reaction mixtures. In addition, the enzymatic preparation from the cellular extract was also able to catalyze the liberation of glucose (6.6%). On the other hand, the extracellular extract and the commercial reference amylase catalyzed the liberation of dextrins, which supposed 18.5% and 20.8% of the total carbohydrate content in the reaction mixture, respectively, in addition to maltose. No glucose was found as the end product in these reactions (Table 2).

Table 2. Percentage of the different products obtained from starch hydrolysis.

	Dextrins (%)	Maltose (%)	Glucose (%)	Starch (%)
Cell-associated amylase	ND	86.1 ± 3.6	6.6 ± 0.8	7.3 ± 2.9
Extracellular amylase	18.5 ± 1.1	79.7 ± 1.3	ND	1.7 ± 0.2
Commercial α-amylase	20.8 ± 3.1	73.8 ± 3.4	ND	5.4 ± 0.3

Comparison of the products obtained from the hydrolysis of starch by cell-associated or extracellular partially purified extracts of *Haloarcula* sp. HS and a commercial α-amylase. The percentage (%) of dextrins, maltose, and glucose produced and the remaining starch are indicated as the mean of three replicates with the corresponding standard deviation. ND, not detected.

With respect to the substrate specificity, neither extracellular nor cellular *Haloarcula* sp. HS extracts were able to hydrolyze other glucose polysaccharides, such as carboxymethyl cellulose, or disaccharides, such as sucrose or lactose, which not contain alpha-1,4-linked glucose.

The most characteristic feature of halophilic enzymes is their ability to operate under very high salinities. As it is shown in Figure 5, the extracellular enzymatic preparation presented the optimal activity at 28% salt and retained less than half of its activity when the salt content was under 20% (Figure 5A), showing that it is more salt-dependent than the cellular one, which instead showed the maximum activity at 16% salinity and retained more than 60% of its activity at all salinities studied (Figure 5B).

The influence of pH in both amylase activities was studied in different buffers, as detailed in Materials and Methods. The optimal activity was found at pH 5 for the extracellular amylase, and at pH 7 for the cellular amylase-enriched extract, as shown in Figure 5C,D, respectively. It should be noted that the cell-associated activity was stable under a wide range of pH values, retaining more than 50% activity at pH values between 2 and 11, and more than 80% activity at pH values comprising pH 5 to 9. Contrarily, the extracellular amylase activity appeared to be more susceptible to extreme pH, losing more than 50% of its activity both at low and high pH values.

The effect of the temperature on the amylase activities showed, once again, that the extracellular amylase activity had a higher dependence on the physicochemical parameters of the assay than the cell-associated one. The extracellular amylase activity showed an optimal temperature of 60 °C, losing more than 65% of its activity below 50 °C or above 60 °C (Figure 5E). The cellular amylase-enriched extract, on the other hand, conserved a high activity over a wide range of temperatures, retaining more than 75% of activity from 30 to 80 °C (Figure 5F). This weak temperature dependence was due to the fact that a mix of three different cell-associated enzymes could contribute to the amylase activity, as later shown by the proteomic analysis of the cellular enzymatic preparation.

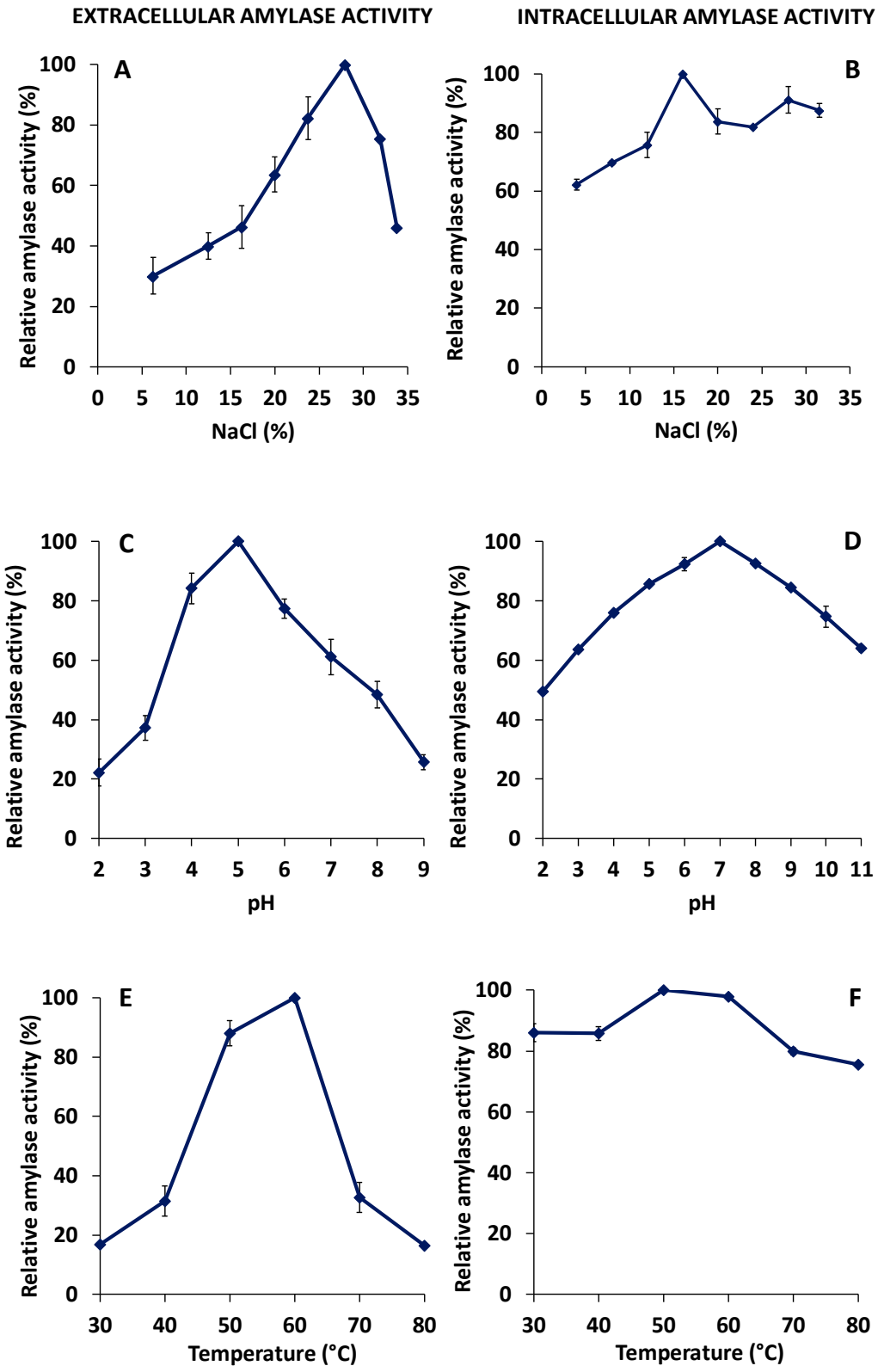

Figure 5. Effect of salt, pH, and temperature on amylase activities. Relative amylase activities in different salt concentrations (%, *w/v*), pH values, and temperatures are shown for the extracellular (**A**,**C**,**E**) and cellular (**B**,**D**,**F**) extracts. Relative activity was defined as the percentage of maximum activity for each case. The 100% activity corresponded to 70 ± 6.4 U mL^{-1} (350 U mg^{-1}) for the extracellular amylase extract and 60 ± 5.6 U mL^{-1} (120 U mg^{-1}) for the mix of cell-associated amylases. Mean and standard deviations are shown.

3.5. Effects of Metals and Surfactants on the Amylase Enzymatic Activities

Many microbial α-amylases are reported to be calcium-dependent metalloenzymes [9]. Therefore, the effect of EDTA, Ca^{2+}, and other metallic ions including Mg^{2+}, Cu^{2+}, Fe^{2+}, and, Fe^{3+} was tested. The results revealed that the addition of Ca^{2+}, Fe^{2+}, or Mg^{2+} causes a slight increase in the amylolytic activity of both extracellular and cellular enzymatic extracts (Figure 6). The possible existence of divalent metals in the partially purified enzymatic preparations makes it difficult to obtain accurate conclusions on the effects of these metals on the amylase activities of *Haloarcula* sp. HS. However, the strong inhibition observed in the presence of the metal chelating agent EDTA confirmed the divalent cation dependence of both, extracellular and cell-associated amylase activities, which decreased to 39% and 33%, respectively, in the presence of EDTA.

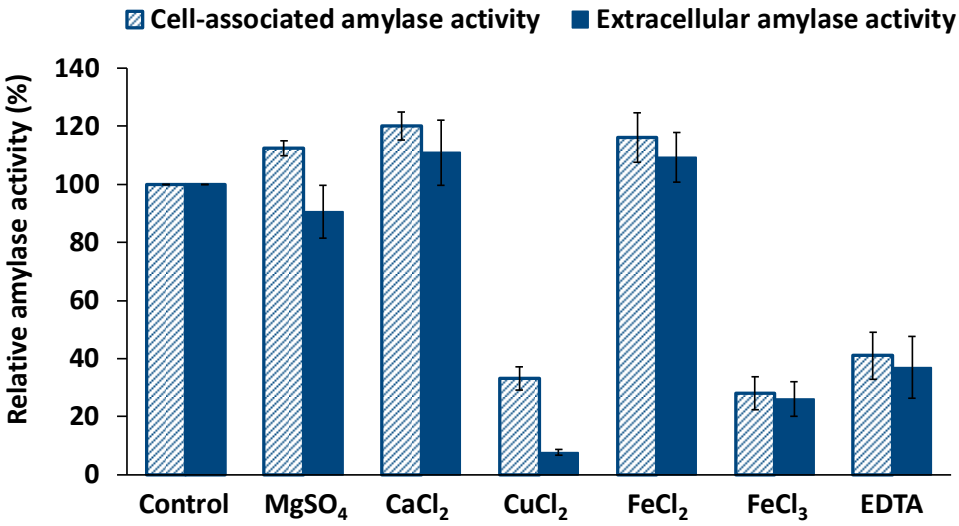

Figure 6. Effect of metal ions on the amylase activities. Extracellular and cell-associated relative amylase activities under the presence of different metal ions and EDTA (10 mM) are represented. Relative activity was defined as the percentage of maximal activity with respect to control, with no additives. The control activity was 70 ± 6.4 U mL^{-1} (350 U mg^{-1}) for the extracellular amylase and 60 ± 5.6 U mL^{-1} (120 U mg^{-1}) for the cellular amylase. Mean and standard deviations are shown.

On the other hand, the presence of Cu^{2+} and Fe^{3+} in the reaction mixture, at a concentration of 10 mM, caused a drastic reduction in both, extracellular and cell-associated amylase activities (Figure 6). The cellular extract only retained 28% of its amylase activity in Fe^{3+}; and similarly, the extracellular amylase conserved 26% of its activity. Under the presence of the cupric ion, the activity of the extracellular amylase dropped to 8%, while the activity of the cell-associated amylase decreased to 33%. This fact suggests the involvement of tiol/carboxyl groups, typically inhibited by Cu^{2+}, in the function of the enzymes [28].

The in vitro effect of anionic (SDS), cationic (SB-12), zwitterionic (CHAPS), and no ionic (Tween 20, Tween 80, and Triton X-100) detergents on the amylase activities were assayed. The obtained results revealed that both activities were very stable in different detergents, retaining more than 80% activity in all, with the exception of SDS, which caused a decrease by almost half in the amylase activities of both, extracellular and cellular amylase enriched extracts.

3.6. Identification of Amylases in Cellular and Extracellular Concentrated Extracts of Haloarcula sp. HS by a Proteomic Approach

A proteomic study of both, extracellular and cellular partially purified extracts with amylase activity, was carried out to identify the sequence of the proteins responsible for these starch-degrading activities in *Haloarcula* sp. HS. Both samples were submitted to

tryptic digestion and analyzed by LC-MS/MS in a triple quadrupole-TOF system, as described in Materials and Methods.

The results revealed that the main extracellular protein secreted to the culture media was α-amylase. The rest of the proteins identified in the extracellular fraction were membrane-ligated proteins, probably from broken cell remains. This extracellular amylase (AMY_HS1) was identified by 42 unique peptides, presenting 73.56% identity and 60% query cover with the α-amylase of *Haloarcula hispanica* N601 (UniProt: V5TMJ3_HALHI). For its part, in the cellular fraction, three different amylases were found. One of them corresponded to the same α-amylase (UniProt: V5TMJ3_HALHI) detected in the extracellular fraction, which in this case was identified according to 13 unique peptides and showed 81.48% identity and 36% query cover. The other two proteins, denoted as AMY_HS2 and AMY_HS3, showed high homology with two different α-amylases of *Haloarcula hispanica* N601 (UniProt codes: V5TRA6_HALHI and V5TQD3_HALHI, respectively), both determined according to 15 unique peptides. AMY_HS2 presented 45.25% identity and 65% query cover with V5TRA6_HALHI, while AMY_HS3 showed 75.76% identity and 31% query cover with V5TQD3_HALHI.

Due to the low percentage of protein covering achieved, the sequences of amylase coding genes were amplified by PCR, as detailed in Material and Methods, with primers designed to target the peptide sequences identified by proteomics for each enzyme. Through this approach, practically the full length of each protein sequence was completed.

The alignment of the three obtained protein sequences revealed that the extracellular amylase only presented a 17% identity with the cell-associated amylases, which in turn showed a 38% identity between them. Nonetheless, as it is shown in their predicted three-dimensional (Figure 7) and secondary structures (Supplementary Material, Figure S3), the three amylase sequences from *Haloarcula* sp. HS conserve the typical structural domains of the GH-13 family, according to the Carbohydrate-Active enZYmes (CAZY) database; including the catalytic $(\beta/\alpha)_8$-barrel (TIM-barrel) located in the domain A, a small domain B located in the loop between the β_3-strand and the α_3-helix of the barrel, and the domain C showing an antiparallel β-sandwich structure in the C-terminal end of the protein. In addition to this typical conformation, the two cellular amylases show an N-terminal domain, which was reported in some maltogenic amylases and seems to be involved in increasing the binding of the enzyme to raw starch. This N domain forms a large groove, the N–C groove, which might be responsible for thermostabilization via oligomerization and substrate affinity modifications in some microbial maltogenic amylases [29]. For its part, the extracellular protein, AMY_HS1, presents the conserved TAT (Twin-Arginine-Translocation) motif and its corresponding processing site (Supplementary Material, Figure S4).

Regarding the physicochemical characteristics, the three alpha-amylases of *Haloarcula* sp. HS had a low isoelectric point, negative net charge, and low hydrophobicity (Table 3) as other haloarchaeal enzymes.

Table 3. Physicochemical properties of the amylase enzymes from *Haloarcula* sp. HS.

Name	N	MW (kDa)	IP	Z	GRAVY	Aliph. Index
AMY_HS1	393	43.70	4.27	−35.577	−0.518	72.72
AMY_HS2	639	70.16	4.43	−66.227	−0.382	73.43
AMY_HS3	549	60.02	4.37	−59.604	−0.463	71.89

Main physicochemical characteristics of the amylase enzymes found in the *Haloarcula* sp. HS strain. N, number of nucleotides; MW, molecular weight; IP, theoretical isoelectric point; Z, net charge; GRAVY (Grand average of hydropathicity), mean of the hydropathy index of each amino acid residue. The aliphatic index stands for the relative volume occupied by the aliphatic side chains.

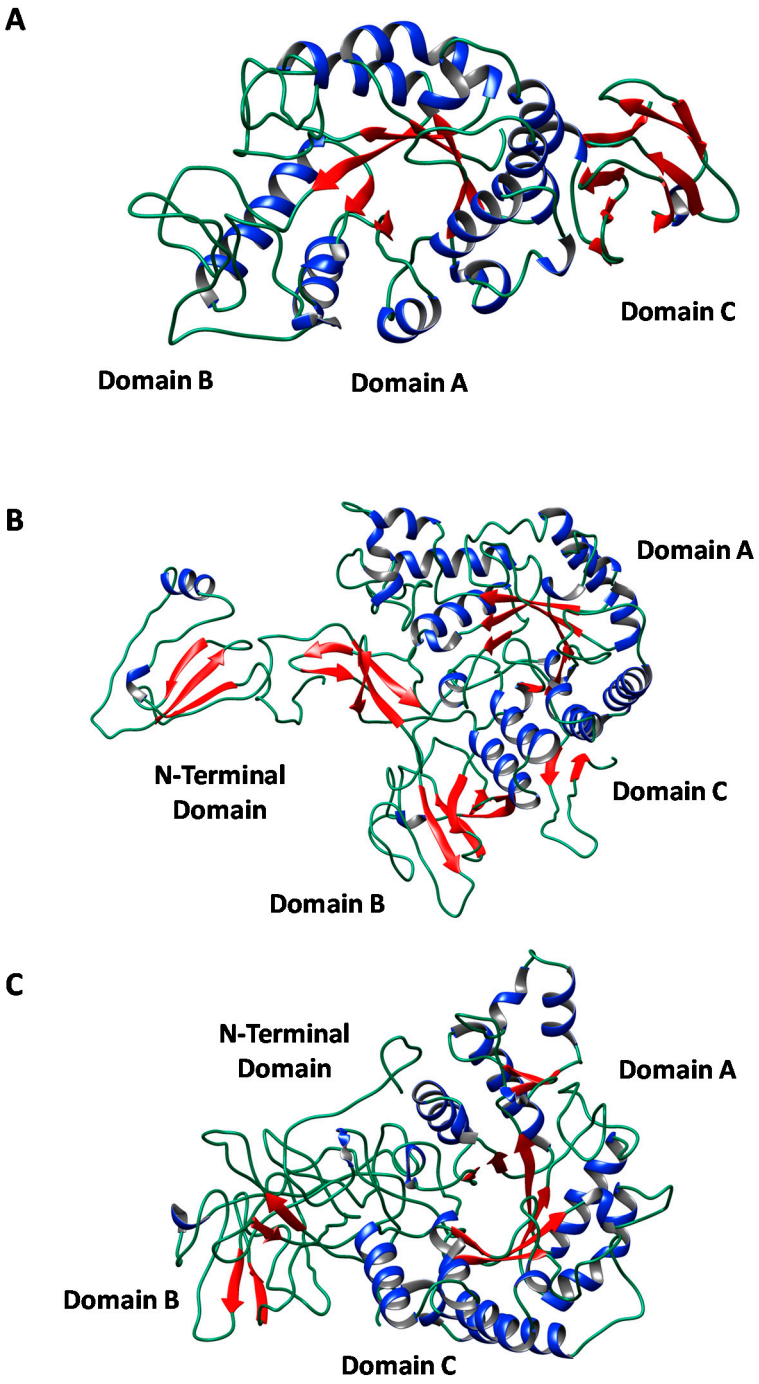

Figure 7. Three-dimensional predicted structures of the three amylase sequences identified in *Haloarcula* sp. HS; (**A**) mature extracellular amylase, AMY_HS1; (**B**) cellular amylase, AMY_HS2; (**C**) cellular amylase, AMY_HS3. Phyre2 software and the Chimera program were employed for 3D structure visualization. Helixes are represented by blue ribbons and strands by red arrows.

Moreover, although the three protein sequences had a low percentage of sequence homology, they conserved the catalytic triad of aspartate, glutamate, and aspartate in the active site, along with other conserved residues that were described to be indispensable for the structure of the enzyme [30]. These conserved amino acids are shown in Figure 8. One of the first consensus amino acids found is aspartic acid, which is essential for active site integrity. This aspartic residue is in the position Asp92 for the mature AMY_HS1 protein after TAT processing, and occupies the position 359 and 303 in AMY_HS2 and AMY_HS3,

respectively (Asp92/359/303). Following the same notation, the rest of the conserved amino acids are distributed as follows—Asn96/363/307, which coordinates the conserved calcium ion between the A and B domains [31]; and His93/360/304, which stabilizes the interaction between the C-terminal of β3 and the rest of TIM barrel through hydrogen bonding to Asn61/328/272 and the backbone oxygen of Tyr57/324/268. The first catalytic residue is Asp177/446/379, located in β4, which is preceded by Arg175/444/377, both of which are indispensable amino acids for the catalytic activity. Lys and His are usually present in this region in the position Asp+3 and +4, binding the reducing end of the glucose chain in the substrate-binding cleft [32], however, these residues were only found in the extracellular amylase. The second catalytic residue is the proton donor Glu205/475/408, which lies in the fifth L-strand of the TIM-barrel. The following conserved residues protect the active site from the solvent and contain the last catalytic amino acid Asp268/539/471, postulated to be involved in substrate binding, substrate distortion, and in elevating the pKa of Glu205/475/408. This residue is usually accompanied in α-amylases by His, Asn, Val, and Phe in the positions −1, −2, −4, and −5, respectively, as it occurs in AMY_HS1, while in AMY_HS2 and AMY_HS3, Phe is substituted by Tyr, and Val is changed by Ala in AMY_HS3. Finally, the other two conserved residues were found in Gly287/564/496, followed by Pro289/566/498 [33–36].

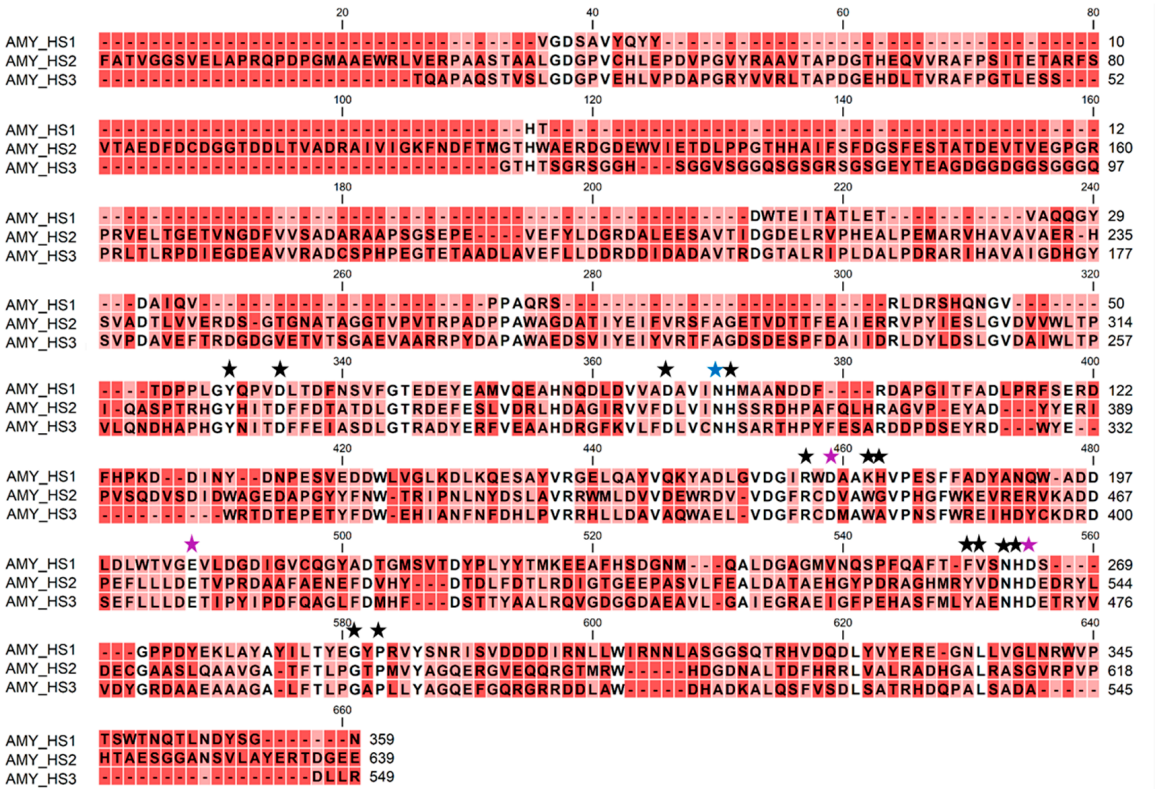

Figure 8. Alignment of the three amylase sequences from *Haloarcula* sp. HS. The mature extracellular protein is named AMY_HS1, while the cell-associated amylases are denoted as AMY_HS2 and AMY_HS3. Purple stars highlight the catalytic triad (Asp-Glu-Asp), blue star denotes the canonical calcium-binding site and the black stars point other essential residues for enzyme structure. Identical residues in the three sequences are shaded in white, residues that coincide in two of the sequences or do not coincide at all are shaded in pink and red, respectively.

Finally, a multispecies study was carried out to compare the degree of conservation among the amylases reported and those from different haloarchaeal members. The protein sequence of the extracellular amylase (AMY_HS1) was aligned and compared to various extracellular amylase sequences available in the NCBI database, selecting different representatives of the order *Halobacteriales* (Supplementary Material, Figure S4). Among these

amylase sequences, different percentages of identity were found with the extracellular amylases from *Haloarcula hispanica* N601 (90%), *Halomicroarcula salina* (73%), *Halapricum salinum* (57%), and *Haloterrigena turkmenika* (40%). Likewise, the two cell-associated amylases (AMY_HS2 and AMY_HS3) from *Haloarcula* sp. HS showed the following percentages that identity with the amylase sequences from *Haloarcula hispanica* N601 (90 and 80%, respectively), *Halomicroarcula salina* (70 and 65%, respectively), *Haloferax mediterranei* (59, and 50%, respectively), *Halogeometricum rufum* (57% with AMY_HS2), and *Halogeometricum limi* (49% with AMY_HS3) (Supplementary Material, Figures S5 and S6). In all alignments, it could be appreciated that the catalytic regions were conserved among the different haloarchaeal species (Supplementary Material, Figures S4–S6).

3.7. Hydrolysis of Bakery Waste

Bakery residues, including dough, flour dust, burnt or rejected bread, and biscuits, can be exploited for the production of fermentable sugars. Among them, bread was chosen as the substrate for this assay, as it is one of the most abundant food waste products worldwide. In addition, many of the discarded by-products during the bread manufacturing process are fundamentally constituted by starch, such as substandard bread and the bread crust removed to make special types of sandwich bread [37].

The extracellular amylase activity was selected for this assay, as it works better in high NaCl concentrations than the cell-associated amylase. This was compared to a commercial thermostable α-amylase. Sodium chloride was found to have a complex effect on the gelatinization and rheological properties of starch. Some studies pointed out that the enthalpy for the gelatinization process decreased at high salt concentrations, an effect of great importance for the production and properties of several cereal-based products, as well as for the manufacture of modified starches [38].

The results proved that a high percentage of the initial starch (75–85%) was hydrolyzed by both enzymes, with maximum activities above 100 U mL^{-1}. However, the concentration of salt was determined in their maximum activities. The extracellular amylase hydrolyzed around 75% of the starch under 20% salt or even under salt saturation, with maximum activities of 107 and 105 U mL^{-1}, respectively; while when no salt was added, the degradation rate decreased to 22%, with an activity of 24.7 U mL^{-1}. Conversely, the commercial α-amylase presented the highest activity (101.8 U mL^{-1}) when no salt was added to the mixture, hydrolyzing 85% of the starch; and its activity dropped drastically to 6–7 U mL^{-1}, under elevated salt concentration, degrading only 5–6% of the starch.

The obtained hydrolysate was very rich in simple sugars that could now be used for the bioproduction of many high-value molecules like glycerol, hydrogen, ethanol, or lactic acid, among others. These molecules are required for different purposes, including renewable energy sources, fuel additives, and food preservers [13]. To our knowledge, this study supposes the first attempt to use a halophilic amylase to degrade starch from bread into simple sugars. The applicability of the amylase from a haloarchaea was tested using starch from agricultural waste [39], however, the starch content of this residue was considerably lower, and also the starch extraction method was costlier.

4. Discussion

Alpha-amylases are a large family of endo-glycosyl hydrolases that cleave the internal α,1-4 glycosidic bonds between the glucose units in polysaccharides, such as amylose and amylopectin. They are common in all kingdoms of life and their general properties, three-dimensional structures, and mechanisms of action are extensively reviewed [40–43].

Alpha-amylases are particularly spread among microbial species, such as bacteria and yeasts. These amylases are often extracellular enzymes that allow microorganisms to use environmental polysaccharides for their nutrition. Thermostable α-amylases were produced and commercially exploited from yeast and bacterial species, such as *Bacillus subtilis*, *B. licheniformis*, or *B. amyloliquefacines* [14]. Some archaea, including halophilic archaea, were found to produce halotolerant α-amylases, which in addition were highly

or moderately thermotolerant. The extracellular α-amylases of *Haloarcula* sp. S-1 [44], *N. amylolyticus* [45], *H. mediterranei* [26], *H. xinjiangense* [46], *Haloferax* sp. HA10 [47], *H.turkmenica* [39], or *Halococcus* GUVSC8 [48] are some examples. Although much less studied, the intracellular α-amylases of some haloarchaea, such as *Haloarcula japonica* [49] were also characterized.

The new strain isolated from the Odiel Marshlands and selected by its high ability to degrade starch in iodine–starch agar plate assays was foumd to be closely related to the genus *Haloarcula*, as shown in the phylogenetic tree (Figure 1). The high homology of its 16S rRNA with that of *Haloarcula hispanica* (98%) *or Haloarcula japonica* (97%) confirmed it. We found that the new strain exhibited a high amylolytic activity when cultured in the presence of starch; this activity was higher in a minimal medium with ammonium acetate (Figure 2).

In agreement with our observations, several reports indicate that amylase production in haloarchaea is induced by starch, as described for *Halorubrum* [46], *Haloferax* [47], *Haloarcula* [50], and some halophilic bacteria [51]. Other culture conditions and nutrients that were reported to influence the induction of alpha-amylases are nitrogen, metal ions, or phosphate [5]. Pérez-Pomares et al. [26], for example, reported low amylase excretion when using a minimal medium containing ammonium acetate as carbon and nitrogen source, plus starch in *Haloferax mediterranei.*

Our observations indicate that the conditions that induce the amylase activity are not the best for growth (Figure 2). Therefore, a two-step culture was set up, in which a large amount of biomass was obtained in a rich medium, followed by transfer to a minimal medium with starch, to induce the production of amylase activity (Figure 3). This two-stage method allowed the improvement of amylase production, and at the same time facilitated the recovery of the extracellular enzyme. Since the minimal medium had no yeast extract, there are no foreign proteins that could interfere with the amylase secreted into the culture medium.

Partially purified extracellular and cellular-amylase-enriched extracts were obtained from *Haloarcula* sp. HS, through ultrafiltration and anion exchange chromatography, respectively, and were electrophoretically separated in native conditions. In situ staining of the obtained acrylamide gel allowed the identification of bands with starch degrading ability, one band in the extracellular enzymatic preparation, and two bands in the cellular extract, with apparent relative molecular masses between 21.6 and 30.4 kDa (Figure 4). The zymogram indicates that the new isolated strain presents amylase activities in both, the supernatant and the crude cell extract, suggesting that there is more than one cell-associated amylase that does not coincide with the extracellular one. The proteomic analysis of the extracts and the subsequent amplification of the whole gene sequences that encode for these amylases allowed us to confirm this hypothesis (Figure 8), and also indicated that the real masses of the amylases were much higher than the apparent molecular masses shown in the electrophoresis gel. These differences could be due to the fact that the electrophoresis was carried out in native conditions and in the presence of starch, which could modify their electrophoretic mobilities, besides the fact that halophilic proteins usually show altered electrophoretic properties [52].

The apparent molecular masses reported for the amylases of other haloarchaea are slightly higher than the molecular weight observed for the amylases of *Haloarcula* sp. HS. For example, the intracellular amylase of *Haloarcula japonica* presented a molecular mass of 83 kDa [49]; the extracellular amylases of *Haloterrigena tukmenica* and *Haloferax* sp. HA10 showed a molecular weight of 66 kDa [39,47], in *Haloferax mediterranei*, the weight of the enzyme was around 50–58 kDa [26], 60 kDa in *Halorubrum xinjiangense* [46], and 74 kDa in *Natronococcus* sp. Ah-36 [45], while in the *Haloarcula* species, the molecular mass varied from 43 to 70 kDa [27,44]. The physicochemical parameters of the new alpha-amylases, with low isoelectric point and negative net charge (Table 3) also meet the usual characteristic of haloarchaeal enzymes, as reported by other authors. Yan and Wu [43] analyzed the sequences of 88 α-amylases from archaea and observed that amylases from haloarchaea

have a highly negatively charged surface, and a higher percentage of acidic residues as a mechanism of adaptation to high salinity. Other authors describe similar features for *H. hispanica*, which has an extracellular amylase with an isoelectric point of 4.2 and a low level of aromatic and hydrophobic residues [27]. In haloarchaea, most studies about amylases focused on extracellular enzymes, given that sometimes no activity was found in the crude cell extract, as was observed in *Haloferax mediterranei* and *Halorubrum xinjiangense* [26,46] or because, as in the case of *Haloterrigena turkmenica*, the amylase activity was quite higher in the supernatant than in the cell extract [39]. With respect to the *Haloarcula* genus, Hutcheon et al. confirmed the overexpression of an extracellular amylase (AmyH) in the mutant strain *Haloarcula hispanica* B3, which was secreted in a folded conformation via the TAT (Twin-Arginine-Translocation) pathway, indicating that it was active in the cytoplasm before the secretion to the media [27]. Additionally, Onodera et al. reported the overexpression of an intracellular amylase (malA), which was not secreted to the media in *Haloarcula japonica* [49]. Based on the above mentioned, it seems that there were diverse amylases with probably different modes of action, which to our knowledge, are not yet deeply elucidated.

Maltose is the main end-product released from the starch hydrolysis by the extracellular and cellular partially purified amylase extracts of *Haloarcula* sp. HS (Table 2). This is the main product of maltogenic α-amylases, like most α-amylases from haloarchaea, e.g., intracellular α-amylase from *Haloarcula japonica* [49] or the extracellular α-amylase from *Haloterrigena tukmenica* [39]. A small proportion of glucose was found in the assay catalyzed by the cell extract. However, it is difficult to predict if it is directly due to the action of the cellular amylases in *Haloarcula* sp. HS or due to the contribution of additional cell-associated enzymes.

With regards to the optimal enzymatic parameters, both cell-associated and extracellular starch-degrading activities exhibited their maximum activities around 60 °C. The low-temperature dependence of the cell-associated amylase, which only loses around 25% of its activity in the temperature range 20–80 °C, is noteworthy. However, it should be considered that this activity might be, as shown in this study, the result of the action of three different amylase enzymes. This fact contributes to broadening the range of optimal temperatures for the cell-associated amylase activity. High retention of enzyme activity over a wide range of temperatures was reported for other partially purified amylases, such as that from *Haloferax* sp. HA10 [47], which showed the highest amylase activity at 55 °C.

The optimal pH values were 7 for the cellular amylase activity, and 5 for the extracellular activity. Additionally, extracellular and cell-associated, amylase activities were extremely halophilic, showing their maximum activities at 25% NaCl. Therefore, it is noteworthy that the cell-associated amylase activity seemed to be more tolerant to changes in salinity, pH, and temperature than the extracellular one (Figure 5). This was probably due to the presence of three different amylases in the cell extract, as was later confirmed in the proteomic analysis. In addition, the high salt and temperature tolerance could be of interest for many industrial applications in which these extreme conditions are needed.

A comparison with the optimal parameters reported for amylases of other related haloarchaea is summarized in Table 4. Most extracellular α-amylases from haloarchaea showed their best activity at temperatures from 45 to 70 °C, pH from 6.5 to 8.7, and in salt concentrations from 1 to 5 M. The extracellular amylase found in *Haloarcula* sp. HS is one of the most halophilic and acidophilic α-amylase described within the haloarchaea group (Table 4).

Table 4. Optimal parameters reported for α-amylase activity in haloarchaea.

Microorganism	Enzyme	NaCl (M)	pH	T[a] (°C)	Ref.
Haloarcula sp. HS	Cellular α-amylase	2.6	7	50	This study
H. japonica	Intracellular α-amylase	2.6	6.5	45	[49]
Haloarcula sp. HS	Extracellular α-amylase	5	5	60	This study
Halococcus GUVSC8	Extracellular α-amylase	2	6	45	[48]
Haloarcula sp. S-1	Extracellular α-amylase	4.3	7	50	[44]
H. hispanica B3	Extracellular α-amylase	4–5	6.5	50	[27]
H. hispanica 2TK2	Extracellular α-amylase	5	6.9	52	[50]
H. xinjiangense	Extracellular α-amylase	4	8.5	70	[46]
Haloferax sp. HA10	Extracellular α-amylase	1	6	55	[47]
H. mediterranei	Extracellular α-amylase	3	7–8	50–60	[26]
H.turkmenica	Extracellular α-amylase	2	8.5	55	[39]
N.amylolyticus	Extracellular α-amylase	2.5	8.7	55	[45]

Additionally, extracellular and cell-associated amylase, activities from *Haloarcula* sp. HS, exhibit a strong inhibition in the presence of the metal chelating agent EDTA (Figure 6). In addition, the analysis of the amylase sequences obtained allowed the identification of the canonical Ca-binding residue in the three amino acidic sequences, as shown in Figure 8, indicating that they must be calcium-dependent. Dependence of calcium is a common feature within haloarchaeal amylases, as was reported for *Haloferax mediterranei*, *Haloarcula hispanica*, *Haloarcula* sp. S-1, *Halorubrum xijiangense*, and [26,27,44,46]. However, some haloarchaeal amylases showed to be resilient to EDTA, indicating no dependence on Ca^{2+}, as revealed by the studies on *Haloterrigena turkmenica* and *Haloarcula japonica* [39,49].

Furthermore, both amylase activities showed high stability in most tested surfactants, excepting the anionic detergent SDS. There are few reports on the stability of amylase from haloarchaea on surfactants. In this context, detergent-stable amylases were recently found in *Haloterrigena tukmenica*, *Halorubrum xijiangense*, and *Haloferax* sp. HA10 [39,46,47]. Additionally, a surfactant-stable amylase was characterized from the halophilic bacteria *Nesterenkonia* sp. F [53]. Therefore, to the best of our knowledge, the two detergent-stable amylase activities described in this work entailed the first report on this specific feature of the amylase activity from the *Haloarcula* genus.

Analyzing the sequences of the peptides generated by the tryptic digestion of the partially purified extracellular and cell extracts, it was possible to identify three different amylases in *Haloarcula* sp. HS. One (AMY_HS1) was found both in cells and in the culture medium, while the other two amylases (AMY_HS2 and AMY_HS3) were exclusively found in the cell extract.

Despite the low percentage of sequence identity that the three amylases of *Haloarcula* sp. HS shared (Figure 8), the three enzymes exhibited a high three-dimensional structure homology, with the three typical domains of alpha-amylases of the glycosyl hydrolase GH-13 family (Figure 7) and many of the key conserved residues (Figure 8). For example, the three amino acids (Asp-Glu-Asp), which constituted the active site of alpha-amylases, were identified in α-amylases of haloarchaeal strains, such as *Halogeometricum borinquense* [30] and *Haloterrigena turkmenica* [39]. These residues were conserved in all alpha-amylases of the GH-13 family of many different origins, which were compiled in the Carbohydrate-Active enZYmes (CAZy) database [54].

The calcium-binding domain located between the 3rd beta-strand and the 3rd alpha-helix contained an asparagine amino acid found in the three amylases of *Haloarcula* sp. HS (Figure 8), as was described for other haloarchaeal amylases [30] and many other α-amylases, which were calcium-dependent metalloenzymes [55]. In some cases, more than one Ca-binding domain was described, as in *H. orenii* [56]. Additional conserved

amino acids reported in alpha-amylases, which help to stabilize the structure or the binding of the substrate [5], were found in the three amylases of *Haloarcula* sp. HS (Figure 8).

Most available archaeal amylase sequences were from the thermophilic archaea and could work at very high temperatures, which was of great industrial interest. The amylases identified from the Odiel Marshlands were medium or highly thermotolerant, in addition to being extremely halophilic. The α-amylases from hyperthermophilic archaea were closely related to plant amylases [57]. However, as new potential α-amylases from the halophilic archaea were identified, evident differences were observed with the sequences of their known hyperthermophilic counterparts. Unfortunately, most of those halophilic amylolytic enzymes were only putative proteins from genome sequencing projects [58], or their complete sequences were not available [26,44,46], making it difficult to establish accurate phylogenetic relationships. In addition, an enormous diversity was observed among the amylases characterized and sequenced from a member of the *Halobacteriaceae* family, which showed similarities with marine bacteria, fungal, or even animal sources [59]. Therefore, more insightful biochemical characterization studies are needed to reveal the exact features of these amylolytic enzymes from haloarchaea.

Although several copies of alpha-amylases appear in the sequenced genomes of haloarchaea, most studies are focused on the extracellular ones. The role of the extracellular amylase in haloarchaea is well-established, as it allows the conversion of starch, produced by the marine plankton, into simple sugars that could be incorporated into the cell and used as a carbon source [60]. Nonetheless, the function of the intracellular amylases is less understood, not only in haloarchaea but also in other heterotrophic microorganisms [61]. Most intracellular amylases of haloarchaea were assigned by sequence homology without a functional characterization, with few exceptions, like the intracellular α-amylase from *H. japonica*, whose activity is well-studied [49]. Further insight is necessary to complete the characterization of haloarchaeal amylases, to understand their role in archaeal metabolism, and to evaluate their biotechnological applications.

5. Conclusions

The detailed biochemical characterization of the cell-associated and the extracellular amylase activities from the new isolated strain *Haloarcula* sp. HS revealed that both are active at high salinity conditions and at considerably high temperatures. These features, joined to their stability under a wide range of surfactants, make them suitable for industrial applications. The proteomic analysis showed that three different cell-associated enzymes, one of which was also found in the extracellular medium, might be responsible for the amylase activities. The three proteins conserve the consensus domains and residues of the α-amylase family. Further studies aim to decipher the function of a hypothetical ancestral gene and to increase our understanding of the biochemical behavior of these polyextremophilic enzymes. Developing new techniques for high-scale production in the industry is also needed.

Supplementary Materials: The following are available online at https://www.mdpi.com/article/10.3390/biology10040337/s1. Figure S1: Full length of the 16S rRNA encoding gene from *Haloarcula* sp. HS. Figure S2: Complete original polyacrylamide gels. Figure S3: Predicted structures of the three amylase sequences identified in *Haloarcula* sp. HS. Figure S4: Multiple alignments of the amino acid sequence of the extracellular amylase identified in *Haloarcula* sp. HS (AMY_HS1). Figure S5: Multiple alignments of the amino acid sequence of the cell-associated amylase from *Haloarcula* sp. HS (AMY_HS2). Figure S6: Multiple alignments of the amino acid sequence of the cell-associated amylase from *Haloarcula* sp. HS (AMY_HS3).

Author Contributions: Conceptualization, J.V., R.L., and P.G.-V.; Funding acquisition, J.V., R.L. and P.G.-V.; Investigation, P.G.-V. and J.V.; Methodology, P.G.-V., B.G. and S.R.; Supervision, J.V. and R.L.; Software: P.G.-V. and L.R. Data curation, P.G.-V., J.V., L.R. and C.G.; Writing—original draft, P.G.-V. and R.L.; Writing—review & editing, P.G.-V., J.V. and R.L. All authors have read and agreed to the published version of the manuscript.

Funding: This research was funded by the Operative FEDER Program-Andalucía 2014–2020, the University of Huelva, the Spanish Agencia Estatal de Investigación (grants PID2019-109785GB-I00 and PID2019-110438RB-C22 -AEI/FEDER) and the SUBV. COOP.ALENTEJO-ALGARVE-ANDALUCIA 2019. P.G.-V. and C.G. acknowledge financial support from the University of Huelva (EPIT 2016-17) and the Junta de Andalucía (grant P18-RT-3154), respectively.

Institutional Review Board Statement: This study did not involve humans or animals.

Informed Consent Statement: Not applicable.

Data Availability Statement: All DNA and protein sequences of the studied enzymes are included as Supplementary Materials; other information is available upon request.

Acknowledgments: Technical support of Rocío Rodríguez from the IBVF-CSIC in the proteomic analysis is acknowledged.

Conflicts of Interest: The authors declare no conflict of interest. The funders had no role in the design of the study; in the collection, analyses, or interpretation of data; in the writing of the manuscript, or in the decision to publish the results.

References

1. Kanekar, P.P.; Kelkar, A.S.; Dhakephalkar, P.K. Halophiles—Taxonomy, Diversity, Physiology and Applications. In *Microorganisms in Environmental Management*; Metzler, J.B., Ed.; Springer: Dordrecht, The Netherlands, 2012; Volume 9789400722, pp. 1–34.
2. Ventosa, A.; Márquez, M.C.; Sánchez-Porro, C.; De La Haba, R.R. Taxonomy of Halophilic Archaea and Bacteria. In *Advances in Understanding the Biology of Halophilic Microorganisms*; Vreeland, R.H., Ed.; Springer: Dordrecht, The Netherlands, 2012; pp. 59–80.
3. Oren, A. Life at high salt concentrations, intracellular KCl concentrations, and acidic proteomes. *Front. Microbiol.* **2013**, *4*, 315. [CrossRef] [PubMed]
4. Mevarech, M.; Frolow, F.; Gloss, L.M. Halophilic enzymes: Proteins with a grain of salt. *Biophys. Chem.* **2000**, *86*, 155–164. [CrossRef]
5. Mehta, D.; Satyanarayana, T. Bacterial and Archaeal α-Amylases: Diversity and Amelioration of the Desirable Characteristics for Industrial Applications. *Front. Microbiol.* **2016**, *7*, 1129. [CrossRef] [PubMed]
6. Cabrera, M. Ángeles; Blamey, J.M. Biotechnological applications of archaeal enzymes from extreme environments. *Biol. Res.* **2018**, *51*, 1–15. [CrossRef]
7. Vaidya, S.; Srivastava, P.; Rathore, P.; Pandey, A. Amylases: A prospective enzyme in the field of biotechnology. *J. Appl. Biosci.* **2015**, *41*, 1–18.
8. Kumar, V.; Sangwan, P.; Singh, D.; Gill, P.K. Global scenario of industrial enzyme market. In *Industrial Enzymes: Trends, Scope and Relevance*; Nova Science Publishers: New York, NY, USA, 2014; pp. 176–196. [CrossRef]
9. Gupta, R.; Gigras, P.; Mohapatra, H.; Goswami, V.K.; Chauhan, B. Microbial α-amylases: A biotechnological perspective. *Process. Biochem.* **2003**, *38*, 1599–1616. [CrossRef]
10. Fernandes, P. Enzymatic processing in the food industry. In *Reference Module in Food Science*; Elsevier BV: Amsterdam, The Netherlands, 2018.
11. Gopinath, S.C.B.; Anbu, P.; Arshad, M.K.M.; Lakshmipriya, T.; Voon, C.H.; Hashim, U.; Chinni, S.V. Biotechnological processes in microbial amylase production. *BioMed Res. Int.* **2017**, *2017*, 272193. [CrossRef]
12. Mobini-Dehkordi, M.; Javan, F.A. Application of alpha-amylase in biotechnology. *J. Biol. Today World* **2012**, *1*, 39–50. [CrossRef]
13. Kumar, V.; Longhurst, P. Recycling of food waste into chemical building blocks. *Curr. Opin. Green Sustain. Chem.* **2018**, *13*, 118–122. [CrossRef]
14. van der Maarel, M.J.; van der Veen, B.; Uitdehaag, J.C.; Leemhuis, H.; Dijkhuizen, L. Properties and applications of starch-converting enzymes of the α-amylase family. *J. Biotechnol.* **2002**, *94*, 137–155. [CrossRef]
15. Taniguchi, H.; Honnda, Y. Amylases. In *Encyclopedia of Microbiology*; Elsevier BV: Amsterdam, The Netherlands, 2009; pp. 159–173.
16. John, J. Amylases-bioprocess and potential applications: A review. *Int. J. Bioinform. Biol. Sci.* **2017**, *5*, 41. [CrossRef]
17. Gómez-Villegas, P.; Vigara, J.; León, R. Characterization of the microbial population inhabiting a solar saltern pond of the odiel marshlands (SW Spain). *Mar. Drugs* **2018**, *16*, 332. [CrossRef] [PubMed]
18. Gómez-Villegas, P.; Vigara, J.; Vila, M.; Varela, J.; Barreira, L.; Léon, R. Antioxidant, Antimicrobial, and Bioactive Potential of Two New Haloarchaeal Strains Isolated from Odiel Salterns (Southwest Spain). *Biology* **2020**, *9*, 298. [CrossRef]
19. Altschul, S.F.; Gish, W.; Miller, W.; Myers, E.W.; Lipman, D.J. Basic local alignment search tool. *J. Mol. Biol.* **1990**, *215*, 403–410. [CrossRef]
20. Bradford, M.M. A rapid and sensitive method for the quantitation of microgram quantities of protein utilizing the principle of protein-Dye binding. *Anal. Biochem.* **1976**, *72*, 248–254. [CrossRef]
21. Kelley, L.A.; Mezulis, S.; Yates, C.M.; Wass, M.N.; Sternberg, M.J.E. The Phyre2 web portal for protein modeling, prediction and analysis. *Nat. Protoc.* **2015**, *10*, 845–858. [CrossRef] [PubMed]

22. Petersen, B.; Petersen, T.N.; Andersen, P.; Nielsen, M.; Lundegaard, C. A generic method for assignment of reliability scores applied to solvent accessibility predictions. *BMC Struct. Biol.* **2009**, *9*, 51. [CrossRef]
23. Pettersen, E.F.; Goddard, T.D.; Huang, C.C.; Couch, G.S.; Greenblatt, D.M.; Meng, E.C.; Ferrin, T.E. UCSF Chimera—A visualization system for exploratory research and analysis. *J. Comput. Chem.* **2004**, *25*, 1605–1612. [CrossRef]
24. Gasteiger, E.; Hoogland, C.; Gattiker, A.; Duvaud, S.; Wilkins, M.R.; Appel, R.D.; Bairoch, A. Protein Identification and Analysis Tools on the ExPASy Server. In *The Proteomics Protocols Handbook*; Walker, J.M., Ed.; Humana Press: New York, NY, USA, 2005; pp. 571–607.
25. Kumar, S.; Stecher, G.; Li, M.; Knyaz, C.; Tamura, K. MEGA X: Molecular evolutionary genetics analysis across computing platforms. *Mol. Biol. Evol.* **2018**, *35*, 1547–1549. [CrossRef]
26. Pérez-Pomares, F.; Bautista, V.; Ferrer, J.; Pire, C.; Marhuenda-Egea, F.C.; Bonete, M.-J.; Marhuenda-Egea, F. α-Amylase activity from the halophilic archaeon *Haloferax mediterranei*. *Extremophiles* **2003**, *7*, 299–306. [CrossRef]
27. Hutcheon, G.W.; Vasisht, N.; Bolhuis, A. Characterisation of a highly stable α-amylase from the halophilic archaeon Haloarcula hispanica. *Extremophiles* **2005**, *9*, 487–495. [CrossRef] [PubMed]
28. Mehta, D.; Satyanarayana, T. Biochemical and molecular characterization of recombinant acidic and thermostable raw-starch hydrolysing α-amylase from an extreme thermophile *Geobacillus thermoleovorans*. *J. Mol. Catal. B Enzym.* **2013**, *85–86*, 229–238. [CrossRef]
29. Tan, T.-C.; Mijts, B.N.; Swaminathan, K.; Patel, B.K.; Divne, C. Crystal Structure of the Polyextremophilic α-Amylase AmyB from Halothermothrix orenii: Details of a Productive Enzyme–Substrate Complex and an N Domain with a Role in Binding Raw Starch. *J. Mol. Biol.* **2008**, *378*, 852–870. [CrossRef] [PubMed]
30. Verma, D.K.; Vasudeva, G.; Sidhu, C.; Pinnaka, A.K.; Prasad, S.E.; Thakur, K.G. Biochemical and Taxonomic Characterization of Novel Haloarchaeal Strains and Purification of the Recombinant Halotolerant α-Amylase Discovered in the Isolate. *Front. Microbiol.* **2020**, *11*, 2082. [CrossRef]
31. Boel, E.; Brady, L.; Brzozowski, A.M.; Derewenda, Z.; Dodson, G.G.; Jensen, V.J.; Petersen, S.B.; Swift, H.; Thim, L.; Woldike, H.F. Calcium binding in alpha.-amylases: An X-ray diffraction study at 2.1-.ANG. Resolution of two enzymes from Aspergillus. *Biochemistry* **1990**, *29*, 6244–6249. [CrossRef] [PubMed]
32. Svensson, B. Protein engineering in the α-amylase family: Catalytic mechanism, substrate specificity, and stability. *Plant Mol. Biol.* **1994**, *25*, 141–157. [CrossRef]
33. Strokopytov, B.; Penninga, D.; Rozeboom, H.J.; Kalk, K.H.; Dijkhuizen, L.; Dijkstra, B.W. X-ray Structure of Cyclodextrin Glycosyltransferase Complexed with Acarbose. Implications for the Catalytic Mechanism of Glycosidases. *Biochemistry* **1995**, *34*, 2234–2240. [CrossRef]
34. Machovič, M.; Janeček, Š. The invariant residues in the α-amylase family: Just the catalytic triad. *Biol. Sect. Cell. Mol. Biol.* **2003**, *58*, 1127–1132.
35. Zona, R.; Chang-Pi-Hin, F.; O'Donohue, M.J.; Janeček, Š. Bioinformatics of the glycoside hydrolase family 57 and identification of catalytic residues in amylopullulanase from Thermococcus hydrothermalis. *JBIC J. Biol. Inorg. Chem.* **2004**, *271*, 2863–2872. [CrossRef]
36. Roth, C.; Moroz, O.V.; Turkenburg, J.P.; Blagova, E.; Waterman, J.; Ariza, A.; Ming, L.; Tianqi, S.; Andersen, C.; Davies, G.J.; et al. Structural and Functional Characterization of Three Novel Fungal Amylases with Enhanced Stability and pH Tolerance. *Int. J. Mol. Sci.* **2019**, *20*, 4902. [CrossRef]
37. Oda, Y.; Park, B.-S.; Moon, K.-H.; Tonomura, K. Recycling of bakery wastes using an amylolytic lactic acid bacterium. *Bioresour. Technol.* **1997**, *60*, 101–106. [CrossRef]
38. Chiotelli, E.; Pilosio, G.; Le Meste, M. Effect of sodium chloride on the gelatinization of starch: A multimeasurement study. *Biopolymers* **2001**, *63*, 41–58. [CrossRef]
39. Santorelli, M.; Maurelli, L.; Pocsfalvi, G.; Fiume, I.; Squillaci, G.; La Cara, F.; Del Monaco, G.; Morana, A. Isolation and characterisation of a novel alpha-amylase from the extreme haloarchaeon *Haloterrigena turkmenica*. *Int. J. Biol. Macromol.* **2016**, *92*, 174–184. [CrossRef]
40. Bertoldo, C.; Antranikian, G. Starch-hydrolyzing enzymes from thermophilic archaea and bacteria. *Curr. Opin. Chem. Biol.* **2002**, *6*, 151–160. [CrossRef]
41. Naidu, M.A.; Saranraj, P. Bacterial amylase: A review. *Int. J. Pharm. Biol. Arch.* **2013**, *4*, 274–287.
42. Saranraj, P.; Stella, D. Fungal amylase-a review. *Int. J. Microbiol. Res.* **2013**, *4*, 203–211. [CrossRef]
43. Yan, S.; Wu, G. Analysis on evolutionary relationship of amylases from archaea, bacteria and eukaryota. *World J. Microbiol. Biotechnol.* **2016**, *32*, 24. [CrossRef]
44. Fukushima, T.; Mizuki, T.; Echigo, A.; Inoue, A.; Usami, R. Organic solvent tolerance of halophilic α-amylase from a Haloarchaeon, *Haloarcula* sp. strain S-1. *Extremophiles* **2004**, *9*, 85–89. [CrossRef]
45. Kobayashi, T.; Kanai, H.; Hayashi, T.; Akiba, T.; Akaboshi, R.; Horikoshi, K. Haloalkaliphilic maltotriose-forming alpha-amylase from the archaebacterium *Natronococcus* sp. strain Ah-36. *J. Bacteriol.* **1992**, *174*, 3439–3444. [CrossRef]
46. Moshfegh, M.; Shahverdi, A.R.; Zarrini, G.; Faramarzi, M.A. Biochemical characterization of an extracellular polyextremophilic α-amylase from the halophilic archaeon *Halorubrum xinjiangense*. *Extremophiles* **2013**, *17*, 677–687. [CrossRef]
47. Bajpai, B.; Chaudhary, M. Production and Characterization of α-Amylase from an Extremely Halophilic Archaeon, *Haloferax* sp. HA10. *Food Technol. Biotechnol.* **2015**, *53*, 11–17. [CrossRef]

48. Salgaonkar, B.B.; Sawant, D.T.; Harinarayanan, S.; Bragança, J.M. Alpha-amylase Production by Extremely Halophilic Archaeon-HalococcusStrain GUVSC8. *Starch Stärke* **2018**, *71*, 1800018. [CrossRef]
49. Onodera, M.; Yatsunami, R.; Tsukimura, W.; Fukui, T.; Nakasone, K.; Takashina, T.; Nakamura, S. Gene Analysis, Expression, and Characterization of an Intracellular α-Amylase from the Extremely Halophilic Archaeon *Haloarcula japonica*. *Biosci. Biotechnol. Biochem.* **2013**, *77*, 281–288. [CrossRef]
50. Erdagi, A.N.; Attar, A.; Basaran-Elalmis, Y.; Yücel, S.; Birbir, M. Production of α-Amylase from Haloarcula hispanica 2TK2 Strain: Optimization of the Parameters That Effecting Activity. *Adv. Sci. Lett.* **2013**, *19*, 3551–3555. [CrossRef]
51. Sanchez-Porro, C.; Martin, S.; Mellado, E.; Ventosa, A. Diversity of moderately halophilic bacteria producing extracellular hydrolytic enzymes. *J. Appl. Microbiol.* **2003**, *94*, 295–300. [CrossRef]
52. Lichi, T.; Ring, G.; Eichler, J. Membrane binding of SRP pathway components in the halophilic archaea Haloferax volcanii. *JBIC J. Biol. Inorg. Chem.* **2004**, *271*, 1382–1390. [CrossRef]
53. Shafiei, M.; Ziaee, A.-A.; Amoozegar, M.A. Purification and biochemical characterization of a novel SDS and surfactant stable, raw starch digesting, and halophilic α-amylase from a moderately halophilic bacterium, *Nesterenkonia* sp. strain F. *Process. Biochem.* **2010**, *45*, 694–699. [CrossRef]
54. Sarian, F.D.; Janeček, Š.; Pijning, T.; Nurachman, Z.; Radjasa, O.K.; Dijkhuizen, L.; Natalia, D.; Van Der Maarel, M.J.E.C. A new group of glycoside hydrolase family 13 α-amylases with an aberrant catalytic triad. *Sci. Rep.* **2017**, *7*, srep44230. [CrossRef] [PubMed]
55. Linden, A.; Mayans, O.; Meyer-Klaucke, W.; Antranikian, G.; Wilmanns, M. Differential Regulation of a Hyperthermophilic α-Amylase with a Novel (Ca,Zn) Two-metal Center by Zinc. *J. Biol. Chem.* **2003**, *278*, 9875–9884. [CrossRef]
56. Sivakumar, N.; Li, N.; Tang, J.W.; Patel, B.K.; Swaminathan, K. Crystal structure of AmyA lacks acidic surface and provide insights into protein stability at poly-extreme condition. *FEBS Lett.* **2006**, *580*, 2646–2652. [CrossRef]
57. Janeček, Š.; Lévêque, E.; Belarbi, A.; Haye, B. Close evolutionary relatedness of α-amylases from archaea and plants. *J. Mol. Evol.* **1999**, *48*, 421–426. [CrossRef]
58. Zorgani, M.A.; Patron, K.; Desvaux, M. New insight in the structural features of haloadaptation in α-amylases from halophilic Archaea following homology modeling strategy: Folded and stable conformation maintained through low hydrophobicity and highly negative charged surface. *J. Comput. Mol. Des.* **2014**, *28*, 721–734. [CrossRef] [PubMed]
59. Janeček, Š. α-amylases from Archaea: Sequences, structures and evolution. *Biotechnol. Extrem.* **2016**, *1*, 505–524.
60. Ştefan Andrei, A.; Banciu, H.L.; Oren, A. Living with salt: Metabolic and phylogenetic diversity of archaea inhabiting saline ecosystems. *FEMS Microbiol. Lett.* **2012**, *330*, 1–9. [CrossRef]
61. El-Fallal, A.; Abou, M.; El-Sayed, A.; Omar, A.E.-S.A.N. Starch and microbial α-amylases: From concepts to biotechnological applications. *Carbohydr. Compr. Stud. Glycobiol. Glycotechnol.* **2012**. [CrossRef]

Supplementary material

GGAATCGATTAGCCCTGCTAGTCGCACGGGTCTTAGACTCCGTAGGCATATAGCTCAGT
AACACGTGGCCAAACTACCCTACAGACCGCGATAACCTCGGGAAACTGAGGCCAATA
GCGGATATAACTCTCAGGCTGGAGTGCCGAGAGTTAGAAACGTTCCGGCGCTGTAGGA
TGTGGCTGCGGCCGATTAGGTAGATGGTGGGGTAACGGCCCACCATGCCGATAATCGG
TACGGGTTGTTGGAGAGCAAGAACCCGGAGACGGTATCTGAGACAAGATACCGGGCCC
TACGGGGCGCAGCAGGCGGGAAACCTTTACACTGCACGACAGTGCGATAGGGGGACTC
CGAGTGTGAGGGCATATAGCCCTCGCTTTTCTGTACCGTAAGGTGGTACAGGAACAAGG
ACTGGGCAAGACCGGTGCCAGCCGCCGCGGTAATACCGGCAGTCCAAGTGATGGCCGA
TATTATTGGGCCTAAAGCGTCCGTAGCTTGCTGTGTAAGTCCGTTGGGAAATCGACCCG
CTCAACGCGTCGGCGTCCAGCGGAAACTGTCCGGCTTGGGGCCGGAAGACTTGGGGGG
TACGTCCGGGGTAGGAGTGAAATCCTGTAATCCTGGACGGACCACCAATGGGGAAACC
ACCTTGAGAAGCCGGACCCGACGGTGAGGGACGAAAGCCAGGGTCTCGAACCGGATT
AGATACCCGGGTAGTCCTAGCTGTAAACGATGCTCGCTAGGTGTGCCGTAGGCCACGA
GCATGCGATGCGCCGTAGGGAAGCCGAGAAGCGAGCCGCCTGGGAAGTACGTCTGCA
AGGATGAAACTTAAAGGAATTGGCGGGGGAGCACCACAACCGGAGGAGCCTGCGGTT
TAATTGGACTCAACGCCGGAAATCTCACCGGTCCCGACAGTAGTAATGACGGTCAGGTT
GACGACTTTACCCGACGCTACTGAGAGGAGGTGCATGGCCGCCGTCAGCTCGTACCGT
GAGGCGTCCTGTTAAGTCAGGCAACGAGCGAGACCCGCACTTCTAGTTGCCAGCAATA
CCCTTGAGGTAGTTGGGTACCCTAGGAGGACTGCCGCTGCTAAAGCGGAGGAAGGAAC
GGGCAACGGTAGGTCAGTATGCCCCGAATGGACCGGGCAACACGCGGGCTACAATGG
CTCTGACAGTGGGATGCAACGCCGAGAGGCGACGCTAATCTCCAAACGGAGTCGTAGT
TCGGATTGCGGGCTGAAACCCGCCCGCATGAAGCTGGATTCGGTAGTAATCGCGTGTCA
GAAGCGCGCGGTGAATACGTCCCTGCTCCTTGCACACACCGCCCGTCAAAGCACCCGA
GTGGGGTCCGGATGAGGCCGTCATGCGACGGTCGAATCCT

Figure S1. Full length of the 16S rRNA encoding gene from *Haloarcula* sp. HS, amplified with the archaeal specific primers 21F (5′-TTCCGGTTGATCCTGCCGGA-3′) and 1492R (5′-GGTTACCTTGTTACGACTT-3′). Polymerase chain reactions (PCR) were performed as indicated in Materials and Methods.

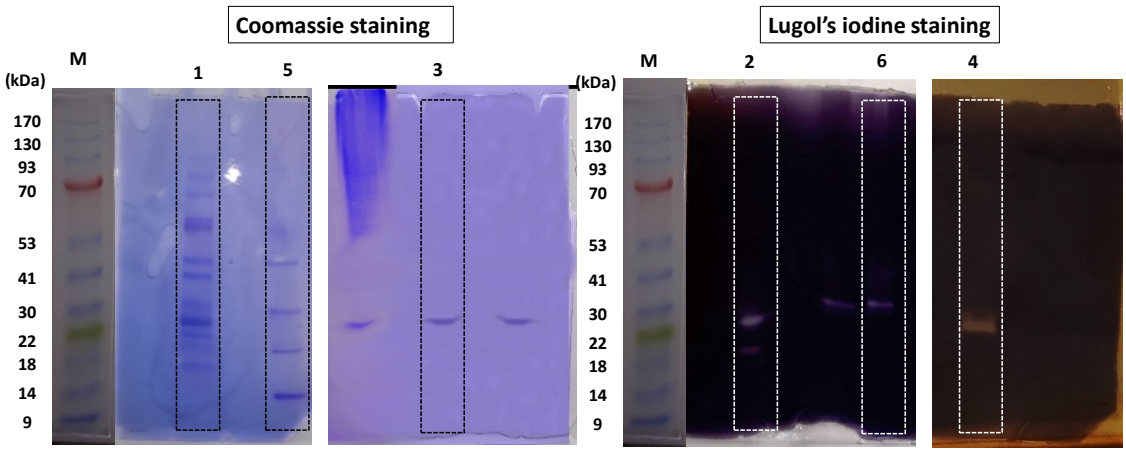

Figure S2. Polyacrylamide gels corresponding to the whole gels of Figure 4. The cropped lanes with their respective numbers are denoted by dashed boxes for Coomassie and Lugol staining.

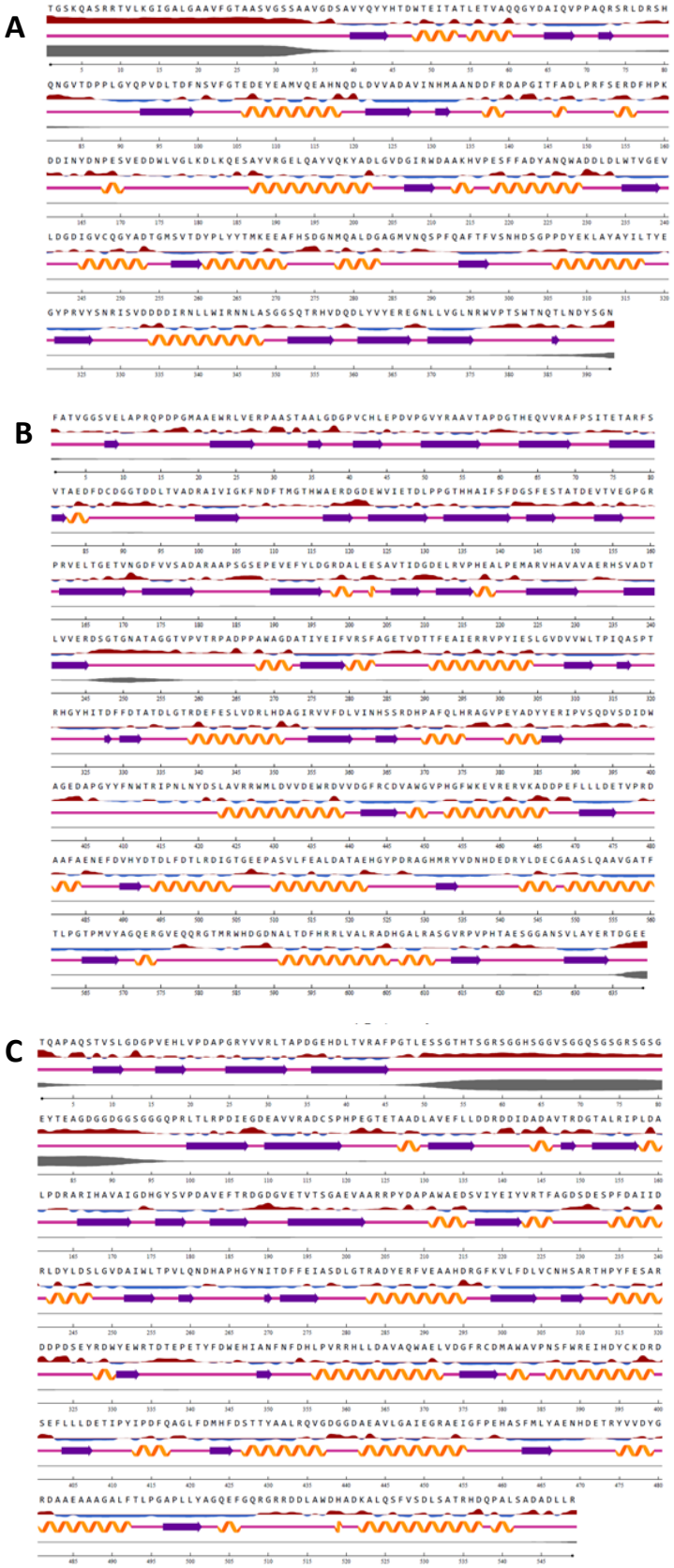

Figure S3. Predicted structures of the three amylase sequences identified in *Haloarcula* sp. HS; A: extracellular amylase, AMY_HS1; B: cell-associated amylase, AMY_HS2; C: cell-associated amylase Amy_HS3. 2D structures were made using the NetSurfP software. Helixes are represented by ribbons and strands by arrows. The red color indicates surface exposition, while the blue color shows buried surfaces.

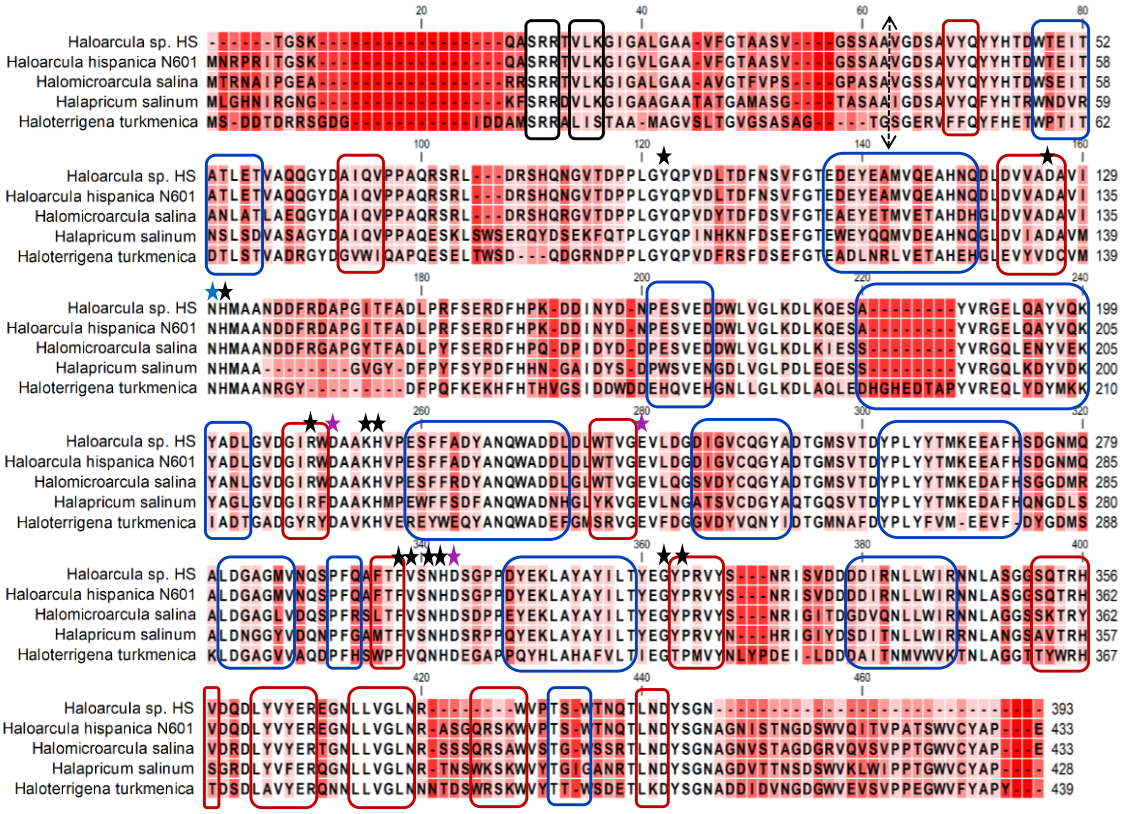

Figure S4. Multiple alignments of the amino acid sequence of the extracellular amylase identified in *Haloarcula* sp. HS (AMY_HS1) with alpha-amylases from different haloarchaea. The sequences are ordered from the top to the bottom with decreasing degree of identity: *Haloarcula hispanica* N601 (WP_014040218.1), *Halomicroarcula salina* (WP_162411878.1), *Halapricum salinum* (WP_049992672.1), and *Haloterrigena turkmenica* (WP_012943282.1). Purple stars highlight the catalytic triad (Asp-Glu-Asp), blue star denotes the canonical calcium-binding site and black stars point other essential residues for enzyme structure. Residues corresponding to the TAT motif are denoted with black boxes and the processing site is indicated by a black dashed double arrow. The gradient from red to white in the background indicates the degree of conservation, with white 100%. Secondary structures, helixes, and strands are denoted by blue and red boxes, respectively, matching with the 3D protein models shown in Figure 8.

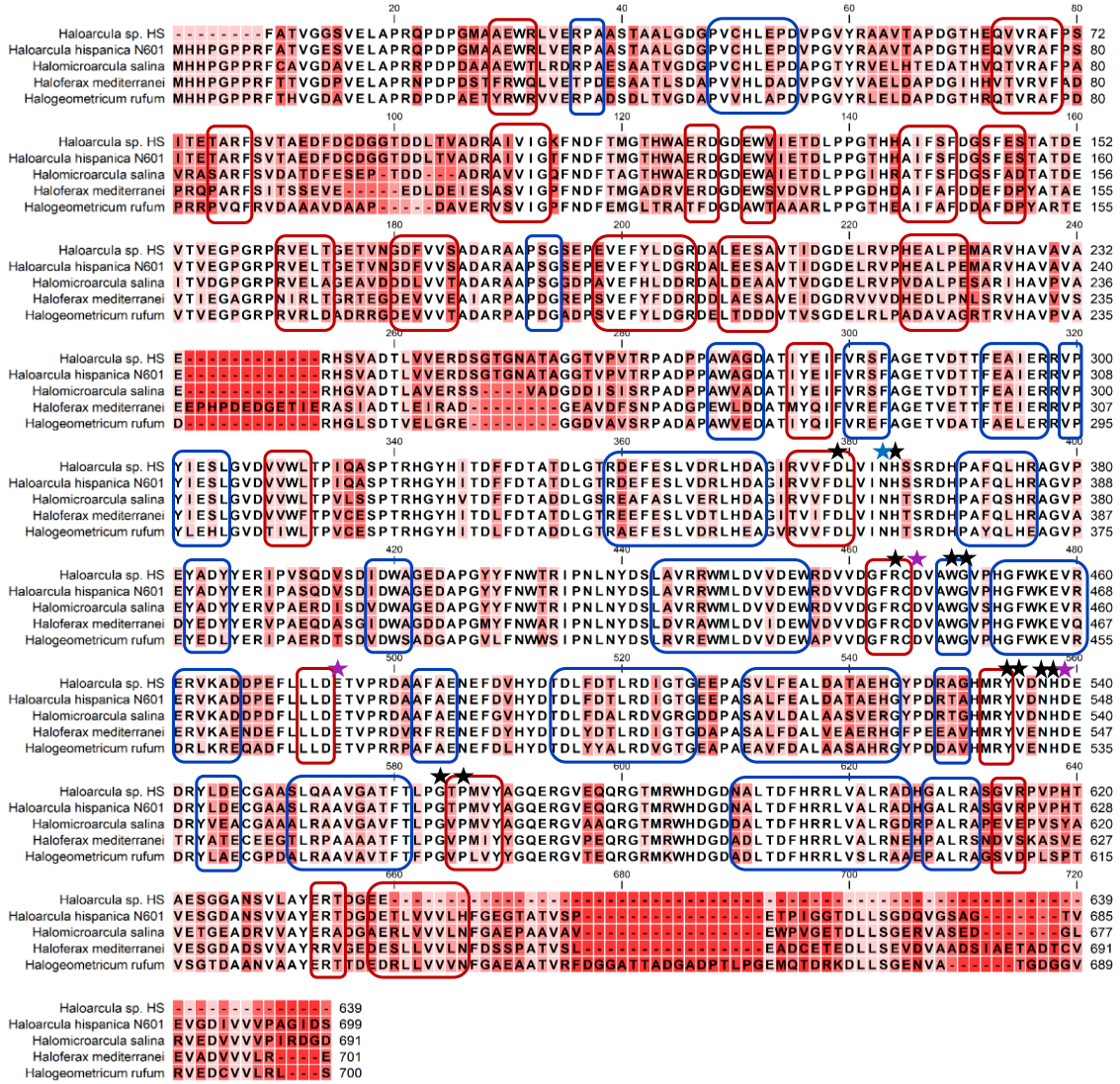

Figure S5. Multiple alignments of the amino acid sequence of the cell-associated amylase from *Haloarcula* sp. HS (AMY_HS2) with alpha-amylases from different haloarchaea. The sequences are ordered from the top to the bottom with decreasing degree of identity: *Haloarcula hispanica* N601 (WP_014040218.1), *Halomicroarcula salina* (WP_162413265.1), *Haloferax mediterranei* (WP_004057797.1), and *Halogeometricum rufum* (WP_089804789.1). Purple stars highlight the catalytic triad (Asp-Glu-Asp), blue star denotes the canonical-calcium binding site and black stars point other essential residues for enzyme structure. The gradient from red to white in the background indicates the degree of conservation, with white 100%. Secondary structures, helixes, and strands are denoted by blue and red boxes, respectively, matching with the 3D protein models shown in Figure 8.

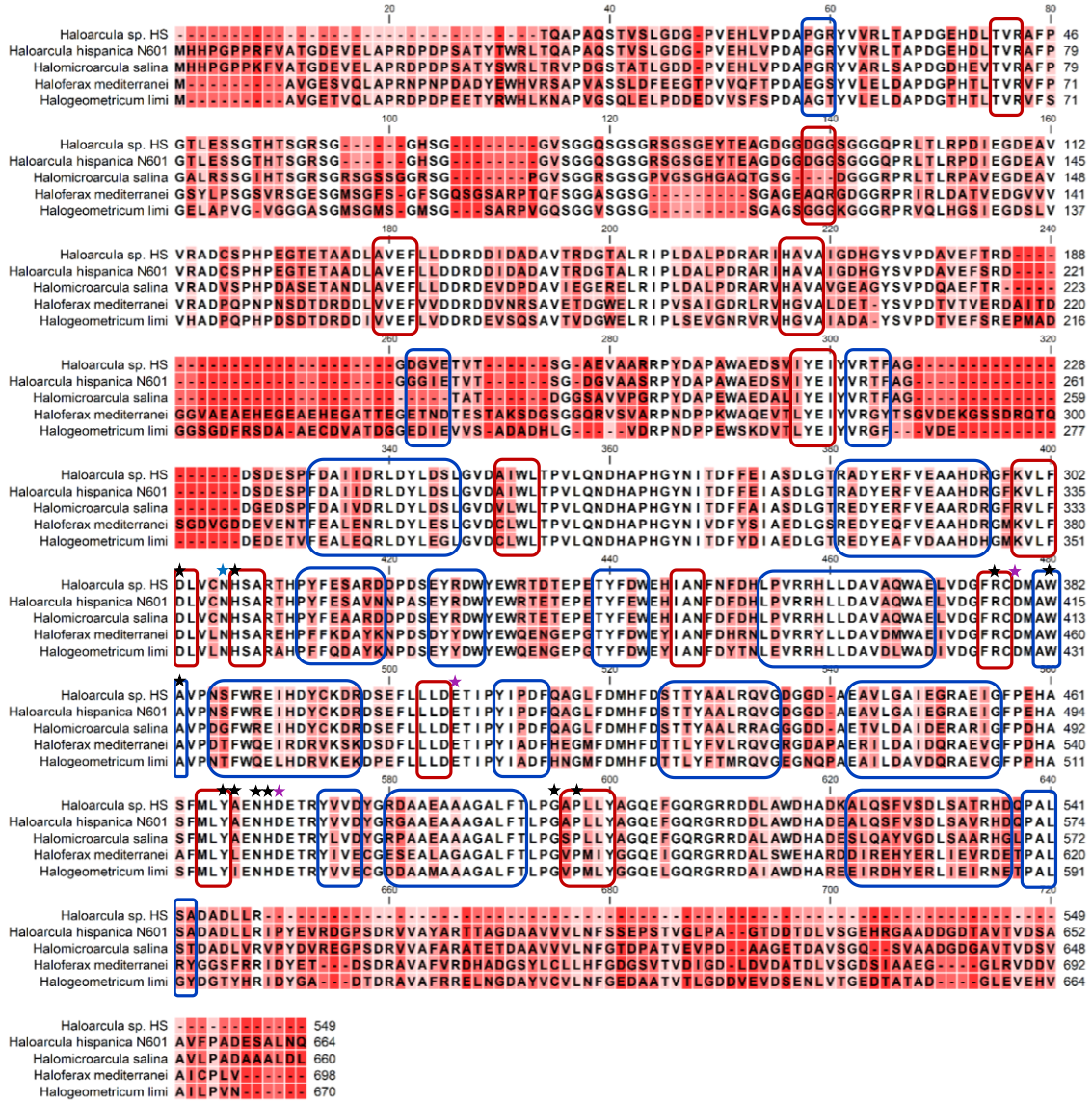

Figure S6. Multiple alignments of the amino acid sequence of the cell-associated amylase from *Haloarcula* sp. HS (AMY_HS3) with alpha-amylases from different haloarchaea. The sequences are ordered from the top to the bottom with decreasing degree of identity: *Haloarcula hispanica* N601 (WP_023843400.1), *Halomicroarcula salina* (WP_162414602.1), *Haloferax mediterranei* (WP_004056521.1), and *Halogeometricum limi* (WP_089883475.1). Purple stars highlight the catalytic triad (Asp-Glu-Asp), blue star denotes the canonical calcium-binding site and black stars point other essential residues for enzyme structure. The gradient from red to white in the background indicates the degree of conservation, with white 100%. Secondary structures, helixes, and strands are denoted by blue and red boxes, respectively, matching with the 3D protein models shown in Figure 8.

Chapter 4

Metagenomic And Pigment Insights Into The Microbiota Dynamics Through The Salinity Gradient In The Odiel Saltern Ponds (SW, Spain)

RESULTS AND DISCUSSION. Chapter 4

El artículo “Metagenomic And Pigment Insights Into The Microbiota Dynamics Through The Salinity Gradient In The Odiel Saltern Ponds (SW, Spain)” en proceso de publicación, debido a restricciones relativas a derechos de autor, ha sido retirado de la tesis.

Abstract: Diverse extreme conditions converge in solar salterns, including high salt concentration, temperature, and solar irradiance. Most environmental factors are similar in the different ponds that comprise the salterns excepting salinity which increases along with the series of ponds until reaching saturation concentrations. Thus, these habitats are exceptional places to study the dynamics of the microbial communities across the salinity gradient. In this work, metagenomics of 16S and 18S rRNA gene coding sequences were employed to characterize the prokaryotic and eukaryotic communities along a salinity gradient (3.5, 7.5, 15, and 30% NaCl). Moreover, the changes in the pigment composition across salinity were studied by spectrophotometry and RP-HPLC, and their possible contribution to the trophic chain was discussed. The results revealed that Chlorophyta dominated the eukaryotic communities at all the studied salinities, although diatoms and alveolates populations were also substantial in seawater. The major microalgae found at medium salinities (7.5 and 15%) belonged to the genus Picochlorum, while at the highest salinity Dunaliella was prevailing. Among prokaryotes, the predominant phylum in seawater was Proteobacteria, but its abundance decreased as salinity increased, being replaced by Bacteroidetes and Euryarcheota. At the highest salinity, the most abundant prokaryotic members were haloarchaea of the family Halobacteriaceae and the bacteria Salinibacter ruber. Finally, the contribution of microbial carotenoids to the pigmentation of the flamingo feathers seems to be conceivable under the actuation of the tiny shrimp Artemia as an intermediate.

Keywords: brines; carotenoids; halophiles; 16S and 18S rRNA metagenomics; Odiel saltern

Conclusions

Conclusions

Based on the objectives proposed in this doctoral thesis and the results obtained in the different chapters, the following conclusions have been reached:

Chapter 1:

1. The two culture-independent methods used to analyze the microbial population in the Odiel salterns, on the one hand, the construction and characterization of two clone PCR amplified-16S rRNA libraries and, on the other, a high throughput 16S rRNA sequencing approach based on the Illumina MiSeq platform, are comparable in terms of determining the majority genera, although mass sequencing provides more information about the less abundant ones.

2. The microbial population of the brine at 33% salinity is composed of a single bacterial species, *Salinibacter ruber*, and a great diversity of halophilic archaea, being *Halorubrum*, *Haloquadratum*, *Halobellus*, and *Halonotius* the most abundant genera.

3. This microbiota has been found to produce and excrete various halotolerant exo-enzymes with amylase, laccase, lipase, cellulase, and protease activity. Besides, antimicrobial compounds, which could be involved in the interspecies competition to proliferate in hypersaline environments, were detected.

Chapter 2:

4. The extracts obtained from two new halophilic archaea isolated from the Odiel salterns, *Haloarcula* sp. HM1 and *Halobacterium* sp. HM2, show high antioxidant and antimicrobial capacity, and promising bioactive properties, being the anti-inflammatory, melanogenic, and acetylcholinesterase inhibitory activities the most outstanding ones.

Chapter 3:

5. The halophilic archaea, *Haloarcula* sp. HS, has been selected by its high amylase activity, which is detected in both the cell extract and the extracellular fraction. Both activities are halotolerant, thermoresistant, and stable under the action of various metals and surfactants, although exhibit different optimal parameters.

6. The analysis of the proteome composition of the partially purified cell-free supernatant and the cellular extracts has allowed the identification of three different enzymes belonging to the α-amylase family in *Haloarcula* sp. HS, two exclusively intracellular and one extracellular, which shows good capacity to degrade bakery residues under high salinity.

Chapter 4:

7. The massive sequencing of the 16S and 18S rRNA coding genes, together with the analysis of the most abundant pigments along the salinity gradient (3.5, 7.5, 15, and 30% NaCl) in Odiel salterns revealed the evolution of the composition of the microbial communities across the salinity gradient.

8. The great microbial diversity present in the seawater is reduced as the salt concentration increases. Green microalgae (*Chlorophyta*) dominate phytoplankton in all the salinities and the phylum *Proteobacteria* is displaced by the phyla *Bacteroidetes* and *Euryarcheaota* as salinity increases.

9. At low salinities phytoplankton dominates the microbial population, being fucoxanthin and chlorophylls the pigments mainly detected, while at the highest salinity bacterioruberin was the predominant carotenoid found.

10. The pigments present in the microbiota of the salterns could be transmitted through the trophic chain, being the precursors of the carotenoids found in higher organisms such as flamingos, with the intervention of the small crustacean *Artemia* as an intermediary.

Conclusiones

En base a los objetivos propuestos en la presente tesis doctoral y a los resultados obtenidos en los distintos capítulos, se han alcanzado las siguientes conclusiones:

Capítulo 1:

1. Los dos métodos independientes de cultivo utilizados para analizar la población microbiana en las salinas de Odiel, por un lado, la construcción y caracterización de dos bibliotecas de ARNr 16S amplificadas por PCR de clones y, por el otro, un enfoque de secuenciación de ARNr 16S de alto rendimiento basado en la plataforma Illumina MiSeq, son comparables en términos de determinación de la mayoría de géneros, aunque la secuenciación masiva proporciona más información sobre los menos abundantes.

2. La población microbiana al 33% de salinidad está compuesta por una única especie bacteriana, *Salinibacter ruber* y una gran diversidad de arqueas halófilas, siendo los géneros mayoritarios *Halorubrum*, *Haloquadratum*, *Halobellus* y *Halonotius*. Además, esta microbiota produce diversas exo-enzimas halotolerantes.

3. Se ha encontrado que esta microbiota produce y excreta varias exo-enzimas halotolerantes con actividad amilasa, lacasa, lipasa, celulasa y proteasa. Además, se detectaron compuestos antimicrobianos, que podrían estar involucrados en la competencia entre especies para proliferar en ambientes hipersalinos.

Capítulo 2:

4. Los extractos obtenidos de las dos nuevas arqueas halófilas aisladas de las salinas de Odiel, *Haloarcula* sp. HM1 y *Halobacterium* sp. HM2, muestran alta capacidad antioxidante y antimicrobiana, y prometedoras propiedades bioactivas, siendo las actividades más destacadas la anti-inflamatoria, melanogénica e inhibitoria de la acetilcolinesterasa.

Capítulo 3:

5. La arquea halófila, *Haloarcula* sp. HS, ha sido seleccionada por su alta actividad amilasa, que se detecta tanto en el extracto celular como en la fracción extracelular. Ambas actividades son halotolerantes, termorresistentes y estables bajo la acción de varios metales y surfactantes, aunque exhiben diferentes parámetros óptimos.

6. El análisis de la composición proteómica del sobrenadante parcialmente purificado libre de células y de los extractos celulares ha permitido la identificación de tres enzimas diferentes pertenecientes a la familia de las α-amilasa en *Haloarcula* sp. HS, dos exclusivamente intracelulares y una extracelular, que muestra buena capacidad para degradar residuos de panadería bajo alta salinidad.

Capítulo 4:

7. La secuenciación masiva de los genes codificantes de ARNr 16S y 18S, junto con el análisis de los pigmentos más abundantes a lo largo del gradiente de salinidad (3.5, 7.5, 15, y 30% NaCl) en Odiel Salterns se reveló la evolución de la composición de las comunidades microbianas a través del gradiente de salinidad.

8. A bajas salinidades el fitoplancton domina la población microbiana, siendo la fucoxantina y las clorofilas los pigmentos principalmente detectados, mientras que a la salinidad más alta se encontró que la bacterioruberina es el carotenoide predominante.

9. Los pigmentos presentes en la microbiota de las salinas podrían transmitirse a través de la cadena trófica, siendo los precursores de los carotenoides encontrados en organismos superiores como los flamencos, con la intervención del pequeño crustáceo *Artemia* como intermediario.

Abbreviations

Abbreviations

ABTS: 2,2′-azino-bis(3-ethylbenzothiazoline-6-sulfonic acid)

AChE: Acetylcholinesterase

AMY_HS: amylase from *Haloarcula* sp. HS

ANOVA: Analysis of variance

BABR: bisanhydroruberin

BHT: Butylated hydroxytoluene

BR: Bacterioruberin

BLAST: Basic local alignment search tool

BSA: Bovine serum albumin

C- Negative control

C+ Positive control

Cas: CRISPR associated

CCA: Copper chelating assay

CECT: Spanish collection of culture type

CHAPS: 3-[(3-Cholamidopropyl) dimethylammonio]-1-propanesulfonate

COX: Cyclooxygenase

CRISPR: Clustered regularly interspaced short palindromic repeats

DGGE: Denaturing gradient gel electrophoresis

DMSO Dimetysulphoside

DPPH: 1,1-Diphenyl-2-picrylhydrazyl

ED-pathway: Entner-Doudoroff pathway

EDTA Ethylenediaminetetraacetic acid

EMBL: European Molecular Biology Laboratory

EMP-pathway: Embden-Meyerhof-Parnas pathway

EPS: Extracellular polysaccharides

FRP: Ferrocyanide reduction potential

GGPP: Geranylgeranyl pyrophosphate

HPLC: High performance liquid chromatography

ICA: Iron chelating assay

IPP: Isopentenyl pyrophosphate

LB medium: Luria–Bertani medium

LC-MS/MS: Liquid chromatography–mass spectrometry

LFS: Life sequencing service

MABR: monoanhydrobacterioruberin

MEGA: Molecular evolutionary genetics analysis

MIC: Minimal inhibitory concentration

MS/MS: tandem mass spectrometry

MUSCLE: Multiple sequence comparison by log- expectation

NCBI: National Center for Biotechnology Information

NGS: Next generation sequencing

NO: Nitric oxide

OTU: Operational taxonomic unit

PAGE: Polyacrylamide gel electrophoresis

PBS: Phosphate-buffered saline

PCR: Polymerase chain reaction

PHA: polyhydroxyalkanoates

PHB: Polyhydroxybutyrate

PHV: Polyhydroxyvalerate

RFLP: Random fragment length polymorphisms

RNAP: RNA polymerase

SB-12: N-Dodecyl-N,N-dimethylammonio-3-propane sulfonate

Sec-pathway: General secretion pathway

SDS: Sodium dodecyl sulfate

SBV: Stabvida sequencing service

TABR: Trisanhydrobacterioruberin

TAP medium: Tris-acetate-phosphate medium

TCA cycle: Tricarboxylic acid cycle

Tat-pathway: Twin-arginine translocation pathway

TOF: time-of-flight

Triton-X100: 2-[4-(2, 4, 4-trimethylpentan-2-yl) phenoxy] ethanol

tRNAs: Transfer RNA

TSB: Tryptic soy broth

Tween 20: Polyoxyethylene (20) sorbitan monolaurate

Tween 80: Polyoxyethylene (80) sorbitan monooleate

TYRO: Tyrosinase

YPD medium: Yeast extract-peptone-dextrose medium

Curriculum vitae

PUBLICATIONS

Gómez-Villegas, P.; Vigara, J.; Romero, L.; Gotor, C.; Raposo, S.; Gonçalves, B.; Léon, R. (2021). Biochemical Characterization of the Amylase Activity from the New Haloarchaeal Strain *Haloarcula* sp. HS Isolated in the Odiel Marshlands. *Biology* 2021, *10*, 337 (3,796;Q1).DOI:10.3390/biology10040337

Gómez-Villegas, P.; Vigara, J.; Vila, M.; Varela, J.; Barreira, L.; Léon, R. (2020). Antioxidant, Antimicrobial, and Bioactive Potential of Two New Haloarchaeal Strains Isolated from Odiel Salterns (Southwest Spain). *Biology* 2020, *9*, 298 (3,796; Q1). DOI: 10.3390/biology9090298

Sahli, K., Gomri, M. A., Esclapez, J., **Gómez-Villegas, P**., Ghennai, O., Bonete, M. J., León, R. Kharroub, K. (2020). Bioprospecting and characterization of pigmented halophilic archaeal strains from Algerian hypersaline environments with analysis of carotenoids produced by *Halorubrum* sp. BS2. *Journal of Basic Microbiology* 2020, 60(7): 624-638 (1,909; Q2). DOI: 10.1002/jobm.202000083

Gómez-Villegas, P.; Vigara, J.; León, R. (2018). Characterization of the Microbial Population Inhabiting a Solar Saltern Pond of the Odiel Marshlands (SW Spain), *Marine drugs*, *16*(9), 332 (3,772; Q1). DOI: 10.3390/md16090332

GRANTS

Predoctoral Research Contract within the framework of the Scientific Policy Strategy of the University of Huelva 2016-2017. June 13, 2017- November 12, 2020.

International mobility aid to Centers of Excellence for doctoral students of the Campus of International Excellence del Mar. October-December 2018.

International mobility aid Erasmus + Internship, Neptune Project 2016/2017. March-May 2017.

Scholarship for Predoctoral stay in Europe of the Campus of International Excellence del Mar 2016/2017. March- May 2017.

CONTRIBUTION TO CONGRESS

P. Gómez-Villegas, A. León, A. Molina, R. Rengel, M. Vila, I. Giráldez, J. Vigara, R. León. Oral presentation: ***"Algared"***. European Researchers Night 2020. Huelva, November 27, 2020.

P. Gómez-Villegas, J. Vigara, R. León. Oral presentation: "***Halophilic microorganisms as marine bioproducers***". II Coasts of Andalusia Course. CEI-Mar Andalusian Universities, July 20-24, 2020.

P. Gómez-Villegas, J. Vigara, R. León. Oral presentation: ***"Halophilic archaea a source of bioactive compounds"***. V Conference of Doctoral Students, Industrial and Environmental Science and Technology Program. University of Huelva, 6-7 November 2019.

P. Gómez-Villegas, J. Vigara, R. León. Oral presentation: ***"Biodiversity of halophilic microorganisms inhabiting Odiel solar salterns in Huelva, Spain"***. II Congress of Young Researchers of the Sea (International). Málaga, 1-4 October 2019.

P. Gómez, A. León, A. Molina, R. Rengel, M. Vila, I. Giráldez, J. Vigara, R. León. Oral presentation: ***"The chemistry of life"***. European Researchers' Night 2019. Huelva, September 27, 2019.

P. Gómez-Villegas, A. León-Vaz, M. Vila, J. Vigara, R. León. Poster: ***"Description of the eukaryotic microbial population in a solar saltern pond of the Odiel marshlands (SW Spain)"***. Halophiles International Conference 2019: Cluj Napoca (Romania), June 24-28, 2019.

P. Gómez-Villegas, J. Vigara, R. León.Poster: ***"Characterization of the prokaryotic diversity inhabiting a solar saltern pond of the Odiel marshlands (SW Spain)"***. Halophiles International Conference 2019: Cluj Napoca (Romania), June 24-28, 2019.

P. Gómez-Villegas, J. Vigara, R. León. Oral presentation: *"**Microbial diversity of Odiel salterns and its biotechnological applications***". Technical Conference: Biotechnological Potential of the salt flats of the Algarve-Andalusian coast. Huelva, April 10, 2019.

P. Gómez-Villegas, J. Vigara, R. León. Oral presentation: "***Characterization and biotechnological potential of halophilic microorganisms from Odiel salterns, Huelva"***. IV Conference of Doctoral Students, Industrial and Environmental Science and Technology Program. University of Huelva, November 8, 2018.

P. Gómez, E. García, A. León, A. Molina, R. Rengel, M. Vila, P. Ruíz, E. Morales, J. Vigara, R. León, I. Giráldez. Oral presentation: ***"Clams and their medicinal properties and photographic exhibition on the colors of the sea"***. Science Week 2018. Faculty of Experimental Sciences, University of Huelva, November 5-9, 2018.

P. Gómez-Villegas, J. Vigara, R. León. Oral presentation: ***"Characterization and biotechnological potential of halophilic microorganisms from the Odiel salt flats, Huelva"***. I Congress of Young Researchers of the Sea. Cádiz, 3-5 October 2018.

P. Gómez-Villegas, J. Vigara, R. León. Poster: *"**Study of the microbial population of the Odiel salt flats by means of culture-independent methods***". I Congress of Young Researchers of the Sea. Cádiz, 3-5 October 2018.

P. Gómez-Villegas, A. León, A. Molina, R. Rengel, M. Vila, E. García, I. Giráldez, J. Vigara, R. León. Oral presentation: ***"The colors of the sea"***. European Night of Researchers 2018. Huelva, September 28, 2018.

P. Gómez-Villegas, J. Vigara, R. León. Oral presentation: ***"Bioprospecting of new species and bioactive compounds"***. ALGARED + project days. Faculty of Experimental Sciences, University of Huelva, June 4, 2018.

P. Gómez-Villegas, J. Vigara, R. León. Oral presentation and poster: ***"Characterization of the microbial diversity of the Odiel salt flats, Huelva"***. IX Conference on Aquaculture in the South Atlantic Coast. Cartaya, Huelva, May 9-10, 2018.

Gómez-Villegas P, Marquez J, M, García-Maroto F, Cuesta A, Vila M, Vigara J, León R. Poster presentation: *"**Subcloning of the nnv-cpn gene in a microalgal expression vector for the preparation of oral vaccines against the nerve necrosis virus**"*. IX Conference on Aquaculture in the South Atlantic Coast. Cartaya, Huelva, May 9-10, 2018.

P. Gómez-Villegas, M. de la Vega, A. Sayago, J. Ariza, A. García-Barneto, M. Vila, J. Vigara, R. León. Poster: *"**Characterization of the microbial population of the crystallization basins of the Odiel salt flats and their carotenoid content**"*. National Meeting on Carotenoids in Microorganisms, Plants, Food and Health. Valencia, November 16-17, 2017.

R. León, M. Vila, A. Molina A. León, **P. Gómez-Villegas**, R. Rengel, C. J. Vigara. Conference: *"**Design and obtaining functional phytoplankton**"*. European Researchers' Night 2017. Huelva. September 29, 2017.

Gómez-Villegas P., Vila M., Vigara J., León R. Oral Presentation: ***"Screening the microbial population inhabiting the solar saltern ponds of the Odiel river marshlands in the south of Spain for their ability to produce halostable exoenzymes"***. National Congress of Biotechnology. Murcia, June 18-21, 2017.

J. Konečná, D. Horák, A. Španová, **P. Gómez-Villegas**, R. León. Poster: ***"Comparison and optimalization of DNA extraction methods using new magnetic particles for analysis of Haloarcula"***. National Congress of Biotechnology. Murcia, June 18-21, 2017.

León R., Vila M., **Gómez-Villegas P**., García-Maroto F., López-Alonso D., Cuesta A., Morillo AJ., Vigara J. Poster: ***"Preparation of microalgae entrapped in hydrogel microspheres as a vehicle for delivery of oral vaccines aquaculture"***. National Congress of Biotechnology. Murcia, June 18-21, 2017.

INTERNATIONAL STAYS

Biocenter, Department of Biology, University of Copenhagen, Denmark. International Predoctoral Stay. October-December 2018. Task: Genetic manipulation of extremophilic archaea using the CRISPR-Cas system. Supervisor: Qunxin She.

Center for Marine Sciences (CCMar), University of the Algarve, Faro, Portugal. International Predoctoral Stay. March-May 2017. Task: Study of the bioactive capacity of extreme halophilic archaea isolated from the Odiel salt flats (Huelva). Supervisors: Dr. João Varela and Dra. Luisa Custodio.

TEACHING ACTIVITY

Practical teaching in the Biochemistry-Molecular Biology subject of the Degree in Chemistry at the University of Huelva. 3 Credits, course 2020/2021.

Practical teaching in the Biochemistry-Molecular Biology and Food Biochemistry subjects of the Degree in Chemistry at the University of Huelva. 1 Credit, course 2019/2020.

Practical teaching in the Biochemistry-Molecular Biology subject of the Degree in Chemistry at the University of Huelva. 1 Credits, academic year 2018/2019.

Practical teaching in the subjects of Biomolecules and Biochemistry-Molecular Biology of the Degree in Chemistry at the University of Huelva. 2 Credits, academic year 2017/2018.

Co-direction of the Final Degree Project: "Subcloning a viral antigenic protein into an expression vector for microalgae" of the Degree in Chemistry at the University of Huelva the course 2017/2018.

Co-direction of the Final Degree Project: "Kinetic characterization of the amylase activity from the haloarquea *Haloarcula* sp." of the Degree in Chemistry at the University of Huelva the course 2018/2019.

Co-direction of the Final Degree Project: "Laccase activity in *Haloarcula hispanica*, strain *onubensis*, and its biotechnological potential" of the Degree in Chemistry at the University of Huelva, the course 2019/2020.

Co-direction of the Final Degree Project: "Characterization of the carotenoid pigments of the extremophile microorganisms isolated from the Odiel marshes and their presence in the marine trophic chain" of the Degree in Chemistry at the University of Huelva, the course 2020/2021.